SYRINGOLIN-TRIGGERED RESISTANCE IN POWDERY MILDEW-INFECTED ARABIDOPSIS: A MOLECULAR AND GENETIC ANALYSIS

Dissertation

zur

Erlangung der naturwissenschaftlichen Doktorwürde

(Dr. sc. nat.)

vorgelegt der

Mathematisch-naturwissenschaftlichen Fakultät

der

Universität Zürich

von

Kathrin Michel

aus

Deutschland

Promotionskomitee

Prof. Dr. Robert Dudler (Leitung der Dissertation)

Prof. Dr. Beat Keller (Vorsitz)

Prof. Dr. Enrico Martinoia

Zürich, 2006

Das schönste Glück des denkenden Menschen ist,
das Erforschliche erforscht zu haben
und das Unerforschliche ruhig zu verehren.

Johann Wolfgang von Goethe

Table of contents

1 Summary

Powdery mildew, caused by the fungus *Blumeria graminis* (DC) Speer, is one of the most important foliar diseases of cereals worldwide. It is an obligate biotrophic parasite, colonising leaf epidermal cells to obtain nutrients from the plant cells without killing them. Syringolin A (sylA), a circular peptide secreted by the phytopathogenic bacterium *Pseudomonas syringae* pv. *syringae*, triggers a hypersensitive cell death reaction (HR) at infection sites when sprayed onto powdery mildew infected wheat which essentially eradicates the fungus. The goal of the present work was to identify genes whose expression was specifically regulated during HR, i.e. genes that might be involved in the switch of compatibility to incompatibility. Microscopic investigations revealed that syringolin inhibits powdery mildew reproduction in both Arabidopsis and cereals in a phenotypically similar way. The model plant *Arabidopsis thaliana* provides excellent molecular and genetic resources such as transcriptome analysis by using the Arabidopsis full genome microarray. Thus, in a first approach to elucidate the syringolin response in Arabidopsis, probes derived from RNA extracted from powdery mildew-infected Arabidopsis treated with sylA or control buffer, respectively, were hybridised to microarrays. Additionally, we performed an experiment with uninfected syringolin-treated plants, which do not undergo HR. Surprisingly, the effect of syringolin on the transcriptome of *Arabidopsis thaliana* was dramatically stronger in uninfected plants than in infected plants. Not only were transcript levels of more genes changed in uninfected plants than in infected plants, but transcripts in infected plants accumulated also to a stronger extent in uninfected plants. Detailed analysis of these results lead to the hypothesis that the cellular response to syringolin was negatively controlled by powdery mildew infection in colonised and neighbouring cells at infection sites. The functional annotation of proteins encoded by sylA-affected

transcripts indicated that sylA affects gene expression as if mitochondrial function and oxidative phosphorylation were impaired. As a consequence, it seems that plants switch to a fermentative metabolism which could help to avoid overreduction of the mitochondrial ubiquinone pool. The observed sylA-induced accumulation of proteasome-related transcripts may reflect an increased demand of proteolytic activity that may help to achieve metabolic changes by selective removal of proteins. The accumulation of transcripts coding for protective proteins may be viewed as a response of the plant to counteract the stress imposed by sylA. This lead to a novel hypothesis according to which the HR in infected and syringolin-treated Arabidopsis could be the result of the pathogen-induced suppression of gene expression that may lead to insufficient production of protective proteins. Transcript abundance specific for infected tissue could be shown for only few genes and these genes were induced only weakly.

Besides microarray experiments, a second approach for the elucidation of molecular events underlying the occurrence of HR in infected sylA-treated plants aimed at the investigation of knock-out mutants harbouring T-DNA insertions in transcripts that accumulated early upon sylA treatment and encoded proteins with regulatory functions. The rational was to identify mutants that exhibited insensitivity to syringolin. None of the 11 analysed T-DNA insertion lines exhibited enhanced sporulation efficiency of powdery mildew after syringolin treatment. However, a mutant harbouring a T-DNA insertion in the At4g12400 gene showed impaired sporulation of the powdery mildew fungus on non-treated leaves. A second mutant line homozygous for an independent T-DNA insertion in the genomic sequence of At4g12400 revealed a similar phenotype, thus supporting the assumption that non-functionality of the encoded protein indeed negatively affects powdery mildew reproduction in Arabidopsis. A homolog of the At4g12400 gene in soybean encodes

a stress inducible gene whose expression is inducible by heat. We speculate that the At4g12400 encoded protein may exhibit a similar stress-related function and may be necessary to counteract cellular stress imposed on the plant during sporulation. This in turn may be beneficial for the biotrophic fungus which depends on a functional cell metabolism and a living host.

In a third approach for the elucidation of the syringolin response in Arabidopsis, EMS-mutagenised plants were screened for less or no impairment in fungal growth after application of syringolin. Transcriptome analysis of one confirmed mutant revealed elevated levels of ABA-related transcripts without syringolin treatment. We hypothesise that this is associated with elevated endogenous ABA-levels which can lead to a suppression of disease resistance. Moreover, mutant plants exhibited elevated abundance of transcripts encoding stress-related proteins. We assume that enhanced expression of stress-related genes may help to support cell survival, thus preventing HR and supporting powdery mildew growth in infected syringolin-treated mutant plants. This assumption is compatible with the hypothesis developed above, i.e. that a pathogen-induced downregulation of genes encoding stress-related and protective proteins could trigger HR and resistance to powdery mildew in sylA-treated wild-type plants. Thus, HR elicited in infected and sylA-treated plants appears not to depend on specific regulation of certain genes, but might rather represent the result of pleiotrophic effects caused by syringolin treatment and fungal invasion. The observation that syringolin-induced gene expression exhibited strong similarity to expression patterns induced by the virulent strain of *P. syringae* is intriguing. We hypothesise that sylA acts as an effector of *P. syringae* pv. *syringae* that helps to put host plant cells into a physiological state, presumably profitably for the bacteria.

2 Zusammenfassung

Echter Mehltau, verursacht durch den Pilz *Blumeria graminis* (DC) Speer, ist weltweit eine der bekanntesten Blattkrankheiten bei Getreide. Es handelt sich dabei um einen obligat biotrophen Erreger, der die Epidermiszellen befällt und Nährstoffe von der pflanzlichen Zelle bezieht, ohne diese zu töten. Syringolin A (SylA), ein zirkuläres Peptid, das von pflanzenpathogenen Stämmen des Bakteriums *Pseudomonas syringae* pv. *syringae* sezerniert wird, vermag eine „Hypersensitive Reaktion“ (HR) in von Mehltau befallenen Weizenpflanzen zu induzieren und verhindert dadurch eine weitere Ausbreitung des Pilzes. Ziel dieser Arbeit war die Identifizierung HR-regulierter Gene, die an einem Wechsel von Kompatibilität zu Inkompatibilität beteiligt sein könnten. Mikroskopische Untersuchungen ergaben, dass Syringolin die Vermehrung des Mehltaupilzes in Arabidopsis und Getreide gleichermassen zu verhindern vermag. Die Modellpflanze *Arabidopsis thaliana* bietet Vorteile bezüglich molekularer und genetischer Forschung, wie z. B. die Untersuchung transkriptioneller Veränderungen mittels des Arabidopsis-Gesamtgenom-Microarrays. In einem ersten Ansatz zur Aufklärung der Syringolinantwort in Arabidopsis wurde RNA aus Blattmaterial von Mehltau befallenen Arabidopsis-Pflanzen nach Syringolinbehandlung bzw. Behandlung mit einer Kontrolllösung isoliert, mit Biotin markiert und anschliessend mit dem Microarray hybridisiert. Des Weiteren wurde ein Experiment mit nicht infizierten und Syringolin-behandelten Pflanzen durchgeführt. Überraschenderweise war die durch Syringolin erzielte Wirkung in nicht infizierten Pflanzen viel stärker als in infizierten Pflanzen. In nicht infizierten Pflanzen veränderte Syringolin die Expressionsstärke von weitaus mehr Genen als in infizierten Pflanzen. Dies führte zu der Annahme, dass eine Infektion mit Mehltau die Antwort von Syringolin in infizierten und benachbarten Zellen negativ beeinflussen kann. Eine

funktionelle Zuordnung der durch Syringolin differenziell exprimierten Produkte deutete an, dass Syringolin direkt oder indirekt mitochondriale Aktivitäten, wie die oxidative Phoshorylierung, negativ beeinflusst. Ein daraus resultierendes Umschalten des pflanzlichen Stoffwechsels hin zu zellulärer Fermentation könnte eine starke Reduktion des mitochondrialen Ubiquinone Pools verhindern. Eine Anreicherung Syringolin-induzierter, proteolytischer Transkripte könnte auf einen erhöhten Bedarf proteolytischer Aktivität in der Zelle hindeuten. Ein selektiver Abbau von Proteinen durch das Proteasom könnte dabei weitreichende Veränderungen im pflanzlichen Metabolismus gewährleisten. Darüber hinaus lässt sich vermuten, dass die erhöhte Anreicherung von Transkripten protektiver Proteine einen Mechanismus der Pflanze darstellt, dem zellulären Stress entgegenzuwirken. Dies führte zur Formulierung einer neuen Hypothese, wonach die HR in infizierten und Syringolin-behandelten Arabidopsis-Pflanzen die Folge einer pathogenabhängigen Unterdrückung der Genexpression darstellen könnte, welches eine unzureichende Synthese protektiver Proteine verursachen könnte. Die Expression nur weniger Gene war spezifisch für infiziertes und Syringolin-behandeltes Gewebe. Darüber hinaus waren diese wenigen Gene nur schwach induziert.

In einem zweiten Ansatz zur Erforschung der molekularen Grundlagen der HR-Auslösung in infizierten SylA-behandelten Pflanzen wurden knock-out-Mutanten, die eine T-DNA in einem Syringolin-induzierbaren Gen trugen, untersucht. Dabei wurden 11 Gene analysiert, deren Expression relativ schnell nach einer Syringolinbehandlung induziert wurde und deren Geneprodukte regulatorische Funktionen besitzen. Das Ziel war die Identifizierung Syringolin-insensitiver Mutanten. Keine dieser Pflanzen zeigte jedoch nach Syringolinbehandlung einen dem Wildtyp vergleichbaren Phänotyp. Eine Mutante, die aufgrund einer T-DNA Insertion im At4g12400-Gen isoliert worden war, zeigte an unbehandelten Blättern eine erhöhte

Resistenz gegenüber Befall mit dem echten Mehltaupilz. Dieser Phänotyp konnte durch eine zweite unabhängige Insertion im At4g12400-Gen bestätigt werden. Ein homologes Stress-induzierbares Gen wurde in Sojabohnen identifiziert. Die Expression dieses Gens kann durch Hitze induziert werden. Es ist anzunehmen, dass At4g12400 ebenfalls für ein Protein kodiert, welches durch zellulären Stress, möglicherweise im Zuge pilzlicher Sporulation hervorgerufen, benötigt wird, um diesem entgegenzuwirken. Dies wiederum könnte den biotrophen Erreger, der von einem funktionellen Wirtsstoffwechsel abhängt, in der Entwicklung unterstützen.

Ein dritter Ansatz zur Aufklärung der Syrigolinantwort in Arabidopsis konzentrierte sich auf die Identifizierung von EMS-mutagenisierten Pflanzen, welche weniger oder gar keine Beeinträchtigung des pilzlichen Wachstums nach einer Syringolinbehandlung zeigten. Dies führte zur Identifizierung einer Mutante. Unbehandeltes Gewebe dieser Mutante wies eine erhöhte Expression von Genen auf, deren Genprodukte eine Rolle in der zellulären Physiologie des pflanzlichen Hormons Abscisinsäure (ABA) spielen. Eine gesteigerte Expression dieser Gene könnte gleichzeitig mit einer erhöhten endogenen ABA-Konzentration einhergehen, was zu einer Unterdrückung der pflanzlichen Abwehr führen kann. Zudem zeigte die Mutante eine erhöhte Expression von Genen, deren kodierten Proteine eine grundsätzliche Funktion während zellulärer Stressreaktionen besitzen. Diese Proteine führen möglicherweise zu einem gesteigerten Schutz sowie dem Überleben der Zelle, was eine Unterdrückung der HR und die erhöhte Anfälligkeit der Mutante gegenüber Mehltau erklären könnte. Diese Annahme unterstützt die anfangs erwähnte Hypothese in dem Sinne, dass die HR eine Folge pathogenabhängiger Unterdrückung der Genexpression darstellen könnte, welche eine unzureichende Synthese protektiver Proteine zur Folge hätte. Demnach scheint das Auftreten der HR in infizierten Syringolin-behandelten Pflanzen eher einen pleiotropen Effekt

darzustellen als eine spezifische Wirkung. Interessanterweise scheint Syringolin das Gen-Expressionsmuster in ähnlicher Weise zu verändern, wie das virulente Stämme des Bakteriums *Pseudomonas syringae* tun. Dies legt die Vermutung nahe, dass SylA als Effektor von *P. syringae* agiert, der hilft, die pflanzliche Wirtszelle in einen für das Bakterium wahrscheinlich profitablen physiologischen Zustand zu bringen.

3 Introduction

Plants are hosts to thousands of infectious diseases caused by a vast array of phytopathogenic bacteria and fungi. A relatively small proportion of potential pathogens is able to successfully invade a specific plant host and cause disease. *Blumeria graminis* (DC.) Speer the causal agent of the powdery mildew disease in cereals is one of the most important foliar diseases worldwide. Powdery mildew is a biotrophic pathogen which requires living host tissue to grow and reproduce. Asexual reproduction starts after landing of a conidial spore on the plant where it exclusively infects epidermal cells. In the course of infection, primary and secondary germ tubes arise from both ends of the conidium. Elongation of the secondary germ tube initiates the differentiation of a swollen appearance referred to as appressorium. The appressorium produces the penetration peg which often successfully penetrates the cell wall and establishes a haustorium. The haustorium which is enclosed by the extrahaustrorial matrix and the invaginated host plasma membrane, is responsible for the nutrient transfer from the host plant to the fungus. Successful colonisation by the fungus is followed by the formation of elongated secondary hyphae and the development of conidiophores which produce new conidia. A compatible interaction between wheat and powdery mildew is illustrated in figure 1.1.

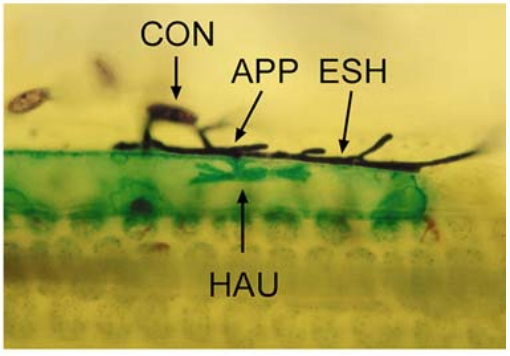

Figure 1.1 Colonisation of a wheat epidermal cell by powdery mildew

A conidium (CON) of powdery mildew formed an appressorium (APP) that successfully penetrated a cell transiently expressing *GUS* and formed a haustorium (HAU) and elongating secondary hyphae (ESH). Epiphytic fungal structures were stained with coomassie blue. The picture was taken 40 hours post inoculation. Modified after Schweizer et al., 1999.

Plants have evolved mechanisms to detect and respond effectively to most pathogens. Recognition of a pathogen-derived avirulence factor by a distinct resistance (R) protein in the host plant triggers defense reactions against certain races of biotrophic pathogens. The hallmark of this race-specific resistance is the hypersensitive reaction (HR), a localised cell and tissue death at the site of infection, which prevents further spread of the infection. Although highly effective for the control of many diseases, these R-genes often are not durable because of selection in the pathogen population for variants that overcome the resistance conferred by the R-gene.

The HR can also trigger non-specific resistance throughout the plant, a phenomenon designated as systemic acquired resistance (Ryals et al., 1996). Once triggered, systemic acquired resistance provides resistance to a wide range of pathogens for days. In moncots, this induced resistance is restricted to the site of induction and designated local acquired resistance. In rice, acquired resistance against the rice blast fungus *Pyricularia oryzae* (telomorph: *Magnaporthe grisea*) can be induced by inoculation with the non-host pathogen *Pseudomonas syringae* pv. s*yringae* (Smith and Métraux, 1991). Resistance to *Pyricularia oryzae* and defence-related transcript levels can also be increased by application of syringolin, an elicitor that is secreted by the bacteria under appropriate conditions (Wäspi et al., 1998). The function of the syringolins in the interaction of *P. syringae* pv. s*yringae* with host plants is currently unknown, however, they represent one of the molecular determinants of *P. syringae* pv. s*yringae* by which rice plants can perceive this nonhost pathogen (Hassa et al., 2000; Wäspi et al., 1998).

Syringolins constitute a family of structurally related cyclic peptides designated syringolin A to F. Syringolin A, the major variant present in conditioned media, consists of a 12-membered ring formed by two nonproteinogenic amino acids, 5-methyl-4-amino-2-hexenoic acid and 3,4-dehydrolysine, bound to a valine that in turn is linked to a second valine via an urea moiety (Figure 1.2).

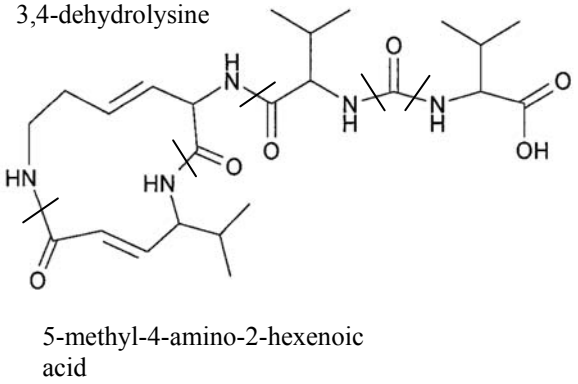

Figure 1.2 Chemical structure of syringolin A

A 12-membered ring structure consisting of 5-methyl-4-amino-2-hexenoic acid and 3,4-dehydrolysine connected to two valines. The valines are connected via an urea moiety. Lines delimit amino acids (Amrein et al., 2004).

Syringolin A (in the following also referred to as syringolin) is synthesised by a non-ribosomal peptide synthetase/polyketide synthetase (Amrein et al., 2004) and its production is controlled by the bacterial *lemA/gacA* two-component regulatory system (Wäspi et al., 1998) necessary for pathogenicity of *Pseudomonas* on host plants (Hrabak and Willis, 1992, 1993). Although syringolin is sufficient to induce resistance and accumulation of defence related transcripts in rice plants, *P. syringae* pv. s*yringae* strains and mutants that do not produce syringolin still elicit resistance, indicating that the syringolin perception system in rice is redundant with respect to the resistance response (Reimmann et al., 1995; Wäspi et al., 1998).

The effect of syringolin on the interaction of powdery mildew with wheat was reported by Wäspi and co-workers (2001). They could show that application of syringolin to powdery mildew-infected wheat essentially eradicates fungal growth when applied 48 hours after infection. Although these effects of syringolin are reminiscent to certain types of fungicides, syringolin does not exhibit fungitoxic activity against numerous fungi tested such as *Pyricularia oryzae*, *Rhodotorula pilimanae*, *Fusarium graminearum* or *Trichoderma viride* (Wäspi et al., 2001). In contrast to treatment with a fungicide, the curative effect of syringolin on infected wheat was associated with the occurrence of hypersensitive cell death at the infection sites (Wäspi et al., 2001), which correlates with autofluorescence. In addition, autofluorescence indicative for HR is exclusively found in infected cells and no autofluorescence occurs in uninfected tissue (Wäspi et al., 2001). Thus, syringolin was hypothesised to directly or indirectly reprogram colonised host cells to undergo hypersensitive cell death in a compatible interaction. The effect of syringolin on powdery mildew-infected cells leading to autofluorescence and fungal arrest is illustrated in figure 1.3.

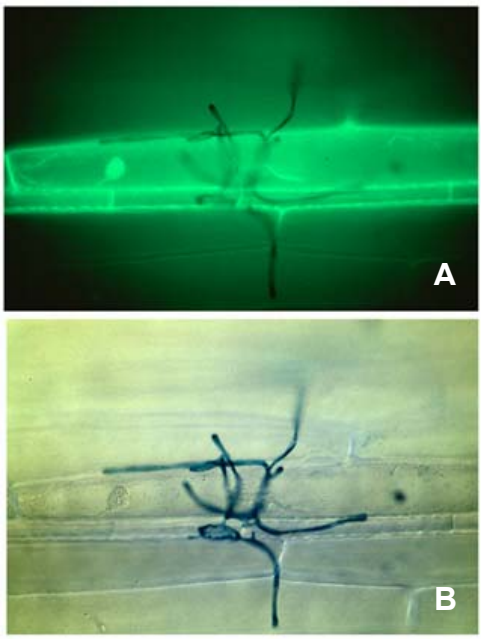

Figure 1.3 Induction of HR by application of syringolin on powdery mildew-infected wheat.

Leaves were infected with wheat powdery mildew and sprayed with 40 µM syringolin 48 hours after infection. Leaves were destained and fungal structures were stained with coomassie blue. Plant-pathogen interactions were photographed under fluorescent (A) and incident light (B), respectively, five days post inoculation (Wäspi et al., 2001).

This thesis shows that a similar curative effect of syringolin is found in powdery mildew-infected *Arabidopsis thaliana*. This offers the possibility to genetically dissect the syringolin response and to use the ATH1 full genome array for transcriptome analysis.

Thus, syringolin treatment or treatment with a control solution was carried out on leaves pre-infected with powdery mildew. In addition, leaf material was collected from uninfected plants that were sprayed with syringolin or the control solution. Subsequent isolation of RNA and hybridisation to the ATH1 gene chip aimed at the identification of genes possibly involved in defence-related HR which might be specifically induced by syringolin treatment of infected Arabidopsis.

To address biological functions of genes transcriptionally upregulated by syringolin treatment, T-DNA insertion lines of selected genes were tested for their ability to support powdery mildew growth upon syringolin treatment.

A second approach aimed at the identification of mutants that exhibit less or no impairment on fungal growth after application of syringolin. Screening of EMS-plants revealed one confirmed mutant. This mutant was characterised microscopically and transcriptional changes were investigated by hybridisation to the ATH1 gene chip.

4 Results

4.1 Syringolin A action in powdery mildew-infected *Arabidopsis thaliana*

Syringolin A (referred to as sylA or syringolin for simplicity), one of the molecular determinants secreted by *Pseudomonas syringae* pv. *syringae*, essentially eradicates powdery mildew from infected wheat plants if applied curatively after inoculation (Wäspi et al., 2001). In contrast to treatment with a fungicide, application of syringolin causes autofluorescence, an indication of the hypersensitive reaction (HR). Syringolin-treated cells were unable to undergo plasmolysis and to take up neutral red, indicating irreversible membrane damage of dying cells. So far, the occurrence of sylA-triggered HR has been shown for powdery mildew-infected monocotyledonous plants such as wheat (*Triticum aestivum*) and barley (*Hordeum vulgare*).

With the aim to genetically dissect syringolin action in plants, we analysed the syringolin-response in the model plant *Arabidopsis thaliana*.

4.1.1 Experimental setup and microscopic evaluations

To visualise the effect of sylA on infected Arabidopsis, 14-day-old seedlings of *Arabidopsis thaliana* (ecotype Columbia) were infected with a compatible strain of the powdery mildew fungus *Erysiphe cichoracearum* (*E.c*). The isolate was recovered from Arabidopsis and was used throughout this study. Since the growth of *Erysiphe* sp. occurs on the leaf surface, early stages of the infection cycle and disease progression can be easily observed by visual inspection or with microscopic techniques. The disease reaction phenotype in compatible interactions is

characterised by the development of macroscopically visible white, snow-like colonies, which first become apparent on the surface of infected leaves about five days post-inoculation (dpi). Figure 4.1 illustrates microscopic investigations of fungal development at different timepoints.

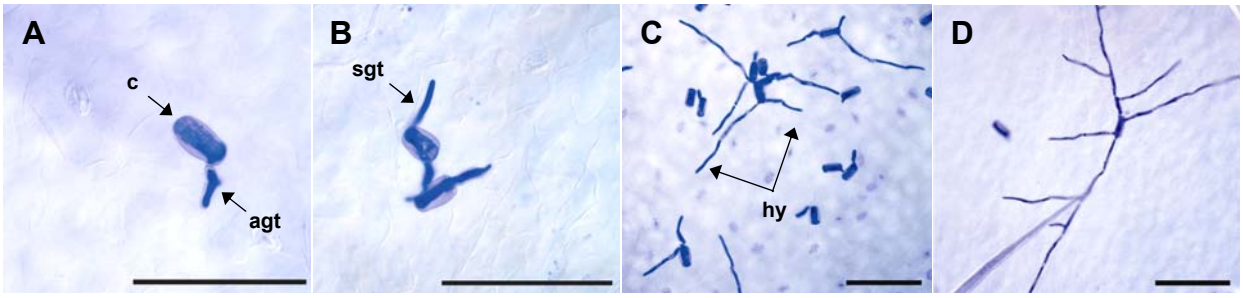

Figure 4.1 Arabidopsis-powdery mildew interaction

Leaves of 14-day-old *Arabidopsis thaliana* plants were infected with a compatible strain of *Erysiphe cichoracearum.* Leaves were destained by over-night incubation in lacto-phenol solution. Fungal structures were stained with coomassie blue and plant-pathogen interactions were investigated by bright field microscopy. **(A)** 12 hours after infection. The appressorial germ tube (agt) has emerged from the conidium (c). **(B)** 24 hours after infection. A second functional germ tube (sgt) has developed. **(C)** 36 hours after infection. Hyphae (hy) arose from both germ tubes and have elongated by two days post-inoculation **(D)**. Scale bar: 100 µm.

Twelve hours after infection (hai), an unlobed germ tube, referred to as appressorial germ tube, had arisen from the end of a conidium (Figure 4.1 A). Often, a second germ tube emerged from the opposite end of a conidium within 24 hai (Figure 4.1 B). By 24 hai, most conidia had germinated. The first germ tube could be distinguished from the second by its slightly enlarged and swollen appearance. Because of its distinct morphology, we refer to the first germ tube as the appressorial germ tube. The appressorial germ tube produced a penetration peg, which often successfully penetrated the cell wall and established a haustorium. By 36 hai, hyphae had arisen from both germ tubes (Figure 4.1 C) and had elongated by two dpi (Figure 4.1 D), and started to form a network on the leaf surface. At this timepoint, plants were treated with a control solution (0,05% Tween 20) or a 20 µM

solution of sylA and leaf material was evaluated under the microscope five dpi, corresponding to 72 hours after treatment (hat). A schematic overview of the experimental setup is illustrated in figure 4.2.

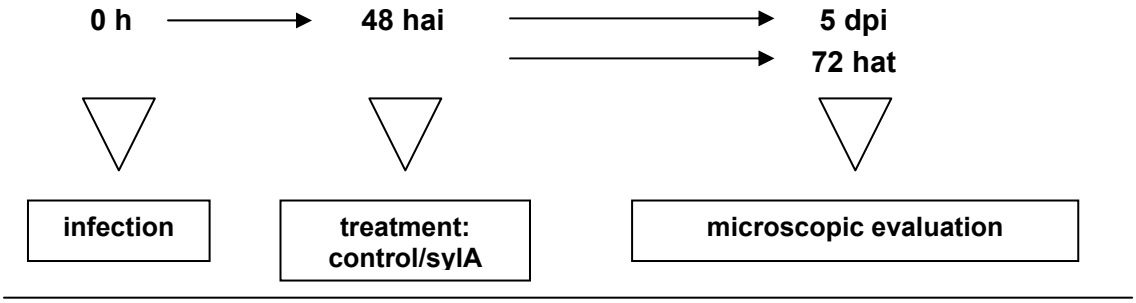

Figure 4.2 Overview of the experimental setup

14-day-old seedlings of *Arabidopsis thaliana* were infected with a compatible strain of *Erysiphe cichoracearum* at timepoint 0 hours (h). At 48 hours after infection (hai), plants were treated with a 20 µM solution of sylA or a control solution (0,05% TWEEN 20). Leaves were destained and stained for fungal structures five days post inoculation (dpi), corresponding to 72 hours after treatment (hat).

Treatment with a control solution had no effect on fungal reproduction and resulted in a compatible interaction. By 24 hat, elongated hyphae had started to form a network on the leaf surface (Figure 4.3 A). The fungal network became dense 48 hat (Figure 4.3 B). At this timepoint young conidiophores were formed and became numerous 72 hat (Figure 4.3 C). Infected plants sprayed with a control solution emitted no autofluorescence at any timepoint (Figure 4.3 D-F).

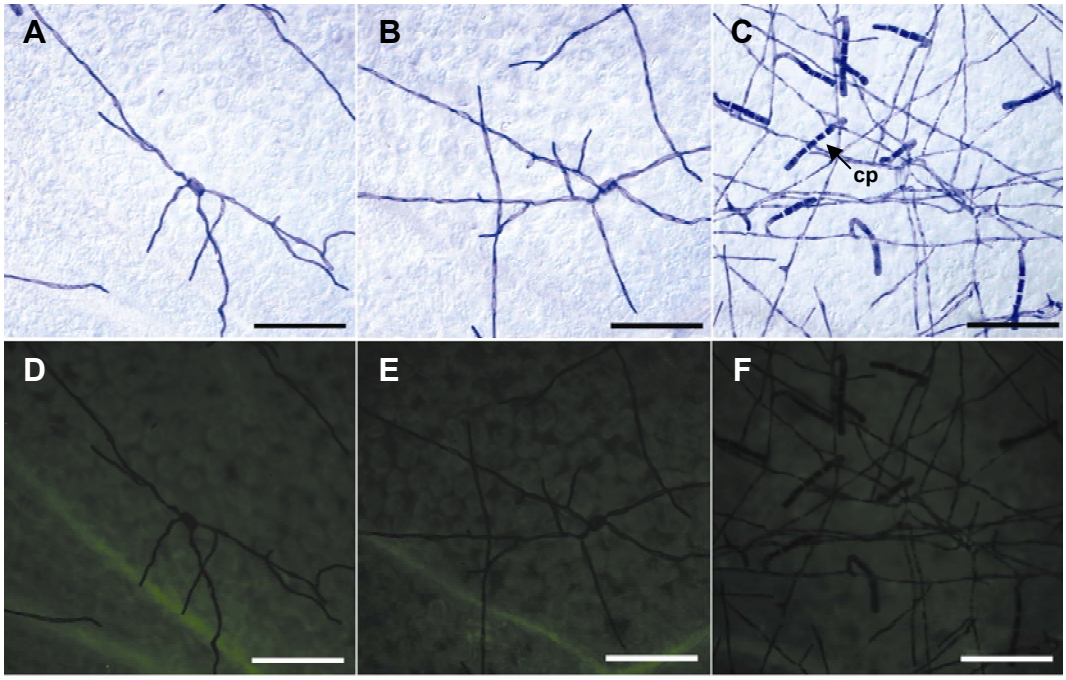

Figure 4.3 Arabidopsis-powdery mildew interactions on control-treated leaves

Leaves of 14-day-old *Arabidopsis thaliana* plants were infected and sprayed with a control solution 48 hours after infection. Leaves were destained by over-night incubation in lacto-phenol solution. Fungal structures were stained with coomassie blue and plant-pathogen interactions were photographed under incident and fluorescent light, respectively, 24 (A, D), 48 (B, E) and 72 (C, F) hours after treatment. With the formation of conidiophores (cp) at five days post-inoculation, the fungus has successfully completed its lifecycle. Scale bar: 100 µm.

When plants were sprayed with a solution of 20 µM sylA 48 hai, fungal growth was arrested. Thus, no further development and sporulation had occurred by 72 hat (Figure 4.4 A). Tissue collapse and autofluorescence at the sites of infection

was apparent 48 hat and became clearly visible 72 hat (Figure 4.4 B). In rare cases no autofluorescence became apparent at the infection sites which was accompanied with a progression of fungal growth. In general, arrest of fungal growth was associated with autofluorescence at 100% of infection sites. Spraying of 20 µM sylA on uninfected plants had no visible effect, neither by eye nor by bright field (Figure 4.4 C) and epifluorescence microscopy (Figure 4.4 D). Killing of the powdery mildew fungus with a fungicide resulted in an arrest of fungal growth (Figure 4.4 E). However, in contrast to a treatment with sylA, no autofluorescence became visible at 88% of infection sites (Figure 4.4 F).

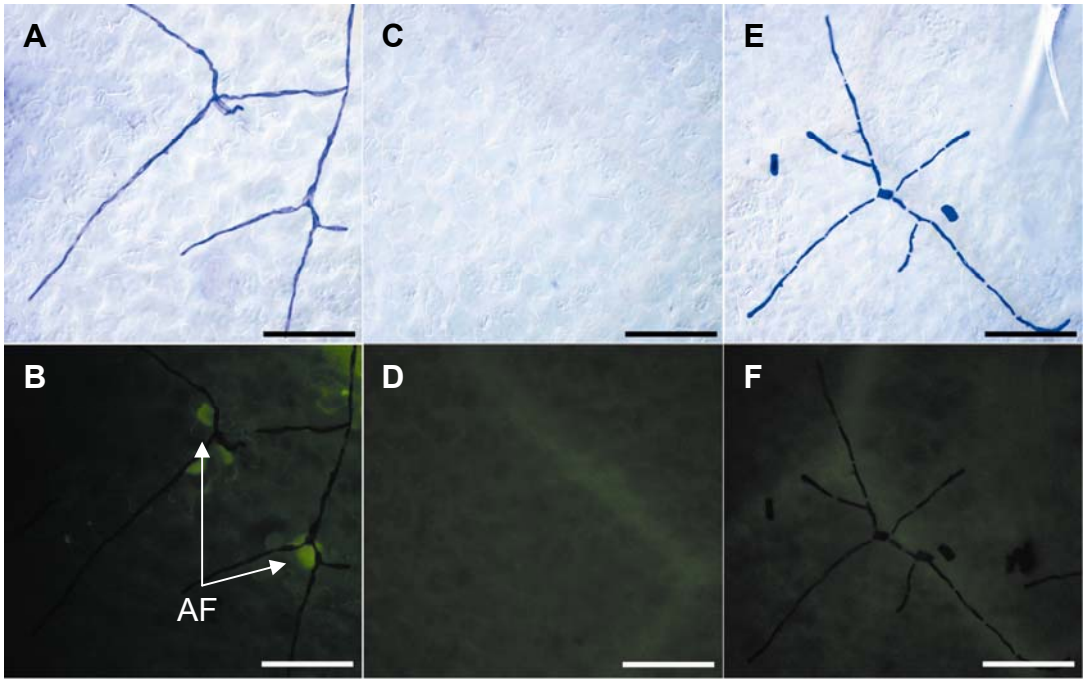

Figure 4.4 Effect of syringolin A on powdery mildew-infected and uninfected Arabidopsis leaves

Infected leaves of *Arabidopsis thaliana* were treated with sylA 48 hours after infection. Seventy-two hours after treatment, leaves were destained by over-night incubation in lacto-phenol solution. Fungal structures were stained with coomassie blue and plant-pathogen interactions were photographed under incident (A) and fluorescent light (B) to visualise cells emitting autofluorescence as indicated by arrows (AF). In uninfected tissue (C) treated with sylA, no autofluorescence was visible 72 hat (D). If plants were infected and treated with a fungicide 48 hours after infection (E), arrest in fungal growth was not correlated with the occurrence of autofluorescence (F). Scale bar: 100 µm.

Powdery mildew penetrates only into the epidermal cells where it forms specialised food absorptive structures called haustoria. Application of syringolin on wheat plants two days after infection with a virulent strain of powdery mildew triggers the accumulation of autofluorescing material specifically in the epidermis (Wäspi et al., 2001). Figure 4.5 illustrates that in infected sylA-treated Arabidopsis autofluorescence was relatively weak in epidermal cells, although clearly visible against a dark background as indicated by arrowheads (eAF). However, autofluorescence was much stronger in mesophyll cells underlying the infection sites (mAF) as indicated by arrows (Figure 4.5).

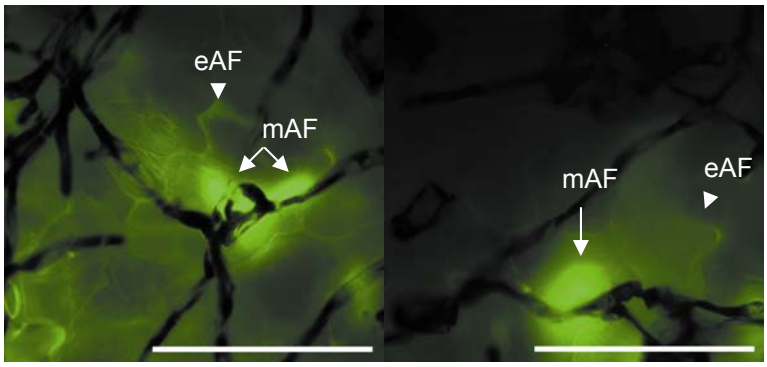

Figure 4.5 Autofluorescence at infection sites on leaves treated with sylA

Infected leaves of *Arabidopsis thaliana* were treated with sylA 48 hours after infection and were photographed under fluorescent light 72 hat. Cells emitted autofluorescence at infection sites. Accumulation of autofluorescing material was weak in epidermal cells (eAF) but clearly visible in the mesophyll cell layer (mAF). Scale bar: 100 µm.

Phytotoxic effects such as yellowing of leaves only became apparent after spraying 40 to 100 µM or higher concentrations of sylA (data not shown). Thus, spray application of a 20 µM sylA solution on powdery mildew-infected Arabidopsis plants converted a compatible interaction into an incompatible one, similar to the effects observed after sylA treatment of powdery mildew-infected wheat (Wäspi et al., 2001).

4.1.2 Transcriptional analysis of the sylA response using ATH1 gene chips

4.1.2.1 Differential expression patterns in sylA-treated plants

To understand the molecular events underlying the conversion of compatibility to incompatibility exerted by sylA, a series of Affymetrix gene chip hybridisation experiments was performed. The aim was to identify genes possibly involved in the switch between compatibility to incompatibility that is exerted by sylA, such as genes activated or repressed after sylA treatment of powdery mildew-infected plants, but not by sylA treatment of uninfected plants. Thus, 14-day-old *Arabidopsis thaliana* plants were inoculated with *Erysiphe cichoracearum* by tapping highly infected Arabidopsis leaves on the leaf surface of experimental plants. This resulted in a high infection density (~200 spores/mm^2, see section Materials and Methods, chapter 6.3.1). After 48 hours, plants were sprayed with a 20 µM solution of sylA or a control buffer solution. RNA was extracted from the plants at 0.5, 1, 2, 4, 8, and 12 hat. Equal amounts of plant material were pooled in pairs, resulting in an early pool, referred to as IS1 for infected sylA-treated plants and sample collection at 0.5-1 hat. A middle pool was obtained from infected and sylA-treated plants collected at 2-4 hat (IS4) and a late RNA pool of plant material collected at 8-12 hat (IS12). The experimental procedure is illustrated in figure 4.6.

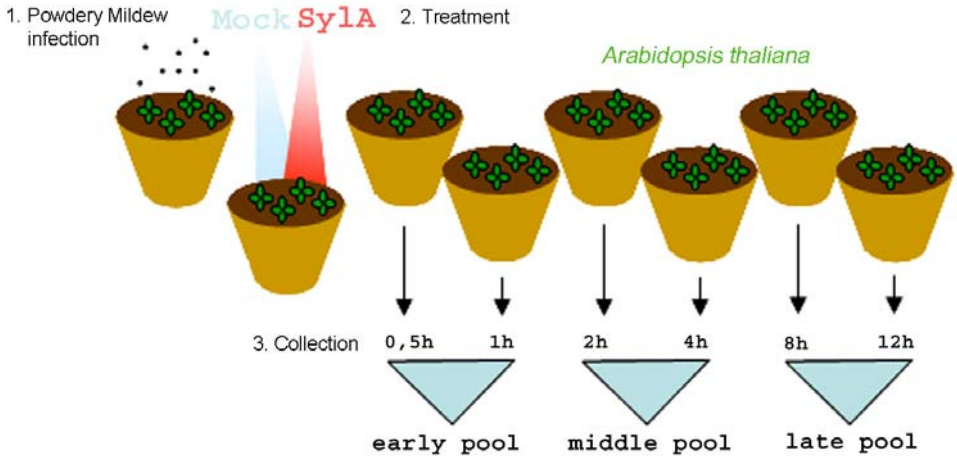

Figure 4.6 Illustration of setup for gene chip hybridisation experiments

Leaves of 14-day-old *Arabidopsis thaliana* seedlings were first infected with a compatible strain of *Erysiphe cichoracearum*. Second, plants were treated with sylA or a control solution 48 hours after infection. Third, total RNA was extracted from leaves collected at six different time points. Starting material for gene chip hybridisation experiments was obtained by combining plant material derived from the two early, two middle, and the two late time points at a ratio of 1:1 (w/w). h: hours

In addition, leaf material was collected at one hat (S1) and at 8-12 hat (S12) from uninfected plants that were sprayed with 20 µM sylA or the control solution. Total RNA was extracted from the plants, labelled and hybridised to Affymetrix ATH1 gene chips representing the complete Arabidopsis genome. An overview of the experiments undertaken is given in table 4.1.

Table 4.1 Overview of gene chip hybridisation experiments

Experiments	Infection	Treatment	Sample collection
IS1	*E. cichoracearum*	control solution vs. syringolin [20 µM]	0,5-1hat[2]
IS4	*E. cichoracearum*	control solution vs. syringolin [20 µM]	2-4 hat
IS12	*E. cichoracearum*	control solution vs. syringolin [20 µM]	8-12 hat
S1	-	control solution vs. syringolin [20 µM]	1 hat
S12	-	control solution vs. syringolin [20 µM]	8-12 hat
I60[1]	uninfected vs. infected plants	control solution	56-60 hai[3]

(1) The effect of infection (I) on transcript abundance was calculated by comparing expression ratios derived from uninfected plants versus infected plants, both treated with a control solution. The timepoint of sample collection corresponded to 56-60 (60) hours after infection (48 hai + 8-12 hat).

(2) Hours after treatment.

(3) Hours after infection.

All experiments were repeated three times independently. Stringent criteria for data analysis were used. The ratios of signal intensities corresponding to treated and control-treated samples (t/c-ratio) were calculated. For statistical analysis, the parametric test using all available error estimates as implemented in the Genespring software (see section Materials and Methods, chapter 6.8.2) was chosen. Furthermore, genes were considered statistically significant if they passed the multiple test correction (MTC) according to Benjamini and Hochberg (Benjamini and Hochberg, 1995). The results in terms of numbers of transcripts whose levels were altered significantly more than 2-fold and 3-fold are presented in table 4.2.

Table 4.2 Numbers of differentially expressed transcripts

Experiments	t/c ratio[1,2]			
	≥ 2	≤ 0,5	≥ 3	≤ 0,333
IS1	0	0 [1]	0	0
IS4	0 [68]	0 [4]	0 [25]	0 [1]
IS12	455 [621]	0 [482]	215 [264]	0 [51]
S1	19	28	1	4
S12	2394	2873	1121	1760
I60	1045	996	555	275

(1) Data derived from three independent experiments. Differentially expressed genes were filtered by the Welch's t-test ($p \leq 0.05$) including multiple test correction (MTC).

(2) Values in brackets designate genes that obtained a p-value ≤ 0.05 but that have not passed the MTC.

Surprisingly, in experiments IS1 and IS4 (plant material collected 0,5-1 hat and 2-4 hat, respectively) the expression of no gene was reproducibly altered more than 2-fold in all three biological independent repetitions. In experiment IS1, only one gene, coding for a germin-like protein 3 (At5g20630), was significantly repressed (t/c ratio: 0,4) as judged by Welch's t-test statistics (p-value ≤ 0.05) when MTC was excluded (Table 4.2). Likewise, no gene has passed the multiple test correction in experiment IS4, but among transcripts that obtained p-values ≤ 0.05, four genes whose expression was lowered more than 2-fold were identified when MTC was excluded and 68 transcripts showed at least a 2-fold increase in abundance.

In IS12, 455 and 215 genes that passed all statistical tests were upregulated 2-fold and 3-fold, respectively, whereas no gene downregulated by sylA treatment passed the multiple test correction. The distributions of the t/c ratios of upregulated genes in experiments IS4, IS12 and S12 are shown in a Venn diagram in figure 4.7.

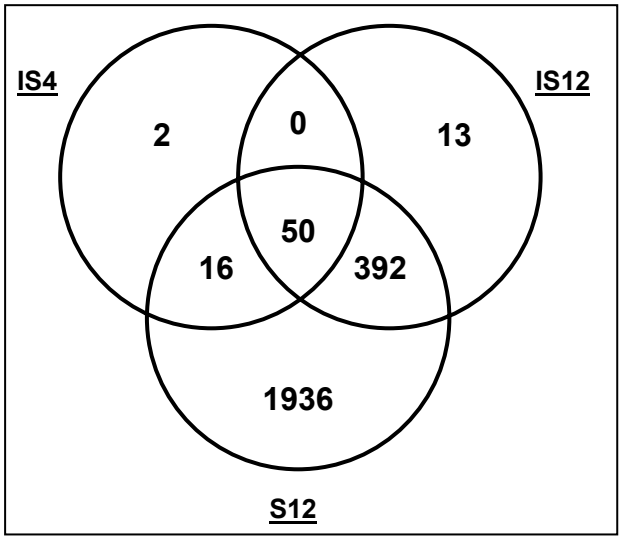

Figure 4.7 Overlap between genes upregulated more than 2-fold in infected and uninfected plants treated with sylA

The Venn diagram represents the distribution of significantly upregulated genes (p-value ≤ 0.05, MTC) in experiments IS12 and S12. Multiple test correction was not applied to genes upregulated in experiment IS4.

Two genes (which did not pass the MTC) were exclusively upregulated in experiment IS4. These genes encoded a mitochondrial pentatricopeptide (PPR) repeat-containing protein (At3g61170) and a zinc finger family protein (At2g24830). To our surprise, all except 13 of the 455 genes which were more than 2-fold upregulated at the 8-12 hat timepoint (IS12) in infected tissue were also included in the set of genes activated when sylA was sprayed on uninfected plants (S12). A list of the 13 genes exclusively present in experiment IS12 is given in table 4.3. It includes genes encoding proteins responding to biotic (Table 4.3, At2g34930, row #1) and abiotic stimuli (Table 4.3, At1g29410, row #10), as well as genes encoding proteins involved in the regulation of transcription (Table 4.3, At2g35340, At5g13080, rows #12, 13). Further genes encoded proteins of unknown biological functions.

Table 4.3 Expression patterns of genes exclusively upregulated by sylA in infected tissue

Row	Description	Locus[1]	Protein	t/c ratio[2]
				IS12
1	disease resistance family protein (contains LRR domain)	At2g34930	-	2,9
2	expressed protein	At1g49930	-	2,3
3	expressed protein	At3g04630	WDL1	3,5
4	expressed protein	At3g51500	-	2,1
5	expressed protein	At4g22960	-	2,6
6	expressed protein	At5g44990	-	2,8
7	expressed protein	At5g47050	-	2,2
8	expressed protein	At5g63220	-	2,1
9	kelch repeat-containing protein	At1g51540	-	2
10	phosphoribosylanthranilate isomerase 1	At1g29410	PAI3	2,4
11	putative heterogeneous nuclear ribonucleoprotein	At5g47620	-	2,2
12	putative RNA helicase	At2g35340	-	2,9
13	WRKY family transcription factor	At5g13080	WRKY75	2,3

(1) The annotation of the genes derived from TAIR, the Arabidopsis Information Resource (http://arabidopsis.org).

(2) Data derived from three independent experiments. Differentially expressed genes were filtered by the Welch's t-test ($p \leq 0.05$) and MTC.

Moreover, transcripts that exhibited higher expression in experiment IS12 compared to experiment S12 might also represent genes that were possibly involved in the induction of HR, which exclusively occurs in infected tissue treated with sylA. Among genes whose transcript levels were altered more than 2-fold by sylA in infected plants (IS12), eighteen genes exhibited higher expression in experiment IS12 compared to the expression of corresponding genes in experiment S12. Significance of difference between t/c ratios of these 18 genes in experiments IS12 and S12 was judged by Student's t-test statistics (p-value ≤ 0.05). This revealed only one gene encoding an expressed protein (At5g14730) whose t/c ratio in experiment IS12 was significantly higher as compared to the corresponding t/c ratio in experiment S12. A list of the 18 genes and the corresponding p-values is given in table 8.1 (Appendix B). Thus, very few genes were identified that were differentially regulated by sylA application on infected plants, which results in HR, as compared to sylA treatment of uninfected plants, which develop no visible symptoms. In addition, these few genes were induced only weakly.

4.1.2.2 Transcript accumulation following powdery mildew infection

The effect of infection alone on transcript abundance was calculated by comparing expression ratios derived from uninfected and infected plants that were both treated with a control solution. Plant material was collected 8-12 hat corresponding to 56-60 hours after infection (I60, Table 4.1).

The venn diagram in figure 4.8 A represents the overlap between genes which were more than 2-fold upregulated in infected (IS12) and uninfected (S12) plants treated with sylA, and genes exhibiting more than 2-fold elevated expression after fungal infection alone (I60). Of the 1045 (570 + 400 + 74 +1) genes which were more than 2-fold upregulated in infected plants (I60), 474 genes (400 + 74) were also induced more than 2-fold by sylA in uninfected tissue and 75 genes (74 + 1) were superinduced by sylA treatment of infected plants.

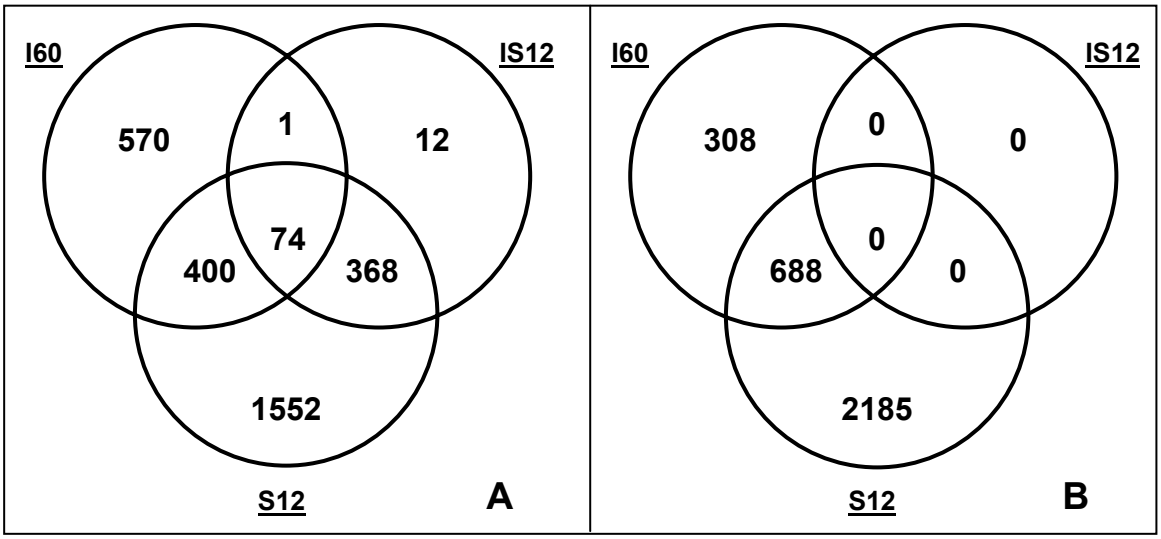

Figure 4.8 Overlap of sylA and powdery mildew-responsive gene expression

The venn diagram represents the distribution of significantly (p-value ≤ 0.05, MTC) upregulated (A) and downregulated (B) genes in experiments I60, IS12 and S12.

None of the genes upregulated by powdery mildew alone was repressed significantly by sylA in experiment IS12, but 60 of these genes were downregulated more than 2-fold by sylA in uninfected tissue in experiment S12 (data not shown in the venn diagram). A list of these genes and their corresponding t/c ratios is given in table 8.2 (Appendix C). Among others, these genes included transcripts involved in cellular transport processes (Table 8.2, rows #4ff) as well as transcripts encoding proteins involved in abiotic and biotic stress response, e.g. disease resistance proteins (Table 8.2, rows #17ff), a glucanase (Table 8.2, At3g57240, row #16), a protein involved in jasmonic acid biosynthesis (Table 8.2, At1g17990, row #21), and a member of the seven-transmembrane-MLO family (Table 8.2, At3g45290, row #25). Moreover, several genes present in the category ‘protein metabolism’ encoded proteins exhibiting kinase activity (Table 8.2, rows #32ff).

Figure 4.8 B represents a comparison of genes whose expression was more than 2-fold downregulated in experiments IS12, S12 and I60. Of the 996 (688 + 308) genes whose corresponding transcript levels were lowered by the fungus (I60), 688 were also downregulated by sylA in uninfected tissue. Among genes upregulated by sylA in infected tissue, the expression of three genes was lowered by fungal infection (not shown in venn diagram), as represented in table 4.4. These genes encoded a disease resistance family protein containing a leucine-rich repeat-domain (Table 4.4, At2g34930, row #1) that was exclusively present in experiment IS12, whereas a mitochondrial internal NAD(P)H dehydrogenase (Table 4.4, At1g07180, row #2) involved in electron transfer, and a MATE efflux protein (Table 4.4, At1g15180, row #3) exhibiting drug transporter activity, were similarly upregulated in uninfected tissue by sylA (S12). In addition, six genes whose transcription levels were repressed by the fungus were not included in experiment IS12. However, these genes were more than 2-fold upregulated in experiment S12 where syringolin was applied on uninfected plants. The corresponding t/c ratios of these genes are presented in table 4.4.

Table 4.4 Expression patterns of genes upregulated by sylA in infected and/or uninfected plants and downregulated by fungal infection alone

Row	Description	Locus[1]	Protein	t/c ratio[2,3]		
				I60	IS12	S12
1	disease resistance family protein (contains LRR-domain)	At2g34930		0,3	2,9	-
2	internal NAD(P)H dehydrogenase	At1g07180	NDA1	0,4	4,2	5,6
3	MATE efflux family protein	At1g15180		0,3	8,9	4,2
4	SEC14 cytosolic factor family protein	At1g30690		0,4	-	2,6
5	expressed protein	At4g33666		0,5	-	2,3
6	U3 ribonucleoprotein (Utp) family protein	At5g08600		0,4	-	2,9
7	elongation factor 1B alpha-subunit 1	At5g12110		0,3	-	2,1
8	expressed protein	At5g24570		0,4	-	3,8
9	PRT1 protein	At3g24800	PRT1	0,5	-	2

(1) The annotation of the genes derived from TAIR, the Arabidopsis Information Resource (http://arabidopsis.org).

(2) Data derived from three independent experiments. Differentially expressed genes were filtered by the Welch's t-test ($p \leq 0.05$) and MTC.

(3) Dashes designate genes that have not passed the Welch's t-test and MTC.

Surprisingly, sylA application on uninfected plants appeared to have a much higher impact on the transcriptome than application on infected plants: 2394 genes were activated more than 2-fold and of 2873 genes the transcript levels were lowered more than 2-fold by sylA treatment of uninfected plants, as compared to 455 activated and 0 repressed genes when sylA application occurred on infected plants (Table 4.2). Thus, in uninfected plants syringolin changed the expression of more genes than in infected plants. This result can be explained partly by the fact that the transcript level ratios of 368 genes activated more than 2-fold in both experiments IS12 and S12, but not in I60 (Figure 4.8 A), was almost always lower in experiment IS12 (sylA on infected plants) than in experiment S12 (sylA on uninfected plants). The average of IS12/S12 over these genes is $0,57 \pm 0,2$, significantly different from 1 (p-value < 0.001; one sample t-test). For only 22 genes is this ratio larger than 1.

There is no indication that this is generally caused by a small induction of these genes by the fungus alone and thus would represent an artefact caused by the chosen cut-off value of 2, because the average of IS12 x I60/S12 over these 368 genes is 0,68 ± 0,3, significantly different from 1 (p-value < 0.001). The corresponding value over all 1920 (1552 + 368) genes activated by sylA alone (S12) but not the fungus alone (I60) is 0,69 ± 0,2 (p-value < 0.001). In contrast, this value over the 75 genes that were activated in experiments IS12 and I60 is 1,08 ± 0,6, which is not significantly different from 1 (p-value > 0.5). Similar relations hold true for genes with t/c ratios ≤ 0,5.

In conclusion, it appears that in infected plants, sylA indeed changed the activity of fewer genes to a lesser extent than in uninfected plants.

These results on the transcriptional changes obtained in infected sylA-treated plants do not allow any conclusion on a hypothesised HR specific regulation of certain genes.

4.1.2.3 Characteristics of transcriptome changes exerted by syringolin application

As described above, the ability of syringolin to selectively induce HR on *E. cichoracearum*-infected plants was found not to be correlated with transcriptional upregulation of putative HR-related genes. However, plants were found to strongly respond to sylA treatment by altering transcription of genes covering a broad range of biological functions. These transcripts were grouped according to biological function GO (Gene Ontology) terms (http://www.arabidopsis.org/tools/bulk/go/). The distributions of biological function GO terms for genes exhibiting t/c ratios altered more than 2-fold upon sylA treatment of infected and uninfected tissue are illustrated in pie diagrams (Figure 4.9).

As evident from figure 4.9, in powdery mildew-infected plants (Figure 4.9 A) the distribution of sylA-induced genes with regard to functional categories was similar to the one found for genes whose expression was induced by sylA treatment of uninfected plants (Figure 4.9 B), although, the number of genes was larger. In uninfected plants the distribution of upregulated genes (Figure 4.9 B) was also similar to the one of downregulated genes (Figure 4.9 C). Unexpectedly, more genes were downregulated than upregulated as previously illustrated in terms of numbers in table 4.2.

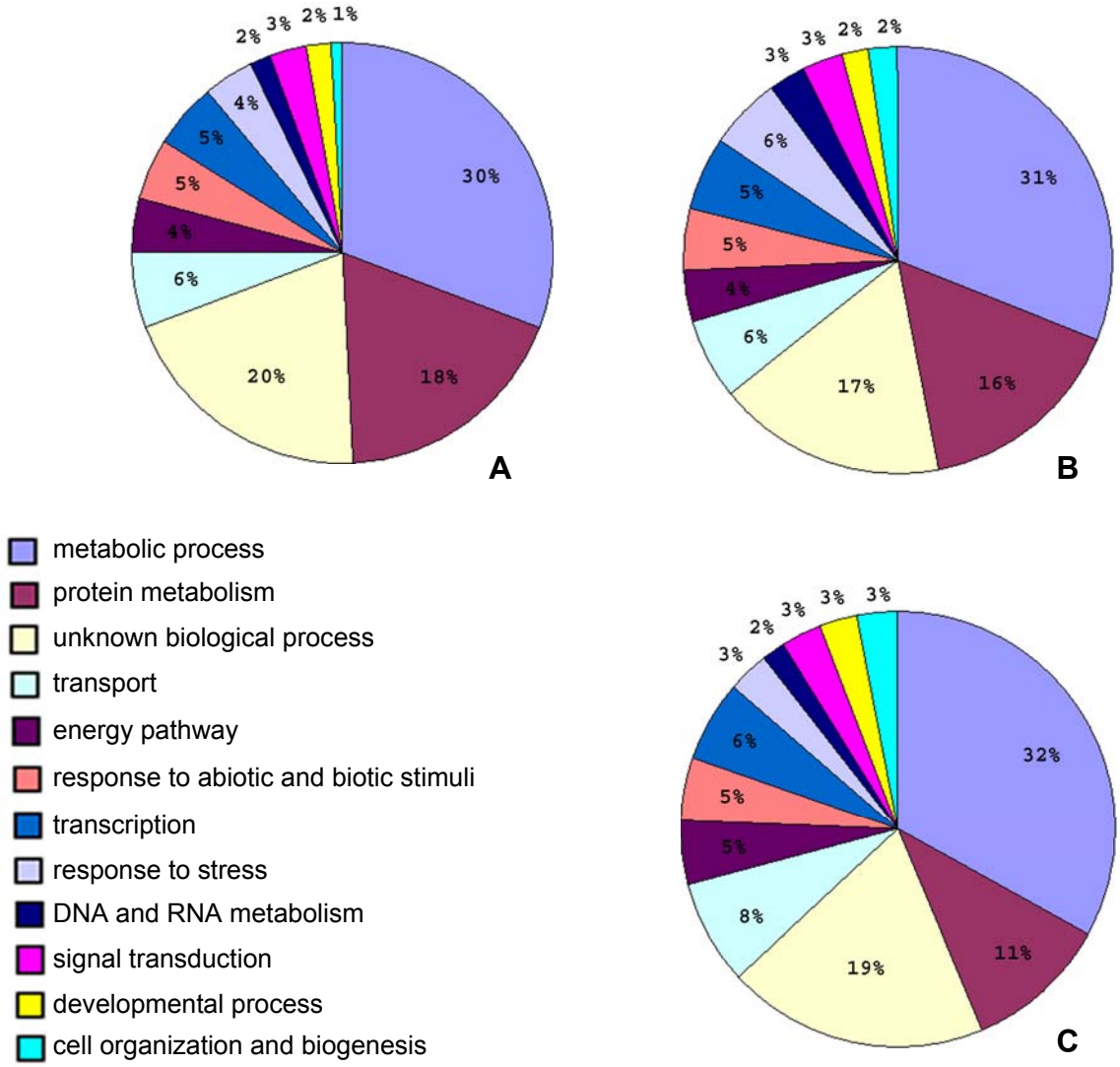

Figure 4.9 Pie-graph illustrating proportions of functional groups involved in the syringolin A response in infected and uninfected tissue

Classification of sylA-responsive genes exhibiting t/c ratios greater than two in infected (A) and uninfected plants (B) and smaller than 0,5 in uninfected tissue (C) 8-12 hat according to biological function GO terms. The corresponding web page can be retrieved by entering the locus identifier on the TAIR web page (http://www.arabidopsis.org/tools/bulk/go/). It should be noted that one gene can have more than one annotated function.

Since syringolin exerted dramatic transcriptional changes when applied on uninfected tissue, the increased or decreased transcript levels where analysed in order to understand the effect of syringolin in uninfected Arabidopsis in general. As seen before, this set of genes included almost all transcripts that were also activated by sylA in infected plants.

In order to decrease the large number of genes significantly altered by sylA application on uninfected plants and for facility of inspection of the data, the cut-off for t/c ratios was set to 3 and 0,333, respectively. Transcripts that accumulated in infected and uninfected plants upon sylA treatment were categorised according to functional pathways as represented in the MAPMAN software (Thimm et al., 2004) and are listed in table 8.3 (Appendix D). In the following, prominent groups of genes are presented in separate tables and figures.

The highest proportion of genes belonged to the functional categories of metabolic processes (including genes involved in physiological, biological and cellular processes, according to TAIR function GO terms), protein metabolism, and to genes that were not linked to any biological process so far.

Figure 4.10 presents an overview of all genes encoding proteins involved in various metabolic processes whose expression was altered by syringolin. Concerning carbohydrate metabolism, syringolin reduced transcript levels of genes encoding enzymes involved in synthesis and degradation of starch (Table 8.3, rows #136ff, 152ff). Similarly, the synthesis of sucrose was inhibited (Table 8.3, rows #147ff) but three genes encoding enzymes involved in sucrose degradation exhibited elevated expression ratios (Table 8.3, rows #164ff). In addition, sylA generally lowered transcript abundances corresponding to enzymes functioning in secondary, lipid, amino acid, sulphate and nucleotide metabolism (Figure 4.10).

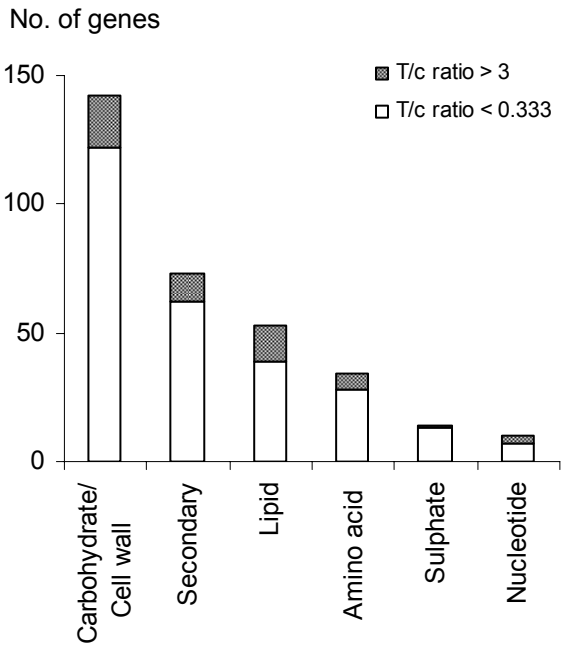

Figure 4.10 Alteration of transcript abundance of genes encoding metabolic proteins

Syringolin application on Arabidopsis alters the expression of genes encoding proteins involved in different metabolic processes (X-axis). The Y-axis represents the number of genes whose expression was enhanced (filled column elements) or lowered more than 3-fold (open column elements) in each category.

Among genes encoding proteins involved in cell wall metabolism the majority exhibited t/c ratios lower than 0,333 and predominantly encompassed genes encoding cell wall modifying and degrading proteins (Table 8.3, rows #59ff, 110ff), but also cell wall proteins and proteins related to the synthesis of the cell wall (Table 8.3, rows #1ff, 33ff, 44ff).

Genes encoding proteins with a function in plant primary metabolism included enzymes involved in glycolysis and the tricarboxylic acid cycle as well as proteins that are involved in fermentation. Corresponding expression values of these genes in infected (IS4, IS12) and uninfected plants (S12) treated with sylA are given in table 4.5.

Table 4.5 Differentially expressed genes of infected an uninfected plants treated with sylA involved in glycolysis, tricarboxylic acid cycle and fermentation

Row	Description	Locus[1]	t/c ratio		
			IS4[2]	IS12[3]	S12[3]
1	**Sucrose degradation**				
2	putative beta-fructofuranosidase	At1g22650	-	-	3,4
3	putative beta-fructofuranosidase	At1g35580	-	-	6,3
4	putative beta-fructofuranosidase	At4g09510	-	-	0,3
5	putative beta-fructosidase	At1g55120	-	-	0,2
6	beta-fructosidase	At1g12240	-	-	0,2
7	**Fructose phosphorylation**				
8	pfkB-type carbohydrate kinase family protein	At5g51830	-	2,5	8
9	**Glucose phosphorylation**				
10	putative phosphoglucomutase	At5g51820	-	-	0,3
11	putative phosphoglucomutase	At1g70820	-	-	0,1
12	**Glycolysis**				
13	phosphofructokinase family protein	At4g29220	-	-	0,3
14	putative pyrophosphate-fructose-6-P-1-phosphotransferase α subunit	At1g76550	-	3,7	7,6
15	putative pyrophosphate-fructose-6-P-1-phosphotransferase β subunit	At1g12000	-	-	4
16	putative pyrophosphate-fructose-6-P-1-phosphotransferase β subunit	At4g04040	-	-	0,2
17	putative fructose-bisphosphate aldolase	At2g36460	-	2,2	4,4
18	putative 2,3-biphosphoglycerate-independent phosphoglycerate mutase	At3g08590	-	2,9	4,6
19	putative pyruvate kinase	At5g56350	-	3,3	9,2
20	putative pyruvate kinase	At3g04050	-	-	4,3
21	**Tricarboxylic acid cycle**				
22	malate dehydrogenase	At5g43330	-	2,6	3,5
23	carbonic anhydrase family protein	At3g52720	-	-	0,1
24	**Fermentation**				
25	putative L-lactate dehydrogenase (LDH1)	At4g17260	-	4,1	9,6
26	putative pyruvate decarboxylase (PDC1)	At4g33070	24,8	241	656,6

(1) The annotation of the genes derived from TAIR, the Arabidopsis Information Resource (http://arabidopsis.org).

(2) Data derived from three independent experiments. Differentially expressed genes were filtered by the Welch's t-test ($p \leq 0.05$). Dashes designate genes that have not passed the Welch's t-test.

(3) Data derived from three independent experiments. Differentially expressed genes were filtered by the Welch's t-test ($p \leq 0.05$) and MTC. Dashes designate genes that have not passed the Welch's t-test and MTC.

These data revealed that more genes encoding glycolytic enzymes were upregulated by sylA than downregulated, suggesting that syringolin might lead to an induction of sucrose breakdown via glycolysis (Table 4.5, rows #13ff). However, the expression of only few genes encoding enzymes of the tricarboxylic acid cycle (Table 4.5, rows #22, 23) was altered by sylA. Enzymes with a function in cellular

fermentation encompassed a lactate dehydrogenase (Table 4.5, At4g17260, row #25) and a pyruvate decarboxylase (Table 4.5, At4g33070, row #26).

With regard to primary metabolism, it is striking that the expression of genes encoding proteins involved in photosynthetic activity were strongly inhibited upon sylA treatment (Table 8.3, rows #422ff). In contrast, genes encoding proteins functioning in mitochondrial processes were induced by syringolin (Table 4.6).

Table 4.6 Differentially expressed genes of infected an uninfected plants treated with sylA involved in mitochondrial electron flow

Row	Description	Protein	Locus[1]	t/c ratio		
				IS4[2]	IS12[3]	S12[3]
1	alternative oxidase 1a, mitochondrial	AOX1A	At3g22370	-	2,3	8,6
2	alternative oxidase 1b, mitochondrial	AOX1B	At3g22360	-	-	22,6
3	putative alternative oxidase	AOX1D	At1g32350	-	7,2	171
4	putative cytochrome c		At4g10040	-	2,6	4,3
5	cytochrome c biogenesis protein family		At1g49380	-	-	0,3
6	expressed protein		At5g12420	-	-	0,1
7	pyridine nucleotide-disulphide oxidoreductase family protein	NDA1	At2g20800	-	51	61,8
8	internal NAD(P)H dehydrogenase in mitochondria	NDB2	At1g07180	-	4,2	5,6

(1) The annotation of the genes derived from TAIR, the Arabidopsis Information Resource (http://arabidopsis.org).

(2) Data derived from three independent experiments. Differentially expressed genes were filtered by the Welch's t-test ($p \leq 0.05$). Dashes designate genes that have not passed the Welch's t-test.

(3) Data derived from three independent experiments. Differentially expressed genes were filtered by the Welch's t-test ($p \leq 0.05$) and MTC. Dashes designate genes that have not passed the Welch's t-test and MTC.

Among genes whose encoded proteins were related to the mitochondrial electron transport, several were upregulated upon sylA treatment, such as genes encoding an external and internal NAD(P)H dehydrogenase (Table 4.6, At2g20800, At1g07180, rows #7, 8). In addition, this also included genes encoding subunits of the alternative oxidase (Table 4.6, At3g22370, At3g22360, At1g32350, rows #1ff),

an enzyme providing a branching point that directs mitochondrial electron flow via an alternative pathway.

Moreover, we identified two genes encoding a stomatin-like protein and a putative prohibitin (Table 8.3, At5g54100, At3g27280, rows #546, 547). These proteins belong to the superfamily of PID (Proliferation, Ion, and Death) proteins also described as band 7 proteins identified in maize which have been associated with hypersensitive reactions involving cell death and pathogen resistance (Nadimpalli et al., 2000). Further genes encoding members of the PID gene family were classified to the category of protein metabolism (Table 8.3, rows #548ff).

A high number of genes encoding proteins involved in cellular degradation processes was found in the functional group of protein metabolism. Proteins related to this category were predominantly identified as subunits of the 26S proteasome core and lid particles including components of the ubiquitination multi-enzymatic system (Table 4.7). Many of the Arabidopsis subunits are encoded by at least a pair of paralogs. Amino acid sequence identity among the paralogs is high (>90%) suggesting that the family members are functionally redundant. The existence of these conserved paralogs in Arabidopsis may simply reflect the absolute requirement for expression of these gene products across a wide range of developmental states and environmental conditions.

Table 4.7 Differentially expressed genes of infected an uninfected plants treated with sylA encoding proteasome subunits

Row	Description	Protein	Locus[1]	t/c ratio		
				IS4[2]	IS12[3]	S12[3]
1	20S proteasome alpha subunit A2	PAA2	At2g05840	-	3,2	4,3
2	20S proteasome alpha subunit B	PAB1	At1g16470	-	4,7	8,5
3	20S proteasome alpha subunit C	PAC1	At3g22110	-	3,7	5,2
4	20S proteasome alpha subunit D	PAD1	At3g51260	-	2,7	5,5
5	20S proteasome alpha subunit D2	PAD2	At5g66140	-	5,3	14,1
6	20S proteasome alpha subunit E1	PAE1	At1g53850	2,1	4,3	8,2
7	20S proteasome alpha subunit E2	PAE2	At3g14290	-	4,1	8,8
8	20S proteasome alpha subunit F1	PAF1	At5g42790	-	3,3	7,8
9	20S proteasome apha subunit F2	PAF2	At1g47250	2	5	11,3
10	20S proteasome alpha subunit G	PAG1	At2g27020	-	2,8	5,3
11	20S proteasome beta subunit B	PBB1	At3g27430	-	2,6	4,7
12	20S proteasome beta subunit B	PBB2	At5g40580	2,5	5,1	12,5
13	20S proteasome beta subunit C1	PBC1	At1g21720	-	2,8	5,4
14	20S proteasome beta subunit C	PBC2	At1g77440	-	4,2	7,7
15	20S proteasome beta subunit D	PBD1	At3g22630	-	3,5	5,5
16	20S proteasome beta subunit D2	PBD2	At4g14800	-	3	6,2
17	20S proteasome beta subunit E1	PBE1	At1g13060	-	2,4	4,9
18	20S proteasome beta subunit F1	PBF1	At3g60820	-	2	3,5
19	20S proteasome beta subunit G1	PBG1	At1g56450	-	2,8	5
20	26S proteasome regulatory subunit S2	RPN1a	At2g20580	-	4,2	8,2
21	putative 26S proteasome regulatory subunit	RPN1b	At4g28470	-	2,6	5,1
22	putative 26S proteasome regulatory subunit	RPN2a	At2g32730	-	2,8	5,7
23	putative 26S proteasome regulatory subunit	RPN2b	At1g04810	-	4,7	8,8
24	putative 26S proteasome regulatory subunit S3	RPN3a	At1g20200	-	3,2	7,6
25	putative 26S proteasome regulatory subunit	RPN5a	At5g09900	-	3,2	6,8
26	putative 26S proteasome regulatory subunit	RPN5b	At5g64760	-	4,8	7,7
27	putative 26S proteasome regulatory subunit	RPN6	At1g29150	-	2,9	7,3
28	putative 26S proteasome regulatory subunit	RPN7	At4g24820	-	3,3	6,2
29	26S proteasome non-ATPase regulatory subunit 7	RPN8a	At5g05780	-	2,5	4,8
30	26S proteasome non-ATPase regulatory subunit 7	RPN8b	At3g11270	2,8	7,7	12,3
31	putative 26S proteasome regulatory subunit	RPN9a	At5g45620	-	-	3,2
32	26S proteasome regulatory subunit S5A	RPN10	At4g38630	-	2,2	5,3
33	putative 26S proteasome regulatory subunit	RPN11	At5g23540	-	4	9,3
34	putative 26S proteasome regulatory subunit	RPN12a	At1g64520	-	3,1	5,2
35	26S proteasome AAA-ATPase subunit	RPT1A	At1g53750	-	2,4	4,5
36	26S proteasome AAA-ATPase subunit	RPT2A	At4g29040	-	3,1	6,5
37	26S proteasome AAA-ATPase subunit	RPT3	At5g58290	-	3	7,1
38	26S proteasome AAA-ATPase subunit	RPT4A	At5g43010	-	2,5	6,4
39	26S proteasome AAA-ATPase subunit	RPT5A	At3g05530	-	2,4	5,4
40	putative 26S proteasome AAA-ATPase subunit	RPT6A	At5g20000	2,4	4,7	9,3

(1) The annotation of the genes derived from TAIR, the Arabidopsis Information Resource (http://arabidopsis.org).

(2) Data derived from three independent experiments. Differentially expressed genes were filtered by the Welch's t-test ($p \leq 0.05$). Dashes designate genes that have not passed the Welch's t-test.

(3) Data derived from three independent experiments. Differentially expressed genes were filtered by the Welch's t-test ($p \leq 0.05$) and MTC. Dashes designate genes that have not passed the Welch's t-test and MTC.

Representatives of all 20S core protease (CP) subunits and of all 19S regulatory particles (RP) were found among genes upregulated by sylA, several were represented by pairs. Transcripts that accumulated already 2-4 hat were identified among RP and CP subunits. All except subunit RPN 9a (Table 4.7, At5g45620, row #31) were transcriptionally induced in infected and uninfected plants treated with sylA, however expression values in uninfected plants were always higher.

The functional category of genes related to development encompassed subunits of the COP9 signalosome (CSN). Representatives of the eight subunits composing the CSN were upregulated more than 2-fold by sylA in uninfected plants and three subunits were also identified among genes upregulated in infected plants upon sylA treatment (Table 4.8, At5g14250, At5g42970, At5g56280). The CSN shares a strong similarity to subunits of the lid complex of the 26S proteasome and has been discussed as a specialised proteasome regulator (Schwechheimer and Deng, 2001). Differentially expressed genes encoding subunits of the CSN and the corresponding lid paralogs are given in table 4.8.

Table 4.8 Differentially expressed genes of infected an uninfected plants treated with sylA encoding members the COP9 signalosome

Description		Lid paralog	Protein	Locus[1]	t/c ratio[2]	
					IS12	S12
COP9 signalosome complex subunit 1	CSN1	RPN7	FUS6	At3g61140	-	4
putative COP9 complex subunit CSN2	CSN2	RPN6		At2g26990	-	3
COP9 signalosome complex subunit 3	CSN3	RPN3	COP13	At5g14250	2,5	4,1
COP9 signalosome complex subunit 4	CSN4	RPN5	COP8	At5g42970	2,2	4
c-JUN coactivator protein	CSN5a	RPN11	AJH1	At1g22920	-	2
COP9 signalosome subunit 6	CSN6a	RPN8	CSN6A	At5g56280	2,1	3,7
COP9 signalosome complex subunit 7	CSN7	RPN9	FUS5	At1g02090	-	5,6
putative COP9 signalosome subunit	CSN8	RPN12	COP9	At4g14110	-	4,4

(1) The annotation of the genes derived from TAIR, the Arabidopsis Information Resource (http://arabidopsis.org).

(2) Data derived from three independent experiments. Differentially expressed genes were filtered by the Welch's t-test ($p \leq 0.05$) and MTC. Dashes designate genes that have not passed the Welch's t-test and MTC.

Furthermore, several components of the SCF (Skp1/Cullin/F-box protein)-type E3 ligase complex were transcriptionally induced by sylA, such as ASK1 (Table 8.3, At2g25700, row #583), the Arabidopsis homolog of SKP1 (S-phase Kinase-associated Protein), and many F-box proteins (Table 8.3, rows #557ff). Further genes encoded members of the AAA (ATPases Associated with different Activities)-type ATPase family responsible for protein-unfolding or dissociation of protein-protein interactions (Table 8.3, rows #524ff).

In addition, we identified a high number of proteins with predicted kinase activity (according to molecular function GO terms), including receptor-like kinases (RLKs) with various extracellular domains (specified in squared brackets in table 8.3, rows #680ff.). Figure 4.11 illustrates sylA-dependent alteration of transcript abundances of genes encoding RLKs categorised into groups according to their extracellular domains.

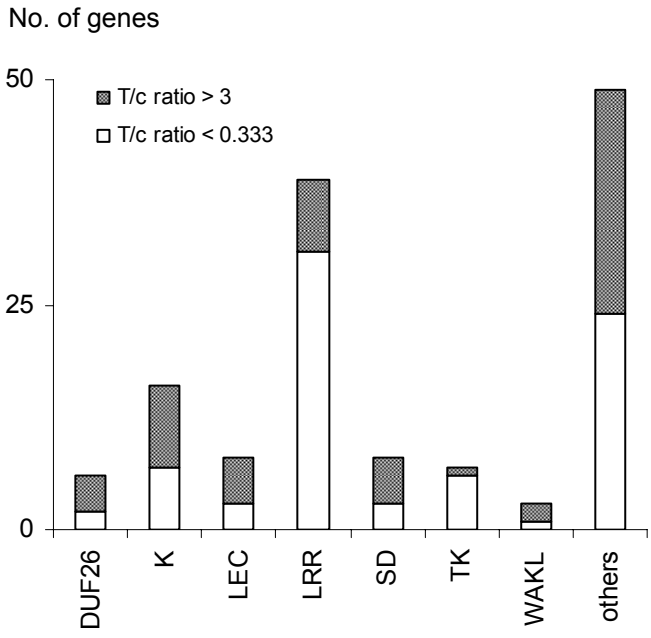

Figure 4.11 SylA-dependent alteration of transcript abundance of genes encoding receptor-like kinases

Syringolin application on Arabidopsis alters the expression of genes encoding RLKs. The X-axis represents groups of RLKs classified according to their extracellular domains. The Y-axis represents the number of genes whose expression was enhanced (filled column elements) or lowered more than 3-fold (open column elements). Abbreviations for the extracellular domains: DUF26, domain of unknown function 26; K, kinase; LEC, legume lectin; LRR, leucine-rich repeat; SD, S-locus glycoprotein-like domain; TK, transmembrane/kinase; WAKL, wall-associated kinase like.

Further proteins with a role in cellular regulative processes included GTP-binding proteins (Table 8.3, rows #844ff) and proteins involved in calcium signalling (Table 8.3, rows #863ff). Corresponding transcripts accumulated upon sylA treatment in infected and uninfected tissue.

Genes that were classified to the group of proteins responding to abiotic and biotic stimuli included many members of the heat shock protein (Hsp) family. An overview of all Hsps present in experiments IS4, IS12 and S12 is given in table 4.9. Of the five major families of Hsps present in infected plants treated with sylA, we identified members of the Hsp70 family together with their co-chaperones (e.g. DnaJ and GrpE), of the Hsp100 family, and several members of the family of small Hsps (Table 4.9). Six of the twelve Hsps present in experiment IS12 also exhibited elevated expression in experiment IS4 where plant material was collected 2-4 hat. All Hsps present in experiments IS4 and IS12 were also included in the set of 3-fold differentially expressed genes in uninfected plants treated with sylA (S12).

Several genes encoding members of the small Hsp family upregulated in experiments IS4 and IS12 were identified as cytosolic class-I (C-I) (Table 4.9, At3g46230, At1g59860, At2g29500, At1g53540, rows #13, 15ff) and class-II (C-II) small Hsps (Table 4.9, At5g12020, At5g12030, rows #14, 18). Two genes encoded mitochondrial (M) small Hsps (Table 4.9, At5g51440, At4g25200, rows #19, 20), both were already upregulated in infected tissue 2-4 hat and one of them (Table 4.9, At5g51440, row #19) exhibited highest expression values among all Hsp genes upregulated by sylA in infected and uninfected plants. Further mitochondrial Hsps transcriptionally induced by sylA included two members of the Hsp70 family (Table 4.9, At4g37910, At5g55200, rows #7, 8), and a chaperonin (Table 4.9, At3g23990, row #1) which belongs to the Hsp60 protein family.

Table 4.9 Differentially expressed genes of infected an uninfected plants treated with sylA encoding heat shock proteins

Row	Description[1]	Protein	Locus[2]	t/c ratio		
				IS4[3]	IS12[4]	S12[4]
1	chaperonin (M)	HSP60	At3g23990	-	-	3,1
2	chaperonin (P)		At1g26230	-	-	0,2
3	heat shock cognate 70 kDa protein 2 (C)	HSP70-2	At5g02490	-	2	13,3
4	heat shock cognate 70 kDa protein 3 (C)	HSC70-3	At3g09440	-	-	3
5	putative heat shock protein 70 (C)		At3g12580	5,8	22,6	71,3
6	putative heat shock protein 70		At1g79920	-	-	4
7	putative heat shock protein 70 (M)		At4g37910	-	-	3,9
8	putative co-chaperone grpE protein (M)		At5g55200	-	6,1	9,5
9	heat shock protein 81-1 (Er)	HSP81-1	At5g52640	2,5	9,5	52,1
10	heat shock protein 81-2	HSP81-2	At5g56030	-	-	3,1
11	heat shock protein 101	HSP101	At1g74310	4,7	4,6	15,1
12	putative heat shock protein 100 (M)		At2g25140	-	2,6	6,6
13	17.4 kDa class I heat shock protein (C-I)	HSP17.4	At3g46230	4,5	-	44,4
14	17.6 kDa class II heat shock protein (C-II)	HSP17.6	At5g12020	3,1	-	4,1
15	17.6 kDa class I heat shock protein (C-I)	HSP17.6A	At1g59860	6	36,8	111,2
16	17.6 kDa class I small heat shock protein (C-I)	HSP17.6BI	At2g29500	5,5	4,9	5,8
17	17.6 kDa class I small heat shock protein (C-I)	HSP17.6C	At1g53540	-	-	4,2
18	17.7 kDa class II heat shock protein 17.6A (C-II)	HSP17.7	At5g12030	11	-	28
19	23.5 kDa mitochondrial small heat shock protein (M)	HSP23.5	At5g51440	12	85,2	114,2
20	23.6 kDa mitochondrial small heat shock protein (M)	HSP23.6	At4g25200	8,3	-	26,6
21	26.5 kDa class P-related heat shock protein (P)		At4g21870	-	-	0,1
22	heat shock protein-related (P)		At5g57710	-	-	0,3
23	DNAJ heat shock N-terminal domain-containing protein		At1g71000	9,1	-	132,1
24	DNAJ heat shock family protein		At2g20560	2,6	-	10,5
25	DNAJ heat shock family protein		At4g28480	-	2,2	5,7
26	DNAJ heat shock N-terminal domain-containing protein		At2g35720	-	2,1	4,8
27	putative DNAJ heat shock protein	AtJ2	At5g22060	-	-	4,8
28	DNAJ heat shock N-terminal domain-containing protein		At5g37440	-	-	3,9
29	DNAJ heat shock N-terminal domain-containing protein (Nu)		At1g74250	-	-	3
30	DNAJ heat shock N-terminal domain-containing protein (P)		At5g03030	-	2,5	2,9
31	DNAJ heat shock N-terminal domain-containing protein (P)		At5g18140	-	-	0,3
32	DNAJ heat shock N-terminal domain-containing protein		At5g16650	-	-	0,3
33	DNAJ heat shock N-terminal domain-containing protein		At4g09350	-	-	0,2
34	DNAJ heat shock N-terminal domain-containing protein		At2g47440	-	-	0,1

(1) Intracellular localisation of the corresponding proteins are indicated in parenthesis: C, cytosol; I or II, class-I or II; M, mitochondrion; P, plastid; Nu, nucleus; Er, endoplasmatic reticulum.

(2) The annotation of the genes derived from TAIR, the Arabidopsis Information Resource (http://arabidopsis.org).

(3) Data derived from three independent experiments. Differentially expressed genes were filtered by the Welch's t-test ($p \leq 0.05$). Dashes designate genes that have not passed the Welch's t-test.

(4) Data derived from three independent experiments. Differentially expressed genes were filtered by the Welch's t-test ($p \leq 0.05$) and MTC. Dashes designate genes that have not passed the Welch's t-test and MTC.

One of the early induced Hsp genes (IS4) was *Hsp81-1* (Table 4.9, At5g52640, row #9), one of the six members belonging to the Arabidopsis Hsp90 family (80-90 kDa). Proteins of the Arabidopsis Hsp90 family exhibit significant similarities to Hsp90 proteins from other organism for which an active role in signal transduction has been reported (Picard et al., 1990). Whether the function of Hsp90 proteins in Arabidopsis is analogous to that of Hsp90 proteins in other systems remains to be determined. Interestingly, three genes encoding Hsps localised in plastids (P) were downregulated by syringolin in uninfected plants (Table 4.9, At1g26230, At4g21870, At5g57710, rows #2, 21, 22).

The number of genes encoding transcription factors (TFs) differentially expressed considerably increased in uninfected plants compared to infected plants treated with sylA (Table 8.3, rows #1243ff). As evident from figure 4.12, transcripts of genes encoding members of the NAM (No Apical Meristem), WRKY, and heat shock transcription factor (Hsf) families strongly accumulated upon sylA treatment.

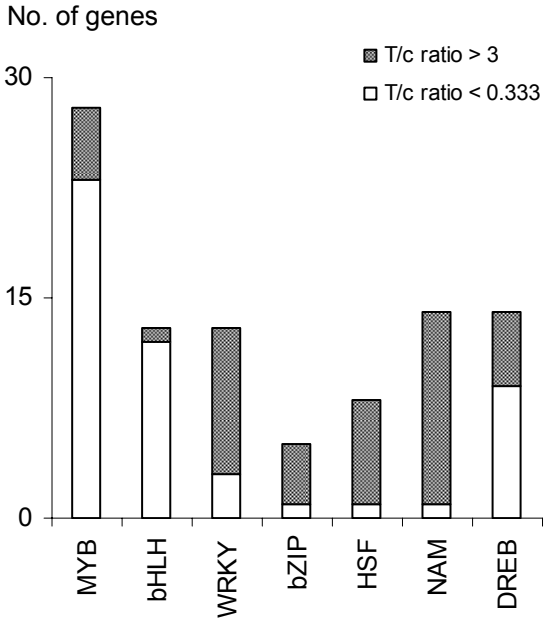

Figure 4.12 SylA-dependent alteration of transcript abundance of genes encoding transcription factors

Syringolin application on Arabidopsis alters the expression of genes encoding members of different transcription factor families (X-axis). The Y-axis represents the number of genes whose expression was enhanced (filled column elements) or lowered more than 3-fold (open column elements) in each category. Abbreviations: bHLH, basic helix loop helix; bZIP, basic leucine zipper; HSF, heat shock factor; NAM, no apical meristem; DREB, drought responsive element binding factor.

Table 4.10 gives an overview of transcription factor families encompassing predominantly members that were transcriptionally induced by syringolin. These included members of the DREB (Drought Responsive Element Binding) TF family that specifically bind to promoter elements of stress responsive genes. Transcript levels of genes encoding members of the subfamily A-2 of DREB TFs were enhanced by sylA and the expression of one of them (Table 4.10, At2g38340, row #1) was strongly upregulated in infected and uninfected plants as reflected by corresponding t/c ratios (67,0 (IS12) and 530,6 (S12), respectively). In contrast, the majority of genes encoding members of the subfamilies A-4, A-5, and A-6 was downregulated by sylA in uninfected plants (Table 4.10, rows #6ff).

The NAM proteins have been implicated in a variety of processes in plant development, including the maintenance of the shoot apical meristem and the formation of lateral roots (Xie et al., 2000). Members of the NAM protein family were transcriptionally upregulated by syringolin, and the gene encoding ANAC094 (Table 4.10, At5g39820, row #26) exhibited high induction values in infected and uninfected plants.

In addition, syringolin predominantly induced the expression of genes belonging to the heat shock transcription factor (Hsf) class A whose members are primarily responsible for stress-inducible activation of heat shock genes (Czarnecka-Verner et al., 2000). The gene encoding HSFA2 (Table 4.10, At2g26150, row #31) was upregulated in infected tissue 2-4 hat (IS4) and exhibited higher expression in experiment S12, where uninfected plant material was collected at the late timepoint of 8-12 hat. Among further Hsfs, the expression of only one gene, encoding HSFC1 (Table 4.10, At3g24520, row #37), was repressed by sylA. Interestingly, HSFC1 proteins compose a new class of Hsfs that is clearly separated from all others Hsfs by sequence details and by the characteristics of the HR-A/B region (Nover et al., 2001).

Finally, WRKY proteins have been shown to be strongly involved in the alteration of gene expression in response to microbial pathogens and pathogen elicitors (Asai et al., 2002; Chen and Chen, 2002; Eulgem et al., 1999). Interestingly, WRKY6, transcriptionally induced by sylA (Table 4.10, At1g62300, row #38), was found to play a role during plant senescence (Robatzek and Somssich, 2002) and was upregulated upon treatment with bacterial flagellin (Navarro et al., 2004).

Table 4.10 Differentially expressed genes of infected an uninfected plants treated with sylA encoding members of transcription factor families

Row	Description	Protein	Locus[1]	t/c ratio		
				IS4[2]	IS12[3]	S12[3]
1	DREB subfamily A-2 of ERF		At2g38340	-	67	530,6
2	DREB subfamily A-2 of ERF		At2g40350	-	5,6	22,3
3	drought-responsive family protein		At1g02750	-	-	3,9
4	member of the DREB subfamily A-2 of ERF	DREB2A	At5g05410	2,5	-	9,6
5	member of the DREB subfamily A-2 of ERF	DREB2B	At3g11020	-	-	3,1
6	member of the DREB subfamily A-4 of ERF		At4g16750	-	-	0,3
7	member of the DREB subfamily A-4 of ERF		At1g01250	-	-	0,1
8	member of the DREB subfamily A-4 of ERF		At4g32800	-	-	0,1
9	member of the DREB subfamily A-4 of ERF	TINY2	At5g11590	-	-	0,2
10	member of the DREB subfamily A-5 of ERF		At3g50260	-	-	5,3
11	member of the DREB subfamily A-5 of ERF		At1g19210	-	-	0,3
12	member of the DREB subfamily A-5 of ERF		At1g74930	-	-	0,1
13	member of the DREB subfamily A-6 of ERF		At2g23340	-	-	0,1
14	member of the DREB subfamily A-6 of ERF		At1g64380	-	-	0,2
15	member of the DREB subfamily A-6 of ERF		At2g22200	-	-	0,3
16	no apical meristem (NAM) family protein	ANAC003	At1g02220	-	-	5
17	no apical meristem (NAM) family protein	ANAC013	At1g32870	-	3,1	5,5
18	no apical meristem (NAM) family protein	ANAC046	At3g04060	-	-	6,1
19	no apical meristem (NAM) family protein	ANAC051	At3g10490	-	2,7	11,6
20	no apical meristem (NAM) family protein	ANAC053	At3g10500	-	-	5,5
21	no apical meristem (NAM) family protein	ANAC062	At3g49530	-	-	3,1
22	no apical meristem (NAM) family protein	ANAC078	At5g04410	-	-	3,2
23	no apical meristem (NAM) family protein	ANAC082	At5g09330	-	2,6	6,2
24	no apical meristem (NAM) family protein	ANAC087	At5g18270	2	6,5	27,1
25	no apical meristem (NAM) family protein	ANAC090	At5g22380	-	-	5,7
26	no apical meristem (NAM) family protein	ANAC094	At5g39820	-	412,1	807,3
27	no apical meristem (NAM) family protein	ANAC100	At5g61430	-	2,9	6,3
28	no apical meristem (NAM) family protein	ANAC103	At5g64060	3,8	10,2	25,5
39	no apical meristem (NAM) family protein	ANAC34/35	At2g02450	-	-	0,2
30	heat shock factor protein 2	HSFA1E	At3g02990	-	-	5,7
31	heat shock transcription factor family protein	HSFA2	At2g26150	5,1	3,5	14,1
32	heat shock transcription factor family protein		At1g77570	-	-	5,7
33	heat shock transcription factor family protein	HSFA3	At5g03720	-	-	3,5
34	heat shock transcription factor 21	HSFA4A	At4g18880	-	-	5,8
35	putative heat shock factor protein	HSFA8	At1g67970	-	-	6,2
36	heat shock factor protein 7	HSFB2B	At4g11660	-	-	4,2
37	heat shock transcription factor family protein	HSFC1	At3g24520	-	-	0,3

Table 4.10 (continued)

Row	Description	Protein	Locus[1]	t/c ratio		
				IS4[2]	IS12[3]	S12[3]
38	WRKY family transcription factor	WRKY6	At1g62300	-	-	5,8
39	WRKY family transcription factor	WRKY15	At2g23320	-	-	3
40	WRKY family transcription factor	WRKY25	At2g30250	-	-	6,7
41	WRKY family transcription factor	WRKY30	At5g24110	-	-	129
42	WRKY family transcription factor	WRKY33	At2g38470	-	2,4	13,3
43	WRKY family transcription factor	WRKY46	At2g46400	-	-	5,4
44	WRKY family transcription factor	WRKY47	At4g01720	-	-	0,3
45	WRKY family transcription factor	WRKY54	At2g40750	-	-	3,2
46	WRKY family transcription factor	WRKY55	At2g40740	-	-	3,2
47	WRKY family transcription factor	WRKY59	At2g21900	-	-	15,9
49	WRKY family transcription factor	WRKY60	At2g25000	-	-	0,2
50	WRKY family transcription factor	WRKY75	At5g13080	-	2,3	-

(1) The annotation of the genes derived from TAIR, the Arabidopsis Information Resource (http://arabidopsis.org).

(2) Data derived from three independent experiments. Differentially expressed genes were filtered by the Welch's t-test ($p \leq 0.05$). Dashes designate genes that have not passed the Welch's t-test.

(3) Data derived from three independent experiments. Differentially expressed genes were filtered by the Welch's t-test ($p \leq 0.05$) and MTC. Dashes designate genes that have not passed the Welch's t-test and MTC.

A further group of genes involved in transcriptional processes was represented by the histone family genes, whose expression was downregulated more than 3-fold by sylA in uninfected plants (Table 8.3, rows #1412ff). Histones have structural roles in the formation of protein cores around which DNA is folded. Chromosome duplication during S phase of the eukaryotic cell cycle requires both replication of genomic DNA and the synthesis of histones, which are assembled with the newly synthesised DNA into chromatin fibers. In addition, syringolin application on uninfected plants enhanced the expression of the *Cdc48* gene (Table 8.3, At3g09840, row #1222) and its homologs. This indicates that syringolin directly or indirectly influences cell cycle progression or cell division.

Several transcripts encoding proteins involved in transport processes were downregulated by sylA application on uninfected plants. This concerned cellular transport of amino acids, lipids, peptides and sugars (Figure 4.13).

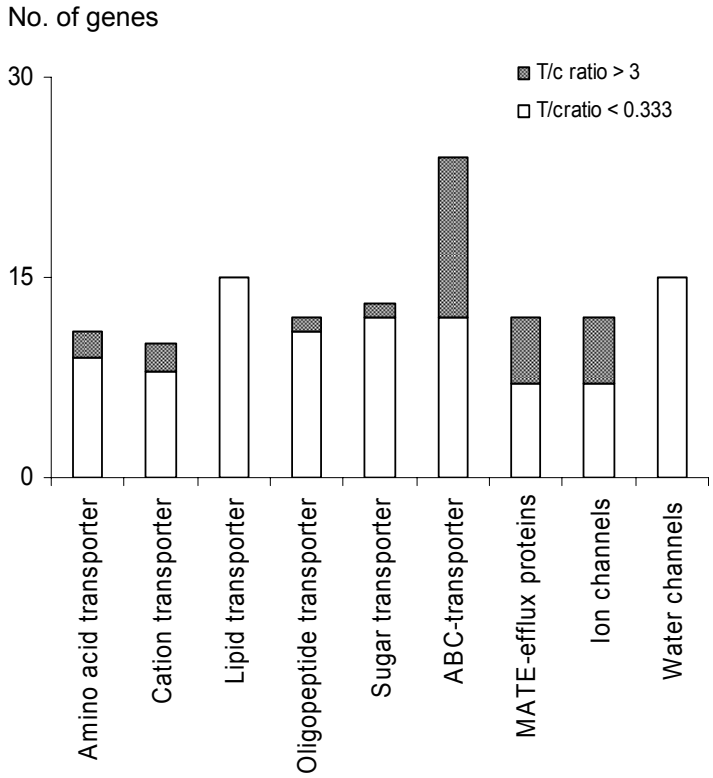

Figure 4.13 Influence of syringolin on cellular transport processes

Syringolin application on Arabidopsis alters the expression of genes encoding proteins involved in different cellular transport processes (X-axis). The Y-axis represents the number of genes whose expression was enhanced (filled column elements) or lowered more than 3-fold (open column elements) in each category.

Genes encoding ABC (ATP-Binding Cassette)-transporters and MATE (Multidrug And Toxic compound Extrusion) efflux proteins, involved in cellular detoxification, were induced by syringolin. A similar number of genes belonging to these protein families was downregulated by syringolin in uninfected plants.

Cyclic nucleotide-gated channels (CNGCs) are activated by cyclic nucleotides and exhibit permeability to monovalent and divalent cations. Genes encoding CNGCs were present among genes upregulated as well as downregulated by sylA.

A high number of genes encoding major intrinsic proteins (MIPs), membrane channels involved in water transport, uncharged solutes, gases and micro-nutrients (Tyerman et al., 2002) was downregulated by sylA. An inhibition of genes encoding

MIPs has been shown in plants during water deficiency (Aharon et al., 2003) and has been reported as a consequence of a drop in cytosolic pH associated with low-oxygen stress (Liu et al., 2005).

In addition, syringolin enhanced transcript abundance of proteins directing transport between different cellular compartments, such as nuclear importin alpha-1 and alpha-2 (Table 8.3, At3g06720, At4g02150, rows #1683, 1684) which mediate nuclear transport, as well as TIM17-1 and TOM20-4 (Table 8.3, At1g20350, At5g40930, rows #1660, 1661), mitochondrial translocases in the inner and outer membrane.

Abundance of transcripts corresponding to genes involved in cellular vesicle trafficking was elevated (Table 8.3, rows #1764ff). This included membrane associated family proteins known as SNAREs which play a role in membrane fusion and are central to the process of secretory vesicle targeting (Bock et al., 2001). The formation of a tight complex between two target SNAREs, syntaxin and a SNAP25-like protein, and one or more vesicular SNAREs is necessary to drive membrane fusion.

Remarkable changes in transcript abundance were also found for auxin-responsive genes. The majority of these genes had lowered expression values after sylA treatment (Table 8.3, rows #904ff). Similarly, the expression of genes encoding proteins involved in gibberellin, cytokinin, brassinosteroid and jasmonate signalling was repressed by sylA (Figure 4.14). For example, genes encoding lipoxygenase 2 and 3 (Table 8.3, At3g45140, At1g17420, rows #985, 986) involved in jasmonate biosynthesis were less expressed, whereas transcript abundance of the lipoxygenase 1 gene (Table 8.3, At1g55020, row #981) was enhanced by sylA. A considerable number of genes involved in ethylene and absciscic acid-signalling was also induced by sylA (Figure 4.14).

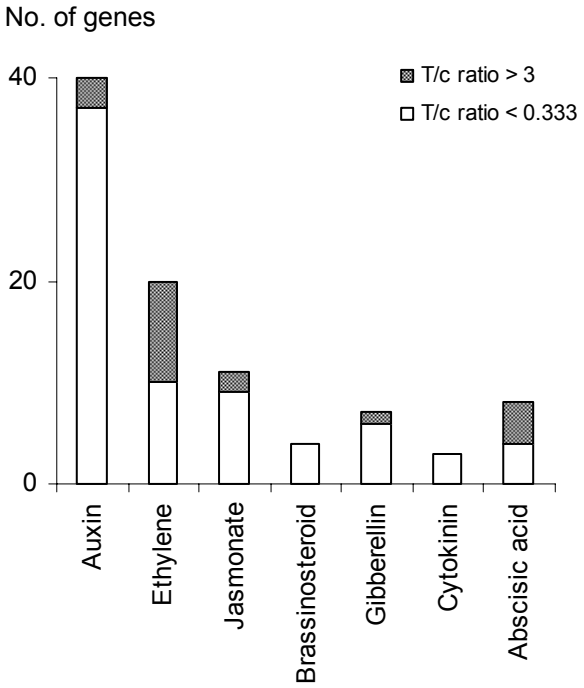

Figure 4.14 SylA-dependent alteration of transcript abundance of genes encoding proteins involved in plant hormone physiology

Syringolin application on Arabidopsis alters the expression of genes encoding proteins related to hormone signalling. The X-axis represents different groups of plant hormones. The Y-axis represents the number of genes whose expression was enhanced (filled column elements) or lowered more than 3-fold (open column elements) in each category.

Syringolin application on uninfected plants enhanced transcript abundance of genes encoding proteins responding to biotic stimuli. This included PAD3 and PAD4 (Table 8.3, rows #1116, 1142), both involved in phytoalexin biosynthesis, together with CPR5, EDS5 and RAR1/PBS1 (Table 8.3, rows #1115, 1131, 1145), which are components of distinct R-gene mediated pathways. Some of them are also required for the expression of basal defences against several virulent pathogen strains. The product of *Yls9/Nhl10* (Table 8.3, At2g35980, row #1138), a homolog of the tobacco *Hin1* gene, belongs to the harpin-induced protein family and was activated 71-fold upon sylA treatment. Interestingly, transcripts of the *Hin1* gene specifically accumulated when host plants were inoculated with avirulent bacterial strains but not after infection with virulent strains (Varet et al., 2003; Zheng et al., 2004), indicating HR-related expression.

However, syringolin was also found to exert repressive effects on disease resistance genes as reflected by downregulation of several of these genes (Table 8.3, rows #1151ff), genes involved in the synthesis of flavonoid and isoflavonoid secondary metabolites (Table 8.3, rows #336ff), and several pathogenesis-related (PR) proteins (Table 8.3, rows #1162ff).

Prominent groups of genes that were not classified to a distinct category according to biological function GO terms are presented in figure 4.15. As shown there, transcripts corresponding to all representatives of the oxidase, glucosidase and GDSL-lipase families and the majority of the glucanases and UDP-glycosyltransferases were lowered in abundance. Transcripts encoding members of the glutathione-S-transferase family increased and decreased by approximately equal numbers after syringolin treatment.

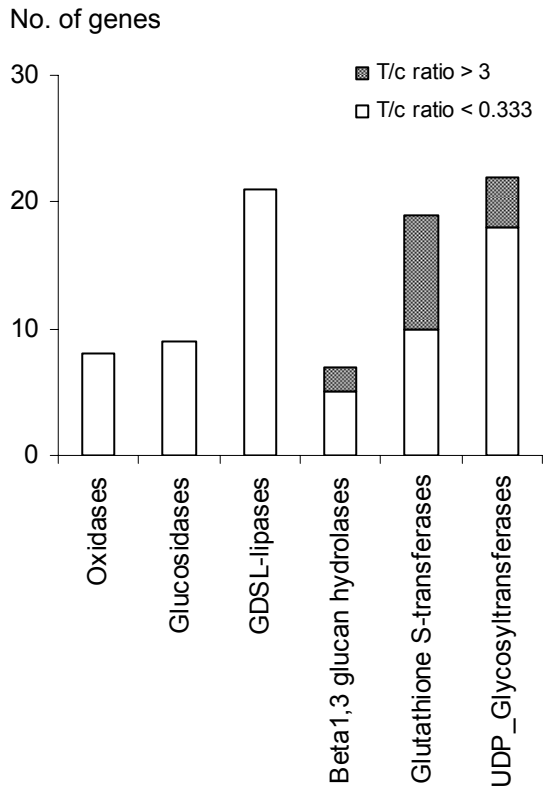

Figure 4.15 Influence of syringolin on enzyme activity

Syringolin application on Arabidopsis alters the expression of genes encoding members of different enzyme families (X-axis). The Y-axis represents the number of genes whose expression was enhanced (filled column elements) or lowered more than 3-fold (open column elements) in each category.

With the aim to gain insight in expression changes in plants very early upon syringolin treatment we analysed alteration in transcript abundance one hour after syringolin application (S1). This revealed that the abundance of the majority of transcripts was reduced by sylA. This repressive effect of sylA was similarly observed at the later timepoints (S12) where the expression of more genes was downregulated by sylA.

As is obvious from table 4.11 which represents all genes more than 2-fold differentially expressed in experiment S1, the gene exhibiting highest induction values encoded the PR-1 (pathogenesis-related) protein (Table 4.11, At2g14610, row #38). Remarkably, the expression of genes encoding pathogenesis-related proteins was repressed by sylA at later timepoints (Table 8.3, rows #1162ff).

In summary, syringolin application on uninfected tissue lead to a change in transcript levels suggesting an inhibition of various metabolic processes, including primary metabolic pathways such as photosynthetic activities. In contrast, cellular processes related to the mitochondrion appear to be induced by syringolin, as reflected by often strong transcriptional induction of several mitochondrial proteins. In fact, activities related to detoxification and drought stress tolerance appeared also to be induced indicated by enhanced transcript abundance of corresponding genes. The expression of genes related to signal transduction was enhanced as represented by elevated transcript abundance of genes encoding members of the WRKY TF family and proteins involved in calcium signalling. In contrast, syringolin was found to have inhibitory effects on the expression of a high number of defence-related genes and genes encoding receptor-like kinases.

Table 4.11 T/c ratios of genes more than 2-fold differentially expressed in experiment S1

Row	Description	Locus[1]	Protein	t/c ratio[2]	
				S1	S12
	METABOLISM				
1	speckle-type POZ protein-related	At3g48360		2,2	0,1
2	methyladenine glycosylase family protein	At5g44680		0,5	0,2
3	multi-copper oxidase type I family protein	At4g38420		0,5	-
4	**Cell wall modification**				
5	xyloglucan:xyloglucosyl transferase	At5g57560		0,4	4,1
6	putative xyloglucan:xyloglucosyl transferase	At4g25810	XTR6	0,4	7,8
7	putative xyloglucan:xyloglucosyl transferase	At1g10550	XTH33	0,3	-
8	putative xyloglucan:xyloglucosyl transferase	At3g23730		0,4	-
9	putative xyloglucan endotransglycosylase/hydrolase	At4g30290		0,5	-
10	expansin family protein	At4g38400	EXLA2	0,3	-
11	**Cell wall degradation**				
12	glycoside hydrolase family 28 protein	At3g06770		0,4	0,1
13	**Secondary metabolism**				
14	transferase family protein	At5g61160		2,1	-
15	**Amino acid metabolism**				
16	putative glutamate decarboxylase	At2g02010		2,8	20,6
17	**CELLULAR REGULATION**				
18	**Protein metabolism**				
19	lectin protein kinase family protein	At4g02410		2	2,4
20	**Protein degradation**				
21	aspartyl protease family protein	At3g54400		0,4	-
22	aspartyl protease family protein	At4g16563		0,4	-
23	serine protease protein -related	At4g17100		0,5	0,4
24	subtilase family protein	At5g45650		0,5	0,2
25	**Signalling in sugar and nutrient physiologie**				
26	putative phosphate-responsive protein	At1g35140	PHI-1	0,1	-
27	putative phosphate-responsive protein	At4g08950		0,2	-
28	phosphate-responsive 1 family protein	At2g17230		0,4	0,2
29	**Calcium signalling**				
30	putative calcium-transporting ATPase, plasma membrane-	At3g63380		2,3	14,3
31	calmodulin-binding family protein	At4g23060		2,1	0,1
32	**TRANSCRIPTION**				
33	DREB subfamily A-5 of ERF/AP2 transcription factor family	At1g21910		0,3	-
34	DREB subfamily A-6 of ERF/AP2 transcription factor family	At1g64380		2,3	0,2
35	myb family transcription factor	At5g05790		0,5	-
36	zinc finger (AN1-like) family protein	At3g28210	PMZ	2,2	82,9
37	**RESPONSE TO ABIOTIC AND BIOTIC STIMULI**				
38	pathogenesis-related protein 1	At2g14610	PR1	6,4	-
39	glycosyl hydrolase family 17 protein	At3g57260		2,2	-
40	macrophage migration inhibitory factor family protein	At3g51660		2,1	4,2
41	germin-like protein	At5g20630	GLP3	0,4	-
42	MATE efflux protein-related	At5g52450		2,3	0,4
43	**DEVELOPMENT**				
44	no apical meristem (NAM) family protein	At5g63790		2,1	-
45	squamosa promoter-binding protein-like 2	At5g43270	SPL2	0,5	0,3

(1) The annotation of the genes derived from TAIR, the Arabidopsis Information Resource (http://arabidopsis.org).

(2) Data derived from three independent experiments. Differentially expressed genes were filtered by the Welch's t-test ($p \leq 0.05$) and MTC. Dashes designate genes that have not passed the Welch's t-test and MTC.

4.2 Functional characterisation of syringolin-responsive genes

Gene disruption by T-DNA insertion is a powerful tool for obtaining knock-out mutants that help in ascertaining biological function of uncharacterised open reading frames.

With the aim to identify genes responsible for sylA-mediated resistance against powdery mildew, we investigated knock-out mutants harbouring T-DNA insertions in genes activated by syringolin. Candidate genes were chosen among transcripts that accumulated early upon sylA treatment and were present in experiment IS4, and genes that exhibited strong induction values in experiment S12 (Table 4.12).

Table 4.12 T-DNA insertion lines for selected genes

Row	Description	T-DNA line	Insertion	Locus[1]	t/c ratio	
					IS4[2]	S12[3]
1	ABC transporter family protein	SALK 120950	Exon	At3g13100	-	35,7
2	PHD finger transcription factor	SALK 041367	Exon	At5g58610	-	13,02
3	ankyrin repeat family protein	SALK 005507	5' UTR	At2g03430	2,4	12,3
4	expressed protein	SALK 123169	Exon	At5g64230	3,7	7,6
5	GCN5-related N-acetyltransferase family protein	SALK 057603	Exon	At1g32020	2,9	9,3
6	leucine-rich repeat family protein	SALK 051751	5' UTR	At1g03440	2,2	5,3
7	member of the DREB subfamily A-2 of ERF	SALK 144950	5' UTR	At2g38340	-	530,6
8	member of the ERFsubfamily B-5 of ERF	SALK 023227[4]	5' UTR	At1g22985	2,2	8,2
9	no apical meristem family protein	GABI 027D08	Exon	At5g39820	-	807,3
10	putative pyruvate decarboxylase 1	SALK 018840	Exon	At4g33070	24,8	656,6
11	putative stress-inducible protein	SALK 000794	Exon	At4g12400	4,7	43,2
12	zinc finger family protein	SALK 021881	Exon	At3g28210	4,6	82,9
13	zinc finger family protein	SALK 143574[4]	Exon	At5g20910	3,0	31,3

(1) The annotation of the genes derived from TAIR, the Arabidopsis Information Resource (http://arabidopsis.org).

(2) T/c ratios of genes that have passed Welch's t-test ($p \leq 0.05$). Dashes designate genes that have not passed Welch's t-test ($p \leq 0.05$).

(3) T/c ratios of genes that have passed Welch's t-test ($p \leq 0.05$) and MTC.

(4) No homozygous plants obtained.

Emphasis was given to proteins that have a function in regulative processes such as transcription factors (Table 4.12, rows #7, 8, 9, 12, 13) and proteins related to cellular signal transduction (Table 4.12, row #6). No homozygous T-DNA insertions were detected for salk_023227 and salk_143574, suggesting that homozygous insertions are lethal.

The isolation and verification of homozygous insertion mutants was performed by PCR. Gene-specific PCR primers flanking the insertion were used in combination with a primer corresponding to the T-DNA left border (primer sequences are given in section Materials and Methods, chapter 6.9.1). PCR amplification using wild type DNA should yield a fragment only with the gene-specific forward (Gf) and reverse (Gr) primers, whilst amplification of a smaller fragment using the respective gene specific primer and the T-DNA left border primer (LBa1 or LBb1) indicates a T-DNA insertion. Following PCR amplification, DNA extracted from plants heterozygous for the insertion should yield a product with either set of primers, whereas DNA from plants homozygous for the insertion would only yield a product with the LBa1/LBb1 and one of the Gf/r primers. A representative example showing the identification of heterozygous and homozygous insertion lines is shown in figure 4.16.

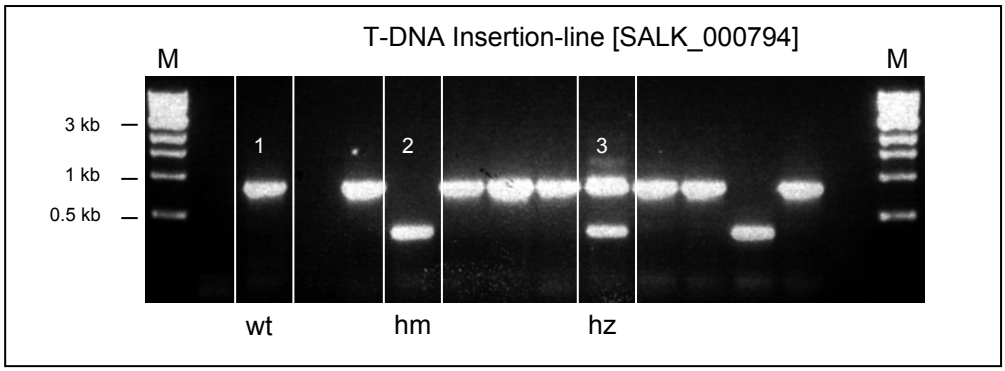

Figure 4.16 Identification of knock-out mutants homozygous for the T-DNA insertion

T-DNA insertion lines were analysed for homozygous insertions by using gene-specific primers (Gr/f). 1: PCR with wild-type DNA (wt - no insertion) should result in a product of 881 bps (from Gf to Gr). 2: DNA from homozygous plants (hm - insertions in both chromosomes) will result in a band of 358 bps (e.g. salk_000794). 3: Heterozygous plants (hz) exhibit both bands. PCR aliquots were analysed on 1,5% agarose gels. M: marker.

Mutant lines successfully reconfirmed for homozygous T-DNA insertions were propagated and analysed for sylA-insensitivity. The assay was based on the microscopic evaluation described in chapter 4.1.2.1. Accordingly, 14-day-old seedlings were infected with powdery mildew and sprayed with a 20 µM syringolin solution 48 hours after infection. To decrease the occurrence of sporadic sporulation which directly correlates with inoculation density, leaves were lightly infected by brushing down spores from highly infected Arabidopsis plants (see section Materials and Methods, chapter 6.3.2). Leaf material was collected for microscopic evaluation 72 hat, at which point first conidiophores started to develop on control-treated leaves (Figure 4.3 C), but no sporulation occurred on sylA-treated wild-type leaves (Figure 4.4 A). Evaluation of plant material at the timepoint when first conidiophores just started to develop increased the stringency of the assay.

Sporulation efficiencies were evaluated according to the scheme shown below in table 4.13:

Table 4.13 Scheme for evaluation of sporulation efficiency

Description	Phenotype
	Number of conidiophores/leaf
weak sporulation	0 - 3
intermediate sporulation	3 - 15
heavy sporulation[1]	> 15

(1) If heavy sporulation was confined to a distinct leaf area, the phenotype was evaluated as 'intermediate sporulation'.

On average, 28 leaves were analysed by bright field microscopy for each insertion line, together with an equal number of wild-type plants. In addition, four to six plants were infected and sprayed with a control solution to visualise proper fungal growth. Sporulation efficiencies were investigated for all T-DNA insertion lines and the results in terms of numbers are given in table 4.14.

Table 4.14 Effect of T-DNA insertion in respective sylA-inducible genes on the response of powdery mildew-infected plants towards syringolin

Experiment[1]	T-DNA line	Sporulation efficiency [%][2]		
		weak sporulation	intermediate sporulation	heavy sporulation
1	wild type	94	6	0
	salk_120950	100	0	0
	salk_018840	100	0	0
2	wild type	98	2	0
	salk_021881	94	4	2
3	wild type	98	2	0
	salk_051751	95	5	0
4	wild type	52	31	17
	gabi_027D08	63	27	10
	salk_144950	64	22	14
5	wild type	54	38	8
	salk_000794	100	0	0
	salk_123169	51	44	5
	salk_057603	95	5	0
	salk_005507	70	24	6
6	wild type	55	31	14
	salk_041367	57	36	7

(1) For each experiment an equal number of wild-type plants was analysed together with the T-DNA insertion lines.

(2) Sporulation efficiency was evaluated according to the scheme presented in table 4.13.

As obvious from table 4.14, all mutant lines exhibited similar responsiveness towards sylA treatment as wild-type plants. Thus, loss-of-function mutation of the 11 genes tested did not result in increased insensitivity towards syringolin. However, unexpectedly, one mutant line revealed an effect independent of syringolin. The respective mutant line (salk_000794), isolated for a T-DNA insertion in the At4g12400 gene (stress-induced protein/ sti1-like protein), showed impaired growth of the powdery mildew fungus on control and non-treated leaves. Macroscopically, we observed yellowed borders of infected salk_000794 leaves (Figure 4.17 A), which became never visible on infected wild-type leaves (Figure 4.17 B). By five days after inoculation, *E. cichoracearum* developed extensive hyphal growth that nearly covered the leaf surface on both salk_000794 and wild-type plants. By day seven, the number of conidiophores was severely reduced on salk_000794 leaves (Figure 4.17 C) whereas, *E. cichoracearum* developed abundant conidiophores on wild-type Columbia plants (Figure 4.17 D). Visible chlorosis in salk_000794 plants just began before the formation of numerous conidiophores macroscopically visible as white powder on wild-type plants six days after infection. The salk_000794 T-DNA insertion line developed only small scattered patches of powder. On uninfected salk_000794 plants, the occurrence of spontaneous lesions such as necrosis or chlorosis was not detectable. Growth and reproduction rate was comparable to wild-type plants (data not shown).

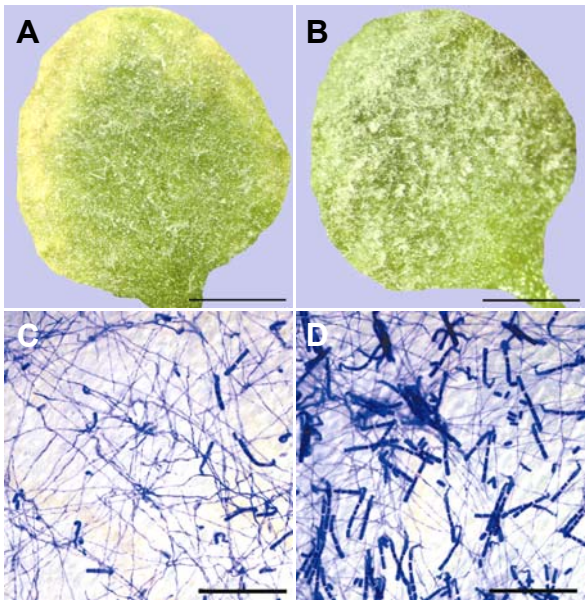

Figure 4.17 Development of powdery mildew on salk_000794 T-DNA insertion line

Salk_000794 mutant plants were infected with powdery mildew. Seven days after infection, symptoms such as chlorosis, starting at the leaf borders, became clearly visible (A) but were not detectable on infected wild-type leaves (B). For bright field microscopy leaves were destained by over-night incubation in lacto-phenol solution and fungal structures were stained with coomassie blue. Microscopic evaluations revealed that sporulation was impaired on salk_000794 mutant plants (C), whereas powdery mildew colonisation was successful on wild-type plants (D). Scale bars in A and B: 2 mm, scale bars in C and D: 100 µm.

Investigation of conidiophores that developed on salk_000794 revealed that sporogenesis was not only reduced but also distorted. The reduced ability to stain conidiophores with coomassie blue as compared to conidiophores from wild-type plants (Figure 4.18 A) indicated degradation of proteins and a starting collapse of conidiophores (Figure 4.18 B and C).

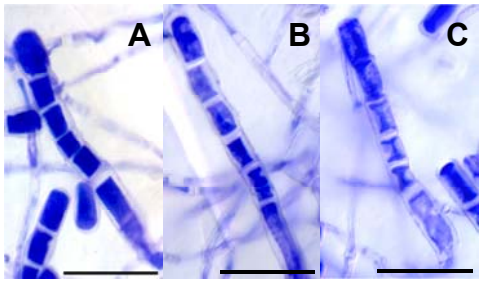

Figure 4.18 Degradation stages of conidiophores on leaves of salk_000794

Leaves of salk_000794 T-DNA insertion line were destained in lacto-phenol solution and were stained for fungal structures with coomassie blue seven days after infection. Intact conidiophores (A). Different stages of protein degradation in conidiophores on leaves of salk_000794 (B and C). Scale bar: 50 µm.

As expected for a line homozygous for a T-DNA insertion the phenotype was maintained in the offspring. The F1 progeny of a cross between the salk_000794 line and the wild type exhibited sporulation efficiencies similar to wild-type plants, indicating that the mutation was recessive.

Plants homozygous for the T-DNA insertion in the genomic sequence of At4g12400 were identified by PCR with T-DNA left border primer LBb1 and the respective gene-specific primers Gf or Gr. The PCR products were then purified and sequenced to precisely determine the location of the T-DNA insertion (Figure 4.19).

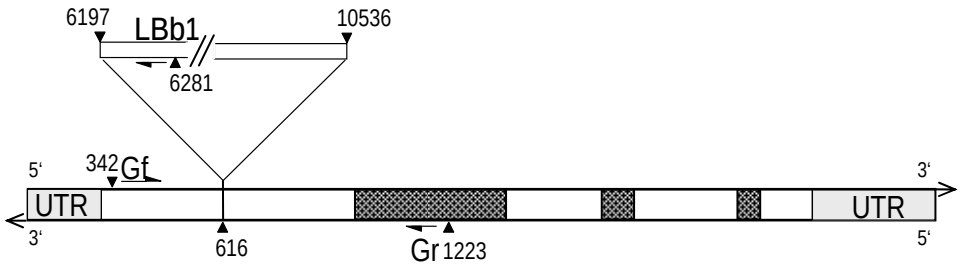

Figure 4.19 Diagram of At4g12400 gene sequence and the positions of T-DNA insertions

Coding regions (exons) are represented by white boxes, non-coding regions are shaded in dark grey (introns) and UTRs at 5' and 3' ends in light grey. Horizontal arrows indicate directions of transcription. Numbers specify positions in the sequence in terms of base pairs. The position of insertion is indicated above the gene diagram, depending on the direction of inserted T-DNA. The scheme is drawn to scale. LBb1: left border primer 1, Gf and Gr: gene specific forward and reverse primers.

As shown in figure 4.19, for insertion line salk_000794 the T-DNA was located within the first exon.

Consistent with gene chip data, semi-quantitative determination of mRNA expression in wild-type plants revealed that the gene (At4g12400) was induced weakly by control treatment but strongly by sylA treatment. As expected, no expression was found in sylA-treated salk_000794 T-DNA insertion lines (Figure 4.20).

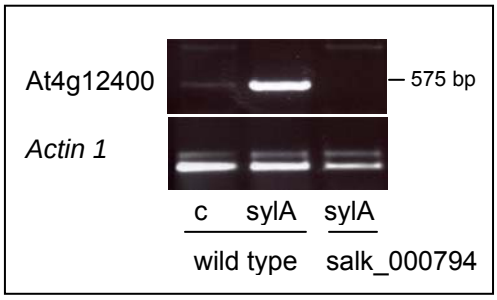

Figure 4.20 mRNA levels of At4g12400

At4g12400 transcript levels were determined by RT-PCR in wild-type (wt) plants and insertion line salk_000794. Plants were treated either with a control solution (c) or a 20 µM solution of sylA (sylA). The PCR product has an expected size of 376 bp. PCR aliquots were analysed on 1,5% agarose gels.

A second independent knock-out line (flag_013C07) with a T-DNA insertion in the genomic sequence of the At4g12400 gene was included in our studies. Preliminary results of plants homozygous for the T-DNA insertion in the At4g12400 genomic sequence revealed a phenotype similar to salk_000794, i.e. impaired sporulation of powdery mildew. This confirmed that loss-of-function of the At4g12400 gene negatively affects powdery mildew reproduction in Arabidopsis.

At present the function of the At4g12400 encoded protein in Arabidopsis is unknown. Homologous genes have been identified in soybean and rice. These genes carry tetratricopeptide repeats which so far are rarely present in plant derived gene sequences. The soybean gene encodes a protein with high identity to the yeast stress-inducible protein and its expression is inducible by heat (Hérnandez Torres et al., 1995). Therefore, it seems likely that the At4g12400 encoded protein may similarly exhibit a stress-related function in Arabidopsis.

4.3 Screening for mutants insensitive to syringolin

In a second approach for the identification of genes responsible for sylA-mediated resistance against powdery mildew a M2 population of 14-day-old EMS-mutagenised Arabidopsis seeds (ecotype Columbia) was screened for less or no impairment of fungal growth after syringolin application. The EMS-mutagenised seeds were purchased from Lehle Seeds (Round Rock, TX, USA). Sporulation efficiency after sylA treatment was tested for 25'250 EMS-plants corresponding to approximately 3000 M2 families. Potential mutants were self-pollinated and offspring (M3) were assayed in a second round of screening. The screening was carried out in cooperation with Dr. Roshani Shakya (a former post-doc in the group of Prof. Robert Dudler) and revealed one confirmed mutant. This mutant was referred to as syl_404.

In general, syl_404 plants were more sensitive to syringolin treatment as expressed by slight osmotic stress symptoms macroscopically visible by slight leaf-wilting shortly after treatment with syringolin. Nevertheless, plants were found to recover within minutes after the liquid had evaporated on the leave surface. On uninfected plants, wilting upon syringolin treatment was observed rarely. The wilting was stronger on plants which were infected prior to syringolin treatment. Recovery was dependent on infection density and on the amount of syringolin applied on the leaf surface. In rare cases, infected and sylA-treated plants were not able to recover and died.

To verify the mutant phenotype conferred by syl_404, 14-day-old seedlings in the M3 generation were infected with powdery mildew as described in chapter 6.3.2. Plants were sprayed with a 20 µM syringolin solution 48 hours after infection and leaf material was collected for microscopic evaluation five days post-inoculation.

Insensitivity of syl_404 plants to syringolin was expressed by the formation of a higher number of conidiophores upon syringolin treatment compared to the number of conidiophores developed on syringolin-treated wild-type plants. Three classes, reflecting the sporulation efficiency upon syringolin treatment, were formed based on the number of conidiophores developed on the plants according to the scheme presented in table 4.13. Figure 4.21 shows typical examples of the three classes: weak sporulation (Figure 4.21 A), intermediate (Figure 4.21 B) and heavy sporulation (Figure 4.21 C). Enlargements illustrate that on leaves exhibiting weak sporulation, the fungus was stopped in further growth (Figure 4.21 a) whereas on leaves classified as heavy sporulation the fungus was able to form conidiophores (Figure 4.21 d). Both phenomena, heavy and weak sporulation, may occur on leaves classified as intermediate (Figure 4.21 b and c).

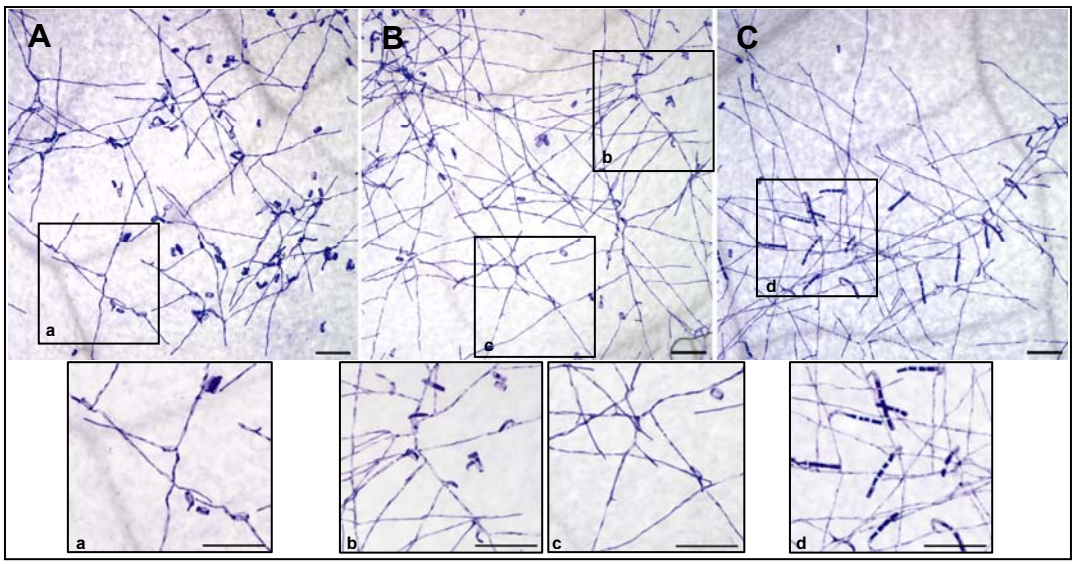

Figure 4.21 Characterisation of plant-pathogen interactions on mutant syl_404

Leaves of mutant syl_404 were infected with powdery mildew and treated with sylA 48 hours after infection. Seventy-two hours after treatment, plant material was destained by over-night incubation in lacto-phenol solution and fungal structures were stained with coomassie blue. Sporulation efficiency was determined according to the scheme presented in table 4.13. Examples of 'weak sporulation' (A), 'intermediate sporulation' (B) and 'heavy sporulation' (C) are illustrated. Representative parts in A-C are enlarged in a-d. Scale bar: 100 µm.

The results derived from two independent experiments are presented in figure 4.22 and corresponding values are given in table 8.4 (Appendix E). For each experiment, on average, 47 leaves of mutant syl_404 and the wild type were analysed microscopically. In addition, four to six wild-type plants were infected and sprayed with a control solution to visualise proper fungal growth.

As shown in figure 4.22, sporulation efficiency after sylA application was drastically enhanced on syl_404 as compared to wild-type plants.

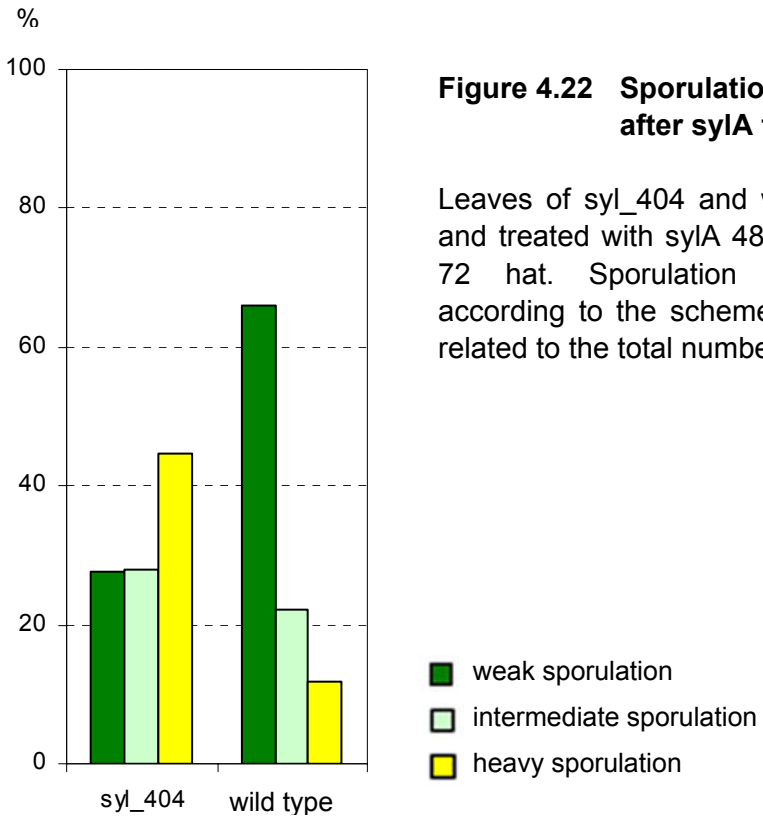

Figure 4.22 Sporulation efficiency on mutant_404 after sylA treatment

Leaves of syl_404 and wild-type plants were infected and treated with sylA 48 hai. Interactions were scored 72 hat. Sporulation efficiency was determined according to the scheme presented in table 4.13 and related to the total number of plants evaluated (100%).

With the aim to eliminate other, additional mutations caused by EMS-mutagenesis, syl_404 was backcrossed to a Columbia wild-type plant and F1 seeds were allowed to self-pollinate to produce F2 seeds. Following this, F2 plants were tested for syringolin-insensitivity. Investigation of 18 F2 plants revealed two plants

exhibiting fungal sporulation after sylA treatment. The segregation ratio of approximately 3:1 in those F2 plants that do not or do support fungal growth with sylA application indicated a recessive mutation (Table 4.15). This suggestion is supported by the finding that infected and sylA-treated F1 plants, which are heterozygous for the mutation, exhibited a wild-type phenotype and did not show increased sporulation efficiency (data not shown).

Table 4.15. Powdery mildew sporulation efficiency on backcross lines

Plants	Sporulation efficiency [number of plants][1]		
	weak sporulation	intermediate sporulation	heavy sporulation
wild type	12	1	0
syl_404 F2 population	14	2	**2**[2]

(1) Sporulation efficiency was evaluated according to the scheme presented in table 4.13.

(2) Plants chosen from F2 population exhibiting heavy sporulation after sylA treatment.

The F2 individuals exhibiting sporulation were referred to as syl_404_bc1 (bc=backcross) and syl_404_bc2. These putative sylA-insensitive mutant lines were infected and treated with sylA as described. The results obtained for syl_404_bc1 and syl_404_bc2 in six independent experiments are illustrated in figure 4.23 and corresponding values are given in table 8.5 (Appendix E). For each experiment an equal number of plants from original syl_404 (M3 plants) and wild-type plants was analysed together with the backcross lines.

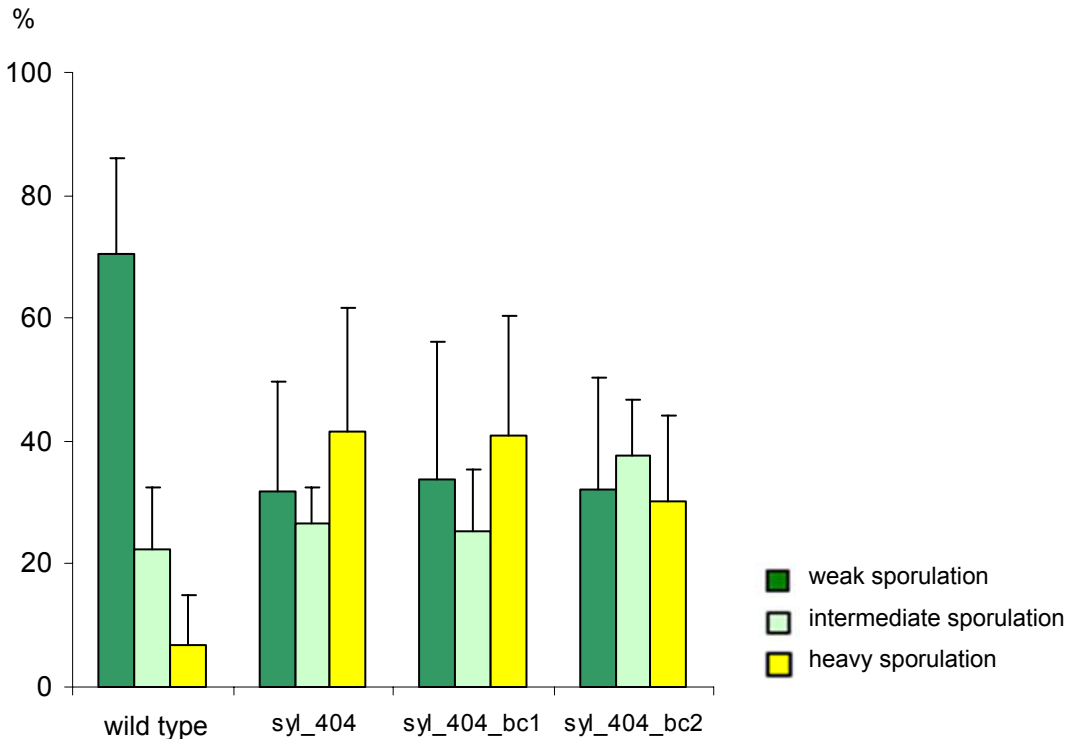

Figure 4.23 Sporulation efficiency on backcross mutant lines

Plants derived from the F2 population of syl_404_bc1 and syl_404_bc2, the original parental line and wild-type plants were infected and treated with sylA 48 hai. Interactions were scored 72 hat. Sporulation efficiency was evaluated according to the scheme presented in table 4.13 and related to the total number of plants evaluated (100%).

Figure 4.23 shows that fungal sporulation efficiency was enhanced on backcross lines syl_404_bc1 and syl_404_bc2 as compared to infected and sylA-treated wild-type plants. Reduced sporulation efficiency was comparable to the results obtained for powdery mildew-infected and sylA-treated original syl_404.

In summary, these results indicate that syl_404 harbours a mutation in a gene that might be involved in the curative effect of syringolin on powdery mildew-infected *Arabidopsis thaliana* plants.

4.3.1 Transcriptional analysis

With the aim to identify transcriptional differences in the syringolin response between syl_404 and wild-type plants, we compared transcript accumulation between sylA-treated backcross line syl_404_bc2 (in the following referred to as syl_404 for simplicity) and sylA-treated wild-type plants using the ATH1 Affymetrix gene chip. To reduce the impact of pool sampling on data variation, plant material was collected from a single timepoint experiment eight hours after treatment. In the following this experiment is referred to as experiment S8.

The experiments were repeated in duplicates. In case of few replicates available, Genespring recommends to statistically filter on relevant genes by assuming that variances are equal between two groups (see section Materials and Methods, chapter 6.8.2). Consequently, reliable data were filtered using Student's t-test (variances equal) including a multiple testing correction according to Benjamini and Hochberg (Benjamini and Hochberg, 1995).

RNA extraction was performed according to previous experiments. Synthesis of labelled cRNA was performed according to the Affymetrix one-sample protocol. For the one-sample protocol *in vitro* transcription was extended from 4,5 hours to over-night incubation.

The results in terms of numbers of transcripts whose levels were enhanced and lowered more than 2-fold and more than 3-fold in experiment S8 are presented in table 4.16.

Table 4.16 Numbers of differentially expressed transcripts

	t/c ratio[1]			
	≥ 2	≤ 0,5	≥ 3	≤ 0,333
wild type	1629	1973	973	1231
syl_404	1959	2093	1096	1459

(1) Data derived from two independent experiments. Differentially expressed genes were filtered by Student's t-test ($p \leq 0.05$) and MTC.

Reproducibility of transcriptional changes caused by syringolin application in experiment S8 was investigated by comparing transcript accumulation in sylA-treated wild-type plants to a previously performed experiment (S12) where RNA derived from uninfected sylA-treated wild-type plant material collected 8 and 12 hat. This revealed that out of the 1629 genes whose expression was enhanced more than 2-fold in experiment S8, the expression of 1206 transcripts was similarly enhanced more than 2-fold in experiment S12. As shown for experiment S8 in table 4.16, the majority of more than 2-fold differentially expressed genes was downregulated by syringolin in syl_404 and wild-type plants. Concerning the 1973 genes downregulated more than 2-fold in the wild type by syringolin (S8), the abundance of 1622 transcripts was also lowered more than 2-fold in the wild type by syringolin in experiment S12. Accordingly, transcriptional changes exerted by syringolin appear to be comparable. However, it seems likely that different timepoints of sample collection as well as modification of target labelling and gene chip hybridisation (see section Materials and Methods, chapter 6.8.1) might have provoked a certain transcriptional variability. The distributions of values of differentially expressed genes 8 hat in wild-type and syl_404 plants are given in a Venn diagram in figure 4.24.

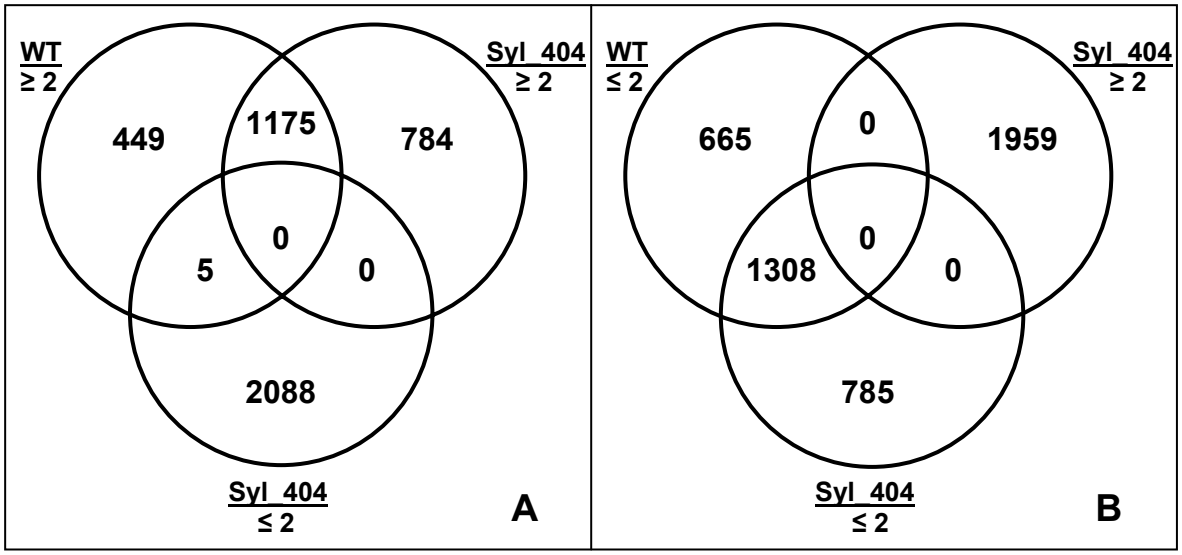

Figure 4.24 Comparison of sylA-responsive gene expression in syl_404 and wild-type plants

The Venn Diagram represents the distribution of more than 2-fold significantly (p-value ≤ 0.05, MTC) expressed genes in syl_404 and wild-type (WT) plants. (A): overlap between differentially expressed genes in syl_404 and upregulated genes in wild-type plants. (B): overlap between differentially expressed genes in syl_404 and downregulated genes in wild-type plants.

We focused on genes differentially expressed between wild-type plants and syl_404, such as genes more than 2-fold upregulated in wild-type plants but downregulated in syl_404, which was the case for five genes (Figure 4.24 A). These genes and corresponding t/c ratios are given in table 4.17.

Table 4.17 Genes more than 2-fold differentially expressed between wild-type and syl_404 plants

Row	Description	Protein	Locus[1]	t/c ratio[2]	
				wt	syl_404
1	MATE efflux family protein		At3g23550	12,4	0,3
2	fibrillarin 2 identical to fibrillarin 2	Fib2	At4g25630	2,3	0,5
3	curculin-like (mannose-binding) lectin family protein		At5g18470	4,9	0,3
4	auxin conjugate hydrolase	ILL5	At1g51780	2,1	0,4
5	WRKY family transcription factor	WRKY53	At4g23810	5,8	0,4

(1) The annotation of the genes derived from TAIR, the Arabidopsis Information Resource (http://arabidopsis.org).

(2) Data derived from two independent experiments. Differentially expressed genes were filtered by the Student's t-test (p ≤ 0.05) and MTC. wt: wild type.

The reverse case, i.e. genes downregulated in the wild type and upregulated in syl_404, was not found (Figure 4.24 B). Among genes with an absent call for the detection value in all experiments performed with RNA derived from syl_404 plants, seven genes were found that received a present call in wild-type plants. However, these genes were neither upregulated nor transiently expressed but downregulated at least 1,6-fold by syringolin in the wild type (data not shown).

Inspection of raw values obtained from control (0,05% TWEEN 20)-treated wild-type and syl_404 plants made it obvious that the abundance of many transcripts was already altered in the mutant without sylA treatment. Consequently, this resulted in decreased t/c ratios of these genes. To compare absolute transcript abundances between wild-type and syl_404 plants, ratios were calculated derived from sylA-treated wild-type and syl_404 plants. Similarly, mutant/wild-type ratios (m/wt ratios) were calculated from the data derived from control-treated wild-type and syl_404 plants.

In total, m/wt ratios ≥ 3 and ≤ 0,333 were found for 514 genes in control-treated syl_404 plants and for 333 genes in syringolin-treated syl_404 plants, respectively. However, average signal values over all genes obtained from control- and syringolin-treated syl_404 plants were similar.

Genes whose m/wt ratios were altered more than 3-fold by control and/or syringolin treatment in syl_404 were grouped according to biological function GO (Gene Ontology) terms and are listed in table 8.6 (Appendix F). The distribution of transcripts in functional categories for control (c) or syringolin (s) treatment is illustrated in figure 4.25.

For several functional categories transcript abundance in syl_404 was higher than in the wild type without sylA treatment (Figure 4.25). Remarkably, strongest alteration in transcript abundance upon control treatment in syl_404 compared to wild-type plants was found for genes encoding proteins responding to abiotic and biotic stimuli.

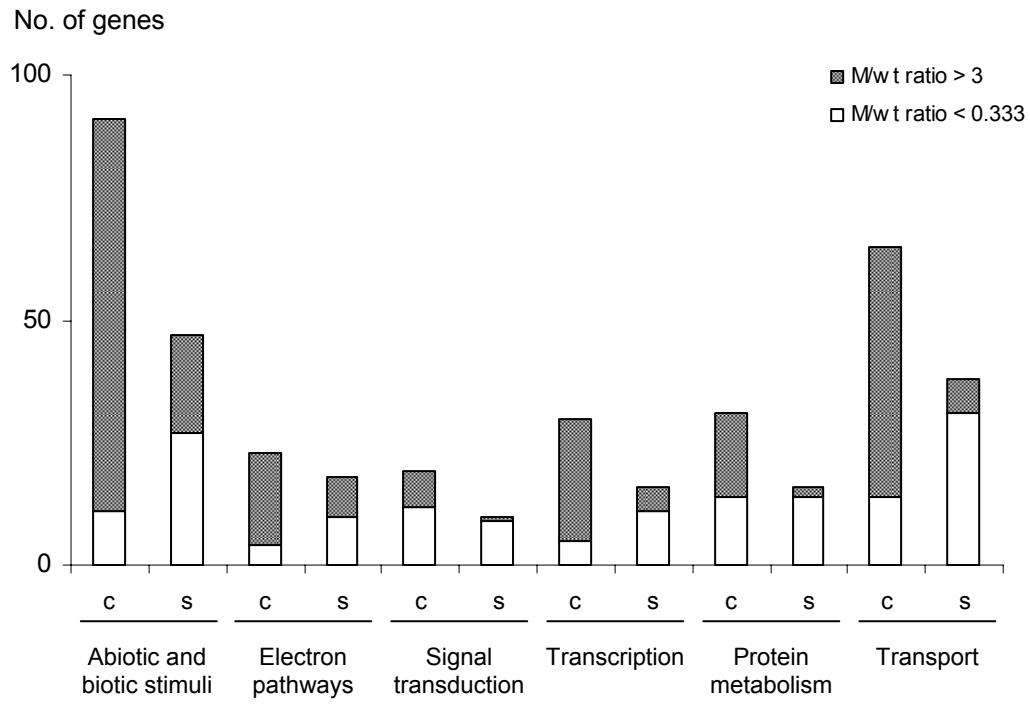

Figure 4.25 Impact of control and syringolin treatment on gene expression in syl_404 plants

Genes differentially expressed between wild-type and syl_404 plants upon treatment with a control solution (c) or syringolin (s). Transcripts were categorised according to biological function GO terms as represented on the X-axis. The Y-axis represents the number of genes whose expression was enhanced (filled column elements) and lowered more than 3-fold (open column elements) in each category.

Table 4.18 represents an overview of transcripts whose abundances were altered more than 10-fold by control and/or syringolin treatment in syl_404 as compared to the wild type.

Table 4.18 Functional groups of genes exhibiting m/wt ratios ≥ 10 and ≤ 0,1 in syl_404 upon control and/or syringolin treatment

Row	Description[1]	Locus[2]	m/wt ratio		t/c ratio[5]	
			Control[3]	Syringolin[4]	wt	syl_404
	RESPONSE TO ABIOTIC AND BIOTIC STIMULI					
	Abscisic acid/ Dehydration stress					
1	ABA-responsive protein-related	At3g02480	**491,6**	**142,8**	6,7	1,9
2	calcium-binding RD20 protein	At2g33380	**9,65**	**30,09**	**0,11**	**0,33**
3	dehydrin	At1g20450	**7,18**	**18,56**	**0,24**	0,62
4	dehydrin xero2	At3g50970	**34,65**	**20,46**	**7**	**4,11**
5	putative dehydrin	At4g38410	**24,07**	2,8	0,5	**0,06**
6	lipid transfer protein 4	At5g59310	**42,28**	10,67	0,61	**0,16**
7	member of the DREB subfamily A-6 of ERF	At4g28140	**31,66**	**12,64**	2,43	0,97
8	myb family transcription factor	At4g05100	**32,56**	**181,6**	0,17	0,96
9	**Jasmonic acid signalling**					
10	putative allene oxide cyclase	At3g25780	**14,74**	3,84	1,23	**0,32**
11	putative aminotransferase	At2g24850	**37,71**	0,6	3,3	**0,05**
12	putative lipoxygenase	At1g17420	**7,9**	**10,62**	0,32	**0,44**
13	putative plant defensin-fusion protein	At2g02130	**0,44**	**0,1**	**0,37**	**0,08**
14	vegetative storage protein 2	At5g24780	**32,76**	0,06	0,38	**0,001**
15	**Pathogen**					
16	putative chitinase	At2g43620	**14,27**	**2,84**	**2,73**	**0,54**
17	pathogenesis-related thaumatin family protein	At4g36010	**18,46**	**2,42**	**19,23**	**2,52**
18	protein with putative ankyrin	At4g14400	**0,65**	**0,06**	**0,36**	**0,04**
19	putative trypsin inhibitor	At2g43510	**18,01**	**3,8**	**2,36**	0,5
20	putative trypsin inhibitor	At2g43550	1,48	**0,08**	**0,13**	**0,01**
21	**Cellular redox state**					
22	catalase 3 (SEN2)	At1g20620	**1,23**	**0,08**	**0,29**	**0,02**
23	putative glutathione S-transferase (ERD9)	At1g10370	**11,94**	**1,6**	**7,2**	0,97
24	peroxidase 21	At2g37130	**14,02**	0,44	0,11	**0,001**
25	peroxidase 42	At4g21960	**0,66**	**0,09**	**0,22**	**0,03**
26	putative peroxidase	At5g05340	**17,71**	0,76	0,8	0,03
27	plastocyanin-like domain-containing protein	At5g20230	**11,46**	1,1	**17,31**	**1,67**
28	senescence-associated protein	At4g35770	**19,47**	2,08	1,12	**0,12**
29	**Heat**					
30	17.6 kDa class II heat shock protein	At5g12020	4,04	**11,84**	3,71	**10,86**
31	17.6 kDa class I small heat shock protein	At1g53540	5,22	**24,22**	7,23	33,53
32	17.7 kDa class II heat shock protein	At5g12030	5,99	**24,92**	16	**66,51**
33	**others**					
34	gibberellin-regulated family protein	At5g14920	**0,6**	**0,03**	**0,22**	**0,01**
35	putative 2-oxoacid-dependent oxidase (DIN11)	At3g49620	**315,7**	0,75	64,05	**0,15**
36	putative mannitol dehydrogenase	At4g37990	**61,14**	**85,32**	2,26	3,15
37	MERI-5 protein	At4g30270	**13,56**	**1,45**	**5,5**	0,54
38	**ELECTRON PATHWAYS**					
39	alcohol dehydrogenase	At1g77120	2,66	**14,87**	0,38	**2,15**
40	putative cytochrome P450	At2g30770	**20,32**	1,58	**21,62**	**1,68**
41	cytochrome P450 family protein	At3g48520	**29,54**	1,77	0,61	**0,04**
42	putative cytochrome P450	At2g45570	2,37	**15,87**	1,36	**9,14**
43	putative glutamate decarboxylase	At2g02010	**90,79**	1,34	**1817**	**26,84**
44	**TRANSCRIPTION**					
45	putative AP2 domain-containing transcription factor	At2g20880	**37,1**	4,45	1,72	**0,21**
46	member of the ERF subfamily B-4 of ERF	At1g43160	**856,7**	7,85	1,59	**0,015**
47	member of the ERF subfamily B-4 of ERF	At5g13330	**14,97**	3,17	1,68	**0,37**

Table 4.18 (continued)

Row	Description[1]	Locus[2]	m/wt ratio		t/c ratio[5]	
			Control[3]	Syringolin[4]	wt	syl_404
48	member of the ERF subfamily B-4 of ERF	At5g61890	**12,37**	0,69	0,47	**0,03**
49	no apical meristem (NAM) family protein	At1g52890	**26,2**	14,09	0,49	**0,27**
50	transcription factor jumonji domain-containing protein	At3g20810	**0,47**	**0,08**	**0,33**	**0,06**
51	WRKY family transcription factor	At5g49520	**21,61**	**4,5**	4,63	0,97
52	WRKY family transcription factor	At4g31800	**11,39**	**2,03**	**4,17**	0,74
53	WRKY family transcription factor	At4g18170	**11,07**	6,88	0,6	**0,37**
54	**PROTEIN METABOLISM**					
55	germin-like protein	At5g20630	**0,3**	**0,01**	**0,28**	**0,01**
56	palmitoyl protein thioesterase family protein	At4g17470	**13,29**	2,16	0,19	**0,03**
57	**TRANSPORT**					
58	putative 4-alpha-glucanotransferase	At5g64860	0,54	**0,06**	**0,27**	**0,03**
59	ABC transporter family protein	At2g39350	**20,76**	3,6	0,36	**0,06**
60	amino acid permease family protein	At4g21120	**10,42**	2,13	3,53	0,72
61	carboxyl methyltransferase family protein	At3g44860	**36,63**	2,24	1,55	**1,94**
62	putative cation exchanger	At5g17860	**10,46**	**1,93**	3,69	0,68
63	GCN5-related N-acetyltransferase family protein	At2g39030	**113,5**	1,31	1,57	**0,02**
64	glucosyltransferase-related	At4g16590	**12,63**	0,34	1,18	0,04
65	putative high-affinity nitrate transporter	At3g45060	**10,13**	1,19	0,39	**0,05**
66	MATE efflux family protein	At1g61890	**13**	**3,58**	0,43	**0,12**
67	MATE efflux family protein	At3g23550	**10,37**	**0,22**	**12,4**	**0,26**
68	O-methyltransferase family 2 protein	At1g76790	**11,15**	0,86	0,8	**0,06**
69	putative proline transporter	At2g36590	**12,94**	2,09	0,14	**0,02**
70	lipid transfer protein	At3g22120	0,83	**0,07**	**0,24**	**0,02**
71	lipid transfer protein	At5g55450	1,05	**0,07**	1	0,07
72	lipid transfer protein	At3g22600	**37,53**	**2,18**	**45,56**	**2,6**
73	lipid transfer protein	At3g22620	**24,51**	8,31	0,45	0,15
74	lipid transfer protein	At4g22470	**20,92**	2,18	1,54	0,16
75	oligopeptide transport family protein	At1g52190	**0,36**	**0,05**	**0,17**	**0,02**
76	oligopeptide transport family protein	At5g46050	**17,78**	0,5	2,12	**0,06**
77	sulfotransferase family protein	At5g07010	**94,33**	3,6	0,55	**0,02**

(1) Transcripts were grouped according to biological function GO (Gene Ontology) terms. Genes with unknown biological functions were excluded from table 4.18.

(2) The annotation of the genes derived from TAIR, the Arabidopsis Information Resource (http://arabidopsis.org).

(3) Data derived from two independent experiments: m/wt ratios were calculated from the data derived from control-treated syl_404 (m) and wild-type (wt) plants. Genes that passed statistical filtering based on Student's t-test ($p \leq 0.05$) are highlighted in bold.

(4) Data derived from two independent experiments: m/wt ratios were calculated from the data derived from syringolin-treated syl_404 (m) and wild-type (wt) plants. Genes that passed statistical filtering based on Student's t-test ($p \leq 0.05$) are highlighted in bold.

(5) Data derived from two independent experiments: t/c ratios were calculated from the data derived from wild-type (wt) and syl_404 plants. Genes that passed statistical filtering based on Student's t-test ($p \leq 0.05$) and MTC are highlighted in bold.

Transcripts exhibiting strong syringolin-independent expression in syl_404 included genes encoding proteins related to abscisic acid (ABA) signalling and drought stress (Table 4.18, rows #1ff). Among them, the gene encoding an ABA-responsive protein revealed a dramatic expression ratio in control-treated and syringolin-treated syl_404 plants (Table 4.18, At3g02480, row #1). In some cases, low m/wt ratios in syringolin-treated syl_404 plants resulted from elevated expression levels of the respective genes in the wild type upon syringolin treatment as reflected by corresponding t/c ratios.

Genes with high transcript levels in control-treated syl_404 plants were also related to the jasmonic acid signalling pathway (Table 4.18, rows #10ff), which is generally involved in a number of biotic and abiotic stress responses. The abundances of the majority of these transcripts were lower in syringolin-treated syl_404 plants and downregulated by syringolin in the wild type. Interestingly, drought stress and endogenous ABA can upregulate a number of wound-inducible genes (Chao et al., 1999), and cellular responses to jasmonic acid can involve concomitant activation of ethylene response pathways (Creelman et al., 1992; Creelman and Mullet, 1995; Penninckx et al., 1998). Indeed, transcripts of genes encoding members of the ERF (Ethylene Responsive Factor) transcription factor family revealed high m/wt ratios in control-treated plants (Table 4.18, rows #46ff). Comparison to data available through the Genevestigator database (Zimmermann et al., 2004), which collects hundreds of microarray expression data sets, revealed that all except one (Table 4.18, At5g61890, row #48) of the ERF and WRKY transcription factors present in table 4.18 were transcriptionally inducible by ozone and infection with *Pseudomonas syringae*, indicating a role of these proteins in abiotic and biotic stress responses.

In addition, further genes involved in cellular stress responses, such as genes encoding proteins functioning during oxidative stress (Table 4.18, rows #22ff) revealed high transcript abundance in control-treated syl_404. Transcripts of these genes exhibited lower abundances in syringolin-treated syl_404. In addition, the majority of these genes was downregulated by syringolin in wild-type and syl_404 plants as reflected by corresponding t/c ratios. In contrast, genes encoding members of the cytosolic small Hsps revealed higher expression in syringolin-treated compared to control-treated syl_404 plants (Table 4.18, rows #30ff). Similarly, the gene encoding a glutamate decarboxylase (Table 4.18, At2g02010, row #43) exhibited higher expression in syringolin-treated syl_404 plants and its expression was dramatically upregulated by syringolin in the wild type.

In conclusion, it was found that only few genes exhibited antagonised expression in syl_404 compared to wild-type plants upon syringolin treatment. In general, transcriptional responsiveness of syl_404 differs from that in the wild type with regard to high expression of many stress-responsive genes without syringolin treatment. Transcripts of genes related to dehydration stress and ABA-signalling strongly accumulated in abundance in control-treated and syringolin-treated syl_404 plants and genes encoding small heat shock proteins exhibited high m/wt ratios in syringolin-treated syl_404 plants.

5 Discussion

5.1 Syringolin A action in *Arabidopsis thaliana*

In wheat, syringolin treatment effectively protects the plant from colonisation with virulent isolates of *Blumeria graminis* f. sp. *tritici*. This is also true for the interaction of powdery mildew (*Erysiphe cichoracearum*) with *Arabidopsis thaliana.* Arabidopsis offers several important advantages for the study of plant disease mechanisms in general and of powdery mildew disease in particular. Microscopic examination revealed that powdery mildew disease progressed similarly on Arabidopsis and on cereals, suggesting that information about the Arabidopsis-powdery mildew interaction will aid in understanding the more economically important powdery mildew disease of cereals. However, *Erysiphe cichoracearum* does differ morphologically from *Blumeria graminis* in germ tube development, conidiophore foot cell shape, and haustorium shape (Adam and Somerville, 1996).

Characterisation of the syringolin response in Arabidopsis revealed that syringolin efficiently protects the plant from colonisation by powdery mildew when applied two days after infection. By this time, the fungus has invaded the host cells and produced haustoria. By their feeding activities, biotrophic fungi create a nutrient sink at the infection site, so that the host is disadvantaged but not killed. Since powdery mildew depends on living host cells, plant cell death strategies are commonly most effective against this biotrophic fungus (Carver et al., 1999). Indeed, syringolin treatment of infected Arabidopsis causes autofluorescence, indicative for the occurrence of a hypersensitive reaction (Figure 4.4 B). In contrast to sylA-treated wheat, where autofluorescence was predominantly observed in epidermal cells, autofluorescence in Arabidopsis was weak in epidermal cells but strongly detectable

in underlying mesophyll cells at this timepoint (Figure 4.5). This is similar to the phenotypes conferred by *edr1* (*enhanced disease resistance 1*) plants with regard to inoculation with *E. cichoracearum* (Frye and Innes, 1998) and to phenotypes conferred by the late-acting resistance gene *Mla12* (*Mildew-resistance Locus A*) in barley (Hückelhoven and Kogel, 1998). In both cases, powdery mildew growth was affected after the development of secondary hyphae, but before conidiophore production. In addition, incompatible interactions in *Mla12* plants are associated with the accumulation of large masses of dead mesophyll cells (Boyd et al., 1995; Hyde and Colhoun, 1975). However, since powdery mildew does not infect mesophyll cells, and sylA does not lead to HR in uninfected tissue, sylA-triggered cell death in infected tissue must be in part due to effects the fungus exerts on neighbouring mesophyll cells. It is tempting to speculate that fungal infection triggers the diffusion of signal molecules such as ions or simple metabolites between infected and uninfected cells leading to HR in the surrounded tissue. Alternatively, membrane- or cell wall-bound macromolecules participating in the control of interactions between neighbouring cells may also be responsible for the signal transduction between infected and uninfected cells.

5.2 Transcript profiling of syringolin-treated powdery mildew-inoculated Arabidopsis

Microarray comparison between powdery mildew-infected and uninfected syringolin-treated Arabidopsis was carried out in order to identify genes transcriptionally involved in the localised induction of HR in *E. cichoracearum*-infected Arabidopsis plants.

Unexpectedly, no gene exhibiting a t/c ratio ≥ 2 in experiments IS1 and IS4 (plant material collected at 0.5-1 hat and 2-4 hat, respectively), has passed the statistical filtering when multiple testing correction was included (Table 4.2). However, we found a set of 47 genes differentially expressed more than 2-fold in uninfected plants treated with sylA (experiment S1). Thus, it appears that in uninfected plants more genes are reproducibly altered by sylA than in infected plants. This indicates that both parameters, infection and sylA treatment, applied together to the plant, might have provoked various cellular stresses leading to diffuse transcriptional changes at the early timepoint experiments (IS1 and IS4). In addition, large variation in gene expression very early after syringolin treatment together with low expression at these timepoints (data not shown) might have contributed to the reasons why no candidate gene passed stringent statistical filtering. However, one gene (At5g20630), encoding a germin-like protein 3 (GLP3), was more than 2-fold repressed in experiment IS1 when excluding the false positive correction (MTC) from the statistical filtering process. Because germins with oxalate-oxidase activity are involved in the elicitation of HR at lower concentrations of hydrogen peroxide and the destruction of oxalate, which is an inhibitor of the hypersensitive response (Lane, 2002), it was hypothesised that downregulation of *Glp3* by sylA might counteract the induction of HR. However, to date, the function of germin-like proteins from dicots remains uncharacterised with regard to their biochemical properties or antimicrobial activities (Lane, 2002).

Seventy-two genes were differentially expressed at least two-fold in experiment IS4 when MTC was excluded from statistical filtering (Table 4.2). All but two of the 68 genes (p-value ≤ 0.05, no MTC) upregulated in infected tissue 2-4 hat were also included in the set of sylA-responsive genes upregulated in infected and uninfected plants by 8-12 hat. This finding indicates that the major changes exerted by sylA took place at later timepoints. This observation is supported by the high number of differentially expressed transcripts 8-12 hat in infected and uninfected tissue (Table 4.2). The remarkable changes in the transcriptome at the late timepoint (8-12 hat) of our hybridisation experiments is in accordance with earlier findings in syringolin-treated wheat leaves, where important transcriptional changes occurred 10 hours after syringolin application (Wäspi et al., 2001).

To our surprise, the effect of sylA on the transcriptome of *Arabidopsis thaliana* was dramatically higher in uninfected plants than in infected plants. It seems that the cellular response to syringolin was found to be negatively controlled by powdery mildew infection. Our microarrary data suggest that in general this was not explicable by powdery mildew-induced accumulation of sylA-induced transcripts. Therefore, it was hypothesised that the observed reduced sylA response of powdery mildew-infected tissue may be due to a suppressive effect on gene expression the fungus exerts in colonised and neighbouring cells and was observed for a few specific genes in wheat (Wäspi et al., 2001).

However, 13 transcripts were identified that exclusively accumulated in infected tissue treated with sylA (Table 4.3). Apart from transcripts encoding proteins with unknown biological functions (Table 4.3, rows #2ff), two encoded a disease resistance protein containing a leucine-rich repeat domain and the WRKY75 transcription factor, respectively (Table 4.3, At2g34930, At5g13080, rows #1 and 13).

Interestingly, the WRKY75 transcription factor has a function during H_2O_2-mediated programmed cell death (Gechev et al., 2005) and was upregulated during programmed cell death (PCD) triggered in Arabidopsis by the fungal AAL-toxin (Gechev et al., 2004). Furthermore, this also included the *Pai3* gene (Table 4.3, At1g29410, row #10) encoding a protein involved in tryptophane biosynthesis. Since *Pai* isogenes were found to respond to environmental stresses, the expression of *Pai3* was possibly enhanced by excessive cellular stress imposed by a coincidence of both powdery mildew infection and syringolin treatment.

Thus, one hypothesis is that these transcripts might be linked to the occurrence of HR. Whether these genes might indeed encode proteins involved in the onset of HR in infected and sylA-treated tissue or whether the expression of these genes might rather be considered as a consequence of distinct cellular processes leading to HR remains to be determined.

Since one of the hypothesised functions of syringolin was to suppress a suppression of host responses imposed by the colonising fungus (Wäspi et al., 2001), we were interested in genes upregulated by powdery mildew infection but downregulated by syringolin. The single effect of infection on transcript abundance was calculated by comparing expression ratios derived from uninfected plants to infected plants, both treated with a control solution (I60). We identified 60 genes upregulated by powdery mildew infection alone but downregulated by syringolin application on uninfected plants (S12). Genes whose expression was induced by powdery mildew and repressed by sylA predominantly encoded proteins categorised to cellular transport, proteins that respond to biotic and abiotic stimuli as well as proteins involved in protein metabolism (Appendix C, Table 8.2).

Another interesting group is formed by three genes whose expression was repressed by the pathogen but enhanced by syringolin in infected tissue (Table 4.4). These genes encoded a disease resistance protein containing a leucine-rich repeat domain, an internal NAD(P)H dehydrogenease, and a MATE efflux (Multidrug And Toxic compound Extrusion) protein (Table 4.4, rows #1ff). Internal NAD(P)H dehydrogenases exhibit protective activity by providing a mechanism for plants to remove excess reducing power (Rasmusson et al., 2004). MATE efflux proteins play a role during cellular drug stress tolerance. In addition, six genes whose transcription levels were repressed by the fungus were more than 2-fold upregulated in uninfected plants by sylA (Table 4.4, rows #4ff).

In summary, several genes differentially expressed upon powdery mildew inoculation were found to exhibit opposite transcriptional regulation by syringolin. The encoded proteins might represent candidates that counteract fungal life to varying extent. However, it remains an open question how these proteins may contribute to antagonise powdery mildew growth on Arabidopsis. Moreover, transcriptional alteration by syringolin specific for infected tissue could only be shown for relatively few genes. Still, these genes encode proteins that might play a role during hypothesised HR in infected and sylA-treated cells. Nevertheless, these genes were induced only weakly.

5.3 Syringolin-induced genes in terms of biological functions

Plants infected with powdery mildew prior to sylA treatment apparently responded weaker to sylA. In contrast, in uninfected plants a large number of transcripts encoding proteins of a broad range of biological functions were affected. In the following, putative functions of these genes and their integration into different metabolic and regulative pathways are discussed.

5.3.1 Ubiquitin/26S proteasome pathway

In plants, the ubiquitin (Ub)/proteasome (26S) is involved in degrading a wide range of proteins. The importance of the Ub/26S system in plants is reflected by the identified high number of more than 1'300 genes (~5% of the total genome) in the Arabidopsis genome encoding Ub/26S components (Vierstra, 2003). A schematic overview of the Ub/26S pathway is shown in figure 5.1.

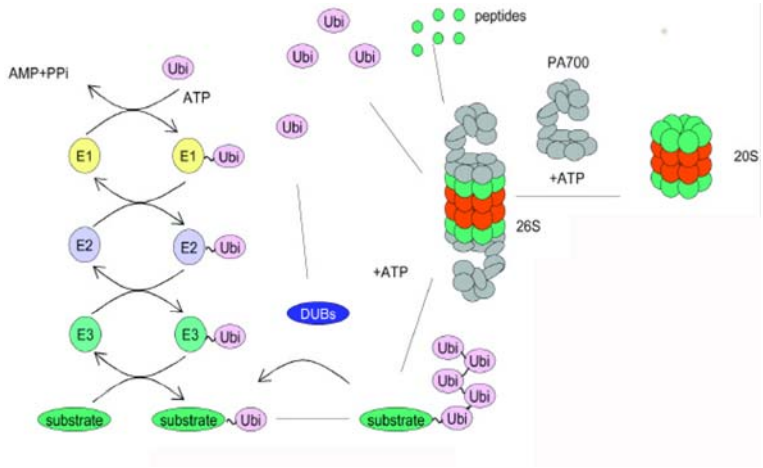

Figure 5.1 Schematic overview of the ubiquitin-proteasome pathway

E3 enzymes recognise substrates and mediate the transfer of ubiquitin from an E2. The latter receives its ubiquitin by transfer from an E1. Polyubiquitinated proteins are targeted for degradation by the 26S proteasome. Mono- and polyubiquitinated proteins can be deubiquitinated by the action of numerous deubiquitinating enzymes (DUBs). The 26S proteasome releases free ubiquitin and degrades the substrate to short peptides. The 26S multicatalytic proteinase complex is made up of the core 20S proteasome and PA700 activator (19S cap) (modified after Wojcik, 2002).

The 26S proteasome has a general function in the selective removal of various short-lived proteins that were first covalently linked to ubiquitin. Several of these proteins control key aspects of plant growth, development and defence (Callis and Vierstra, 2000; Hellmann and Estelle, 2002). The process of ubiquitination starts with the ubiquitin-activating enzyme (E1) which recruits ubiquitin and passes it to the ubiquitin-conjugating enzyme (E2), which transfers the ubiquitin to the ubiquitin ligase

protein (E3). The E3 is generally considered to be most important in controlling target specifity since it is responsible for recruiting the target protein (Vierstra, 2003).

The 26S proteasome complex consists of a 20S core protease (CP) capped by two particles of the PA700 proteasome activator, also called the 19S regulatory particle (RP). The 2.4 MDa proteolytic 26S proteasome complex of *Arabidopsis thaliana* has been isolated recently (Yang et al., 2004). The genomes of Arabidopsis and rice contain gene pairs for many CP and RP subunits (Fu et al., 1998). The 20S core particles carries two copies of the seven different α and β subunits arranged in four stacked rings. Representatives of all seven α and β subunits were found among genes upregulated by sylA, several were represented by pairs (Table 4.7).

The RP is subdivided into lid and base. Collectively, the RP assists in recognising appropriate substrates, unfolding them, opening the α-ring gate, and then directing the unfolded polypeptides into the lumen of the CP for breakdown. Genes encoding pairs or single representatives of all of these subunits exhibited elevated expression upon sylA treatment. Four genes encoding RP and CP subunits exhibited enhanced expression already 2-4 hat (Table 4.7).

At present, only the functions of a few of the core RP subunits are known. For the majority of subunits both pairs were induced by syringolin. An exception was found for RPN12a (Table 4.7, At1g64520, row #34), indicating that paralogs might exhibit different activities. Indeed, RPN12a and RPN12b display enough structural divergence to support this assumption (Yang et al., 2004). Another exception was subunit RPN3a (Table 4.7, At1g20200, row #24), which is distinguished from its paralog by the absence of a nuclear localisation signal (Yang et al., 2004).

An increase of the 26S proteasome level might reflect a higher demand for protein degradation via the ubiquitin pathway after sylA treatment. In fact, the presence of a distinct set of proteasome subunits together with the finding that some transcripts which accumulated already 2-4 hat encoded RP and CP subunits might hint at the formation of specialised proteasome complexes upon sylA treatment (Table 4.7).

In addition, all subunits of the COP9 signalosome (CSN) complex were present among genes more than 2- and 3-fold upregulated by sylA in uninfected plants (Table 4.8). The eight subunits of the CSN show remarkable similarity to the lid subcomplex of the 19S regulatory particle (Wei et al., 1998). This indicates that the CSN has a direct role in protein degradation, possibly as the lid for a specialised CSN proteasome (Schwechheimer and Deng, 2001). Insights have been gained that link the COP9 signalosome closely to the function of the multiprotein ubiquitin ligase (E3) complex, the SCF [Skp/Cullin/F-box] complex (Lyapina et al., 2001; Schwechheimer and Deng, 2001).

Moreover, the RAR1 protein (Table 8.3, At5g51700, row #1145), which functions downstream of multiple R-gene-mediated resistance pathways, was upregulated by sylA in uninfected plant tissue. In plants, SGT1, a positive regulator of E3 ubiquitin ligase complexes, has been found to interact with RAR1 (Azevedo et al., 2002; Liu et al., 2002). Therefore, it is possible that RAR1 cooperates with SGT1 to target negative regulators of disease resistance for degradation. A model for involvement of the CSN, RAR1, the SCF ubiquitin ligase complex, and the 26S proteasome in disease resistance is shown in figure 5.2.

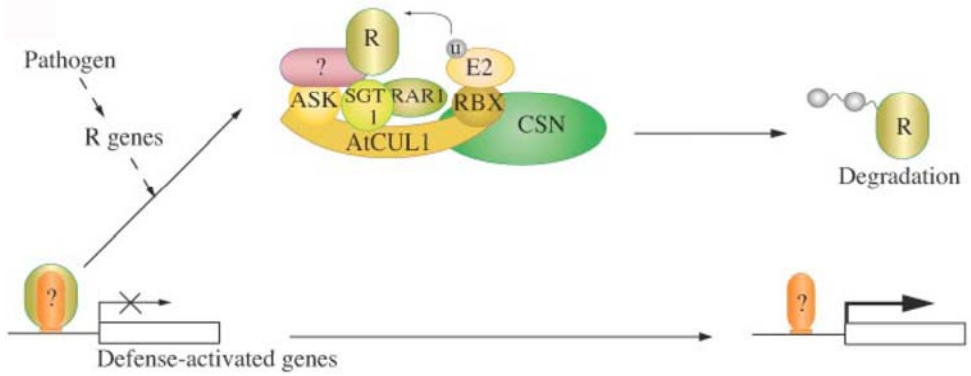

Figure 5.2 Model of regulated protein degradation and its function in disease resistance

RAR1 cooperates with SGT1 that is associated with components of the SCF ubiquitin ligase complex to target negative regulators of disease resistance. The SCF complex is regulated by CSN to promote ubiquitination of target proteins. Degradation of target proteins occurs by the 26S proteasome in which the COP9 signalosome replaces the lid (modified after Serino and Deng, 2003).

Since the Arabidopsis genome encompasses about 700 F-box proteins, variable components of the SCF complex, the CSN has the potential to control many E3 ubiquitin ligases and thereby their mediated processes (Gagne et al., 2002). The finding that syringolin alters the abundance of many transcripts encoding F-box proteins (Table 8.3, rows #557ff, 611ff, 620ff) could indicate that syringolin induces selective protein degradation via the CSN.

In conclusion, our results indicate that one crucial effect exerted by syringolin appears to enhance protein degradation which directly or indirectly might allow the plant to influence the presence of key components of disease resistance in plants.

5.3.2 Chaperones

Syringolin application on infected and uninfected plants provoked accumulation of several transcripts encoding heat shock proteins (Hsps). This encompassed members of the five major families of Hsps: Hsp70, the chaperonins (GroEL and Hsp60), the Hsp90, the Hsp 100, and the low molecular weight small Hsps (Table 4.9). Studies of the protective ability of Hsps have focused on their role as chaperones to prevent misfolding of proteins. Hsps/chaperones are known to be expressed in plants not only during high temperature stress but also in response to a wide range of other environmental insults. Most likely, Hsps/chaperones play a crucial role in the re-establishment of cellular homeostasis (Boston et al., 1996; Vierling, 1991). In Arabidopsis, six members of the Hsp90 family have been isolated ranging from 80 to 90 kDa (Takahashi et al., 1992; Yabe et al., 1994). The expression of two genes encoding *Hsp81-1/Hsp90.1* and *Hsp81-2/Hsp90.2* (Table 4.9, At5g52640, At5g56030, rows #9, 10) was upregulated by sylA. It was shown that heat shock had a greater effect on the expression level of *Hsp81-1/Hsp90.1* than on those of *Hsp81-2/Hsp90.2* (Takahashi et al., 1992). This corresponds to expression patterns obtained after sylA treatment. Syringolin application on infected plants enhanced the expression of *Hsp81-1/Hsp90.1* already 2-4 hat (t/c ratio: 2,5) and even more when sylA was sprayed on uninfected plants (t/c ratio: 52,1). Interestingly, HSP81-1/HSP90.1 is required for full R-gene mediated resistance against *Pseudomonas syringae* pv. *tomato* DC3000 carrying the avirulence gene *avrRpt* (Takahashi et al., 2003). In addition, accumulation of RPM1 (Resistance to *P. syringae* pv. *maculicola*), conferring resistance against *Pseudomonas syringae* strains that carry the avirulence genes *avrB* and *avrRpm1*, is greatly diminished in specific *hsp81-2/hsp90.2* missense mutants (Hubert et al., 2003). In general, HSP90

proteins may determine whether NBS-LRR proteins are functional in disease resistance by transiently binding of non-native proteins to assist its proper folding (Sangster and Queitsch, 2005; Young et al., 2001). In this context, it was speculated that RAR1 might act as a co-chaperone protecting HSP90-associated NBS-LRR proteins from SGT1b mediated degradation (Holt et al., 2005).

A high number of Hsps transcriptionally induced after sylA treatment was present in the group of the Hsp70 chaperones. Upregulation of Hsp70 genes positively correlated with the acquisition of thermo-tolerance (Lee and Schoffl, 1996). Moreover, Hsp70 proteins were found to interact with signalling molecules including cell-death regulators, thereby negatively affecting the mitochondrial pathway of apoptosis (Beere, 2004, 2005). Interestingly, transcripts encoding mitochondrial Hsp70 and the mitochondrial co-chaperone GrpE were also accumulating after sylA application (Table 4.9, At4g37910, At5g55200, rows #7, 8).

In Arabidopsis, 13 different small Hsps are grouped into five classes in accordance with their molecular phylogeny and localisation in the cell (Vierling, 1991). We detected strong induction of genes encoding small Hsps. The majority belonged to cytosolic class I and II small Hsps (Table 4.9, row #13ff), but highest transcript abundance was found for a gene encoding the mitochondrial *Hsp23.5* (Table 4.9, At5g51440, row #19). This gene exhibited highest expression ratios in infected tissue already 2-4 hat and its expression was enhanced 8-12 hat in infected and uninfected plants. Expression of the gene *Hsp23.6*, encoding a mitochondrial small Hsp (Table 4.9, At4g25200, row #20), was also already more than 2-fold enhanced 2-4 hours after sylA treatment. Since the capability of mitochondria to tolerate heat has a great impact on the whole cell activity and survival, it has been suggested that mitochondrial small Hsps play a major role in the heat tolerance of

plant mitochondria (Sanmiya et al., 2004). In this context, mitochondrial small Hsps of maize were shown to improve mitochondrial electron transport, mainly by protection of the NADH:ubiquinone oxireductase activity of complex I (Downs and Heckathorn, 1998; Hamilton and Heckathorn, 2001). Therefore, a protective role for mitochondrial small Hsps during sylA-dependent stress responses might exist.

Surprisingly, three small Hsps localised in the plastids were transcriptionally downregulated in syringolin-treated plants (Table 4.9, rows #2, 21, 22). Plastid small Hsps protect photosynthetic electron transport during heat stress (Heckathorn et al., 1998). Recently, Zou and co-workers (2005) have shown that destruction of PSII proteins lead to photooxidation of molecules in the PSII which results in ROS (Reactive Oxygen Species) formation and a decrease of photosynthetic activity. In this context, it is conspicuous that syringolin was found to exert strong inhibitory effect on photosynthetic gene expression such as genes encoding chlorophyll a/b binding proteins and components of photosystem I and II (Table 8.3, rows #422ff). This might indicate that chloroplast integrity was negatively affected by syringolin but in contrast to mitochondria, the expression of protective genes was inhibited.

The transcription of Hsp-encoding genes is controlled by regulatory proteins called heat shock transcription factors (Hsfs). The Arabidopsis genome contains 21 genes encoding Hsfs distributed to Hsf-classes A, B, and C (Nover et al., 2001). In contrast to class A Hsfs of plants, a considerable number of Hsfs assigned to classes B and C have evidently no function as transcription activators during heat stress (Baniwal et al., 2004). Syringolin predominantly induced the expression of Hsfs genes belonging to class A (Table 4.10, rows #30ff). In infected tissue syringolin exclusively enhanced transcript abundance of *HsfA2* (Table 4.10, At2g26150, row #31) that, in addition, exhibited highest induction values in uninfected plants treated

with sylA. HSFA2 is exclusively found after heat shock induction in complexes (heat shock granules) which are mainly formed by the cytosolic small Hsps and Hsp70 influencing its activity and intracellular distribution (Baniwal et al., 2004). Moreover, synthesis of HSFA2 seems to be strictly heat stress dependent, especially in periods of repeated heat stress and recovery (Nover et al., 2001).

These results imply that heat shock proteins and transcription factors play an important role in plant response to sylA, perhaps by directly supporting recovery from stress induced by sylA, thus preventing cell damage and cell death.

5.3.3 Mitochondria

Mitochondria are the energy factories of the cells producing ATP molecules, the energy supply for the processes of life. Remarkably, a considerable number of genes upregulated by sylA in infected and uninfected plants encodes proteins located in mitochondria.

Since most of the mitochondrial proteins are synthesised in the cytosol, the import of proteins into mitochondria is achieved by a number of oligomeric protein complexes. A single translocase of the outer membrane (TOM) contains the receptors to target proteins that are subsequently passed to two translocases of the inner membrane (TIM) (Koehler, 2004). Two Arabidopsis homologs of these import components were transcriptionally induced by syringolin, namely TIM17 and TOM20 (Table 8.3, At1g20350, At5g40930, row #1660, 1661). In addition, transcriptional upregulation was found for proteases responsible for a rapid breakdown of mitochondrial targeting pre-sequences. This included FtsH (Table 8.3, At1g06430, At1g07510, rows #537f), Clp (Table 8.3, At5g51070, row #541), DegP (Table 8.3, At3g03380, row #556) and Lon proteases (Table 8.3, At5g26860, At3g05790, rows #571f).

Next to several members of the mitochondrial substrate carrier family (Table 8.3, rows #1662ff), transcriptional upregulation was found for a gene encoding a porin family protein located at the outer mitochondrial membrane (Table 8.3, At1g50400, row #1621). The feature of voltage gating porins has been used to name the family of these proteins, the voltage-dependent anion channel (VDAC) family. VDAC, along with the adenine nucleotide translocator, cyclophilin D, and other proteins form a complex called permeability transition pore complex (PTPC) (Crompton et al., 2002). Pro- and anti-apoptotic factors of the Bcl-2 family proteins are thought to be involved in regulating the function of the PTPC (Shimizu et al., 1999; Shimizu et al., 2000). In addition, an increase of VDAC channels can result in closing of the VDAC, thereby suppressing ATP release from the mitochondria in the cytosol (Lemeshko, 2002; Lemeshko and Lemeshko, 2004). Since VDAC closure also affects cytochrome c release in the cytosol, one might speculate that this could directly counteract the induction of cell death.

Among further transcripts encoding mitochondrial proteins that accumulated upon sylA treatment we identified a putative prohibitin (Table 8.3, At3g27280, row #547). Since prohibitin is localised at the inner mitochondrial membrane, it is speculated to have impact on mitochondrial membrane potential and ATP production (McClung et al., 1995). Prohibitins have anti-proliferation activity, are ubiquitously expressed, and appear to be essential for cell survival. Based on sequence and structural similarities, prohibitin together with stomatin and a subgroup of HIR- (Hypersensitive Induced Reaction) plant defence-related proteins belong to a superfamily of plant proteins named PID (Proliferation, Ion, and Death) also designated as ‘band 7’ proteins which may be involved in signalling and regulation of PCD via modulation of ion channel activity (Nadimpalli et al., 2000). Transcripts

encoding representatives of band 7 family proteins such as a stomatin-like protein and several HIR-proteins accumulated in sylA-treated tissue (Table 8.3, rows #546ff).

Oxidative phosphorylation is the process by which cells obtain energy (ATP) when oxygen is present in the cell. Structural basis for oxidative phosphorylation in mitochondria are five protein complexes I-V located at the inner mitochondrial membrane. Syringolin appears to activate a plant-specific bypass of the classic respiratory chain by enhancing transcript abundance of genes encoding rotenone-insensitive NADH dehydrogenases and subunits of the alternative oxidase (AOX). Alternative oxidase, which appears to play an antioxidant role in plant mitochondria, is encoded by five genes in Arabidopsis, four Aox1 types and one Aox2 type (Considine et al., 2002). Transcriptional upregulation of *Aox1a*, which is the predominantly expressed isoform, and *Aox1b* (Table 4.6, At3g22370, At3g22360, rows #1, 2) was found in plants treated with sylA. An unexpected change in gene expression was the relatively high level of *Aox1d* transcripts (Table 4.6, At1g32350, row #3). Previously, *Aox1d* transcript levels had been found to be barely detectable in any tissues (Thirkettle-Watts et al., 2003). However, because *Aox1d* transcript levels were enhanced in phytotron experiments using high light conditions (Fiorani et al., 2005) *Aox1d* expression in sylA-treated plants might reflect a situation of cellular stress response.

Unlike the cytochrome pathway, which is coupled to ATP synthesis, electron transport from ubiquinol to AOX is nonphosphorylating and releases energy as heat, thereby preventing overreduction of the ubiquinol pool and ROS generation. Electron flow of the alternative pathway, starting with the oxidation of NADH by the rotenone-insensitive NADH dehydrogenases via the ubiquinone pool to the AOX, allows the oxidation of NADH by mitochondria to continue. Because less ATP is produced, this

results in a decreasing ATP/ADP ratio. Seven types of the rotenone-insensitive NAD(P)H dehydrogenase (ND) identified in the Arabidopsis genome were grouped into three families A, B, and C. Genes encoding NDA1 and NDB2 enzymes exhibited enhanced expression ratios upon sylA treatment (Table 4.6, At2g20800, At1g07180, rows #7, 8).

Interestingly, co-expression of *Aox1a* and *Ndb2* was observed under various cellular stress conditions. Clifton and co-workers (2005) suggested that both AOX1a and NDB2 are capable of forming a functionally alternative respiratory chain allowing oxidation of cytosolic NAD(P)H which is uncoupled from oxidative phosphorylation (Figure 5.3).

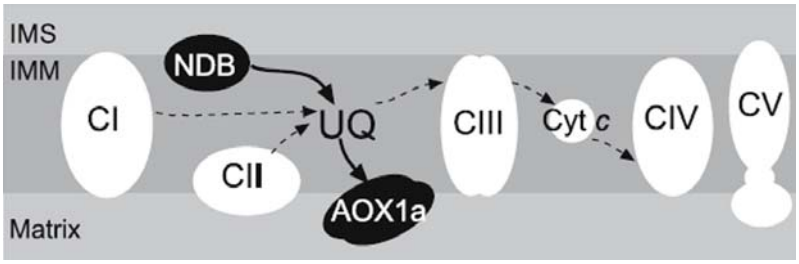

Figure 5.3 Diagrammatic representation of the plant mitochondrial electron transport chain

The multi subunit complexes I, II, III, IV, and cytochrome c, which comprise the cytochrome electron transport chain, are shown in white. The stress inducible alternative external NADH dehydrogenase (NDB) and alternative oxidase (AOX1a) are shown in black. The flow of electrons is indicated by arrows with the proposed stress inducible pathway indicated by solid arrows. IMS = intermembrane space, IMM = inner mitochondrial membrane, UQ = ubiquinone (modified after Clifton et al., 2005).

In general, the alternative mitochondrial pathway decreases ROS formation when mitochondria are overflooded with reducing substrate. In this way, activation of the alternative bypass by syringolin would counteract a high reduction state of the ubiquinone (UQ) pool which may result from high NAD(P)H supply and/or the inhibition/dysfunction of the cytochrome pathway (Maxwell et al., 1999; Millenaar and

Lambers, 2003; Moore et al., 2002). The activation of alternative pathways results in decreasing cellular ATP yield which in turn might induce increased glycolytic and TCA cycle turnover to produce reducing substrates such as NAD(P)H. Indeed, a number of genes encoding proteins responsible for sucrose breakdown and glycolytic enzymes were upregulated by syringolin, suggesting that glycolytic activity was enhanced (Table 4.5). In general, this allows effective balancing of cellular NAD(P)H/NAD(P)$^+$ and ATP/ADP ratios, thus linking respiratory energy coupling with demands for carbon skeletons (Gray et al., 2004). However, in the case of a restricted cytochrome pathway, stimulation of glycolytic activities would rather overflood mitochondria with reductive substrates, which in turn would stimulate the activity of alternative pathways. As detailed below, a number of transcripts encoding fermentative enzymes were also strongly accumulating.

5.3.4 Metabolic changes

If mitochondrial membrane permeability and ATP supply by oxidative phosphorylation are indeed affected by syringolin one may expect significant effects on bioenergetics and cellular metabolism. Indeed, syringolin leads to considerable transcriptional changes of a high number of genes encoding proteins involved in various metabolic processes. Unexpectedly, transcript abundance of the majority of these genes was lowered by syringolin as represented in figure 4.10. Concerning carbohydrate metabolism, upregulated transcription was exclusively found for enzymes functioning in sucrose break-down, glycolysis, as well as ethanolic and lactate fermentation (Table 4.5).

Strong transcriptional induction of the *pyruvate decarboxylase 1* gene (Table 4.5, At4g33070, row #26) was indicative for the induction of fermentative catabolic activity. Fermentation is the metabolic breakdown of glucose without net oxidation, allowing for the maintenance of ATP generation by glycolysis under anerobic conditions. Since the pathway from pyruvate to acetaldehyde and ethanol involves the activities of pyruvate decarboxylase (PDC) and alcohol dehydrogenase (ADH), it was striking that transcript abundance of the gene encoding the corresponding ADH1 protein was not enhanced by sylA. This might be explained by the findings that normal levels of *Adh1* expression were shown to be critical for plant survival under low oxygen conditions and that increased expression of ADH did not affect hypoxia tolerance (Dolferus et al., 2003; Ismond et al., 2003). Moreover, PDC was found to be the main regulatory enzyme in this pathway (Kürsteiner et al., 2003).

In Arabidopsis, four genes encode PDC proteins. Among them, *Pdc1* is the main anaerobically induced gene whereas *Pdc2* is constitutively expressed at low levels (Ismond et al., 2003). In addition, the onset of cellular fermentation in sylA-treated cells was emphasised by transcriptional induction of the *Ldh1* (*lactate dehydrogenase 1*) gene (Table 4.5, At4g17260, row #25) encoding an enzyme which catalyses the lactate fermentation pathway from pyruvate to lactate.

High glucose levels stimulate glycolysis. If the increasing glycolytic rate exceeds that of the glycolytic enzyme pyruvate dehydrogenase, responsible for metabolising pyruvate to acetyl-CoA, the activity of PDC directing carbon flow via ethanolic fermentation can be stimulated (Gass et al., 2005). Furthermore, pyruvate is a strong activator of AOX as shown in both soybean (Day et al., 1994; Millar et al., 1993) and tobacco (Vanlerberghe et al., 1995). In this way, electron transport to AOX might help support high rates of carbon flow and helps to modulate pyruvate levels when electron flux through the Cyt pathway is saturated or limited (Vanlerberghe et al., 1995).

However, induction of genes encoding AOX in sylA-treated plants seems not to prevent the engagement of these fermentative activities by the accumulation of pyruvate.

The fact that *Pdc1* overexpression improves low oxygen stress survival only when sugar supply is adequate explains why sugar availability strongly enhances anoxia tolerance (Vartapetian and Jackson, 1997). Interestingly, we observed transcriptional induction of sucrose degrading enzymes by sylA (Table 4.5, rows #2ff). These findings suggest that syringolin application may reflect a physiological situation similar to hypoxia.

This is supported by the observation that syringolin enhanced transcript abundance of a gene encoding a class 1 nonsymbiotic hemoglobin (Table 8.3, At2g16060, row #1195). Overexpression of the class 1 hemoglobin gene, *Glb1* from *Lotus japonica* in potato tubers leads to the formation of hypertrophic lenticels and to higher internal oxygen concentrations in growing tissue (Geigenberger, 2003) indicating that GLB1 might directly interact with a cellular oxygen sensing system.

To test the correspondence between syringolin and anoxia-related gene expression, publicly available microarray data obtained from six-day-old seedlings of *Arabidopsis thaliana* (ecotype Columbia *glabra*) treated under anoxia for six hours (Loreti et al., 2005) were compared to expression patterns obtained in sylA-treated plants. Similar statistical filtering criteria for relevant genes were used in both experiments. A detailed overview of statistical parameters applied to both experiments is given in table 8.7 (Appendix G).

In accordance with sylA-experiments, in anoxic plants the expression of more genes was repressed than enhanced (135 genes ≥ 2-fold upregulated, 344 genes ≥ 2-fold downregulated). This might result from decreasing ATP availability and was reflected by an inhibition of various metabolic processes in both systems. Of the 5339 genes whose expression was altered more than 2-fold by syringolin in

uninfected plants 8-12 hat (Student's t-test, no MTC), transcript abundance of 148 genes was similarly altered more than 2-fold in plants exposed to anoxia.

A strong overlap of more than 2-fold differentially expressed genes was found for transcripts encoding auxin-responsive proteins whose expression was dramatically repressed under oxygen deprivation and syringolin treatment, respectively. Moreover, this also encompassed several members of the cytosolic small Hsp family, suggesting that Hsps which were hypothesised to support recovery from stress induced by sylA might similarly play a role in survival at low oxygen concentrations.

In addition, transcripts of the *Pdc1* gene that strongly accumulated in sylA-treated plants (Table 4.5, At4g33070, row #26), also exhibited dramatic increase in abundance in plants exposed to anoxia. Therefore, these data support the hypothesis that syringolin indeed triggers an anoxia-like response.

Fermentative activities are responsible for the synthesis of acetaldehyde, ethanol, and lactate that may be toxic to plants, leading to a slow death process, despite plants being in external aerobic conditions (Gaston et al., 2002). In line with that, syringolin application dramatically enhanced the expression of a gene encoding glutamate decarboxylase 1 (Table 8.3, At5g17330, row #172), a Ca^{2+}/calmodulin-dependent enzyme that converts glutamate to GABA (γ-aminobutyric acid) which has been proposed to play a role in counteracting cytosolic acidification during anoxia (Gout et al., 2001) and is essential for the restriction of ROS levels in plants (Bouche et al., 2003).

In summary, genes transcriptionally preventing damage or facilitating recovery to maintain cell survival were induced by syringolin. As detailed above, this encompassed a number of transcripts encoding enzymes of the alternative mitochondrial electron pathway that allow maintenance of NAD(P)H oxidation and decrease in ROI formation as well as enzymes involved in fermentation. In addition,

the accumulation of transcripts encoding heat shock proteins/chaperones may increase the capability to disaggregate, refold, and renature misfolded proteins and offset the otherwise fatal consequences of damaging stimuli. Moreover, transcriptional induction of prohibitin, exhibiting anti-apoptotic activities, might also contribute to promote cell survival.

5.3.5 Transport and detoxification

Several cellular transport-processes appeared to be strongly inhibited by sylA as indicated by a high number of respective genes whose expression was downregulated (Figure 4.13). Repression of lipid, sugar, amino acid, and oligopeptide transport might directly correlate with an inhibition of various metabolic processes by sylA as described above.

Surprisingly, syringolin seems to inhibit water efflux, reflected by decreased expression of several genes encoding major intrinsic proteins (MIP), such as aquaporines, which are localised at the vacuolar membrane (TIPs, Tonoplast Intrinsic Proteins) and the plasma membrane (PIPs, Plasma membrane Intrinsic Proteins, Table 8.3, rows #1772ff). An inhibition of water channel activity in roots was described as a result from a drop in cytosolic pH associated with low-oxygen stress (Tournaire-Roux et al., 2003). One may speculate that sylA-dependent repression of genes encoding proteins involved in water transport activities represents a consequence of acidification caused by accumulating fermentation products such as acetaldehyde, ethanol, and lactate. In addition, downregulation of genes encoding plasma membrane intrinsic proteins (PIPs) hints at a mechanism that minimises water flow through cell membranes, which in turn might counteract further loss of turgor during drought stress.

SylA application lead to increased transcript levels of genes generally associated with detoxification. This included members of the MATE (Multidrug And Toxic compound Extrusion) and ABC (ATP-Binding Cassette) transporter families as well as glutathione-S-transferases (Figure 4.13 and 4.15, Table 8.3, rows #1565ff, 1646ff, 1898ff). ABC-transporters catalyse the efflux of drugs by utilising the energy released upon the hydrolysis of ATP.

Moreover, syringolin increased transcript abundance of genes encoding members of the syntaxin family. Syntaxins are components of vesicle-trafficking. Among them, SYP121 (Table 8.3, At3g11820, row #1769) was postulated to have a function during pathogen-defence, such as the production of large vesicles at infection sites that stain positively for hydrogen peroxide and were implicated to have a function in cell wall strengthening, defence signalling, and antimicrobial activity (Collins et al., 2003). SYP122 (Table 8.3, At3g52400, row #1770) is involved in defence against a broad range of bacterial, viral, and fungal pathogens (Assaad et al., 2004) and is phosphorylated in response to the bacterial elicitor flagellin (Nuhse et al., 2003). Accordingly, it is likely that upregulation of SYP122 and possibly other components of the membrane trafficking machinery by syringolin could play a role in diffuse secretion.

In summary, the functional group of transport-related proteins encompassed a high number of putative detoxifying and secretory proteins whose corresponding transcripts accumulated upon sylA treatment. This may indicate that activities related to cellular detoxification were enhanced in sylA-treated cells. However, it has to be mentioned that ABC transporters are also involved in various cellular processes such as plant growth and development (Martinoia et al., 2002).

5.3.6 Hormones

Syringolin application enhanced transcript abundance of ABA (abscisic acid)-responsive genes (Table 8.3, rows #951f) and a gene involved in ABA biosynthesis (Table 8.3, At1g16540, row #953). Furthermore, one gene that exhibited high transcript abundance encoded the ABI3-interacting protein 2, a member of the zinc-finger transcription factor family (Table 8.3, At5g20910, row #604). Mutation in *Abi3* causes ABA insensitivity (Koornneef et al., 1984). In contrast, syringolin also induced the expression of *Era1* (Table 8.3, At5g40280, row #954), encoding a negative regulator of the ABA-response during germination (Cutler et al., 1996). However, upregulation of *Era1* (*Enhanced response to ABA 1*) might occur in the context of negative feedback tuning ABA signalling. Yet, sylA-dependent downregulation of the *Fry1* (*Fiery 1*) gene (Table 8.3, At5g63980, row #956), encoding an inositol polyphosphate 1-phosphatase, favours a role of sylA in stimulating ABA-responses, because mutation of the *Fry1* gene has been found to dramatically enhance the expression of ABA- and stress responsive genes (Xiong et al., 2001).

In general, ABA enhances seed dormancy and is involved in drought stress response regulating transpiration by reducing water loss via rapid induction of stomata closure (Buchanan et al., 2001). As detailed above, syringolin reduced transcript accumulation of genes encoding aquaporines indicative for cellular drought stress. In addition, syringolin exerted a dramatic inhibitory effect on cell wall modifying genes (Table 8.3, rows #59ff), which might result from reduced cellular turgor pressure during water deficiency which is important for cell extension. Accordingly, it can be speculated that ABA-responsive gene expression was enhanced due to celluar drought stress which might be stimulated in sylA-treated cells.

Surprisingly, the expression of a high number of auxin-responsive genes was downregulated by syringolin (Figure 4.14, Table 8.3, rows #904ff). As noted before, similar negative effects on auxin-related gene expression were also found during anoxia. It has been suggested that either auxin level or signalling is altered by anoxia (Loreti et al., 2005). In addition, it was found that H_2O_2 can negatively regulate the auxin response (Kovtun et al., 2000).

Syringolin application also alters the transcript abundance of genes involved in ethylene-signalling. The expression of genes encoding members of the ERF (Ethylene Response Factor) transcription factor family increased and decreased by approximately equal numbers after syringolin treatment (Table 8.3, rows #963ff, 972ff, Figure 4.14) which gives only weak information of sylA-dependent interference with ethylene signalling. However, syringolin was found to induce the expression of *Ein4* encoding an ethylene receptor (Table 8.3, At3g04580, row #960).

Only few genes involved in the jasmonate hormone response exhibited responsiveness towards syringolin (Figure 4.14). The expression of the *Lox1* gene, encoding lipoxygenase 1 (Table 8.3, At1g55020, row #981), which is involved in jasmonic acid biosynthesis, was upregulated by sylA, whereas transcript abundance of the *Lox2* gene (Table 8.3, At3g45140, row #985) was lowered by sylA. These findings correspond to results obtained in senescencing Arabidopsis leaves (He et al., 2002). However, the expression of more genes encoding senescence-associated proteins was downregulated by syringolin (Table 8.3, rows #1806f and 1841ff), indicating that sylA may rather counteract senescence.

To conclude, it remains an open question whether ABA is an integral part of the syringolin action or whether regulatory factors involved in ABA-signalling were upregulated due to secondary effects exerted by sylA. Furthermore, syringolin exerted

dramatic repressive effect on auxin-related gene expression whereas the accumulation of distinct transcripts indicates the induction of ethylene-signalling. Finally, a role for jasmonate as a part of the syringolin response could not be defined.

5.3.7 Transcription factors

Genes encoding transcription factors (TFs) whose expression was altered by sylA included several major families. While transcripts encoding basic helix-loop-helix and Myb TFs were predominantly downregulated by sylA (Table 8.3, rows #1373ff, #1456ff), bZIP, HSF, NAM and WRKY TF transcripts increased in abundance (Table 8.3, rows #1247ff, 1266ff, 1283ff, 1324ff and figure 4.12).

A further group of TFs is formed by the DREB (Drought Responsive Element Binding) TF family. Members belonging to the subfamily A-2 of the DREB TF family, which are involved in drought and salt stress tolerance (Liu et al., 1998), were transcriptionally upregulated by sylA (Table 4.10, rows #1ff), one of them dramatically in both infected and uninfected plants (Table 4.10, At2g38340, row #1). In contrast, several members of subfamilies A4 to A6 of the DREB TF family that so far have not been implicated in drought tolerance were downregulated by sylA (Table 4.10, rows #6ff).

The complexity of plant drought response is represented by the existence of four transcriptional regulatory systems, of which two are ABA-independent and two are ABA-dependent (Shinozaki and Yamaguchi-Shinozaki, 2000). Members of the DREB A2 family function in the ABA-independent drought response, however, crosstalk between these pathways has been suggested (Narusaka et al., 2003).

Interestingly, transcriptional responsiveness of several TF genes involved in drought stress tolerance, together with enhanced transcript abundance of genes encoding proteins involved in ABA signalling as well as transcriptional repression of

water channel proteins suggests that in Arabidopsis, syringolin indeed triggers a drought stress response.

A second group of genes encoding transcription factors is formed by the NAM (No Apical Meristem) protein family. The expression of the majority of NAM TF genes was enhanced by sylA. NAM TFs are involved in plant development and morphogenesis (Souer et al., 1996). Moreover, members of the superfamily of NAC (petunia NAM and Arabidopsis ATAF1, ATAF2, and CUC2) proteins, to which NAM proteins belong, share a conserved role in hormone control and defence responses (Collinge and Boller, 2001), and NAC proteins were postulated to improve resistance against drought stress, as some of them exhibit ABA-responsiveness (Fujita et al., 2004). Thus, NAM proteins may also contribute to improve dehydration tolerance that seems to be triggered by syringolin in Arabidopsis. Global alteration of transcript abundance of Arabidopsis genes can be examined using the Genevestigator database which collects hundreds of microarray expression data sets. The Genevestigator database can be retrieved from www.genevestigator.ethz.ch (Zimmermann et al., 2004). This revealed that the gene encoding the NAM transcription factor ANAC094, which exhibited strongest expression upon sylA treatment (Table 4.10, At5g39820, row #26), was not enhanced by drought stress but strongly inducible by ozone. Since the toxicity of ozone is linked with an increase of reactive oxygen species (Sharma and Davis, 1994) it is tempting to speculate that the expression of *ANac094* was enhanced by the accumulation of reactive oxygen species (ROS). Accordingly, besides assuming that syringolin lead to cellular drought stress in Arabidopsis, these results suggest that syringolin might also trigger ROS accumulation and oxidative stress.

Further proteins transcriptionally activated by sylA belonged to the family of WRKY TF proteins. Members of this family (74 in Arabidopsis) have diverse biological functions ranging from stress responses to development (Kalde et al., 2003). Interestingly, the two developmental processes in which WRKY transcription

factors were implicated are trichome development and senescence (Johnson et al., 2002; Robatzek and Somssich, 2002).

Wrky6, which was transcriptionally induced by sylA (Table 4.10, At1g62300, row #38) exhibited enhanced transcript abundance in senescent leaves as well as in response to infection by pathogenic bacteria (Robatzek and Somssich, 2001). Accordingly, by enhancing transcript abundance of *WRKY6*, syringolin-treated plants might indirectly regulate the expression of a number of leaf senescence-associated genes.

5.3.8 Defence-related proteins

The *Pad4* and *Eds5* genes encoding a triacylglycerol lipase and a homolog of the MATE transporter family, respectively, are functionally involved in the accumulation of salicylic acid during infection with virulent *Pseudomonas syringae* (Glazebrook, 2001; Nawrath et al., 2002). In Arabidopsis, PAD4 and EDS5 also play a role in the resistance towards the virulent powdery mildew strain *Erisyphe orontii*, indicating that PAD4 and EDS5 play key roles in defence signalling pathways (Reuber et al., 1998).

Moreover, syringolin induced the expression of two genes encoding CLH1 (chlorophylase1) and CLH2 (Table 8.3, At1g19670, At5g43860, rows #1149 and 366) responsible for chlorophyll breakdown which was postulated to be correlated with senescence (Tsuchiya et al., 1999). Interestingly, the gene encoding CLH2 was upregulated by sylA, indicating chlorophyll degradation and possibly the onset of senescence, whereas CLH1 was transcriptionally repressed by sylA. Kariola and co-workers (2005) found that silencing of *Clh1* resulted in reduced lesion formation and was correlated with enhanced pathogen resistance. This was interpreted to be caused by higher ROS-levels resulting from an accumulation of phototoxic

chlorophyll which in turn might strongly enhance SA-dependent defence. These results, together with transcriptional induction of PAD4 and EDS5, which are both involved in the accumulation of SA, indicated that effects triggered by syringolin might directly involve SA or SA-related pathways.

Syringolin was also found to downregulate several disease resistance genes (Table 8.3, rows #1151ff), genes encoding phenylalanine ammonia-lyases (Table 8.3, rows #336ff) required for flavonoid and isoflavonoid synthesis (Dixon et al., 2002), trypsin-inhibitory proteins (Table 8.3, rows #1172ff), and several pathogenesis-related (PR) proteins (Table 8.3, rows #1162ff). Interestingly, the gene encoding PR-1 was identified as the gene that exhibited strongest induction values one hour after syringolin application on uninfected plants (experiment S1, Table 4.11, At2g14610, row #38). The expression of *Pr-1* decreased 8-12 hours after treatment (experiment S12), enhancing the assumption that syringolin indeed might suppress plant defence.

In summary, the accumulation of transcripts encoding enzymes of the alternative mitochondrial electron pathway may indicate that syringolin affects mitochondrial integrity. In this context, the activation of the alternative mitochondrial pathway could help to counteract a high reduction state of the ubiquinol pool possibly resulting from an inhibition of the cytochrome pathway. Transcripts encoding mitochondrial and cytosolic heat shock proteins that assist to renature misfolded proteins may support recovery from stress induced by syringolin. At the same time, metabolism seems to switch to cellular fermentation. In general, induction of the mitochondrial alternative pathway and cellular fermentation provoke a decreasing cellular ATP/ADP ratio. This can stimulate glycolysis. Interestingly, syringolin application lead to an increase of transcripts encoding enzymes involved in sucrose degradation and glycolysis. Strong transcriptional induction of fermentative and glycolytic enzymes may indicate that syringolin triggers an anoxia-like response in Arabidopsis.

In addition, it appears that syringolin also triggers a drought stress response as reflected by the upregulation of genes related to ABA-signalling and genes encoding members of the DREB transcription factor family functioning in the ABA-independent drought stress response.

We found indications that syringolin induces salicylic acid-dependent pathways. Moreover, we speculate that syringolin-dependent induction of a high number of genes involved in protein degradation may directly allow the plant to influence the presence of key components of disease resistance in plants. However, the expression of many disease resistance genes was downregulated by syringolin, indicating an inhibition of cellular defence. This may likely be a consequence of far reaching inhibition of many biosynthetic processes which occurs during low oxygen metabolism and impaired ATP supply (Geigenberger, 2003).

5.4 Transcriptome analysis of the syl_404 mutant

An EMS-mutant screen for the identification of plants that react insensitively towards syringolin treatment revealed one confirmed mutant, designated syl_404. Sporulation efficiency on syl_404 was significantly enhanced upon syringolin treatment compared to infected and syringolin-treated wild-type plants (Figures 4.22 and 4.23).

Microarray analysis was performed to compare expression patterns in syl_404 and wild-type plants upon syringolin treatment. For five genes, the expression was induced in the wild type but repressed in syl_404 (Table 4.17). At present we can only speculate that downregulation of these genes in syl_404 could favour fungal growth on plants treated with syringolin. The transcription factor WRKY53 (Table 4.17, At4g23810, row #5) was found to be expressed during early events of leaf senescence (Hinderhofer and Zentgraf, 2001). Inhibition of senescence-related *WRKY53* expression in syl_404 indicates that syl_404 plants might be able to counteract senescence-related gene expression.

Inspection of raw values obtained from control- and syringolin-treated syl_404 plants revealed high expression of many genes already without syringolin treatment. As is obvious from figure 4.25 and table 8.6 (Appendix F), many transcripts were present in the category of proteins involved in abiotic and biotic stress tolerance. Interestingly, transcripts of genes encoding proteins related to cellular drought stress, including proteins involved in abscisic acid (ABA)-signalling, which is the major hormone involved in water balance and in the response to dehydration stress, exhibited strong expression already in control-treated syl_404 plants (Table 4.18, rows #1ff, Table 8.6, rows #15ff).

Assuming that enhanced expression of ABA-responsive genes may directly be associated with an accumulation of endogenous ABA, one may speculate that syl_404 plants exhibit elevated ABA levels. Interestingly, enhanced ABA levels correlate with increased susceptibility to pathogens (Mohr and Cahill, 2003; Thaler and Bostock, 2004). With regard to ABA-induced susceptibility, it is worth noting that several fungal pathogens can produce ABA (Crocoll et al., 1991). Current evidence suggests that ABA affects disease resistance mainly negatively by interfering with salicylic acid-based resistance (Audenaert et al., 2002). Assuming that syl_404 plants indeed accumulate high levels of endogenous ABA this could explain why syl_404 plants exhibit increased susceptibility to powdery mildew infection upon syringolin treatment.

The majority of transcripts related to ABA-signalling and dehydration stress revealed similarly high expression in control- and syringolin treated syl_404 plants. In contrast, transcripts of genes encoding members of the small heat shock protein (sHsp) family accumulated stronger in syringolin-treated than in control-treated syl_404 plants and stronger than in wild-type plants (Table 4.18, rows #30ff). Small Hsps were found to protect cells from the detrimental effects such as heat (Lee et al., 1997), desiccation (Wehmeyer et al., 1996), and osmotic stress. Thus, enhanced expression of genes encoding sHsps may promote cell survival in the syl_404 mutant.

As detailed before, we have identified 13 genes exclusively upregulated in infected sylA-treated wild-type plants (IS12). We hypothesised that these transcripts might be linked to the occurrence of HR in infected and sylA-treated tissue which was correlated with a restriction of powdery mildew growth (see chapter 5.2). Interestingly, of these 13 genes only two, At2g34930 and At3g04630 (Table 4.3, rows #1, 3), exhibited m/wt ratios ≥ 2 in control- and syringolin-treated syl_404 plants, respectively.

Since sporulation efficiency of powdery mildew was less restricted in syl_404 compared to wild-type plants upon syringolin treatment, this is compatible with the hypothesis that at least some of the 13 genes may indeed be associated with fungal growth restriction and the occurrence of HR in sylA-treated wild-type plants.

Moreover, we have identified 60 genes downregulated by sylA in uninfected wild-type plants (S12) but upregulated by fungal infection (I60). We hypothesised that the encoded proteins might represent candidates that favour fungal life to varying extent (see chapter 5.2). We investigated whether these genes exhibited high transcript levels in syl_404 plants. While none of the genes revealed high expression in syringolin-treated syl_404 plants, transcripts of 10 genes accumulated to a stronger extent in control-treated syl_404 compared to control-treated wild-type plants. These genes are highlighted in bold in table 8.2 (Appendix C). In addition, two genes whose expression was upregulated by syringolin but downregulated by fungal infection in wild-type plants also exhibited m/wt ratios ≤ 2 in control-treated syl_404 plants (Table 4.4, At1g15180, At5g12110, rows #3, 7), and one gene exhibited a m/wt ratio ≤ 2 in syringolin-treated syl_404 plants, respectively (Table 4.4, At5g08600, row #6). Thus, one may speculate that abundances of these transcripts specific for fungal infection contribute to support powdery mildew reproduction in syl_404.

In summary, transcriptional profiling revealed elevated expression of many stress-responsive genes in syl_404 plants already without syringolin treatment, indicating basal expression of these genes in non-treated syl_404 plants, or, perhaps less likely, induction by control treatment. Members of the small Hsp family that exhibited strong expression in syringolin-treated syl_404 plants may contribute to enhance cell survival, which can directly promote powdery mildew reproduction after

sylA application. In addition, gene expression specific for fungal infection may similarly support powdery mildew reproduction in syl_404 plants.

Beyond this, we hypothesise that elevated abundance of transcripts encoding proteins related to ABA-signalling in syl_404 plants may indicate elevated levels of ABA. Since ABA is a key factor in the suppression of disease resistance, higher ABA levels in syl_404 plants may represent the factor that promotes susceptibility to powdery mildew infection. In general, endogenous ABA levels increase during drought stress. Whether syl_404 plants indeed suffer drought stress is speculative. High abundance of transcripts related to drought stress and ABA-signalling in syl_404 plants without syringolin-treatment may indicate that these genes exhibit increased basal expression. Nevertheless, the finding that syl_404 plants showed slight wilting upon syringolin treatment supports the assumption that syl_404 plants exhibit enhanced sensitivity to drought stress which appears to be triggered by syringolin but was never observable in syringolin-treated wild-type plants. We assume that syl_404 plants exhibit enhanced sensitivity to drought stress which is accompanied by a generally elevated transcript abundance of drought-responsive genes. We can further speculate that higher transcript abundance of these genes was associated with enhanced ABA levels and enhanced susceptibility to powdery mildew infection. Thus, relatively minor drought stress might contribute to increase susceptibility to powdery mildew in syl_404 plants.

5.5 Comparison to microarray data in publicly available databases

5.5.1 *Pseudomonas syringae* and pathogen-associated molecular patterns (PAMPs)

Publicly available microarray data from Arabidopsis infected with virulent and avirulent *avrRpm1* carrying strains of *Pseudomonas syringae* pv*. tomato* were compared to transcriptional changes exerted by sylA treatment. Microarray data were obtained from five-week-old seedlings of *Arabidopsis thaliana* (ecotype Columbia). Bacterial infiltrations were performed with 10^{-8} cfu/ml in 10 mM $MgCl_2$ and data derived from plant material collected 24 hat were compared to expression patterns obtained in experiment S12 where plant material was collected 8-12 h after sylA application. An overview of statistical parameters applied to the experiments and corresponding references are given in table 8.7 (Appendix G). The overlap of genes differentially expressed in Arabidopsis after syringolin treatment or infiltration with virulent and avirulent strains of *P. syringae* pv*. tomato* is given in figure 5.4.

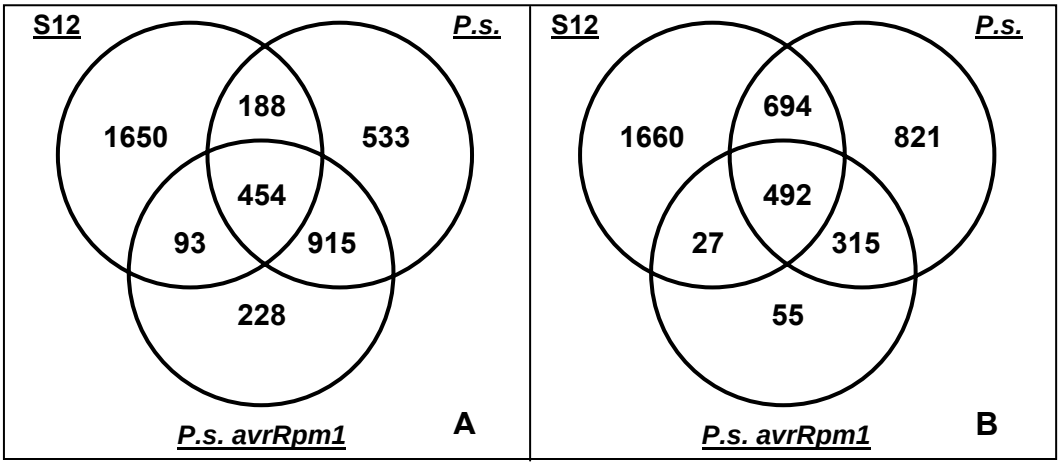

Figure 5.4 Overlap between genes more than 2-fold differentially expressed after bacterial infiltration and syringolin treatment

The Venn Diagram represents the distribution of significantly (p-value ≤ 0.05, MTC) upregulated (A) and downregulated (B) genes in Arabidopsis infiltrated with virulent (*P.s*) and avirulent (*P.s. avrRpm1*) strains of *P. syringae* pv. *tomato* and in plants upon syringolin treatment (S12).

As shown in figure 5.4., a high number of genes was similarly regulated by syringolin and the virulent bacterial strain (*P.s.)*, although fewer genes were found in the overlap between genes differentially expressed by syringolin and the avirulent strain of *P. syringae* pv*. tomato* (*P. s. avrRpm1*)*.*

Genes upregulated by sylA, avirulent and virulent strains of *P. syringae* pv*. tomato* encoded proteins belonging to different families of heat shock proteins (Hsps), predominantly members of the small Hsps family and heat shock transcription factors. In addition, this also included genes encoding components of the mitochondrial alternative respiratory chain, such as subunit A of the alternative oxidase (AOX1a) and an alternative NADH dehydrogenase (NDB2). As detailed before, activation of these genes may prevent cellular damage and support recovery from stress induced by sylA. Accordingly, it seems that cells challenged with bacteria similarly require enhanced abundance of transcripts encoding proteins with protective functions possibly to counteract cellular stress imposed by bacterial infection.

Moreover, syringolin treatment and infiltration with either avirulent or virulent strains of *P. syringae* negatively affect the expression of photosynthesis-related gene expression. Since downregulation of photosynthesis was similar to that found in *P. syringae*-infected soybean (Zou et al., 2005), it seems likely that transcriptional repression of photosynthetic genes by syringolin represents a bacteria-specific effect which is provoked by syringolin.

The two virulent strains *P. syringae* pv. *tomato* DC3000 and *P. syringae* pv. *maculicola* ES4326 cause water-soaked patches on infected leaves of *Arabidopsis* plants (ecotype Columbia). This is the first sign of disease in a compatible interaction and might result from stimulation of cells to ‘leak’ nutrients and water into the intercellular space where bacteria live (Katagiri et al., 2002). Remarkably, genes

commonly upregulated in Arabidopsis by syringolin (S12) and bacterial infections with either avirulent (*P.s. avrRpm1*) or virulent (*P.s*.) strains of *P. syringae* encompassed genes encoding proteins involved in drought tolerance. This included several genes encoding DREB (Drought Responsive Element Binding) transcription factors. Among downregulated genes several encoded proteins involved in cell extension.

Interestingly, genes exclusively differentially expressed by the virulent bacterial strain and syringolin, respectively, included additional drought-responsive genes. Moreover, transcript abundance of genes encoding subunits of the 26S proteasome were also found to increase to a stronger extent in plants infected with the virulent strain. We hypothesise that protein degradation may provide a mechanism by which virulent bacteria achieve compatibility in Arabidopsis.

In summary, it appears that gene expression patterns triggered by syringolin in Arabidopsis are similar in certain aspects to transcriptional changes exerted by infiltration with bacterial strains of *P. syringae* pv. *tomato*. The fact that *P. syringae* pv. *tomato* does not produce syringolin indicates that these effects must be induced by other bacterial compounds than syringolin. In addition, syringolin-induced gene expression exhibited stronger similarity to expression patterns triggered by the virulent strain of *P. syringae* pv. *tomato.* Therefore, it is tempting to speculate that syringolin may act as virulence factor in Arabidopsis.

Basal resistance is activated by conserved pathogen-associated molecular patterns (PAMPs) such as flagellin (Felix et al., 1999), which are present in most bacteria regardless of their pathogenic potential in plants. Flagellin (flg22) was found to be involved in the induction of non-host resistance (Li et al., 2005; Shimizu et al., 2003) and Avr9-induced race specific resistance (Navarro et al., 2004). To test the similarity between the flg22 response and the effect of syringolin exerted on the transcriptome, gene chip data obtained from plants (ecotype Landsburg erecta) treated for 30-min with a 1 µM solution of flg22 (Zipfel et al., 2004) were compared to expression patterns obtained in Arabidopsis upon sylA treatment. An overview of statistical parameters applied to the experiments and corresponding references are given in table 8.7 (Appendix G).

As illustrated in figure 5.5, a high proportion of genes more that 2-fold upregulated by flg22 was similarly regulated by syringolin in Arabidopsis. However, in contrast to syringolin treatment, only a small number of genes was downregulated in flg22-treated Arabidopsis.

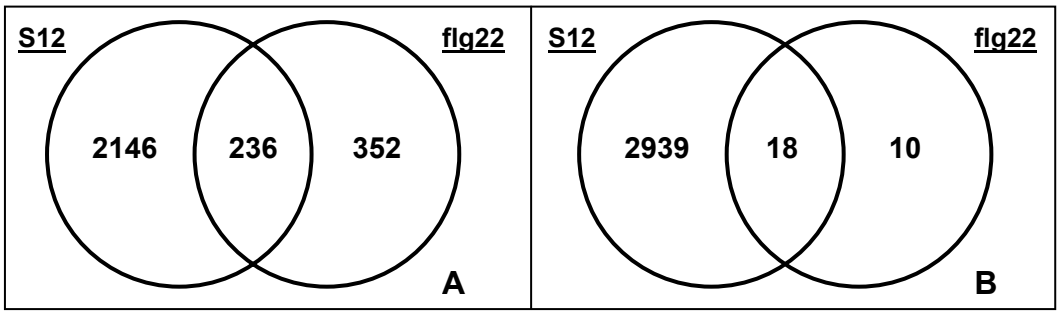

Figure 5.5 Overlap between genes more than 2-fold differentially expressed by flagellin and syringolin treatment

The Venn Diagram represents the distribution of significantly (p-value ≤ 0.05) upregulated (A) and downregulated (B) genes in Arabidopsis by flagellin (flg22) and upon syringolin treatment (S12).

Transcripts whose abundances commonly increased in Arabidopsis after syringolin and flg22 treatment included RNAs encoding receptor-like kinases, protein kinases, phosphatases, and proteins involved in calcium signalling. Therefore, it seems likely that similar defence-related pathways may be triggered in both systems. As detailed before, we found indications that syringolin may exhibit virulence activity in Arabidopsis. However, these results indicate that syringolin may also act as an elicitor in certain aspects.

5.5.2 Abiotic stress responses

Experimental clustering revealed that expression patterns obtained in syringolin-treated plants exhibit resemblance in certain aspects to expression patterns in Arabidopsis (ecotype Columbia) observed upon fumigation with ozone (500ppb) for six hours and cycloheximide (10 µM) treatment. Cycloheximide is a translational inhibitor whereas ozone was found to trigger the production of reactive oxygen species (ROS) leading to an oxidative burst (Schraudner et al., 1998). In addition, we investigated transcriptional changes in 14-day-old Arabidopsis cell cultures (ecotype Landsburg erecta) one hour after heat treatment. Expression patterns were also investigated in Arabidopsis protoplasts (ecotype Landsburg erecta) treated with the PCD-inducing mycotoxin Fumonisin (20 mM). RNA was extracted at timepoints where 0%, 20% and 30% of protoplast had died in this experiment. An overview of statistical parameters applied to all experiments and corresponding references are given in table 8.7 (Appendix G).

Expression patterns obtained in plants upon heat stress and treatment with fumonisin exhibited only weak similarity to the expression patterns triggered in plants by syringolin. In contrast, many genes whose transcript levels were altered more than 2-fold by syringolin (S12) were similarly altered in plants treated with cycloheximide and in plants exposed to ozone (Figure 5.6).

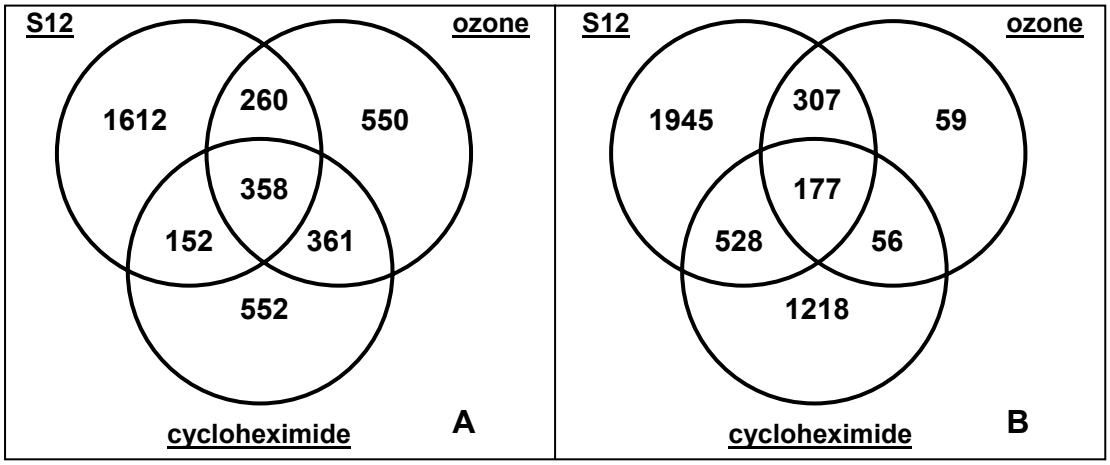

Figure 5.6 Overlap between genes more than 2-fold differentially expressed by syringolin, ozone, and cycloheximide.

The Venn Diagram represents the distribution of significantly (p-value ≤ 0.05) upregulated (A) and downregulated (B) genes in plants by syringolin (S12), cycloheximide, and exposure to ozone.

Among genes commonly upregulated by ozone and syringolin (Figure 5.6 A), a high number encoded heat shock proteins (Hsps), including several members of the small Hsp family, heat shock transcription factors as well as subunit 1a of the alternative oxidase (AOX1a). The AOX1a and a 23.5 kDa mitochondrial Hsp were similarly transcriptionally upregulated by cycloheximide, ozone and syringolin. The encoded proteins support recovery from stress, predominantly imposed on mitochondria. Accordingly, it seems likely that ozone and cycloheximide affect mitochondrial integrity, similar to the effect exerted by syringolin in Arabidopsis.

Transcripts whose abundances were commonly lowered by syringolin, cycloheximide, and ozone (Figure 5.6 B) encompassed various functional groups of genes. Among them, a prominent group included genes encoding proteins involved in photosynthesis, indicating that syringolin, cycloheximide, and exposure to ozone can negatively affect photosynthetic activity in Arabidopsis.

5.6 A mutant with enhanced resistance to powdery mildew

Besides screening EMS-mutagenised plants (see chapter 5.4), in a second approach for the identification of mutants that exhibit insensitivity to syringolin, we investigated knock-out mutants harbouring T-DNA insertions in a selection of genes upregulated by syringolin. Unfortunately, none of the T-DNA insertion lines was found to exhibit enhanced sporulation efficiency of powdery mildew after syringolin treatment. Thus, despite strong upregulation of these genes by syringolin, none of them appears to encode a protein involved in the curative effect of syringolin on powdery mildew infected *Arabidopsis thaliana* plants.

However, the line isolated for a T-DNA insertion in the At4g12400 gene (encoding a stress-induced protein) revealed an effect independent of syringolin. The respective mutant line (salk_000794) showed impaired growth of the powdery mildew fungus on control and non-treated leaves. Resistance to *E. cichoracearum* on salk_000794 plants was manifested at a relatively late stage in the infection. Spores germinated on the leaf surface and developed networks of secondary hyphae on both salk_000794 and wild-type plants. However, conidiophore formation was dramatically reduced on salk_000794 plants.

Interestingly, this phenotype was similar to the one observed in powdery mildew infected Arabidopsis *edr1* (*enhanced disease resistance 1*) mutants. The *edr1* mutant displays enhanced resistance to *E. cichoracearum*, but does not constitutively express pathogenesis related genes (Frye and Innes, 1998). These observations suggest that the resistance response in *edr1* and salk_000794 plants affects the fungus primarily after onset of conidiophore formation at day four, indicating that the fungus is stopped at a relatively late stage.

The respective gene (At4g12400) was induced in infected syringolin-treated plants 2-4 hat (IS4) and its expression increased in uninfected tissue 8-12 hat (S12). General transcript levels of At4g12400 were compared in the Genevestigator database (Zimmermann et al., 2004). This revealed transcriptional induction of At4g12400 by different chemical compounds. In addition, transcript abundance was enhanced by heat and upon challenge with *Pseudomonas syringae*. Whether salk_000794 displays resistance to *P. syringae* or whether the encoded protein represents a susceptibility factor for these bacteria remains to be determined. However, transcript abundance of At4g12400 was not enhanced by fungal infection (I60). Therefore, basal expression of At4g12400 seems to be sufficient to promote fungal growth. Alternatively, upregulation of the gene may occur in the course of later infection stages at the onset of sporulation.

Recently, we have isolated a second plant homozygous for an independent T-DNA insertion in the genomic sequence of At4g12400 which exhibits reduced sporulation of powdery mildew. Thus, this supports the assumption that non-functionality of the At4g12400 gene indeed negatively affects powdery mildew reproduction in Arabidopsis.

How non-functionality of the At4g12400 gene enables powdery mildew reproduction is not clear. It is conceivable that the corresponding gene product functions as an inhibitor of a certain resistance gene that now responds to *E. cichoracearum*. The identification of a homologous gene in soybean which is inducible by heat shock (Hernández Torres et al., 1995) let us assume that the At4g12400 encoded protein may similarly be involved in cellular stress responses. Speculating that the At4g12400 encoded protein in Arabidopsis has a function in counteracting cellular stresses, the absence of the protein may provoke excessive cellular stress in the infected plant, which in turn can negatively affect successful reproduction of the biotrophic pathogen.

5.6 Conclusions and outlook

Syringolin A was originally hypothesised to directly or indirectly reprogram colonised host cells to undergo hypersensitive cell death in a compatible interaction (Wäspi et al., 2001). In order to better understand the effect of sylA at the molecular level, the aim of this thesis was to monitor transcriptional changes accompanying the HR triggered by sylA in powdery mildew-infected plants. Microscopic investigations revealed that syringolin inhibits powdery mildew reproduction in both Arabidopsis and cereals in a phenotypically similar way. This offered the possibility to investigate transcriptional changes underlying the syringolin response by using the Arabidopsis full genome gene chip. Unexpectedly, microarray experiments revealed that in uninfected plants, syringolin changed the expression of more genes than in infected plants, and transcripts accumulating in infected plants also accumulated, to even higher levels, in uninfected plants. These results lead to the hypothesis that the cellular response to syringolin was negatively controlled by powdery mildew infection in colonised and neighbouring cells. Changes in transcript abundance by syringolin specific for infected tissue could be shown for 13 genes. We hypothesise that these genes might be linked to the occurrence of HR, although it is not clear whether this is a cause or a consequence of HR. In addition, these few genes were induced only weakly.

The functional annotation of proteins encoded by sylA-affected transcripts lead to the hypothesis that sylA affects mitochondrial function and oxidative phosphorylation. There is evidence that sylA induces a switch to a fermentative metabolism. Direction of electron flux via cellular fermentation could help to avoid overreduction of the ubiquinone pool. In this context, the induction of genes encoding enzymes of the alternative mitochondrial electron pathway supports the assumption that mitochondria in syringolin-

treated cells indeed are overflooded with reductive substrate and that the mitochondrion may represent a target of the syringolin action. If we assume that mitochondrial alternative pathways and cellular fermentation are activated in sylA-treated cells, we expect a decreasing ATP/ADP ratio. Thus, the observed inhibition of metabolic processes and energy consuming defence pathways by syringolin may likely be a consequence of impaired cellular energy supply. We speculate that metabolic changes and the switch to alternative pathways may be achieved and regulated by selective removal of proteins by the activity of the 26S proteasome. Impaired mitochondrial function may directly or indirectly lead to enhanced cellular stress in sylA-treated cells. In this context, the accumulation of transcripts encoding protective proteins may be viewed as a response of the plant to counteract the stress imposed by syringolin. If the assumption holds true that the observed reduced sylA response of powdery mildew-infected tissue may be due to a suppressive effect on gene expression the fungus exerts in colonised and neighbouring cells, then the HR in infected and sylA-treated Arabidopsis could be the result of the pathogen-induced suppression of gene expression that may lead to insufficient production of protective proteins.

Assuming that the mitochondrion may represent a direct target in the syringolin response, future work will focus on the ability of syringolin to directly or indirectly inhibit electron flow via the mitochondrial cytochrome pathway. Therefore, changes in the membrane potential of isolated mitochondria could be monitored as recommended by Yao et al. (2002). Alternatively, respiratory rates could be monitored on isolated mitochondria treated with sylA. In addition, determination of acetaldehyde and ethanol concentrations in syringolin-treated tissue would provide evidence whether products of ethanolic fermentation indeed accumulate upon syringolin treatment.

Another approach for the elucidation of the syringolin response in Arabidopsis could focus on the investigation of knock-out mutants harbouring T-DNA insertions in a selection of genes upregulated by syringolin. Investigation of 11 loss-of-function mutants for insensitivity to syringolin, e.g. enhanced sporulation efficiency of powdery mildew after syringolin treatment, revealed no candidate. A mutant harbouring a T-DNA insertion in the *Sti1-like* gene (At4g12400) revealed an effect independently of syringolin, i.e. showed impaired sporulation of the powdery mildew fungus on non-treated leaves. A second mutant line homozygous for an independent T-DNA insertion in the genomic sequence of At4g12400 revealed a similar phenotype, thus supporting the assumption that non-functionality of the *Sti1-like* gene (At4g12400) indeed negatively affects powdery mildew reproduction in Arabidopsis. The fungus is only affected at the sporulation stage on the At4g12400 mutant. Sporulation may be particularly stressful for the host plant. Thus, the At4g12400 encoded protein may be necessary to keep colonised cells alive long enough for the fungus to complete its live cycle. Currently, we are investigating whether basal expression of At4g12400 is sufficient to promote fungal growth or whether upregulation of the gene may occur in the course of later infection stages at the onset of sporulation.

An unexpected aspect of the syringolin response is represented by the finding that syringolin also triggers a drought stress response in Arabidopsis as reflected by the upregulation of genes related to ABA-signalling and genes encoding proteins involved in the ABA-independent drought response. In this context, it is intriguing that virulent strains of *Pseudomonas syringae* cause water-soaked patches on infected leaves of Arabidopsis plants as a visible sign of nutrient and water leakage into the intercellular space. Whether the syringolin triggered drought response may be related to bacteria-induced water leakage observed in Arabidopsis

is speculative. In any case, the finding that syringolin-induced gene expression exhibited stronger similarity to expression patterns triggered by the virulent strain of *P. syringae* suggests that syringolin may act as virulence factor in Arabidopsis.

Remarkably, the topic of a drought stress response recurred with regard to the phenotype of a mutant with reduced resistance to powdery mildew infection upon syringolin treatment. This mutant revealed enhanced abundance of ABA-related transcripts without syringolin treatment. We hypothesise that this was associated with elevated endogenous ABA-levels in these plants. Because endogenous ABA can suppress disease resistance, this would explain why syl_404 plants exhibit enhanced susceptibility to powdery mildew infection upon syringolin treatment. Unexpectedly, syl_404 mutant plants exhibited slight wilting upon syringolin treatment whereas wilting was never observed in syringolin-treated wild-type plants. Syringolin was found to induce the accumulation of transcripts encoding proteins involved in the ABA-dependent and ABA-independent drought response in wild-type plants. Thus, it is tempting to hypothesise that syringolin indeed triggers a drought stress response in Arabidopsis. We further speculate that wilting in syl_404 plants resulted from enhanced sensitivity of these plants to respond to drought stress. In addition, syl_404 plants revealed elevated abundance of many transcripts encoding stress-related proteins. Accordingly, enhanced expression of stress-related genes may help to support cell survival and thus prevent HR in infected syringolin-treated syl_404 plants. This hypothesis is compatible with the scenario developed above, i.e. that a pathogen-induced downregulation of genes encoding stress-related and protective proteins could trigger HR and resistance to powdery mildew in sylA-treated wild-type plants. Identification of the respective gene bearing the mutation by mapping using ecotype-specific PCR-based markers will help to understand the phenotypic and

transcriptional changes in syl_404 plants that underly the reduced resistance to powdery mildew infection upon syringolin treatment.

Thus, HR elicited in infected and sylA-treated plants appears not to depend on specific regulation of certain genes, but might rather represent the result of pleiotrophic effects caused by syringolin treatment and fungal invasion. Another aspect of the syringolin response was represented by the assumption that syringolin may exhibit virulence activity in Arabidopsis. It is tempting to speculate that sylA acts as an effector of *P. syringae* pv. *syringae* that helps to put host plant cells into a physiological state from which the bacteria may profit. Intriguingly, a number of effectors secreted by *P. syringae* DC3000, which exhibit virulence activity in *Arabidopsis thaliana*, have been shown to suppress the HR in nonhost plants (Abramovitch et al., 2003; Bretz, et al., 2003; Jamir et al., 2004). Thus, transcriptional changes induced by sylA in Arabidopsis could be interpreted in the light of a putative virulence activity exerted by syringolin that may include the suppression of HR. The study of syringolin-negative *P. syringae* pv. *syringae* mutants on a host plant species may help to shed light on this subject.

6 Materials and Methods

6.1 Plant material and fungal strains

Microarray experiments were carried out in the susceptible *Arabidopsis thaliana* ecotype Columbia. EMS mutagenised Arabidopsis seeds (Col-0) were purchased from Lehle Seeds (Round Rock, TX, USA). T-DNA insertion lines were obtained from the SIGnAL collection of the Salk Institute for Genomic Analysis Laboratory (Alonso et al., 2003) via the Nottingham Arabidopsis Stock Centre, http://signal.salk.edu. T-DNA insertion lines were generated in the Columbia and Wassilewskija ecotypes of *Arabidopsis thaliana*.

A culture of a powdery mildew pathogen was isolated from an infected *Arabidopsis thaliana* plant (ecotype Columbia) growing in a climate chamber at the Institute of Plant Biology in Zürich and was used throughout these studies. Database searches of the 16S rRNA sequence revealed that this strain was most closely to the two species *Erysiphe cichoracearum* and *Erysiphe orontii*. Microscopic investigations of culture specific morphological characteristics such as conidiophore foot cells and septation were performed by Prof. R. Honegger and revealed the isolation of a culture of *Erysiphe cichoracearum*.

6.2 Plant and fungal growth conditions

Four to six plants were grown in 5-cm-diameter pots filled with commercial compost (Einheitserde, Type ED 73, Buchenberg, Germany). Pots were covered with plastic wraps to ensure high humidity and were stratified for three days at 4°C before being placed in growth chambers. Plants were grown with a 16 h photoperiod (100-150 μmol m^{-2} sec^{-1}) at 21°C to 22°C and 80-90% relative humidity. Covers were removed after the seeds sprouted and the first leaves were emerging. Adult plants (12-14 days after germination) were used for experimental analysis.

For the reproduction of powdery mildew inoculum, *Arabidopsis thaliana* plants with six to eight leaves (about three to four weeks old) were inoculated weekly. Inoculation of Arabidopsis with *Erysiphe cichoracearum* was performed in a wind still chamber. Heavily infected leaves of former infection rounds were slightly dapped on the surface of four to five rosette leaves until the whole leaf surface was covered with spores. After inoculation, plants were again transferred to the growth chambers, covered with a plastic lid for 12 hours, and kept under the conditions given above.

6.3 Infections

6.3.1 Infection of plant material used for gene chip experiments

Leaves of 14-day-old plants used for RNA extraction and hybridisation of ATH1 gene chips were infected with *Erysiphe cichoracearum* by tapping highly sporulating leaves of Arabidopsis on the leaf surface of experimental plants. Infection density was quantified by single spore counting and determined to be ~200 spores/mm^2.

6.3.1.1 Estimation of proportion of powdery mildew-infected cells in Arabidopsis leaves

Microscopic investigations on leaf cross-sections revealed an average number of 6400 mesophyll cells and 160 epidermal cells on the adaxial leaf side per field of view. Estimating a similar number of epidermal cells on the abaxial side, it was calculated that the leaves consist of 95% mesophyll cells (6400 cells/field of view) and of only 5% epidermal cells (2 x 160 cells/field of view). Since the abaxial side remained uninfected in all gene chip experiments, the total number of uninfected cells corresponded to 6560 cells (6400 + 160), resulting in 2,4% adaxial epidermal cells per leaf.

Arabidopsis seedlings were infected at high spore density (~200 spores/mm^2) following protocols described above. Eighteen hours after infection, successful interactions, represented by germinated spores forming either appressoria or primary and secondary hyphae, respectively, were determined. This revealed 47 interactions on 160 adaxial epidermal cells per field of view. Accordingly, 29% of all cells on the adaxial leaf side were successfully infected by powdery mildew. Finally, it was calculated that the proportion of infected cells in relation to all cells of the leaf was 0.7% (0.29 x 0.024) on average.

6.3.2 Infection of plant material used for microscopic evaluation

Plant material used for microscopic investigations and for determination of sporulation efficiency of T-DNA insertion lines as well as of EMS-mutagenised plants was infected at ~180 spores/mm^2. Inoculation was performed with an artist's fine brush to gently dislodge conidia from highly infected leaves to avoid clotting of spores. Infected plants were held approximately two cm above experimental plants to

brush down spores on the primary leaves. Furthermore, slight blowing ensured distribution of spores on the leaf surface. Afterwards, plants were covered for 12 hours and kept under conditions described above.

6.4 Syringolin A isolation

Syringolin A was isolated from still cultures of *Pseudomonas syringae* pv. *syringae strain* B301D-R as described by Wäspi et al. (1999). Three-step purification included partition chromatography on an Amberlite XAD 16 column (2.6x 40 cm; Rohm and Haas, Philadelphia (PA), USA), reversed phase HPLC on a Nucleosil 100 7 C18 250/20 column (Macherey-Nagel, Duren, Germany), and FPLC on a Superdex 30 16/60 gel filtration column (Pharmacia, Uppsala, Sweden; for details see (Wäspi et al., 2001)).

6.5 Syringolin treatment

Syringolin treatment of infected plants was carried out 48 hours after inoculation. Plants were sprayed with distilled water containing 20 µM syringolin and 0,05% (v/v) TWEEN 20 or a control solution (0,05% (v/v) TWEEN 20). Cyprodinil (Novartis AG, Basel, Switzerland) was kindly provided by Dr. M. Oostendrop (Novartis Crop Protection AG, Basel, Switzerland). The substance was dissolved in acetone and diluted with water to a final concentration of 0,05%. The solution was sprayed as described above. Control plants were treated with the solvent only. Plant material was collected at various timepoints after treatment. For microscopic as well as molecular analyses, primary leaves were harvested, exclusively.

6.6 Microscopy

To investigate fungal infection stages by bright field microscopy and to monitor autofluorescence of plant cells, Arabidopsis leaves were destained by overnight immersion at room temperature in a 1:2 (v/v) dilution of a lacto-phenol stock solution (phenol : lactic acid : glycerol : water = 1:1:2:1) with ethanol. Fungal structures were stained with coomassie blue (0.6% (w/v)) in ethanol. Leaves were incubated for no longer than one minute in the staining solution and cleared immediately after staining in sterile water. Leaf segments were mounted onto microscopic slides in 40% (v/v) glycerol. Microscopic inspection with an Axioplan microscope (Carl Zeiss AG, Oberkochen, Germany) was done by bright-field or blue light incident fluorescence microscopy (excitation filter 450-490 nm; bypass filter 515-565 nm). Images were captured with the Magna Fire 2.0 digital camera (Optronics, Goleta (CA), USA) using auto exposure settings.

6.7 RNA extraction

Plant material was ground to a fine powder in liquid nitrogen using pestle and mortar. Alternatively, 50-100 mg plant material was homogenised with an electrical homogeniser by totally adding 750 µl of Trizol extraction buffer (Invitrogen BV, Groningen, Netherlands). Subsequently, RNA was extracted according to the manufacturer's protocol (Chomczynski and Sacchi, 1987). The RNA was then further purified using the RNeasy Kit (Qiagen, Basel, Switzerland) according to the protocols of the manufacturer.

6.8 Microarray experiments

6.8.1 Target preparation and hybridisation

The integrity of RNA used for gene chip hybridisation experiments was checked on a bioanalyser (Agilent Technologies, Inc., Palo Alto (CA), USA). For gene chip experiments described in chapter 4.1.2, double stranded cDNA was synthesised with the SuperScript kit (Invitrogen, Basel, Switzerland) using 15-20 µg total RNA as starting material. Purification was done with the Affymetrix GeneChip Cleanup module (Affymetrix, Bucks, UK). The probe was labelled with the Ambion MEGA Script T7 kit (Ambion, Huntingdon, UK) and finally purified again with the Affymetrix GeneChip Sample Cleanup module. Three independent biological replicates were performed for all experiments. For gene chip experiments performed on wild type and mutant syl_404, probe preparation was carried out according to the one-cycle target labelling and control reagent package (Affymetrix, Bucks,UK) by Marzanna Künzli-Gontarczyk (Functional Genomics Centre, Zürich). Experiments were repeated in duplicates. After purification of the cRNA, the quality of labelled cRNA was checked on a bioanalyzer (Agilent Technologies, Inc., Palo Alto (CA), USA). Fragmentation of the labelled RNA and chip hybridisation were performed as recommended by Affymetrix (Affymetrix, Bucks, UK). The technical manual was provided by Affymetrix (http://www.affymetrix.com/support/technical/manual/expression_manual.affx).

6.8.2 Data analysis

Raw data were processed with the Affymetrix Microarray Suite 5.0 software package. Data analysis was performed using GeneSpring 7.0 software (Silicon Genetics, Redwood City, CA).

Genes with an “absent” call for the detection value in all replicates of one gene chip experiment were excluded from the list (flag filtering). Furthermore, genes were filtered based on their control strength, representing a value calculated from all normalisations applied to the experiment. In the case of experiments consisting of three biological replicates, the Cross-Gene Error Model (GEM) was activated to determine between-sample variation. Thereby, deviation for each gene signal is based on how its intensities vary across replicate samples. In general, the Cross-Gene Error Model provides a more accurate estimate for the precision of a gene signal by combining measurement variation and between-sample variation information. A variance components analysis is performed using the estimates of measurement variation to estimate standard errors and to compare mean expression levels between experimental conditions. If replicates are available, the variance is calculated on the basis of biological variability (sample variation).

In the absence of visualisation or diagnostic methods (Genespring currently has none), it is safest to assume that variability may differ between treatment and control. This rules out the use of Student’s t-test. The Welch’s t-test corrects for differences in variability. Because we assumed that our data are normally distributed, Welch’s t-test was chosen, although three replicates are not enough to determine normal distribution, it is generally thought to be a reasonably safe assumption. Therefore, differentially expressed genes were identified by computing two-sample Welch’s t-test statistics based on variances calculated by the Cross Gene Error

Model including multiple test correction according to Benjamini and Hochberg (Benjamini and Hochberg, 1995). Genes that exhibited a larger than 2-fold difference in their signal values between control and treatment were extracted.

In the case of few replicates, Genespring software recommends to increase stringency of statistical filtering by assuming that variances of gene expression were equal. Thereby, parameters that had to be determined were reduced by assuming that variances of both samples were equal instead of calculating variances for the two groups. Consequently, for experiments that were based on two replicates, differentially expressed genes were identified by computing Student's t-test including multiple test correction according to Benjamini and Hochberg (Benjamini and Hochberg, 1995).

6.9 Identification of plants homozygous for T-DNA insertions

The majority of T-DNA insertion lines was obtained from the SIGnAL collection of the Salk Institute for Genomic Analysis Laboratory (Alonso et al., 2003) via the Nottingham Arabidopsis Stock Centre. The *Arabidopsis thaliana* NAM-insertion line GABI-Kat 027D08 (At5g39820) was kindly provided by Patrick Schweizer (IPK Gatersleben).

6.9.1 Primers and PCR

DNA was extracted from seedlings of M2 populations of T-DNA insertion lines according to Fulton et al. (1995). For PCR, primers flanking the insertion were used in combination with a primer corresponding to the T-DNA left border to verify plants homozygous for the T-DNA insertion. The oligonucleotides were obtained from Microsynth AG (Balgach, Switzerland) and are listed in table 6.1.

Table 6.1 Primers used for verification of homozygous T-DNA insertions

Target	Primer	Sequence (5'-3')
T-DNA left border	LBa1[1]	TGGTTCACGTAGTGGGCCATCG
	LBb1[2]	GCGTGGACCGCTTGCTGCAAC
	FLAG[3]	CGTGTGCCAGGTGCCCACGGAATAGT
	GABI-KAT[4]	CCCATTTGGACGTGAATGTAGACAC
At4g12400 (salk_000794)	Gf[5]	AGCCGATTAGGTGCTGCGTTT
	Gr[6]	TCCATCATGAAGCCATAAACCCT
At4g12400 (flag_013C07)	Gf	TGCTTCACTGCCTCTGGATAC
	Gr	GGAGAGGCAGAAGAAGGAGAG
At2g03430	Gf	AAAAATTTCCGTCATATTTTGTGA
	Gr	GATGAATCTCCCCATTCCGCT
At5g64230	Gf	TTTCACAAGGAAACTTAATTACTG
	Gr	GCCTTACTATTCAAAGAAGCCAAGG
At1g32020	Gf	CATGTTGAGTGACTTGATTCTTGA
	Gr	TCAACAAGTGCCTCAAGCCTTTC
At1g03440	Gf	TTCTGAGACCACGAACCTCGC
	Gr	TGATGTGAGTACAAAGAGAAAGA
At2g38340	Gf	CCAATTTGACATCTTCCATCAACG
	Gr	TAACGTCGCTTCCACTGGCTC
At1g22985	Gf	TGGGTTCTTTCAGGTGGGCTT
	Gr	AATCAACATCAGGACGGCCAA
At4g33070	Gf	GCCGTCACTTAGCTCGTCGTC
	Gr	CATCATCGCCAAAGCATAGCC
At3g28210	Gf	CAGCTCCCTCTTCCACACCCT
	Gr	AATATAGCCCACGAGTTTCTGA
At5g20910	Gf	CATCTTACGGTTGATCGTGAGCC
	Gr	GGAAAGACAATGGGAGTGTGCC
At5g39820	Gf	AACGGCAAAATTCAAGATTCA
	Gr	CCTTTGTTGCGGGTAAAGCAA
At5g58610	Gf	TCAACCTTTTGAGCAATTTCGGA
	Gr	GCATTGGTCTCATAAACCGCC
At3g13100*		

(1) Left border primer a1 (SALK insertion line)

(2) Left border primer b1 (SALK insertion line)

(3) Left border primer (FLAG insertion line)

(4) Left border primer (GABI-KAT-insertion line)

(5) Gene specific primer forward

(6) Gene specific primer reverse

(*) Plants homozygous for the T-DNA insertion in the gene were kindly provided by Sonia Plaza, Institute of Plant Biology, University of Zurich

PCR was carried out in a 20 µl volume containing 1 µl DNA-template (0,5-1 µg), 2 µl of dNTP mix (1 mM), 0,4 µl of each primer (10 pmol/µl), 2 µl of 10x reaction buffer and 0,2 µl Taq-polymerase (5 units/µl) (Sigma-Aldrich, Buchs SG, Switzerland). The thermocycling conditions were: 94°C 3', [94°C 45'', annealing temperature 45'', 72°C 60''] x 25-30 cycles, 70°C 10'. PCR reactions were mixed with 2 µl gel loading buffer (30% glycerol, 1x TBE, 0,25% bromphenole blue) and were separated on a 1,5% agarose gel.

6.9.2 Sequencing

For sequencing, PCR products obtained with T-DNA left border primer and the respective gene specific primers were purified with GFX spin columns (Amersham Biosciences, Uppsala, Sweden) prior to sequencing. The dideoxy termination method (Sanger et al., 1977) was used for sequencing and sequences were determined using an automated sequencer (ABI377, Applied Biosystems, Foster City, U.S.A.).

6.9.3 Southern blot hybridisation

For southern blots hybridisations, DNA was extracted from leaves of 2-week-old plants according to Fulton et al. (1995). After digestion of the DNA with *BamHI*, DNA was separated by electrophoresis on a 0.8% agarose gel and let run for four to six hours at 50 V. DNA transfer to a cellulose membrane (Hybond^{TM}-N+, Amersham Bioscience, UK) was carried out overnight. The probe was amplified from the pBIN-pROK2 insertion sequence (http://signal.salk.edu/pBIN-pROK2.txt-new) by PCR with the primer pairs given in table 6.2 and separated on a low-melting agarose gel. Labelling with ^{32}P and hybridisation were performed according to Stein et al. (2000).

Table 6.2 Primers used for amplification of the probe sequence

Target	Primer	Sequence (5'-3')
pBIN_pROK2[1]	Probe fw	AACAGCTGATTGCCCTTCAC
	Probe rev	TTTGGGTGATGGTTCACGTA

(1) Vector containing T-DNA sequence

6.9.4 RT-PCR

Total RNA from Arabidopsis leaves was extracted as described in chapter 6.7. The reverse transcription was performed with Superscript™ II RNase Reverse Transcriptase kit (Invitrogen, Basel, Switzerland) as follows: 10 µg of RNA were incubated with 1 µl of oligo (dT) (500 µg/ml) and 1 µl of dNTP mix (10 mM) for five minutes at 65°C. The samples were chilled on ice and 4 µl of 5x first-strand buffer, 2 µl DTT (0.1 M) and 1 µl RNase Out (40 units/µl) were added (Invitrogen AG, Basel, Switzerland). The samples were incubated two minutes at 42°C and 1 µl (200 units) of Superscript™ II Reverse Transcriptase was added. For reverse transcription, the samples were incubated 90 minutes at 42°C. The reaction was stopped by incubation at 70°C for 15 minutes. Subsequently, the cDNAs were used for regular PCR with gene specific primers.

7 References

Abramovitch, R.B., Kim, Y.J., Chen, S., Dickman, M.B., and Martin, G.B. (2003). Pseudomonas type III effector AvrPtoB induces plant disease susceptibility by inhibition of host programmed cell death. Embo J 22, 60-69.

Adam, L., and Somerville, S.C. (1996). Genetic characterization of five powdery mildew disease resistance loci in *Arabidopsis thaliana*. Plant J 9, 341-356.

Aharon, R., Shahak, Y., Wininger, S., Bendov, R., Kapulnik, Y., and Galili, G. (2003). Overexpression of a plasma membrane aquaporin in transgenic tobacco improves plant vigor under favorable growth conditions but not under drought or salt stress. Plant Cell 15, 439-447.

Alonso, J.M., Stepanova, A.N., Leisse, T.J., Kim, C.J., Chen, H., Shinn, P., Stevenson, D.K., Zimmerman, J., Barajas, P., Cheuk, R., Gadrinab, C., Heller, C., Jeske, A., Koesema, E., Meyers, C.C., Parker, H., Prednis, L., Ansari, Y., Choy, N., Deen, H., Geralt, M., Hazari, N., Hom, E., Karnes, M., Mulholland, C., Ndubaku, R., Schmidt, I., Guzman, P., Aguilar-Henonin, L., Schmid, M., Weigel, D., Carter, D.E., Marchand, T., Risseeuw, E., Brogden, D., Zeko, A., Crosby, W.L., Berry, C.C., and Ecker, J.R. (2003). Genome-wide insertional mutagenesis of Arabidopsis thaliana. Science 301, 653-657.

Amrein, H., Makart, S., Granado, J., Shakya, R., Schneider-Pokorny, J., and Dudler, R. (2004). Functional analysis of genes involved in the synthesis of syringolin A by *Pseudomonas syringae* pv. *syringae* B301 D-R. Mol Plant Microbe In 17, 90-97.

Asai, T., Tena, G., Plotnikova, J., Willmann, M.R., Chiu, W.L., Gomez-Gomez, L., Boller, T., Ausubel, F.M., and Sheen, J. (2002). MAP kinase signalling cascade in *Arabidopsis* innate immunity. Nature 415, 977-983.

Assaad, F.F., Qiu, J.L., Youngs, H., Ehrhardt, D., Zimmerli, L., Kalde, M., Wanner, G., Peck, S.C., Edwards, H., Ramonell, K., Somerville, C.R., and Thordal-Christensen, H. (2004). The PEN1 syntaxin defines a novel cellular compartment upon fungal attack and is required for the timely assembly of papillae. Mol Biol Cell 15, 5118-5129.

Audenaert, K., De Meyer, G.B., and Hofte, M.M. (2002). Abscisic acid determines basal susceptibility of tomato to Botrytis cinerea and suppresses salicylic acid-dependent signaling mechanisms. Plant Physiol 128, 491-501.

Azevedo, C., Sadanandom, A., Kitagawa, K., Freialdenhoven, A., Shirasu, K., and Schulze-Lefert, P. (2002). The RAR1 interactor SGT1, an essential component of R gene-triggered disease resistance. Science 295, 2073-2076.

Baniwal, S.K., Bharti, K., Chan, K.Y., Fauth, M., Ganguli, A., Kotak, S., Mishra, S.K., Nover, L., Port, M., Scharf, K.D., Tripp, J., Weber, C., Zielinski, D., and von Koskull-Doring, P. (2004). Heat stress response in plants: a complex game with chaperones and more than twenty heat stress transcription factors. J Biosciences 29, 471-487.

Beere, H.M. (2004). "The stress of dying": the role of heat shock proteins in the regulation of apoptosis. J Cell Sci 117, 2641-2651.

Beere, H.M. (2005). Death versus survival: functional interaction between the apoptotic and stress-inducible heat shock protein pathways. J Clin Invest 115, 2633-2639.

Benjamini, Y., and Hochberg, Y. (1995). Controlling the False Discovery Rate - a Practical and Powerful Approach to Multiple Testing. J Roy Stat Soc B Met 57, 289-300.

Bock, J.B., Matern, H.T., Peden, A.A., and Scheller, R.H. (2001). A genomic perspective on membrane compartment organization. Nature 409, 839-841.

Boston, R.S., Viitanen, P.V., and Vierling, E. (1996). Molecular chaperones and protein folding in plants. Plant Mol Biol 32, 191-222.

Bouche, N., Fait, A., Bouchez, D., Moller, S.G., and Fromm, H. (2003). Mitochondrial succinic-semialdehyde dehydrogenase of the gamma-aminobutyrate shunt is required to restrict levels of reactive oxygen intermediates in plants. Proc Natl Acad Sci USA 100, 6843-6848.

Boyd, L.A., Smith, P.H., Foster, E.M., and Brown, J.K.M. (1995). The Effects of Allelic Variation at the Mla Resistance Locus in Barley on the Early Development of Erysiphe-Graminis F Sp Hordei and Host Responses. Plant J 7, 959-968.

Bretz, J.R., Mock, N.M., Charity, J.C., Zeyad, S., Baker, C.J., and Hutcheson, S.W. (2003). A translocated protein tyrosine phosphatase of *Pseudomonas syringae* pv. *tomato* DC3000 modulates plant defence response to infection. Mol Microbiol 49, 389-400.

Buchanan, B.B., Gruissem, W., and Jones, R.L. (2001). Biochemistry & Molecular Biology of Plants. Rockville, Maryland, USA: American Society of Plant Physiologists.

Callis, J., and Vierstra, R.D. (2000). Protein degradation in signaling. Curr Opin Plant Biol 3, 381-386.

Carver, T.L.W., Lyngkjaer, M.F., Neyron, L., and Strudwicke, C.C. (1999). Induction of cellular accessibility and inaccessibility and suppression and potentiation of cell death in oat attacked by *Blumeria graminis* f.sp *avenae*. Physiol Mol Plant P 55, 183-196.

Chao, W.S., Gu, Y.Q., Pautot, V.V., Bray, E.A., and Walling, L.L. (1999). Leucine aminopeptidase RNAs, proteins, and activities increase in response to water deficit, salinity, and the wound signals systemin, methyl jasmonate, and abscisic acid. Plant Physiol 120, 979-992.

Chen, C., and Chen, Z. (2002). Potentiation of developmentally regulated plant defense response by AtWRKY18, a pathogen-induced *Arabidopsis* transcription factor. Plant Physiol 129, 706-716.

Chomczynski, P., and Sacchi, N. (1987). Single-step method of RNA isolation by acid guanidinium thiocyanate-phenol-chloroform extraction. Anal Biochem 162, 156-159.

Clifton, R., Lister, R., Parker, K.L., Sappl, P.G., Elhafez, D., Millar, A.H., Day, D.A., and Whelan, J. (2005). Stress-induced co-expression of alternative respiratory chain components in *Arabidopsis thaliana*. Plant Mol Biol 58, 193-212.

Collinge, M., and Boller, T. (2001). Differential induction of two potato genes, Stprx2 and StNAC, in response to infection by *Phytophthora infestans* and to wounding. Plant Mol Biol 46, 521-529.

Collins, N.C., Thordal-Christensen, H., Lipka, V., Bau, S., Kombrink, E., Qiu, J.L., Huckelhoven, R., Stein, M., Freialdenhoven, A., Somerville, S.C., and Schulze-Lefert, P. (2003). SNARE-protein-mediated disease resistance at the plant cell wall. Nature 425, 973-977.

Considine, M.J., Holtzapffel, R.C., Day, D.A., Whelan, J., and Millar, A.H. (2002). Molecular distinction between alternative oxidase from monocots and dicots. Plant Physiol 129, 949-953.

Creelman, R.A., and Mullet, J.E. (1995). Jasmonic acid distribution and action in plants: regulation during development and response to biotic and abiotic stress. Proc Natl Acad Sci USA 92, 4114-4119.

Creelman, R.A., Tierney, M.L., and Mullet, J.E. (1992). Jasmonic acid/methyl jasmonate accumulate in wounded soybean hypocotyls and modulate wound gene expression. Proc Natl Acad Sci USA 89, 4938-4941.

Crocoll, C., Kettner, J., and Dörffling, K. (1991). Abscisic acid in saprophytic and parasitic species of fungi. Phytochemistry, 30, 1059-1060.

Crompton, M., Barksby, E., Johnson, N., and Capano, M. (2002). Mitochondrial intermembrane junctional complexes and their involvement in cell death. Biochimie 84, 143-152.

Cutler, S., Ghassemian, M., Bonetta, D., Cooney, S., and McCourt, P. (1996). A protein farnesyl transferase involved in abscisic acid signal transduction in Arabidopsis. Science 273, 1239-1241.

Czarnecka-Verner, E., Yuan, C.X., Scharf, K.D., Englich, G., and Gurley, W.B. (2000). Plants contain a novel multi-member class of heat shock factors without transcriptional activator potential. Plant Mol Biol 43, 459-471.

Day, D.A., Millar, A.H., Wiskich, J.T., and Whelan, J. (1994). Regulation of Alternative Oxidase Activity by Pyruvate in Soybean Mitochondria. Plant Physiol 106, 1421-1427.

Dixon, R.A., Achnine, L., Kota, P., Liu, C.-J., Reddy, M.S., and Wang, L. (2002). The phenylpropanoid pathway and plant defense: A genomics perspective. Mol Plant Pathol 3, 371-390.

Dolferus, R., Klok, E.J., Delessert, C., Wilson, S., Ismond, K.P., Good, A.G., Peacock, W.J., and Dennis, E.S. (2003). Enhancing the anaerobic response. Ann Bot (Lond) 91 Spec No, 111-117.

Dong, H., Delaney, T.P., Bauer, D.W., and Beer, S.V. (1999). Harpin induces disease resistance in *Arabidopsis* through the systemic acquired resistance pathway mediated by salicylic acid and the NIM1 gene. Plant J 20, 207-215.

Downs, C.A., and Heckathorn, S.A. (1998). The mitochondrial small heat-shock protein protects NADH:ubiquinone oxidoreductase of the electron transport chain during heat stress in plants. FEBS Lett 430, 246-250.

Eulgem, T., Rushton, P.J., Schmelzer, E., Hahlbrock, K., and Somssich, I.E. (1999). Early nuclear events in plant defence signalling: rapid gene activation by WRKY transcription factors. Embo J 18, 4689-4699.

Felix, G., Duran, J.D., Volko, S., and Boller, T. (1999). Plants have a sensitive perception system for the most conserved domain of bacterial flagellin. Plant J 18, 265-276.

Fiorani, F., Umbach, A.L., and Siedow, J.N. (2005). The alternative oxidase of plant mitochondria is involved in the acclimation of shoot growth at low temperature. A study of *Arabidopsis* AOX1a transgenic plants. Plant Physiol 139, 1795-1805.

Frye, C.A., and Innes, R.W. (1998). An *Arabidopsis* mutant with enhanced resistance to powdery mildew. Plant Cell 10, 947-956.

Fu, H., Doelling, J.H., Arendt, C.S., Hochstrasser, M., and Vierstra, R.D. (1998). Molecular organization of the 20S proteasome gene family from *Arabidopsis thaliana*. Genetics 149, 677-692.

Fujiki, Y., Yoshikawa, Y., Sato, T., Inada, N., Ito, M., Nishida, I., and Watanabe, A. (2001). Dark-inducible genes from *Arabidopsis thaliana* are associated with leaf senescence and repressed by sugars. Physiol Plant 111, 345-352.

Fujita, M., Fujita, Y., Maruyama, K., Seki, M., Hiratsu, K., Ohme-Takagi, M., Tran, L.S.P., Yamaguchi-Shinozaki, K., and Shinozaki, K. (2004). A dehydration-induced NAC protein, RD26, is involved in a novel ABA-dependent stress-signaling pathway. Plant J 39, 863-876.

Fulton, T.M., Chunwongse, J., and Tanksley, S.D. (1995). Microprep protocol for extraction of DNA from tomato and other herbaceous plants. Plant Mol Biol Rep 13, 207-209.

Gagne, J.M., Downes, B.P., Shiu, S.H., Durski, A.M., and Vierstra, R.D. (2002). The F-box subunit of the SCF E3 complex is encoded by a diverse superfamily of genes in *Arabidopsis*. Proc Natl Acad Sci USA 99, 11519-11524.

Gass, N., Glagotskaia, T., Mellema, S., Stuurman, J., Barone, M., Mandel, T., Roessner-Tunali, U., and Kuhlemeier, C. (2005). Pyruvate decarboxylase provides growing pollen tubes with a competitive advantage in petunia. Plant Cell 17, 2355-2368.

Gaston, S., Zabalza, A., Gonzalez, E.M., Arrese-Igor, C., Aparicio-Tejo, P.M., and Royuela, M. (2002). Imazethapyr, an inhibitor of the branched-chain amino acid biosynthesis, induces aerobic fermentation in pea plants. Physiol Plant Pathol 114, 524-532.

Gechev, T.S., Gadjev, I.Z., and Hille, J. (2004). An extensive microarray analysis of AAL-toxin-induced cell death in *Arabidopsis thaliana* brings new insights into the complexity of programmed cell death in plants. Cell Mol Life Sci 61, 1185-1197.

Gechev, T.S., Minkov, I.N., and Hille, J. (2005). Hydrogen peroxide-induced cell death in *Arabidopsis*: Transcriptional and mutant analysis reveals a role of an oxoglutarate-dependent dioxygenase gene in the cell death process. Iubmb Life 57, 181-188.

Geigenberger, P. (2003). Response of plant metabolism to too little oxygen. Curr Opin Plant Biol 6, 247-256.

Glazebrook, J. (2001). Genes controlling expression of defense responses in *Arabidopsis*-2001 status. Curr Opin Plant Biol 4, 301-308.

Gomez-Gomez, L., and Boller, T. (2002). Flagellin perception: a paradigm for innate immunity. Trends Plant Sci 7, 251-256.

Gout, E., Boisson, A., Aubert, S., Douce, R., and Bligny, R. (2001). Origin of the cytoplasmic pH changes during anaerobic stress in higher plant cells. Carbon-13 and phosphorous-31 nuclear magnetic resonance studies. Plant Physiol 125, 912-925.

Gray, G.R., Maxwell, D.P., Villarimo, A.R., and McIntosh, L. (2004). Mitochondria/nuclear signaling of alternative oxidase gene expression occurs through distinct pathways involving organic acids and reactive oxygen species. Plant Cell Rep 23, 497-503.

Hassa, P., Granado, J., Freydl, E., Waspi, U., and Dudler, R. (2000). Syringolin-mediated activation of the Pir7b esterase gene in rice cells is suppressed by phosphatase inhibitors. Mol Plant Microbe In 13, 342-346.

Hamilton, E.W., 3rd, and Heckathorn, S.A. (2001). Mitochondrial adaptations to NaCl. Complex I is protected by anti-oxidants and small heat shock proteins, whereas complex II is protected by proline and betaine. Plant Physiol 126, 1266-1274.

He, Y., Fukushige, H., Hildebrand, D.F., and Gan, S. (2002). Evidence supporting a role of jasmonic acid in Arabidopsis leaf senescence. Plant Physiol 128, 876-884.

Heckathorn, S.A., Downs, C.A., Sharkey, T.D., and Coleman, J.S. (1998). The small, methionine-rich chloroplast heat-shock protein protects photosystem II electron transport during heat stress. Plant Physiol 116, 439-444.

Hellmann, H., and Estelle, M. (2002). Plant development: regulation by protein degradation. Science 297, 793-797.

Hernandez Torres, J., Chatellard, P., and Stutz, E. (1995). Isolation and characterization of gmsti, a stress-inducible gene from soybean (Glycine max) coding for a protein belonging to the TPR (tetratricopeptide repeats) family. Plant Mol Biol 27, 1221-1226.

Hinderhofer, K., and Zentgraf, U. (2001). Identification of a transcription factor specifically expressed at the onset of leaf senescence. Planta 213, 469-473.

Holt, B.F., 3rd, Belkhadir, Y., and Dangl, J.L. (2005). Antagonistic control of disease resistance protein stability in the plant immune system. Science 309, 929-932.

Hrabak, E.M., and Willis, D.K. (1992). The lemA gene required for pathogenicity of *Pseudomonas syringae* pv. *syringae* on bean is a member of a family of two-component regulators. J Bacteriol 174, 3011-3020.

Hrabak, E.M., and Willis, D.K. (1993). Involvement of the *Iem*A gene in production of syringomycin and protease by *Pseudomonas syringae* pv. *syringae*. Mol Plant Microbe In 6, 368-375.

Hubert, D.A., Tornero, P., Belkhadir, Y., Krishna, P., Takahashi, A., Shirasu, K., and Dangl, J.L. (2003). Cytosolic HSP90 associates with and modulates the Arabidopsis RPM1 disease resistance protein. Embo J 22, 5679-5689.

Hückelhoven, R., and Kogel, K.-H. (1998). Tissue-Specific Superoxide Generation at Interaction Sites in Resistant and Susceptible Near-Isogenic Barley Lines Attacked by the Powdery Mildew Fungus (*Erysiphe graminis* f. sp. *hordei*). Mol Plant Microbe In 11, 292-300.

Hyde, P.M., and Colhoun, J. (1975). Structure and evolution of the rp1 complex conferring rust resistance in maize. Phytopathology 35, 293-310.

Ismond, K.P., Dolferus, R., de Pauw, M., Dennis, E.S., and Good, A.G. (2003). Enhanced low oxygen survival in *Arabidopsis* through increased metabolic flux in the fermentative pathway. Plant Physiol 132, 1292-1302.

Jamir, Y., Guo, M., Oh, H.S., Petnicki-Ocwieja, T., Chen, S., Tang, X., Dickman, M.B., Collmer, A., and Alfano, J.R. (2004). Identification of *Pseudomonas syringae* type III effectors that can suppress programmed cell death in plants and yeast. Plant J 37**,** 554-565.

Johnson, C.S., Kolevski, B., and Smyth, D.R. (2002). TRANSPARENT TESTA GLABRA2, a trichome and seed coat development gene of *Arabidopsis*, encodes a WRKY transcription factor. Plant Cell 14, 1359-1375.

Kalde, M., Barth, M., Somssich, I.E., and Lippok, B. (2003). Members of the *Arabidopsis* WRKY group III transcription factors are part of different plant defense signaling pathways. Mol Plant Microbe In 16, 295-305.

Kariola, T., Brader, G., Li, J., and Palva, E.T. (2005). Chlorophyllase 1, a damage control enzyme, affects the balance between defense pathways in plants. Plant Cell 17, 282-294.

Katagiri, F., Thilmony, R., and He, S. (2002). The *Arabidopsis thaliana-Pseudomonas syringae* interaction. American Society of Plant Biologists.

Kaufman, R.J. (1999). Stress signaling from the lumen of the endoplasmic reticulum: coordination of gene transcriptional and translational controls. Genes Dev 13, 1211-1233.

Koehler, C.M. (2004). New developments in mitochondrial assembly. Annu Rev Cell Dev Biol 20, 309-335.

Koornneef, M., Reuling, G., and Karssen, C.M. (1984). The isolation and characterization of abscisic acid-insensitive mutants of *Arabidopsis thaliana*. Physiol Plant Pathol 61, 377-383.

Kovtun, Y., Chiu, W.L., Tena, G., and Sheen, J. (2000). Functional analysis of oxidative stress-activated mitogen-activated protein kinase cascade in plants. Proc Natl Acad Sci USA 97, 2940-2945.

Krause, M., and Durner, J. (2004). Harpin inactivates mitochondria in *Arabidopsis* suspension cells. Mol Plant Microbe In 17, 131-139.

Kürsteiner, O., Dupuis, I., and Kuhlemeier, C. (2003). The pyruvate decarboxylase1 gene of *Arabidopsis* is required during anoxia but not other environmental stresses. Plant Physiol 132, 968-978.

Lane, B.G. (2002). Oxalate, germins, and higher-plant pathogens. Iubmb Life 53, 67-75.

Lee, G.J., Roseman, A.M., Saibil, H.R., and Vierling, E. (1997). A small heat shock protein stably binds heat-denatured model substrates and can maintain a substrate in a folding-competent state. Embo Journal 16, 659-671.

Lee, J.H., and Schoffl, F. (1996). An Hsp70 antisense gene affects the expression of HSP70/HSC70, the regulation of HSF, and the acquisition of thermotolerance in transgenic *Arabidopsis thaliana*. Mol Gen Genet 252, 11-19.

Lemeshko, V.V. (2002). Model of the outer membrane potential generation by the inner membrane of mitochondria. Biophys J 82, 684-692.

Lemeshko, V.V., and Lemeshko, S.V. (2004). The voltage-dependent anion channel as a biological transistor: theoretical considerations. Eur Biophys J 33, 352-359.

Li, X., Lin, H., Zhang, W., Zou, Y., Zhang, J., Tang, X., and Zhou, J.M. (2005). Flagellin induces innate immunity in nonhost interactions that is suppressed by *Pseudomonas syringae* effectors. Proc Natl Acad Sci USA 102, 12990-12995.

Liu, F., Vantoai, T., Moy, L.P., Bock, G., Linford, L.D., and Quackenbush, J. (2005). Global transcription profiling reveals comprehensive insights into hypoxic response in *Arabidopsis*. Plant Physiol 137, 1115-1129.

Liu, Q., Kasuga, M., Sakuma, Y., Abe, H., Miura, S., Yamaguchi-Shinozaki, K., and Shinozaki, K. (1998). Two transcription factors, DREB1 and DREB2, with an EREBP/AP2 DNA binding domain separate two cellular signal transduction pathways in drought- and low-temperature-responsive gene expression, respectively, in *Arabidopsis*. Plant Cell 10, 1391-1406.

Liu, Y., Schiff, M., Serino, G., Deng, X.W., and Dinesh-Kumar, S.P. (2002). Role of SCF ubiquitin-ligase and the COP9 signalosome in the N gene-mediated resistance response to Tobacco mosaic virus. Plant Cell 14, 1483-1496.

Loreti, E., Poggi, A., Novi, G., Alpi, A., and Perata, P. (2005). A genome-wide analysis of the effects of sucrose on gene expression in *Arabidopsis* seedlings under anoxia. Plant Physiol 137, 1130-1138.

Lyapina, S., Cope, G., Shevchenko, A., Serino, G., Tsuge, T., Zhou, C., Wolf, D.A., Wei, N., and Deshaies, R.J. (2001). Promotion of NEDD-CUL1 conjugate cleavage by COP9 signalosome. Science 292**,** 1382-1385.

Martinoia, E., Klein, M., Geisler, M., Bovet, L., Forestier, C., Kolukisaoglu, U., Muller-Rober, B., and Schulz, B. (2002). Multifunctionality of plant ABC transporters--more than just detoxifiers. Planta 214, 345-355.

Maxwell, D.P., Wang, Y., and McIntosh, L. (1999). The alternative oxidase lowers mitochondrial reactive oxygen production in plant cells. Proc Natl Acad Sci USA 96, 8271-8276.

McClung, J.K., Jupe, E.R., Liu, X.T., and Dell'Orco, R.T. (1995). Prohibitin: potential role in senescence, development, and tumor suppression. Exp Gerontol 30, 99-124.

Merlot, S., Mustilli, A.C., Genty, B., North, H., Lefebvre, V., Sotta, B., Vavasseur, A., and Giraudat, J. (2002). Use of infrared thermal imaging to isolate *Arabidopsis* mutants defective in stomatal regulation. Plant J 30, 601-609.

Millar, A.H., Wiskich, J.T., Whelan, J., and Day, D.A. (1993). Organic acid activation of the alternative oxidase of plant mitochondria. FEBS Lett 329, 259-262.

Millenaar, F.F., and Lambers, H. (2003). The alternative oxidase: in vivo regulation and function. Plant Biology 5, 2-15.

Mohr, P., and Cahill, D. (2003). Abscisic acid influences the susceptibility of Arabidopsis thaliana to Pseudomonas syringae pv. tomato and Peronospora parasitica. Funct Plant Biol 30, 461-469.

Moore, A.L., Albury, M.S., Crichton, P.G., and Affourtit, C. (2002). Function of the alternative oxidase: is it still a scavenger? Trends Plant Sci 7, 478-481.

Nadimpalli, R., Yalpani, N., Johal, G.S., and Simmons, C.R. (2000). Prohibitins, stomatins, and plant disease response genes compose a protein superfamily that controls cell proliferation, ion channel regulation, and death. J Biol Chem 275, 29579-29586.

Narusaka, Y., Nakashima, K., Shinwari, Z.K., Sakuma, Y., Furihata, T., Abe, H., Narusaka, M., Shinozaki, K., and Yamaguchi-Shinozaki, K. (2003). Interaction between two cis-acting elements, ABRE and DRE, in ABA-dependent expression of Arabidopsis rd29A gene in response to dehydration and high-salinity stresses. Plant J 34, 137-148.

Navarro, L., Zipfel, C., Rowland, O., Keller, I., Robatzek, S., Boller, T., and Jones, J.D. (2004). The transcriptional innate immune response to flg22. Interplay and overlap with Avr gene-dependent defense responses and bacterial pathogenesis. Plant Physiol 135, 1113-1128.

Nawrath, C., Heck, S., Parinthawong, N., and Metraux, J.P. (2002). EDS5, an essential component of salicylic acid-dependent signaling for disease resistance in *Arabidopsis*, is a member of the MATE transporter family. Plant Cell 14, 275-286.

Nover, L., Bharti, K., Doring, P., Mishra, S.K., Ganguli, A., and Scharf, K.D. (2001). *Arabidopsis* and the heat stress transcription factor world: how many heat stress transcription factors do we need? Cell Stress Chaperon 6, 177-189.

Nuhse, T.S., Boller, T., and Peck, S.C. (2003). A plasma membrane syntaxin is phosphorylated in response to the bacterial elicitor flagellin. J Biol Chem 278, 45248-45254.

Penninckx, I.A., Thomma, B.P., Buchala, A., Metraux, J.P., and Broekaert, W.F. (1998). Concomitant activation of jasmonate and ethylene response pathways is required for induction of a plant defensin gene in *Arabidopsis*. Plant Cell 10, 2103-2113.

Picard, D., Khursheed, B., Garabedian, M.J., Fortin, M.G., Lindquist, S., and Yamamoto, K.R. (1990). Reduced levels of hsp90 compromise steroid receptor action in vivo. Nature 348, 166-168.

Pontier, D., Miao, Z.H., and Lam, E. (2001). Trans-dominant suppression of plant TGA factors reveals their negative and positive roles in plant defense responses. Plant J 27, 529-538.

Rasmusson, A.G., Soole, K.L., and Elthon, T.E. (2004). Alternative NAD(P)H dehydrogenases of plant mitochondria. Annu Rev Plant Biol 55, 23-39.

Reimmann, C., Hofmann, C., Mauch, F., and Dudler, R. (1995). Characterization of a rice gene induced by *Pseudomonas syringae* pv. *syringae:* Requirement for the bacterial *lemA* gene function. Physiol Mol Plant P 46, 71-81.

Reuber, T.L., Plotnikova, J.M., Dewdney, J., Rogers, E.E., Wood, W., and Ausubel, F.M. (1998). Correlation of defense gene induction defects with powdery mildew susceptibility in *Arabidopsis* enhanced disease susceptibility mutants. Plant J 16, 473-485.

Robatzek, S., and Somssich, I.E. (2001). A new member of the *Arabidopsis* WRKY transcription factor family, AtWRKY6, is associated with both senescence- and defence-related processes. Plant J 28, 123-133.

Robatzek, S., and Somssich, I.E. (2002). Targets of AtWRKY6 regulation during plant senescence and pathogen defense. Genes Dev 16, 1139-1149.

Ryals, J.A., Neuenschwander, U.H., Willits, M.G., Molina, A., Steiner, H.Y., and Hunt, M.D. (1996). Systemic Acquired Resistance. Plant Cell 8, 1809-1819.

Sanger, F., Nicklen, S., and Coulson, A.R. (1977). DNA Sequencing with Chain-Terminating Inhibitors. Proc Natl Acad Sci USA 74**,** 5463-5467.

Sangster, T.A., and Queitsch, C. (2005). The HSP90 chaperone complex, an emerging force in plant development and phenotypic plasticity. Curr Opin Plant Biol 8, 86-92.

Sanmiya, K., Suzuki, K., Egawa, Y., and Shono, M. (2004). Mitochondrial small heat-shock protein enhances thermotolerance in tobacco plants. FEBS Lett 557, 265-268.

Schraudner, M., Moeder, W., Wiese, C., Van Camp, W., Inze, D., Langebartels, C., and Sandermann, H. (1998). Ozone-induced oxidative burst in the ozone biomonitor plant, tobacco Bel W3. Plant J 16, 235-245.

Schwechheimer, C., and Deng, X.W. (2001). COP9 signalosome revisited: a novel mediator of protein degradation. Trends Cell Biol 11, 420-426.

Schweizer, P., Christoffel, A., and Dudler, R. (1999). Transient expression of members of the germin-like gene family in epidermal cells of wheat confers disease resistance. Plant J 20, 541-552.

Serino, G., and Deng, X.W. (2003). The COP9 signalosome: regulating plant development through the control of proteolysis. Annu Rev Plant Biol 54, 165-182.

Sharma, Y.K., and Davis, K.R. (1994). Ozone-Induced Expression of Stress-Related Genes in *Arabidopsis thaliana*. Plant Physiol 105, 1089-1096.

Shimizu, R., Taguchi, F., Marutani, M., Mukaihara, T., Inagaki, Y., Toyoda, K., Shiraishi, T., and Ichinose, Y. (2003). The DeltafliD mutant of *Pseudomonas syringae* pv. *tabaci*, which secretes flagellin monomers, induces a strong hypersensitive reaction (HR) in non-host tomato cells. Mol Genet Genomics 269, 21-30.

Shimizu, S., Narita, M., and Tsujimoto, Y. (1999). Bcl-2 family proteins regulate the release of apoptogenic cytochrome c by the mitochondrial channel VDAC. Nature 399, 483-487.

Shimizu, S., Ide, T., Yanagida, T., and Tsujimoto, Y. (2000). Electrophysiological study of a novel large pore formed by Bax and the voltage-dependent anion channel that is permeable to cytochrome c. J Biol Chem 275, 12321-12325.

Shinozaki, K., and Yamaguchi-Shinozaki, K. (2000). Molecular responses to dehydration and low temperature: differences and cross-talk between two stress signaling pathways. Curr Opin Plant Biol 3, 217-223.

Smith, J.A., and Métraux, J.P. (1991). *Pseudomonas syringae* pv. *syringae* induces systemic resistance to *Pyricularia oryzae* in rice. Physiol Mol Plant P 39, 451-461.

Souer, E., van Houwelingen, A., Kloos, D., Mol, J., and Koes, R. (1996). The no apical meristem gene of Petunia is required for pattern formation in embryos and flowers and is expressed at meristem and primordia boundaries. Cell 85, 159-170.

Stein, N., Feuillet, C., Wicker, T., Schlagenhauf, E., and Keller, B. (2000). Subgenome chromosome walking in wheat: a 450-kb physical contig in *Triticum monococcum* L. spans the Lr10 resistance locus in hexaploid wheat (*Triticum aestivum* L.). Proc Natl Acad Sci USA 97, 13436-13441.

Sun, W., Bernard, C., van de Cotte, B., Van Montagu, M., and Verbruggen, N. (2001). At-HSP17.6A, encoding a small heat-shock protein in *Arabidopsis*, can enhance osmotolerance upon overexpression. Plant J 27, 407-415.

Takahashi, A., Casais, C., Ichimura, K., and Shirasu, K. (2003). HSP90 interacts with RAR1 and SGT1 and is essential for RPS2-mediated disease resistance in *Arabidopsis*. Proc Natl Acad Sci USA 100, 11777-11782.

Takahashi, T., Naito, S., and. (1992). Isolation and Analysis of the Expression of Two Genes for the 81-Kilodalton Heat-Shock Proteins from *Arabidopsis*. Plant Physiol 99, 383-390.

Thaler, S., and Bostock, R. (2004). Interactions between abscisic-acidmediated responses and plant resistance to pathogens and insects. Ecology 85, 48-58.

Thimm, O., Blasing, O., Gibon, Y., Nagel, A., Meyer, S., Kruger, P., Selbig, J., Muller, L.A., Rhee, S.Y., and Stitt, M. (2004). MAPMAN: a user-driven tool to display genomics data sets onto diagrams of metabolic pathways and other biological processes. Plant J 37, 914-939.

Thirkettle-Watts, D., McCabe, T.C., Clifton, R., Moore, C., Finnegan, P.M., Day, D.A., and Whelan, J. (2003). Analysis of the alternative oxidase promoters from soybean. Plant Physiol 133, 1158-1169.

Tournaire-Roux, C., Sutka, M., Javot, H., Gout, E., Gerbeau, P., Luu, D.T., Bligny, R., and Maurel, C. (2003). Cytosolic pH regulates root water transport during anoxic stress through gating of aquaporins. Nature 425, 393-397.

Tsuchiya, T., Ohta, H., Okawa, K., Iwamatsu, A., Shimada, H., Masuda, T., and Takamiya, K. (1999). Cloning of chlorophyllase, the key enzyme in chlorophyll degradation: finding of a lipase motif and the induction by methyl jasmonate. Proc Natl Acad Sci USA 96, 15362-15367.

Tyerman, S.D., Niemietz, C.M., and Bramley, H. (2002). Plant aquaporins: multifunctional water and solute channels with expanding roles. Plant Cell Environ 25, 173-194.

Vanlerberghe, G.C., Day, D.A., Wiskich, J.T., Vanlerberghe, A.E., and McIntosh, L. (1995). Alternative Oxidase Activity in Tobacco Leaf Mitochondria (Dependence on Tricarboxylic Acid Cycle-Mediated Redox Regulation and Pyruvate Activation). Plant Physiol 109, 353-361.

Varet, A., Hause, B., Hause, G., Scheel, D., and Lee, J. (2003). The *Arabidopsis* NHL3 gene encodes a plasma membrane protein and its overexpression correlates with increased resistance to *Pseudomonas syringae* pv. *tomato* DC3000. Plant Physiol 132, 2023-2033.

Vartapetian, B.B., and Jackson, M.B. (1997). Plant Adaptations to Anaerobic Stress. Ann Bot-London 79, 3-20.

Vierling, E. (1991). The Roles of Heat-Shock Proteins in Plants. Annu Rev Plant Physiol Plant Mol Biol 42, 579-620.

Vierstra, R.D. (2003). The ubiquitin/26S proteasome pathway, the complex last chapter in the life of many plant proteins. Trends Plant Sci 8, 135-142.

Wäspi, U., Blanc, D., Winkler, T., Ruedi, P., and Dudler, R. (1998). Syringolin, a novel peptide elicitor from *Pseudomonas syringae* pv. *syringae* that induces resistance to *Pyricularia oryzae* in rice. Mol Plant Microbe In 11, 727-733.

Wäspi, U., Hassa, P., Staempfli, A.A., Molleyres, L.P., Winkler, T., and Dudler, R. (1999). Identification and structure of a family of syringolin variants: Unusual cyclic peptides from *Pseudomonas syringae* pv. *syringae* that elicit defense responses in rice. Microbiol Res 154, 89-93.

Wäspi, U., Schweizer, P., and Dudler, R. (2001). Syringolin reprograms wheat to undergo hypersensitive cell death in a compatible interaction with powdery mildew. Plant Cell 13**,** 153-161.

Wehmeyer, N., Hernandez, L.D., Finkelstein, R.R., and Vierling, E. (1996). Synthesis of small heat-shock proteins is part of the developmental program of late seed maturation. Plant Physiol 112, 747-757.

Wei, N., Tsuge, T., Serino, G., Dohmae, N., Takio, K., Matsui, M., and Deng, X.W. (1998). The COP9 complex is conserved between plants and mammals and is related to the 26S proteasome regulatory complex. Curr Biol 8, 919-922.

Wojcik, C. (2002). Regulation of apoptosis by the ubiquitin and proteasome pathway. J Cell Mol Med 6, 25-48.

Xie, Q., Frugis, G., Colgan, D., and Chua, N.H. (2000). *Arabidopsis* NAC1 transduces auxin signal downstream of TIR1 to promote lateral root development. Genes Dev 14, 3024-3036.

Xiong, L., Lee, B., Ishitani, M., Lee, H., Zhang, C., and Zhu, J.K. (2001). FIERY1 encoding an inositol polyphosphate 1-phosphatase is a negative regulator of abscisic acid and stress signaling in *Arabidopsis*. Genes Dev 15, 1971-1984.

Yabe, N., Takahashi, T., and Komeda, Y. (1994). Analysis of tissue-specific expression of *Arabidopsis thaliana* HSP90-family gene HSP81. Plant Cell Physiol 35, 1207-1219.

Yang, P.Z., Fu, H.Y., Walker, J., Papa, C.M., Smalle, J., Ju, Y.M., and Vierstra, R.D. (2004). Purification of the *Arabidopsis* 26 S proteasome - Biochemical and molecular analyses revealed the presence of multiple isoforms. J Biol Chem 279, 6401-6413.

Yao, N., Tada, Y., Sakamoto, M., Nakayashiki, H., Park, P., Tosa, Y., and Mayama, S. (2002). Mitochondrial oxidative burst involved in apoptotic response in oats. Plant J 30, 567-579.

Young, J.C., Moarefi, I., and Hartl, F.U. (2001). Hsp90: a specialized but essential protein-folding tool. J Cell Biol 154, 267-273.

Zheng, M.S., Takahashi, H., Miyazaki, A., Hamamoto, H., Shah, J., Yamaguchi, I., and Kusano, T. (2004). Up-regulation of *Arabidopsis thaliana* NHL10 in the hypersensitive response to Cucumber mosaic virus infection and in senescing leaves is controlled by signalling pathways that differ in salicylate involvement. Planta 218, 740-750.

Zimmermann, P., Hirsch-Hoffmann, M., Hennig, L., and Gruissem, W. (2004). GENEVESTIGATOR. *Arabidopsis* microarray database and analysis toolbox. Plant Physiol 136, 2621-2632.

Zipfel, C., Robatzek, S., Navarro, L., Oakeley, E.J., Jones, J.D., Felix, G., and Boller, T. (2004). Bacterial disease resistance in *Arabidopsis* through flagellin perception. Nature 428, 764-767.

Zou, J., Rodriguez-Zas, S., Aldea, M., Li, M., Zhu, J., Gonzalez, D.O., Vodkin, L.O., DeLucia, E., and Clough, S.J. (2005). Expression profiling soybean response to *Pseudomonas syringae* reveals new defense-related genes and rapid HR-specific downregulation of photosynthesis. Mol Plant Microbe In 18, 1161-1174.

8 Appendix

Abbreviations

SylA	syringolin A
HR	hypersensitive reaction
ROS	reactive oxygen species
PCD	programmed cell death
E. c.	*Erysiphe cichoracearum*
Sti	*stress-induced*
Col	Columbia
Ler	Landsburg erecta
dpi	days post-inoculation
hai	hours after infection
hat	hours after treatment
MTC	multiple test correction
LRR	leucine-rich repeat
SA	salicylic acid
Flg22	flagellin
P. s.	*Pseudomonas syringae*

Table 8.1 P-values of sylA-responsive genes exhibiting higher t/c ratios in infected plants (IS12) compared to uninfected plants (S12)

Description	Protein	Locus[1]	t/c ratio[2]		p-value
			IS12	S12	
expressed protein		At5g14730	6,7	3,5	0,02
hypothetical protein		At5g57510	4,3	2,6	0,07
putative glutathione S-transferase	GSTU1	At2g29490	17,8	13,9	0,08
expressed protein		At2g35480	8,4	6,3	0,11
MATE efflux family protein		At1g15180	8,8	4,2	0,13
putative galactinol synthase		At1g60470	2,7	2,1	0,18
expressed protein		At5g06190	7,2	4,7	0,20
putative calcium-dependent protein kinase		At3g56760	2,8	2,6	0,22
expressed protein		At5g11290	15,0	12,5	0,25
lectin-related, low similarity to lectin 3		At2g43730	6,8	5,5	0,25
autophagy 8e		At2g45170	3,6	3,3	0,28
expressed protein	FRL1	At5g16320	2,3	2,2	0,30
putative chromosome-associated kinesin		At5g60930	2,9	2,6	0,32
putative splicing factor		At4g38780	3,9	3,6	0,33
hydroxyproline-rich glycoprotein family protein		At3g45230	2,2	2,1	0,33
putative sugar transporter		At2g48020	3,1	2,9	0,35
expressed protein		At5g23460	2,6	2,5	0,38
expressed protein		At5g64230	7,8	7,6	0,45

(1) The annotation of the genes derived from TAIR, the Arabidopsis Information Resource (http://arabidopsis.org).

(2) Data derived from three independent experiments. Differentially expressed genes were filtered by the Welch's t-test ($p \leq 0.05$) and MTC.

Table 8.2 T/c ratios of genes downregulated by sylA in uninfected plants (S12) and upregulated by fungal infection alone (I60)

Row	Description	Locus[2]	Protein	t/c ratio[3]	
	Functional categories[1]			S12	I60
	Transcription factors				
1	ethylene-responsive element-binding factor 2	**At5g47220**		0,19	2,65
2	WRKY family transcription factor	At4g01720	WRKY47	0,26	2,89
3	**Transport**				
4	auxin efflux carrier family protein	At1g76520		0,29	2,12
5	glucose transporter	At1g11260	STP1	0,33	3,19
6	haloacid dehalogenase-like hydrolase family protein	At1g72700		0,38	5,51
7	oligopeptide transporter OPT family protein	At5g64410		0,24	3,58
8	putative metal transporter	At1g05300	ZIP5	0,24	2,22
9	putative metal transporter	At1g55910	ZIP11	0,35	2,10
10	putative UDP-galactose/UDP-glucose transporter	At1g14360		0,37	2,42
11	sodium:solute symporter family protein	At5g45380		0,32	6,82
12	sulfate transporter	At1g78000	Sultr1;2	0,17	2,41
13	UDP-galactose/UDP-glucose transporter	At2g02810		0,43	3,96
14	**Response to abiotic and biotic stimuli**				
15	auxin-responsive family protein	At3g12830		0,37	2,89
16	beta-1,3-glucanase	**At3g57240**	BG3	0,30	25,81
17	disease resistance family protein	At2g15080		0,07	4,03
18	disease resistance family protein	At3g23110		0,49	4,02
19	disease resistance response protein-related	At1g55210		0,44	2,70
20	polygalacturonase inhibiting protein 1	**At5g06860**	PGIP1	0,39	2,34
21	putative 12-oxophytodienoate reductase	At1g17990		0,32	2,65
22	putative 9-cis-epoxycarotenoid dioxygenase	**At3g14440**	NCED3	0,38	3,04
23	putative anthranilate synthase beta subunit	At5g57890		0,37	2,27
24	receptor-like protein kinase, putative	At3g45860		0,46	10,13
25	seven-transmembrane MLO family protein	At3g45290	MLO3	0,48	5,76
26	**Protein metaboism**				
27	aspartyl protease family protein	**At5g10760**		0,18	5,21
28	DNAJ heat shock N-terminal domain-containing protein	At3g13310		0,49	2,12
29	shepherd protein	At4g24190	SHD	0,34	2,45
30	small ubiquitin-like modifier 3 (SUMO)	At5g55170	SUM3	0,44	2,67
31	Kinase activity				
32	leucine-rich repeat family protein	At5g49760		0,40	2,60
33	protein kinase family protein	At4g04540		0,24	3,05
34	protein kinase family protein	**At4g23220**		0,24	6,31
35	protein kinase family protein	At5g25440		0,29	3,90
36	putative S-receptor protein kinase	At1g65790	ARK1	0,34	2,34
37	putatve leucine-rich repeat transmembrane protein kinase	At5g45800		0,27	3,46
38	**Hydrolase activity**				
39	acid phosphatase type 5	At3g17790	ACP5	0,45	2,28
40	GDSL-motif lipase/hydrolase family protein	At5g03610		0,43	3,26
41	glycosyl hydrolase family 17 protein	At3g13560		0,33	2,51
42	glycosyl hydrolase family 17 protein	At4g34480		0,37	2,61
43	glycosyl hydrolase family 3 protein	At5g20950		0,24	2,20
44	pectinesterase family protein	**At4g02330**		0,09	2,50
45	pectinesterase family protein	At5g53370		0,29	2,71
46	**Biological process unknown**				
47	ankyrin repeat family protein	At2g24600		0,28	2,41
48	ankyrin repeat family protein	At5g54610		0,15	3,60
49	C2 domain-containing protein	At3g18370		0,41	2,06
50	calcineurin-like phosphoesterase family protein	At1g13750		0,46	3,34
51	calnexin, putative	At5g07340		0,35	3,17
52	calreticulin 2	At1g09210	CRT2	0,32	3,32
53	expressed protein	At1g74440		0,36	2,02
54	expressed protein	At4g23880		0,35	2,58
55	expressed protein	At4g30500		0,41	2,82
56	expressed protein	At5g19875		0,49	2,35
57	expressed protein	At5g45480		0,39	2,33
58	expressed protein	**At5g53110**		0,33	3,11
59	expressed protein	At5g52540		0,40	2,50
60	glycosyltransferase family 14 protein	At3g15350		0,44	2,41
61	glycosyltransferase family protein 47	At1g80290		0,39	2,03
62	kelch repeat-containing F-box family protein	At1g80440		0,29	2,73
63	MutT/nudix family protein	At2g01670		0,37	2,39
64	phytochelatin synthetase-related	**At5g60950**		0,11	4,42
65	proteasel (pfpI)-like protein	**At2g38860**	YLS5	0,36	4,01
66	transferase family protein	At3g50280		0,14	2,02

(1) Transcripts were grouped according to biological function GO (Gene Ontology) terms.

(2) The annotation of the genes derived from TAIR, the Arabidopsis Information Resource (http://arabidopsis.org). In bold: genes that exhibited m/wt ratios ≥ 2 in control-treated syl_404 plants (data derived from two independent experiments and relevant genes were filtered by the Student's t-test ($p \leq 0.05$)).

(3) Data derived from three independent experiments. Differentially expressed genes were filtered by the Welch's t-test ($p \leq 0.05$) and MTC.

Table 8.3 T/c ratios of genes more than 2-fold differentially expressed in infected sylA-treated plants (IS12) and more than 3-fold differentially expressed in uninfected plants treated with sylA (S12)

Row	Description	Locus[2]	Protein	t/c ratio[3]	
	Functional categories[1]			IS12	S12
	METABOLISM				
	Cell wall proteins				
1	arabinogalactan-protein	At5g64310	AGP1	-	3.4
2	arabinogalactan-protein	At2g22470	AGP2	-	6.2
3	arabinogalactan-protein	At4g09030	AGP10	-	3.3
4	arabinogalactan-protein	At5g40730	AGP24	5.1	5.4
5	proline-rich family protein	At5g12880		2.4	5.8
6	arabinogalactan-protein	At2g14890	AGP9	-	0.3
7	arabinogalactan-protein	At5g56540	AGP7	-	0.3
8	arabinogalactan protein	At3g13520	AGP12	-	0.3
9	arabinogalactan-protein	At5g65390	AGP14	-	0.3
10	arabinogalactan protein	At2g23130	AGP17	-	0.3
11	arabinogalactan protein	At4g37450	AGP18	-	0.1
12	arabinogalactan protein	At1g55330	AGP21	-	0.2
13	arabinogalactan-protein family	At4g16980		-	0.2
14	fasciclin-like arabinogalactan-protein	At5g55730	FLA1	-	0.2
15	fasciclin-like arabinogalactan-protein	At2g04780	FLA7	-	0.3
16	fasciclin-like arabinogalactan-protein	At2g45470	FLA8	-	0.1
17	fasciclin-like arabinogalactan-protein	At1g03870	FLA9	-	0.1
18	fasciclin-like arabinogalactan-protein, putative	At5g44130		-	0.1
19	**Minor CHO family metabolism**				
20	galactinol synthase, putative	At1g60470		2.7	2.1
21	galactinol synthase, putative	At3g28340		-	3.6
22	glycosyl transferase family 20 protein	At2g18700	TPS11	-	5
23	2-dehydro-3-deoxyphosphooctonate aldolase, putative	At1g16340		-	0.3
24	aldo/keto reductase family protein	At5g53580		-	0.2
25	aldo/keto reductase family protein	At2g37790		-	0.3
26	aldo/keto reductase, putative	At1g59960		-	0.3
27	sorbitol dehydrogenase, putative	At5g51970		-	0.2
28	sugar isomerase (SIS) domain-containing protein	At5g52190		-	0.1
29	trehalose-6-phosphate phosphatase	At5g51460	TPPA	-	0.3
30	trehalose-6-phosphate phosphatase, putative	At4g39770		-	0.2
31	trehalose-6-phosphate synthase, putative	At1g70290	TPS8	-	0.1
32	**Cell wall precursor synthesis**				
33	NAD-dependent epimerase/dehydratase family protein	At3g46440	UXS5	2.6	9
34	NAD-dependent epimerase/dehydratase family protein	At5g44480	DUR	-	4.5
35	UDP-D-xylose 4-epimerase, putative	At1g30620	MUR4	-	4.3
36	UDP-glucose 4-epimerase, putative	At4g23920		-	3.7
37	UDP-glucose 4-epimerase, putative	At1g63180		-	4.1
38	UDP-glucose 6-dehydrogenase, putative	At5g15490		-	3
39	UDP-glucuronic acid decarboxylase	At5g59290	UXS3	2.1	2.2
40	NAD-dependent epimerase	At3g23820	GAE6	-	0.1
41	Nucleotide-rhamnose synthase	At1g63000	NRS/ER	-	0.3
42	phosphomannose isomerase type I family protein	At3g02570		-	0.2
43	**Cell wall synthesis**				
44	pectinesterase family protein	At2g45220		-	6.8
45	cellulose synthase, catalytic subunit	At4g39350	CESA2	-	0.3
46	cellulose synthase, catalytic subunit, putative	At5g09870	CESA5	-	0.2
47	glucosyltransferase-related	At4g16590	CSLA01	-	0.03
48	glycosyl transferase family 2 protein	At1g23480	CSLA03	-	0.1
49	glycosyl transferase family 2 protein	At5g03760	CSLA09	-	0.1
50	glycosyl transferase family 2 protein	At1g24070	CSLA10	-	0.1
51	glycosyl transferase family 2 protein	At5g16190	CSLA11	-	0.2
52	glycosyl transferase family 2 protein	At4g13410	CSLA15	-	0.04
53	glycosyl transferase family 2 protein	At4g31590	CSLC05	-	0.2
54	cellulose synthase family protein	At1g55850	CSLE1	-	0.2
55	cellulose synthase family protein	At2g32540		-	0.2
56	galactosyl transferase GMA12	At2g22900		-	0.3
57	galactosyltransferase family protein	At4g26940		-	0.3
58	**Cell wall modification**				
59	expansin family protein	At2g18660		-	21.1
60	putative xyloglucan endotransglycosylase	At4g30280		3,1	8,9
61	xyloglucan fucosyltransferase, putative	At2g15390	FUT4	-	3.8
62	xyloglucan:xyloglucosyl transferase	At5g57560	TCH4	-	4.1
63	xyloglucan:xyloglucosyl transferase, putative	At4g25810	XTR6	-	7.8
64	expansin-related	At4g17030	EXLB1	-	0.1
65	expansin, putative	At1g69530	EXPA1	-	0.1
66	expansin, putative	At2g37640	EXPA3	-	0.1
67	expansin, putative	At2g39700	EXPA4	-	0.1
68	expansin, putative	At3g29030	EXPA5	-	0.1
69	expansin, putative	At2g28950	EXPA6	-	0.1
70	expansin, putative	At2g40610	EXPA8	-	0.1
71	expansin, putative	At1g26770	EXPA10	-	0.2
72	expansin, putative	At1g20190	EXPA11	-	0.1
73	beta-expansin, putative	At4g28250	EXPB3	-	0.2
74	invertase/pectin methylesterase inhibitor family protein	At5g62360		-	0.05
75	invertase/pectin methylesterase inhibitor family protein	At5g62350		-	0.1
76	invertase/pectin methylesterase inhibitor family protein	At3g47380		-	0.1
77	invertase/pectin methylesterase inhibitor family protein	At1g14890		-	0.2
78	invertase/pectin methylesterase inhibitor family protein	At4g12390		-	0.2
79	invertase/pectin methylesterase inhibitor family protein	At1g23205		-	0.2
80	invertase/pectin methylesterase inhibitor family protein	At1g47960	C/VIF1	-	0.2

Row	Description	Locus[2]	Protein	t/c ratio[3]	
	Functional categories[1]			IS12	S12
81	invertase/pectin methylesterase inhibitor family protein	At5g64620	C/VIF2	-	0,3
82	pectin methylesterase, putative	At1g11580		-	0,1
83	pectinacetylesterase family protein	At5g23870		-	0,3
84	pectinacetylesterase, putative	At3g05910		-	0,2
85	pectinacetylesterase, putative	At5g45280		-	0,2
86	pectinacetylesterase, putative	At1g57590		-	0,2
87	pectinacetylesterase, putative	At4g19410		-	0,3
88	pectinesterase family protein	At4g02330		-	0,1
89	pectinesterase family protein	At4g33220		-	0,1
90	pectinesterase family protein	At1g53840	PME1	-	0,1
91	pectinesterase family protein	At3g14310	PME3	-	0,1
92	pectinesterase family protein	At3g43270		-	0,1
93	pectinesterase family protein	At5g09760		-	0,3
94	pectinesterase family protein	At3g59010		-	0,3
95	pectinesterase family protein	At5g53370		-	0,3
96	pectinesterase like protein	At5g66920		-	0,2
97	pectinesterase like protein pectinesterase	At4g22010		-	0,2
98	pectinesterase, putative	At3g10720		-	0,1
99	pectinesterase, putative	At1g41830		-	0,3
100	pectinesterase, putative	At1g76160		-	0,2
101	xyloglucan:xyloglucosyl transferase	At1g14720	XTR2	-	0,2
102	xyloglucan:xyloglucosyl transferase	At2g01850	EXGT-A3	-	0,3
103	xyloglucan:xyloglucosyl transferase	At2g06850	EXGT-A1	-	0,2
104	xyloglucan:xyloglucosyl transferase, putative	At3g44990	XTR8	-	0,04
105	xyloglucan:xyloglucosyl transferase, putative	At5g65730		-	0,03
106	xyloglucan:xyloglucosyl transferase, putative	At4g37800		-	0,1
107	xyloglucan:xyloglucosyl transferase, putative	At2g36870		-	0,1
108	xyloglucan:xyloglucosyl transferase, putative	At1g11545		-	0,3
109	**Cell wall degradation**				
110	beta-galactosidase, putative	At3g13750	BGAL1	-	0,1
111	beta-galactosidase, putative	At3g52840		-	0,1
112	beta-galactosidase, putative	At4g36360	BGAL3	-	0,1
113	beta-galactosidase, putative	At1g45130		-	0,1
114	BURP domain-containing protein	At1g70370		-	0,1
115	endo-1,4-beta-glucanase, putative	At1g64390		-	0,1
116	glycoside hydrolase family 28 protein	At3g61490		-	0,3
117	glycoside hydrolase family 28 protein	At3g06770		-	0,1
118	glycoside hydrolase family 28 protein	At3g15720		-	0,1
119	glycoside hydrolase family 28 protein	At3g62110		-	0,1
120	glycoside hydrolase family 28 protein	At4g23820		-	0,1
121	glycoside hydrolase family 28 protein	At4g33440		-	0,2
122	glycosyl hydrolase family 3 protein	At1g78060		-	0,2
123	glycosyl hydrolase family 3 protein	At5g10560		-	0,3
124	glycosyl hydrolase family 3 protein	At5g20950		-	0,2
125	glycosyl hydrolase family 9 protein	At1g19940		-	0,2
126	pectate lyase family protein	At5g48900		-	0,1
127	pectate lyase family protein	At3g09540		-	0,2
128	pectate lyase family protein	At1g67750		-	0,03
129	pectate lyase family protein	At4g24780		-	0,1
130	pectate lyase family protein	At5g63180		-	0,04
131	pectate lyase family protein	At1g04680		-	0,1
132	pectate lyase family protein	At3g07010		-	0,2
133	polygalacturonase inhibiting protein 2	At5g06870	PGIP2	-	0,1
134	polygalacturonase, putative / pectinase, putative	At1g60590		-	0,1
135	**Starch synthesis**				
136	pectinesterase family protein	At1g61800		-	8,7
137	ADP-glucose pyrophosphorylase subunit	At5g19220	ADG2	-	0,3
138	glucose-1-phosphate adenylyltransferase large subunit 3	At4g39210	APL3	-	0,2
139	glycogen synthase, putative	At3g01180		-	0,2
140	isoamylase, putative	At4g09020		-	0,2
141	isoamylase, putative	At1g03310		-	0,1
142	isoamylase, putative 9	At2g39930		-	0,2
143	starch synthase, putative	At1g32900		-	0,2
144	starch synthase, putative	At1g11720		-	0,2
145	starch synthase-related protein	At4g18240		-	0,3
146	**Sucrose synthesis**				
147	sucrose-phosphatase 1	At2g35840		-	0,3
148	sucrose-phosphatase 2	At3g52340	SPP2	-	0,3
149	sucrose-phosphate synthase, putative	At5g20280		-	0,3
150	sucrose-phosphate synthase, putative	At4g10120		-	0,1
151	**Starch degradation**				
152	4-alpha-glucanotransferase, putative	At5g64860	DPE1	-	0,2
153	alpha-glucosidase 1	At5g11720		-	0,2
154	alpha-xylosidase	At1g68560	XYL1	-	0,1
155	beta-amylase	At4g15210	BETA-AMY	-	0,04
156	beta-amylase	At4g17090	CT-BMY	-	0,2
157	beta-amylase, putative	At4g00490		-	0,3
158	beta-amylase, putative	At2g32290		-	0,1
159	glucan phosphorylase, putative	At3g29320		-	0,3
160	glycoside hydrolase family 77 protein	At2g40840		-	0,2
161	starch excess protein	At1g10760	SEX1	-	0,2
162	starch phosphorylase, putative	At3g46970		-	0,2
163	**Sucrose degradation**				
164	beta-fructofuranosidase, putative	At1g22650		-	3,4

Row	Description	Locus[2]	Protein	t/c ratio[3]	
	Functional categories[1]			IS12	S12
165	beta-fructofuranosidase, putative	At1g35580		-	6.3
166	pfkB-type carbohydrate kinase family protein	At5g51830		2.5	8
167	beta-fructofuranosidase, putative	At4g09510		-	0.3
168	beta-fructosidase	At1g12240		-	0.2
169	beta-fructosidase, putative	At1g55120		-	0.2
170	**Amino acid metabolism**				
171	aspartate aminotransferase	At5g19550		2.1	4.6
172	glutamate decarboxylase 1	At5g17330	GAD1	25.8	480.7
173	glutamate decarboxylase, putative	At2g02000		-	20.6
174	prephenate dehydratase family protein	At5g22630		-	4
175	prephenate dehydratase family protein	At3g44720		-	3
176	proline oxidase, putative	At5g38710		2.2	2.6
177	2-isopropylmalate synthase 2	At5g23020	MAM-L	-	0.04
178	2-isopropylmalate synthase 3	At5g23010	MAM1	-	0.1
179	3-isopropylmalate dehydrogenase	At1g31180		-	0.2
180	aminotransferase, putative	At2g20610	SUR1	-	0.1
181	arginase, putative	At4g08870		-	0.2
182	asparagine synthetase 2	At5g65010	ASN2	-	0.2
183	aspartate aminotransferase	At1g62800	ASP4	-	0.1
184	aspartate kinase, lysine-sensitive, putative	At3g02020		-	0.1
185	aspartate-glutamate racemase family	At1g15410		-	0.3
186	bifunctional aspartate kinase	At1g31230		-	0.1
187	branched-chain amino acid aminotransferase, putative	At3g19710		-	0.1
188	chorismate mutase, putative	At1g69370	CM3	-	0.3
189	cystathionine beta-lyase	At3g57050	CBL	-	0.2
190	cysteine synthase, putative	At5g28020	CYSD2	-	0.2
191	cysteine synthase, putative	At3g61440	CYSC1	-	0.2
192	cysteine synthase, putative	At5g28030		-	0.1
193	cysteine synthase, putative	At3g04940	CYSD1	-	0.2
194	dihydrodipicolinate reductase family protein	At5g52100		-	0.2
195	homocysteine S-methyltransferase 3	At3g22740	HMT3	-	0.1
196	lactoylglutathione lyase, putative	At1g11840	GLX1	-	0.3
197	phosphoethanolamine N-methyltransferase 1	At3g18000	NMT1	-	0.3
198	prephenate dehydratase family protein	At2g27820		-	0.2
199	prephenate dehydratase family protein	At1g08250		-	0.2
200	prephenate dehydratase family protein	At1g11790		-	0.2
201	sarcosine oxidase family protein	At2g24580		-	0.3
202	shikimate kinase-related	At2g35500		-	0.3
203	threonine synthase, putative	At1g72810		-	0.2
204	tryptophan synthase-related	At5g38530		-	0.3
205	urease accessory protein	At2g34470	UREG	-	0.2
206	**Lipid metabolism**				
207	acetyl-CoA carboxylase 2	At1g36180		4.2	9.7
208	acyl-(acyl-carrier-protein) desaturase, putative	At5g16230		-	3.3
209	acyl-CoA binding family protein	At5g27630		-	3.7
210	acyl-CoA oxidase	At5g65110		2.4	3.2
211	AMP-binding protein, putative	At3g23790		-	3.9
212	diacylglycerol kinase, putative	At2g20900		-	3.4
213	glycerophosphoryl diester phosphodiesterase family protein	At5g58170		-	6
214	lipase class 3 family protein	At1g30370		5.2	21.1
215	longevity-assurance	At3g19260	LAG1	-	3.5
216	phospholipase D beta 1	At2g42010	PLDBETA1	-	4.2
217	serine C-palmitoyltransferase, putative	At3g48790		-	4.7
218	steroid sulfotransferase, putative	At2g03760		9.5	13.8
219	sterol carrier protein 2 (SCP-2) family protein	At5g42890		2.7	3.4
220	transducin family protein	At3g18860		3.6	6.7
221	3-oxo-5-alpha-steroid 4-dehydrogenase family protein	At3g55360		-	0.2
222	3-oxoacyl-(acyl-carrier-protein) synthase III	At1g62640	KAS III	-	0.3
223	acetyl-CoA C-acyltransferase 1	At5g48880		-	0.2
224	acyl CoA reductase, putative	At5g22500		-	0.04
225	acyl-activating enzyme 14	At1g30520		-	0.1
226	AMP-binding protein, putative	At5g16340		-	0.3
227	AMP-binding protein, putative	At1g75960		-	0.1
228	beta-ketoacyl-CoA synthase family protein	At1g07720		-	0.1
229	beta-ketoacyl-CoA synthase, putative	At2g26640		-	0.2
230	beta-ketoacyl-CoA synthase, putative	At1g04220		-	0.1
231	ceramidase family protein	At2g38010		-	0.2
232	eceriferum protein	At4g24510	CER2	-	0.2
233	enoyl-CoA hydratase/isomerase family protein	At4g14440		-	0.1
234	enoyl-CoA hydratase/isomerase family protein	At1g06550		-	0.2
235	esterase/lipase/thioesterase family protein	At1g52760		-	0.2
236	expressed protein	At2g03550		-	0.1
237	fatty acid elongase 3-ketoacyl-CoA synthase 1	At1g01120	KCS1	-	0.1
238	fatty acid elongase, putative	At2g15090		-	0.2
239	glycerol-3-phosphate acyltransferase	At1g32200	ATS1	-	0.3
240	glycerophosphoryl diester phosphodiesterase family protein	At1g66970		-	0.2
241	glycerophosphoryl diester phosphodiesterase family protein	At1g74210		-	0.3
242	glycine-rich protein / oleosin	At5g56100		-	0.2
243	lipase	At1g28670	ARAB-1	-	0.1
244	lipase class 3 family protein	At4g10955		-	0.1
245	lipase, putative	At2g42690		-	0.1
246	long-chain-fatty-acid--CoA ligase	At1g49430	LACS2	-	0.1
247	long-chain-fatty-acid--CoA ligase family protein	At2g47240		-	0.1
248	long-chain-fatty-acid--CoA ligase, putative	At1g64400		-	0.2

Row	Description	Locus[2]	Protein	t/c ratio[3]	
	Functional categories[1]			IS12	S12
249	naphthoate synthase, putative	At1g60550		-	0,2
250	peroxisomal protein	At3g16910		-	0,1
251	phospholipase A2 family protein	At2g06925		-	0,2
252	quinone reductase family protein	At5g58800		-	0,3
253	squalene monooxygenase 1.1 / squalene epoxidase 1.1	At5g24150	SQP1	-	0,2
254	squalene monooxygenase 1.2 / squalene epoxidase 1.2	At5g24160		-	0,2
255	sterol 24-C-methyltransferase, putative	At5g13710	SMT1	-	0,2
256	sterol desaturase family protein	At4g22756	SMO1-2	-	0,1
257	sterol desaturase family protein	At4g22753	SMO1-3	-	0,1
258	sulfotransferase family protein	At2g03750		-	0,1
259	thromboxane-A synthase, putative	At2g26170	CYP711A1	-	0,3
260	**N-metabolism**				
261	ferredoxin--nitrite reductase, putative	At2g15620	NIR1	-	0,2
262	haloacid dehalogenase-like hydrolase family protein	At5g57440	GS1	-	0,3
263	**Nucleotide metabolism**				
264	guanylate kinase 2	At3g57550	GK-2	2,1	5,1
265	inosine-5'-monophosphate dehydrogenase	At1g79470		-	4,3
266	thymidine kinase, putative	At3g07800		-	4,4
267	adenine phosphoribosyltransferase 2	At1g80050		-	0,3
268	adenylosuccinate lyase, putative	At4g18440		-	0,1
269	deoxyuridine 5'-triphosphate nucleotidohydrolase family	At3g46940		-	0,2
270	inosine-uridine preferring nucleoside hydrolase family protein	At5g18860		-	0,2
271	nucleoside phosphatase family protein	At1g14250		-	0,3
272	type I phosphodiesterase	At4g29700		-	0,01
273	uridylate kinase, putative	At3g60180		-	0,3
274	**S-assimilation**				
275	adenylylsulfate kinase, putative	At5g67520		-	7,1
276	5'-adenylylsulfate reductase	At4g21990		-	0,1
277	5'-adenylylsulfate reductase (APR1)	At4g04610		-	0,1
278	5'-adenylylsulfate reductase 2	At1g62180		-	0,2
279	adenylylsulfate kinase 2	At4g39940	AKN2	-	0,1
280	APS kinase mRNA	At2g14750	APK	-	0,1
281	dihydrofolate synthetase/folylpolyglutamate synthetase	At3g55630	ATDFD	-	0,1
282	dihydroneopterin aldolase, putative	At5g62980		-	0,3
283	methylenetetrahydrofolate reductase	At2g44160	MTHFR2	-	0,3
284	similar to dihydrofolate synthetase	At3g10160	ATDFC	-	0,3
285	sulfate adenylyltransferase 2	At1g19920	APS2	-	0,1
286	sulfate adenylyltransferase 3	At4g14680	APS3	-	0,2
287	sulfite reductase	At5g04590	SIR	-	0,3
288	tetrahydrofolate dehydrogenase/cyclohydrolase, putative	At3g12290		-	0,3
289	**Secondary metabolism**				
290	caffeoyl-CoA 3-O-methyltransferase, putative	At1g67980		-	3,6
291	FAD-binding domain-containing protein	At5g44390		5,3	12,8
292	FAD-binding domain-containing protein	At1g26380		-	87,9
293	FAD-binding domain-containing protein	At1g26390		-	47
294	FAD-binding domain-containing protein	At1g26420		-	14,1
295	FAD-binding domain-containing protein	At4g20860		-	4,9
296	long-chain-alcohol O-fatty-acyltransferase family protein	At3g51970		2,3	3,3
297	O-methyltransferase family 2 protein	At1g33030		2,7	9,6
298	strictosidine synthase family protein	At3g57020		-	3,2
299	transferase family protein	At5g39090		-	3,4
300	transferase family protein	At5g39050		-	4,1
301	4-coumarate--CoA ligase 1	At1g51680	4CL1	-	0,2
302	4-coumarate--CoA ligase 2	At3g21240	4CL2	-	0,3
303	4-coumarate--CoA ligase 3	At1g65060	4CL3	-	0,1
304	alliinase C-terminal domain-containing protein	At1g70560		-	0,3
305	amine oxidase family protein	At3g09580		-	0,1
306	amine oxidase-related	At5g49555		-	0,3
307	beta-ketoacyl-CoA synthase family	At2g26250		-	0,1
308	carbonic anhydrase family protein	At1g58180		-	0,3
309	CER1 protein	At1g02205	CER1	-	0,2
310	CER1 protein, putative	At5g57800	WAX2	-	0,2
311	CER1 protein	At1g02200		-	0,07
312	chalcone-flavanone isomerase family protein	At5g05270		-	0,3
313	cinnamoyl-CoA reductase-related	At2g23910		-	0,2
314	cinnamoyl-CoA reductase-related	At4g30470		-	0,2
315	cytochrome P450 84A1	At4g36220	FAH1	-	0,2
316	dihydroflavonol 4-reductase	At5g42800	DFR	-	0,1
317	FAD-binding domain-containing protein	At2g34810		-	0,1
318	FAD-binding domain-containing protein	At4g20840		-	0,2
319	FAD-binding domain-containing protein	At5g44410		-	0,2
320	flavin-containing monooxygenase family protein	At1g65860		-	0,1
321	flavonoid 3'-monooxygenase	At5g07990	TT7	-	0,1
322	flavonol synthase	At5g08640		-	0,1
323	glycosyltransferase family protein	At5g54060		-	0,1
324	ivinyl protochlorophyllide 8-vinyl reductase	At5g18660	PCB2	-	0,3
325	jacalin lectin family protein	At1g52000		-	0,04
326	jacalin lectin family protein	At2g39330		-	0,2
327	leucoanthocyanidin dioxygenase, putative	At4g22870		-	0,03
328	leucoanthocyanidin dioxygenase-like protein	At5g05600		-	0,1
329	lycopene beta cyclase	At3g10230	LYC	-	0,3
330	mannitol dehydrogenase, putative	At4g39330		-	0,1
331	mevalonate diphosphate decarboxylase, putative	At3g54250		-	0,3
332	myrosinase-associated protein, putative	At1g54020		-	0,2

Row	Description	Locus[2]	Protein	t/c ratio[3]	
	Functional categories[1]			IS12	S12
333	myrosinase-associated protein, putative	At3g14210		-	0,3
334	oxidoreductase family protein	At1g68540		-	0,2
335	oxidoreductase, 2OG-Fe(II) oxygenase family protein	At3g19000		-	0,1
336	phenylalanine ammonia-lyase 1	At2g37040	PAL1	-	0,2
337	phenylalanine ammonia-lyase 2	At3g53260	PAL2	-	0,2
338	phenylalanine ammonia-lyase 3	At5g04230	PAL3	-	0,2
339	phytoene synthase	At5g17230	PSY	-	0,3
340	pseudogene, transferase family	At1g03495		-	0,1
341	putative catechol O-methyltransferase	At1g76790		-	0,2
342	short-chain dehydrogenase/reductase family protein	At2g29340		-	0,1
343	strictosidine synthase family protein	At3g51450		-	0,1
344	strictosidine synthase family protein	At3g51420		-	0,1
345	transferase family protein	At2g39980		-	0,1
346	transferase family protein	At3g29590		-	0,1
347	transferase family protein	At3g50270		-	0,1
348	transferase family protein	At3g50280		-	0,1
349	transferase family protein	At5g07860		-	0,3
350	transferase family protein	At5g39080		-	0,3
351	transferase family protein	At5g48930		-	0,2
352	transferase family protein	At5g67150		-	0,04
353	tropinone reductase, putative	At2g29290		-	0,1
354	tropinone reductase, putative	At1g07440		-	0,1
355	tropinone reductase, putative	At2g29310		-	0,1
356	tropinone reductase, putative	At2g29320		-	0,1
357	tyrosine decarboxylase, putative	At2g20340		-	0,2
358	UbiA prenyltransferase family protein	At1g60600		-	0,2
359	UDP-glucoronosyl/UDP-glucosyl transferase family protein	At1g01420		-	0,1
360	UDP-glucoronosyl/UDP-glucosyl transferase family protein	At1g30530		-	0,1
361	UDP-glucoronosyl/UDP-glucosyl transferase family protein	At4g01070		-	0,2
362	very-long-chain fatty acid condensing enzyme	At1g68530	CUT1	-	0,2
363	very-long-chain fatty acid condensing enzyme, putative	At1g25450		-	0,2
364	very-long-chain fatty acid condensing enzyme, putative	At2g16280		-	0,2
365	**Tetrapyrrol synthesis**				
366	chlorophyllase	At5g43860	CLH2	2,8	8,8
367	errochelatase I	At5g26030		-	3,1
368	flavodoxin family protein	At3g02280		2,4	2,8
369	glutamyl-tRNA reductase, putative	At2g31250		-	5,1
370	magnesium-protoporphyrin O-methyltransferase, putative	At4g25080		-	0,2
371	protochlorophyllide reductase A	At5g54190	PORA	-	0,2
372	protochlorophyllide reductase B	At4g27440	PORB	-	0,2
373	protochlorophyllide reductase C	At1g03630	POR	-	0,3
374	urophorphyrin III methylase	At5g40850	UPM1	-	0,2
375	**Electron pathways**				
376	catalytic LigB subunit	At4g15093		2,5	3,7
377	cytochrome P450, putative	At5g61320	CYP89A3	18.8	43.9
378	cytochrome P450, putative	At3g03470	CYP89A9	-	3.9
379	cytochrome P450, putative	At2g21910	CYP96A5	-	3.5
380	cytochrome P450 family protein	At2g34500	CYP710A1	3,1	11,4
381	cytochrome P450 71B23, putative	At3g26210	CYP71B23	-	3.2
382	cytochrome P450, putative	At1g33720	CYP76C6	2,3	5.7
383	cytochrome P450, putative	At1g13150	CYP86C4	-	6,6
384	cytochrome P450, putative	At4g37370	CYP81D8	2,3	15.4
385	cytochrome P450, putative	At5g57220	CYP81F2	-	24,1
386	cytochrome P450 family protein	At5g67310	CYP81G1	3,2	3,6
387	electron transport SCO1/SenC family protein	At4g39740		2.4	5
388	Encodes a protein with 14.6% glycine residues	At4g33930		4,7	25
389	uclacyanin II	At2g44790	UCC2	-	17
390	trehalose-6-phosphate phosphatase, putative	At2g22190		-	0,1
391	chlorophyll A-B binding protein	At3g08940	LHCB4.2	-	0,3
392	cytochrome P450 family protein	At3g14650	CYP72A11	-	0,2
393	cytochrome P450 family protein	At4g39510	CYP96A12	-	0,3
394	cytochrome P450 family protein	At5g52320	CYP96A4	-	0,1
395	cytochrome P450 family protein	At3g20100	CYP705A19	-	0,3
396	cytochrome P450, putative	At4g12310	CYP706A5	-	0,1
397	cytochrome P450 family protein	At4g19230	CYP707A1	-	0,2
398	cytochrome P450 family protein	At1g78490	CYP708A3	-	0,2
399	cytochrome P450 family protein	At2g34490	CYP710A2	-	0,2
400	cytochrome P450 family protein	At5g25120	CYP71B11	-	0,2
401	cytochrome P450 family protein	At1g13080	CYP71B2	-	0,2
402	cytochrome P450 family protein	At3g26300	CYP71B34	-	0,2
403	cytochrome P450 71B36, putative	At3g26320	CYP71B36	-	0,2
404	cytochrome P450 family protein	At4g27710	CYP709B3	-	0,2
405	cytochrome P450 family protein	At2g45560	CYP76C1	-	0,3
406	cytochrome P450 family protein	At2g27690	CYP94C1	-	0,2
407	cytochrome P450 81D1	At5g36220	CYP81D1	-	0,3
408	cytochrome P450 family protein	At4g37330	CYP81D4	-	0,2
409	cytochrome P450 family protein	At4g37310	CYP81H1	-	0,3
410	cytochrome P450 family protein	At3g44970		-	0,3
411	ferredoxin family protein	At4g14890		-	0,1
412	ferric chelate reductase	At5g50160		-	0,1
413	ferric chelate reductase, putative	At5g49730		-	0,1
414	glucosamine	At5g24420		-	0,2
415	glucose-6-phosphate dehydrogenase	At5g35790		-	0,1
416	hydroperoxide lyase	At4g15440	HPL1	-	0,1
417	oxidoreductase N-terminal domain-containing protein	At1g66130		-	0,1

Row	Description	Locus[2]	Protein	t/c ratio[3]	
	Functional categories[1]			IS12	S12
418	phosphoenolpyruvate carboxylase, putative	At2g42600	ATPPC2	-	0,3
419	plastocyanin-like domain-containing protein	At4g12880		-	0,1
420	rubredoxin family protein	At5g17170		-	0,2
421	**Photosynthesis**				
422	ribose 5-phosphate isomerase-related	At1g71100		-	4.7
423	phosphoribulokinase/uridine kinase family protein	At2g01460		-	4.6
424	alcohol dehydrogenase, putative	At1g22430		-	0,2
425	chlorophyll A-B binding protein	At2g40100	LHCB4.3	-	0,2
426	chlorophyll A-B binding protein, putative	At1g19150	LHCA2*1	-	0,1
427	expressed protein	At2g28605		-	0,2
428	ferredoxin-related	At3g16250		-	0,2
429	fructose-1,6-bisphosphatase family protein	At5g64380		-	0,2
430	fructose-bisphosphate aldolase	At4g26520		-	0,1
431	fructose-bisphosphate aldolase, putative	At4g26530		-	0,2
432	oxygen evolving enhancer 3 (PsbQ) family protein	At1g14150		-	0,2
433	oxygen evolving enhancer 3 (PsbQ) family protein	At3g01440		-	0,1
434	phosphoribulokinase (PRK) / phosphopentokinase	At1g32060		-	0,3
435	photosystem I reaction center subunit II0 kDa subunit	At1g03130		-	0,3
436	photosystem II 11 kDa protein-related	At1g05385		-	0,2
437	photosystem II 5 kD protein	At1g51400		-	0,2
438	photosystem II reaction center PsbP family protein	At2g39470		-	0,3
439	phytochromobilin:ferredoxin oxidoreductase	At3g09150	HY2	-	0,3
440	plastocyanin	At1g76100		-	0,2
441	ribose 5-phosphate isomerase-related	At5g44520		-	0,2
442	similar to unknown protein	At5g58260		-	0,3
443	thylakoid lumenal 29.8 kDa protein	At1g77090		-	0,3
444	**Mitochondrial electron-transport**				
445	alternative oxidase 1a, mitochondrial	At3g22370	AOX1A	2,3	8,6
446	alternative oxidase 1b, mitochondrial	At3g22360	AOX1B	-	22,6
447	alternative oxidase, putative	At1g32350		7.2	170,6
448	cytochrome c, putative	At4g10040		2,6	4,3
449	Internal NAD(P)H dehydrogenase in mitochondria	At1g07180		4,2	5,6
450	NADH dehydrogenase-related	At4g05020		-	5,5
451	pyridine nucleotide-disulphide oxidoreductase family protein	At2g20800		51	61,8
452	ubiquinol-cytochrome C reductase complex, putative	At5g25450		-	4
453	cytochrome c biogenesis protein family	At1g49380		-	0,3
454	expressed protein	At5g12420		-	0,1
455	**Glycolysis**				
456	2,3-biphosphoglycerate-independent phosphoglycerate mutase, putative	At3g08590		2.9	4.6
457	cytosolic phosphoglycerate kinase (PGK) mRNA	At1g79550	PGK	2,1	2.9
458	fructose-bisphosphate aldolase, putative	At2g36460		2,2	4,4
459	pyrophosphate-fructose-6-P-1-phosphotransferase a subunit, putative	At1g76550		3,7	7.6
460	pyrophosphate-fructose-6-P-1-phosphotransferase b subunit, putative	At1g12000		-	4
461	pyruvate kinase, putative	At3g04050		-	4,3
462	pyruvate kinase, putative, similar to pyruvate kinase	At5g56350		3.3	9,2
463	pyrophosphate-fructose-6-P-1-phosphotransferase b subunit, putative	At4g04040		-	0,2
464	phosphofructokinase family protein	At4g29220		-	0,3
465	phosphoglucomutase, putative	At5g51820		-	0,3
466	pyrophosphate-fructose-6-P-1-phosphotransferaseb subunit, putative	At1g70820		-	0,1
467	**Citric acid cycle**				
468	malate dehydrogenase	At5g43330	UXS3	2,6	3,5
469	carbonic anhydrase family protein	At3g52720		-	0,1
470	**Fermentation**				
471	L-lactate dehydrogenase, putative	At4g17260		4,1	9,6
472	pyruvate decarboxylase, putative	At4g33070		241	656,6
473	aldehyde dehydrogenase family protein,	At4g36250	ALDH3F1	-	0,2
474	**PROTEIN METABOLISM**				
475	**Protein degradation**				
476	20S proteasome alpha subunit A2	At2g05840	PAA2	3,2	4,3
477	20S proteasome alpha subunit B	At1g16470	PAB1	4,7	8,5
478	20S proteasome alpha subunit B, putative	At1g79210		4,2	8,6
479	20S proteasome alpha subunit C	At3g22110	PAC1	3,7	5,2
480	20S proteasome alpha subunit D	At3g51260	PAD1	2,7	5,5
481	20S proteasome alpha subunit D2	At5g66140	PAD2	5,3	14,1
482	20S proteasome alpha subunit E1	At1g53850	PAE1	4,3	8,2
483	20S proteasome alpha subunit E2	At3g14290	PAE2	4,1	8,8
484	20S proteasome alpha subunit F1	At5g42790	PAF1	3,3	7,8
485	20S proteasome alpha subunit F2	At1g47250	PAF2	5	11,3
486	20S proteasome alpha subunit G	At2g27020	PAG1	2,8	5,3
487	20S proteasome beta subunit A	At4g31300	PBA1	3	5,4
488	20S proteasome beta subunit B	At3g27430	PBB1	2,6	4,7
489	20S proteasome beta subunit B	At5g40580	PBB2	5,1	12,5
490	20S proteasome beta subunit C1	At1g21720	PBC1	2,8	5,4
491	20S proteasome beta subunit C	At1g77440	PBC2	4,2	7,7
492	20S proteasome beta subunit D	At3g22630	PBD1	3,5	5,5
493	20S proteasome beta subunit D2	At4g14800	PBD2	3	6,2
494	20S proteasome beta subunit E1	At1g13060	PBE1	2,4	4,9
495	20S proteasome beta subunit F1	At3g60820	PBF1	2	3,5
496	20S proteasome beta subunit G1	At1g56450	PBG1	2,8	5
497	26S protease regulatory complex subunit 4, putative	At2g20140		2.2	4.9
498	26S protease regulatory subunit 6A, putative	At1g09100		7,2	19,8
499	26S proteasome AAA-ATPase subunit	At1g53750	RPT1A	2,4	4,5
500	26S proteasome AAA-ATPase subunit	At4g29040	RPT2A	3,1	6,5
501	26S proteasome AAA-ATPase subunit	At5g58290	RPT3	3	7,1
502	26S proteasome AAA-ATPase subunit	At5g43010	RPT4A	2,5	6,4

Row	Description	Locus[2]	Protein	t/c ratio[3]	
	Functional categories[1]			IS12	S12
503	26S proteasome AAA-ATPase subunit	At3g05530	RPT5A	2.4	5.4
504	26S proteasome AAA-ATPase subunit, putative	At5g20000	RPT6A	4.7	9.3
505	26S proteasome non-ATPase regulatory subunit 7	At5g05780	RPN8a	2.5	4.8
506	26S proteasome non-ATPase regulatory subunit 7	At3g11270	RPN8b	7.7	12.3
507	26S proteasome regulatory complex subunit p42D	At1g45000		3.5	6.5
508	26S proteasome regulatory subunit S2	At2g20580	RPN1a	4.2	8.2
509	26S proteasome regulatory subunit, putative	At4g28470	RPN1b	2.6	5.1
510	26S proteasome regulatory subunit, putative	At2g32730	RPN2a	2.8	5.7
511	26S proteasome regulatory subunit, putative	At1g04810	RPN2b	4.7	8.8
512	26S proteasome regulatory subunit S3, putative	At1g20200	RPN3a	3,2	7,6
513	26S proteasome regulatory subunit, putative	At5g09900	RPN5a	3.2	6.8
514	26S proteasome regulatory subunit, putative	At5g64760	RPN5b	4.8	7.7
515	26S proteasome regulatory subunit, putative	At1g29150	RPN6	2.9	7.3
516	26S proteasome regulatory subunit, putative	At4g24820	RPN7	3.3	6.2
517	26S proteasome regulatory subunit, putative	At5g45620	RPN9	-	3.2
518	26S proteasome regulatory subunit S5A	At4g38630	RPN10	2.2	5.3
519	26S proteasome regulatory subunit, putative	At5g23540	RPN11	4	9.3
520	26S proteasome regulatory subunit, putative	At1g64520	RPN12a	3.1	5.2
521	proteasome maturation factor UMP1 family protein	At5g38650		2.8	6.1
522	proteasome maturation factor UMP1 family protein	At1g67250		6.5	9.9
523	proteasome-related	At3g15180		3.3	8.6
524	AAA-type ATPase family protein	At2g18330		-	3.3
525	AAA-type ATPase family protein	At3g03060		5	11.5
526	AAA-type ATPase family protein	At4g28000		23.6	57
527	AAA-type ATPase family protein	At5g16930		4.3	10
528	AAA-type ATPase family protein	At1g43910		3.9	10.5
529	AAA-type ATPase family protein	At2g18190		6	8.2
530	AAA-type ATPase family protein	At3g28580		2.4	34.5
531	AAA-type ATPase family protein	At5g40010		14.3	25.2
532	AAA-type ATPase family protein	At3g50930		-	21.7
533	AAA-type ATPase family protein	At4g04180		-	4.6
534	AAA-type ATPase family protein	At4g36580		-	14.6
535	AAA-type ATPase family protein	At5g17760		-	3.4
536	AAA-type ATPase family protein	At5g57480		-	4.4
537	FtsH protease	At1g06430		-	4.3
538	FtsH protease	At1g07510		5.4	13.4
539	armadillo/beta-catenin repeat family protein	At5g67340		-	3.2
540	aspartyl protease family protein	At3g12700		4.2	4.4
541	ATP-dependent Clp protease regulatory subunit	At5g51070		-	3.3
542	autophagy 8b (APG8b)	At4g04620		7.5	8.8
543	autophagy 8e (APG8e)	At2g45170		3.6	3.3
544	autophagy 8h (APG8h)	At3g06420		4.5	7.9
545	autophagy 9 (APG9)	At2g31260	APG9	-	4.1
546	stomatin-like protein	At5g54100		4,7	12,7
547	prohibitin, putative	At3g27280		-	3.3
548	band 7 family protein	At3g01290		-	6.1
549	band 7 family protein	At5g51570		-	3.6
550	band 7 family protein	At5g62740		-	3.3
551	band 7 family protein	At1g69840		-	3.4
552	cullin family protein	At4g02570	CUL1	-	3.1
553	cullin family protein	At1g02980		-	5.1
554	chaperonin, putative	At3g02530		-	3
555	cysteine protease inhibitor, putative	At5g05110		-	3.3
556	DegP protease, putative	At3g03380		-	3.1
557	F-box family protein	At5g03970		3	5.2
558	F-box family protein	At1g10110		3.2	5.5
559	F-box family protein	At1g53790		3.2	7.5
560	F-box family protein	At4g27050		-	3.8
561	F-box family protein	At5g27750		-	3.9
562	F-box family protein	At2g16450		-	150.4
563	F-box family protein	At2g24250		-	14.6
564	F-box family protein / SKP1 interacting partner 3-related	At2g02300		-	75.2
565	kelch repeat-containing F-box family protein	At5g03020		-	7
566	kelch repeat-containing F-box family protein	At3g08810		2.1	2.4
567	kelch repeat-containing F-box family protein	At4g38940		2.1	4.9
568	Kelch repeat-containing protein	At1g51540		2	-
569	HECT-domain-containing protein	At5g02880		-	3
570	latex-abundant protein, putative (AMC8)	At1g16420		2,7	36,8
571	LON protease homolog (LON ARA) mRNA	At5g26860		-	4.7
572	Lon protease, putative	At3g05790		-	46.5
573	matrixin family protein	At1g24140		-	12.6
574	nucellin protein, putative	At1g44130		2.8	17.3
575	nucellin protein, putative	At1g77480		3.3	3.4
576	OTU-like cysteine protease family protein	At3g22260		2.3	8.2
577	peptidase M16 family protein	At3g19170		2.3	3.5
578	peptidase M48 family protein	At5g51740		2.8	6.4
579	phosphatase-related	At4g23570	SGT1A	-	5.5
580	phosphatidylinositol 3- and 4-kinase family protein	At2g46500		-	3,1
581	replication protein, putative	At2g06510		2,3	4.1
582	RUB1-conjugating enzyme, putative	At2g18600		-	6
583	SCF complex subunit SKP1/ASK1(At3),putative	At2g25700		4.5	11.9
584	subtilase family protein	At1g32960		-	6.2
585	subtilase family protein	At1g32950		7.3	28.7
586	subtilase family protein	At1g32940		6.5	24.9
587	SWAP	At1g14650		-	3

Row	Description	Locus[2]	Protein	t/c ratio[3]	
	Functional categories[1]			IS12	S12
588	ubiquitin carboxyl-terminal hydrolase family protein	At4g31670		2.7	4.6
589	ubiquitin carboxyl-terminal hydrolase, putative	At4g17510		3.8	8.4
590	ubiquitin family protein	At3g13235		3.2	10.7
591	ubiquitin family protein	At1g64470		-	4.2
592	ubiquitin fusion degradation UFD1 family protein	At2g21270		-	3.2
593	ubiquitin fusion degradation UFD1 family protein	At2g29070		-	3.2
594	ubiquitin-associated (UBA)	At1g04850		2.4	5.4
595	ubiquitin-associated (UBA)	At4g24690		-	4.7
596	ubiquitin-conjugating enzyme 11 (UBC11), E2	At3g08690		-	6.2
597	ubiquitin-conjugating enzyme 13 (UBC13), E2	At3g46460		-	3,7
598	ubiquitin-conjugating enzyme 3 (UBC3), E2	At5g62540		2.2	3.5
599	ubiquitin-conjugating enzyme, putative	At5g50870		2.5	3.9
600	ubiquitin-specific protease 14, putative	At3g20630	UBP14	-	5.1
601	ubiquitin-specific protease 6, putative	At1g51710	UBP6	2.5	5.5
602	ubiquitin-specific protease 7, putative	At3g21280	UBP7	7.4	12.6
603	UBX domain-containing protein	At4g23040		3.7	7.2
604	zinc finger (C3HC4-type RING finger) family protein	At5g20910		7.2	31.3
605	armadillo/beta-catenin repeat family protein	At3g07360		-	0,3
606	ATP-dependent protease La (LON) domain-containing protein	At1g67480		-	0,3
607	ATP-dependent protease La (LON) domain-containing protein	At1g75460		-	0,2
608	cysteine proteinase, putative	At2g27420		-	0,2
609	cysteine proteinase, putative	At3g43960		-	0,3
610	cysteine proteinase, putative	At3g48350		-	0,2
611	F-box family protein	At1g31350		-	0,2
612	F-box family protein	At1g57790		-	0,3
613	F-box family protein	At1g78100		-	0,2
614	F-box family protein	At2g32560		-	0,1
615	F-box family protein	At3g23880		-	0,1
616	F-box family protein-related, similar to A3 protein	At2g03530	UPS2	-	0,3
617	FtsH protease	At5g53170		-	0,3
618	FtsH protease, putative	At3g16290		-	0,3
619	gamma-glutamyl hydrolase	At1g78680		-	0,2
620	kelch repeat-containing F-box family	At3g59940		-	0,1
621	kelch repeat-containing F-box family protein	At1g23390		-	0,2
622	kelch repeat-containing F-box family protein	At1g80440		-	0,3
623	kelch repeat-containing F-box family protein	At2g44130		-	0,2
624	protease HhoA	At4g18370	HHOA	-	0,1
625	serine carboxypeptidase III, putative	At3g45010		-	0,3
626	serine carboxypeptidase S10 family protein	At1g15000		-	0,1
627	serine carboxypeptidase S10 family protein	At1g28110		-	0,3
628	serine carboxypeptidase S10 family protein	At2g22970		-	0,2
629	serine carboxypeptidase S10 family protein	At2g22980		-	0,1
630	serine carboxypeptidase S10 family protein	At2g23000		-	0,2
631	serine carboxypeptidase S10 family protein	At2g27920		-	0,2
632	serine carboxypeptidase S10 family protein	At2g33530		-	0,2
633	serine carboxypeptidase S10 family protein	At2g35780		-	0,2
634	serine carboxypeptidase S10 family protein	At4g30810		-	0,2
635	serine carboxypeptidase S10 family protein	At5g08260		-	0,2
636	serine carboxypeptidase S10 family protein	At5g23210		-	0,2
637	serine carboxypeptidase S10 family protein	At5g42240		-	0,2
638	serine carboxypeptidase S28 family protein	At2g24280		-	0,3
639	serine carboxypeptidase S28 family protein	At5g22860		-	0,2
640	serine carboxypeptidase S10 family protein	At4g30610	BRS1	-	0,2
641	sinapoylglucose:malate sinapoyltransferase	At2g22990	SNG1	-	0,3
642	subtilase family protein	At1g01900		-	0,03
643	subtilase family protein	At1g20160		-	0,1
644	subtilase family protein	At2g05920		-	0,2
645	subtilase family protein	At3g14240		-	0,1
646	subtilase family protein	At4g30020		-	0,1
647	subtilase family protein	At4g34980	SLP2	-	0,1
648	subtilase family protein	At5g45650		-	0,2
649	subtilase family protein	At5g59130		-	0,2
650	ubiquitin-conjugating enzyme 5	At1g63800		-	0,3
651	**CELLULAR REGULATION**				
652	calcineurin-like phosphoesterase family protein	At3g09960		2.5	2.6
653	expressed protein	At5g67600		2.7	3.7
654	GDSL-motif lipase/hydrolase family protein	At5g40990		2.2	28.5
655	leucine-rich repeat family protein	At1g03440		3,9	5,3
656	phosphatidic acid phosphatase family protein	At2g01180	ATPAP1	-	4.8
657	poly (ADP-ribose) polymerase	At4g02390		-	4.2
658	PP1/PP2A phosphatases pleiotropic regulator 2 (PRL2)	At3g16650		2,4	6.1
659	protein phosphatase 2C, putative	At3g62260		-	4.7
660	protein phosphatase 2C, putative	At2g40180		-	97.4
661	serine/threonine protein phosphatase PP1 isozyme 6	At4g11240	TOPP7	-	3.2
662	calcineurin-like phosphoesterase family protein	At5g63140		-	0,2
663	chaperonin, putative	At1g26230		-	0,2
664	CLE12, CLAVATA3/ESR-Related 12	At1g68795	CLE12	-	0,3
665	expressed protein	At3g59400	GUN4	-	0,3
666	legume lectin family protein	At1g53070		-	0,2
667	leucine-rich repeat family protein	At1g68780		-	0,2
668	leucine-rich repeat family protein	At2g33050		-	0,2
669	leucine-rich repeat family protein	At3g17640		-	0,1
670	leucine-rich repeat family protein	At3g20820		-	0,1
671	palmitoyl protein thioesterase family protein	At4g17470		-	0,1
672	palmitoyl protein thioesterase family protein	At5g47330		-	0,1

Row	Description	Locus[2]	Protein	t/c ratio[3]	
	Functional categories[1]			IS12	S12
673	prolifera protein	At4g02060	PRL	-	0.2
674	ribulose-1,5 bisphosphate carboxylase oxygenase, putative	At1g14030		-	0.2
675	tyrosine phosphatase-like protein, putative	At5g59770		-	0.2
676	**Protein kinases ***				
677	casein kinase II beta chain, putative	At5g47080	CKB1	3.1	5.1
678	CBL-interacting protein kinase 20	At5g45820	CIPK20	-	3
679	CBL-interacting protein kinase 22, putative	At2g38490	CIPK22	-	11.5
680	lectin protein kinase family protein [LEC]	At4g28350		-	3.8
681	lectin protein kinase family protein [SD]	At1g67520		-	6.3
682	lectin protein kinase, putative [LEC]	At5g01550		4	16,7
683	lectin protein kinase, putative [LEC]	At3g59700	HLECRK	-	7.9
684	lectin protein kinase, putative [LEC]	At3g53810		2.4	5.6
685	legume lectin family protein [LEC]	At5g65600		-	27.7
686	leucine-rich repeat family protein	At1g33600		-	3.1
687	leucine-rich repeat family protein [LRR22]	At5g25930		-	4.4
688	leucine-rich repeat family protein [LRR23]	At3g13380		-	3
689	leucine-rich repeat protein kinase, putative [LRR3]	At1g51890		-	17.2
690	leucine-rich repeat protein kinase, putative [LRR4]	At5g41180		-	3.9
691	leucine-rich repeat transmembrane protein kinase, putative [LRR10]	At4g39270		-	4.7
692	leucine-rich repeat transmembrane protein kinase, putative [LRR20]	At1g74360		-	6.8
693	leucine-rich repeat transmembrane protein kinase, putative [LRR3]	At5g45840		-	4
694	protein kinase family protein	At3g25250		5.5	31.9
695	protein kinase family protein	At5g49470		-	6.9
696	protein kinase family protein	At5g55560		2.4	6.1
697	protein kinase family protein	At3g46930		2.2	5.1
698	protein kinase family protein	At1g77720		-	3.9
699	protein kinase family protein	At1g60610		2.5	3.7
700	protein kinase family protein	At1g57700		2.3	3.5
701	protein kinase family protein	At1g64300		2.1	3.5
702	protein kinase family protein [CRL4]	At3g55950		-	3.3
703	protein kinase family protein [DUF26]	At4g04490		2	28.7
704	protein kinase family protein [DUF26]	At4g23190	CRK11	-	5.7
705	protein kinase family protein [DUF26]	At4g04500		-	4.9
706	protein kinase family protein [DUF26]	At1g70530		-	3,4
707	protein kinase family protein [K]	At1g66460		-	30.5
708	protein kinase family protein [K]	At2g24370		-	11.1
709	protein kinase family protein [K]	At4g11890		-	4.4
710	protein kinase family protein [K]	At5g58940	CRCK1	-	4
711	protein kinase family protein [K]	At3g17420	GPK1	-	3.4
712	protein kinase family protein [KU]	At5g61560		-	3.3
713	protein kinase family protein [LRKL]	At1g18390		-	4.6
714	protein kinase family protein [LRR22]	At1g55610	BRL1	3	5.7
715	protein kinase family protein [SD]	At3g61960		2.4	4
716	protein kinase family protein [SK]	At5g46080		3,3	25,7
717	protein kinase family protein [TK]	At4g25390		-	4.9
718	protein kinase, putative	At3g01490		-	6
719	protein kinase, putative	At5g20930	TSL	2	3.1
720	protein kinase, putative	At2g45490		-	3.1
721	protein kinase, putative [K]	At5g03320		-	6.7
722	protein kinase, putative [K]	At1g69790		4.5	5.4
723	protein kinase, putative [K]	At5g47070		-	4
724	protein kinase, putative [K]	At2g17220		-	3.7
725	receptor-like protein kinase-related	At5g43980		-	3.7
726	similar to CBL-interacting protein kinase 9	At1g30270	CIPK23	-	6.8
727	similar to WD-40 repeat family protein	At4g22910		-	3.2
728	S-locus lectin protein kinase family protein [SD]	At1g61610		4	18.4
729	S-locus lectin protein kinase family protein [SD]	At4g21390		2,1	4.6
730	S-locus lectin protein kinase family protein [SD]	At1g61370		-	3.8
731	wall-associated kinase, putative [WAKL]	At1g79680		2,1	9
732	wall-associated kinase, putative [WAKL]	At1g21240	WAK3	-	38
733	wall-associated kinase-related	At1g16090	WAKL7	-	3.5
734	WD-40 repeat family protein	At5g42010		-	6.2
735	beta-lg-H3 domain-containing protein	At3g52370		-	0.3
736	CBL-interacting protein kinase 21	At5g57630	CIPK21	-	0.2
737	CBL-interacting protein kinase 9	At1g01140	CIPK9	-	0.3
738	lectin protein kinase, putative [LEC]	At4g02420		-	0,3
739	lectin protein kinase, putative [LEC]	At5g60300		-	0.2
740	lectin protein kinase, putative [LEC]	At5g03140		-	0,04
741	leucine-rich repeat family protein [LRR3]	At1g60800		-	0.2
742	leucine-rich repeat family protein [LRR4]	At5g10290		-	0,3
743	leucine-rich repeat family protein [LRR4]	At5g16000		-	0.2
744	leucine-rich repeat family protein [LRR8]	At4g37250		-	0,3
745	leucine-rich repeat protein kinase, putative [LRR10]	At1g66150	TMK1	-	0.2
746	leucine-rich repeat protein kinase, putative [LRR21]	At5g56040		-	0,2
747	leucine-rich repeat protein kinase, putative [LRR3]	At5g59670		-	0.2
748	leucine-rich repeat transmembrane protein kinase, putative [LRR16]	At2g27060		-	0,2
749	leucine-rich repeat transmembrane protein kinase, putative [LRR18]	At3g56370		-	0,1
750	leucine-rich repeat transmembrane protein kinase, putative [LRR20]	At1g72180		-	0,2
751	leucine-rich repeat transmembrane protein kinase, putative [LRR20]	At3g28040		-	0,1
752	leucine-rich repeat transmembrane protein kinase, putative [LRR22]	At5g65700		-	0,3
753	leucine-rich repeat transmembrane protein kinase, putative [LRR22]	At1g28440		-	0,3
754	leucine-rich repeat transmembrane protein kinase, putative [LRR22]	At3g49670		-	0,3
755	leucine-rich repeat transmembrane protein kinase, putative [LRR22]	At4g20270		-	0,1
756	leucine-rich repeat transmembrane protein kinase, putative [LRR4]	At2g35620		-	0,2
757	leucine-rich repeat transmembrane protein kinase, putative [LRR5]	At5g16590		-	0,3

Row	Description	Locus[2]	Protein	t/c ratio[3]	
	Functional categories[1]			IS12	S12
758	leucine-rich repeat transmembrane protein kinase, putative [LRR5]	At1g31420		-	0,3
759	leucine-rich repeat transmembrane protein kinase, putative [LRR5]	At1g48480	RKL1	-	0,2
760	leucine-rich repeat transmembrane protein kinase, putative [LRR5]	At3g17840	RLK902	-	0,2
761	leucine-rich repeat transmembrane protein kinase, putative [LRR5]	At2g26730		-	0,2
762	leucine-rich repeat transmembrane protein kinase, putative [LRR5]	At5g58300		-	0,1
763	leucine-rich repeat transmembrane protein kinase, putative [LRR6]	At3g14350		-	0,3
764	leucine-rich repeat transmembrane protein kinase, putative [LRR6]	At5g63410		-	0,3
765	leucine-rich repeat transmembrane protein kinase, putative [LRR6]	At2g45340		-	0,2
766	leucine-rich repeat transmembrane protein kinase, putative [LRR7]	At5g67280		-	0,3
767	leucine-rich repeat transmembrane protein kinase, putative [LRR7]	At5g45800		-	0,3
768	leucine-rich repeat transmembrane protein kinase, putative [LRR7]	At1g66830		-	0,2
769	leucine-rich repeat transmembrane protein kinase, putative [LRR8]	At3g03770		-	0,2
770	leucine-rich repeat transmembrane protein kinase, putative [TK]	At1g07650		-	0,2
771	leucine-rich repeat transmembrane protein kinase, putative[LRR6]	At5g51560		-	0,1
772	protein kinase [K]	At2g28930	APK1B	-	0,3
773	protein kinase C substrate	At2g42390		-	0,3
774	protein kinase family protein	At1g65190		-	0,3
775	protein kinase family protein	At5g46570		-	0,3
776	protein kinase family protein	At4g04570		-	0,2
777	protein kinase family protein	At3g22420		-	0,2
778	protein kinase family protein	At1g66980		-	0,2
779	protein kinase family protein	At3g05640		-	0,2
780	protein kinase family protein	At3g04910	WNK1	-	0,2
781	protein kinase family protein	At1g51940		-	0,1
782	protein kinase family protein [CrRLK1L]	At2g23200		-	0,3
783	protein kinase family protein [CrRLK1L]	At5g38990		-	0,3
784	protein kinase family protein [CrRLK1L]	At5g54380		-	0,2
785	protein kinase family protein [DUF26]	At4g23290		-	0,2
786	protein kinase family protein [DUF26]	At5g40380		-	0,01
787	protein kinase family protein [K]	At5g25440		-	0,3
788	protein kinase family protein [K]	At1g20650		-	0,3
789	protein kinase family protein [K]	At4g22130		-	0,3
790	protein kinase family protein [K]	At1g21590		-	0,2
791	protein kinase family protein [K]	At1g80640		-	0,2
792	protein kinase family protein [K]	At4g01330		-	0,2
793	protein kinase family protein [KT]	At1g33260		-	0,2
794	protein kinase family protein [SK]	At5g18500		-	0,3
795	protein kinase family protein [SK]	At1g09440		-	0,3
796	protein kinase family protein [SK]	At1g01540		-	0,2
797	protein kinase family protein [SK]	At2g16750		-	0,1
798	protein kinase family protein [TK]	At1g26150		-	0,3
799	protein kinase family protein [TK]	At1g52290		-	0,3
800	protein kinase family protein [TK]	At4g02630		-	0,2
801	protein kinase family protein [TK]	At1g54820		-	0,1
802	protein kinase family protein [TK]	At4g23220		-	0,2
803	protein kinase family protein [TK]	At2g45590		-	0,2
804	protein kinase, putative	At2g44830		-	0,3
805	protein kinase, putative	At5g28290		-	0,3
806	protein kinase, putative	At5g50180		-	0,2
807	pseudogene, protein kinase family protein [TK]	At4g32710		-	0,3
808	receptor-like protein kinase	At5g60890		-	0,1
809	serine/threonine protein kinase, putative	At1g78290		-	0,2
810	S-locus glycoprotein family protein [SD]	At4g00340	RLK4	-	0,3
811	S-locus lectin protein kinase family protein [SD]	At1g11350		-	0,1
812	S-locus lectin protein kinase family protein [SD]	At4g11900		-	0,04
813	somatic embryogenesis receptor-like kinase 2 [LRR4]	At1g34210	SERK2	-	0,1
814	wall-associated kinase, putative [WAKL]	At4g31110		-	0,2
815	**MAP kinases**				
816	mitogen-activated protein kinase kinase	At1g51660	MKK4	-	3,8
817	mitogen-activated protein kinase kinase	At3g21220	MKK5	-	3,2
818	mitogen-activated protein kinase kinase, putative	At5g40440	MKK3	2,3	3,6
819	mitogen-activated protein kinase, putative	At1g01560	MAPK11	-	5,7
820	**Phosphoinositides**				
821	phosphatidylinositol 3- and 4-kinase family protein	At1g64460		-	3,1
822	phosphatidylinositol-4-phosphate 5-kinase family protein	At1g34260		-	5,4
823	phosphatidylinositol-4-phosphate 5-kinase family protein	At3g09920		-	0,3
824	**C and Nurients**				
825	5'-AMP-activated protein kinase beta-1 subunit-related	At5g39790		-	0,3
826	glutamate receptor family protein	At2g32400	GLR5	-	0,3
827	phosphate-responsive protein, putative	At5g09440		-	0,1
828	phosphate-responsive protein, putative	At5g64260		-	0,3
829	**Light**				
830	chlorophyll A-B binding family protein	At4g14690	ELIP2	8,1	94,5
831	phytochrome and flowering time regulatory protein	At1g25540	PFT1	-	3,1
832	COP1-interacting protein-related	At5g43310		-	0,3
833	leucine-rich repeat protein kinase, putative	At1g51805		-	0,2
834	phototropic-responsive NPH3 family protein	At3g15570		-	0,02
835	phototropic-responsive NPH3 family protein	At3g19850		-	0,2
836	phototropic-responsive NPH3 family protein	At4g31820		-	0,1
837	phototropic-responsive NPH3 family protein	At1g52770		-	0,1
838	phytochrome interacting factor 3	At1g09530	PIF3	-	0,1
839	phytochrome kinase substrate 1	At2g02950	PKS1	-	0,1
840	protein kinase	At3g45780	PHOT1	-	0,2
841	signal transducer of phototropic response	At2g30510	RPT2	-	0,2
842	signal transducer of phototropic response	At2g30520	RPT2	-	0,2

Row	Description	Locus[2]	Protein	t/c ratio[3]	
	Functional categories[1]			IS12	S12
843	transcript accumulation is controlled by the circadian clock	At3g26740		-	0,2
	GTP Proteins				
844	extra-large guanine nucleotide binding protein, putative	At4g34390		-	4,5
845	GTP-binding family protein	At2g27200		-	3
846	GTP-binding protein	At5g42080	ADL1	-	4
847	GTP-binding protein (ERG)	At1g30960		-	3,3
848	GTP-binding protein-related	At5g27540		-	3,7
849	guanine nucleotide exchange family protein	At4g35380		3,5	6,1
850	RabGAP/TBC domain-containing protein	At5g41940		-	3,3
851	rac GTPase activating protein, putative	At1g08340		-	4,6
852	Ras-related GTP-binding family protein	At4g39890		-	4,4
853	Ras-related GTP-binding protein, putative	At1g52280		2	2,6
854	Ras-related GTP-binding protein, putative	At5g64990		2,6	5,3
855	Ras-related GTP-binding protein, putative	At4g17160		-	10
856	Ras-related GTP-binding protein, putative	At4g19640	ARA7	-	3,1
857	Ras-related GTP-binding protein, putative	At4g35860	GB2	-	3,3
858	WD-40 repeat family protein	At5g02430		4,9	10,9
859	Rac-like GTP-binding protein (ARAC4)	At1g20090			0,2
860	Ras-related protein (RAB7)	At1g22740			0,1
861	Rho-GTPase-activating protein-related	At4g35750			0,2
862	**Calcium regulation**				
863	C2 domain-containing protein	At4g34150		-	5
864	calcium-binding EF hand family protein	At4g26470		5,3	22,6
865	calcium-binding EF hand family protein	At5g39670		-	4,6
866	calcium-binding EF hand family protein	At5g04170		-	4,1
867	calcium-binding EF hand family protein	At4g27280		-	4,6
868	calcium-binding EF hand family protein	At4g05520		-	5,4
869	calcium-binding EF-hand protein, putative	At5g54490		-	7,3
870	calcium-dependent protein kinase 2 (CDPK2)	At1g35670	CDPK2	-	3,5
871	calcium-dependent protein kinase family protein	At5g66210	CPK28	-	3,6
872	calcium-dependent protein kinase isoform 2 (CPK2)	At3g10660	CPK2	-	5,2
873	calcium-dependent protein kinase, putative	At4g04740	CPK23	-	3,2
874	calcium-dependent protein kinase, putative	At4g09570	CPK4	-	4,1
875	calcium-dependent protein kinase, putative	At3g56760		2,8	2,6
876	calcium-dependent protein kinase, putative	At1g76040	CPK29	-	3,8
877	calcium-transporting ATPase	At3g22910		2,4	50,7
878	calcium-transporting ATPase	At3g63380		-	14,3
879	calcium-transporting ATPase 2	At4g00900	ECA2	3,7	5,6
880	calmodulin, putative	At1g18530		-	16,5
881	calmodulin-binding family protein	At2g33990		3,3	3,9
882	calmodulin-binding family protein	At2g26410		-	7,5
883	calmodulin-binding protein	At1g73800		-	6,4
884	calmodulin-binding protein	At1g73805		-	8,1
885	calmodulin-binding protein	At5g26920		-	6,9
886	calmodulin-binding protein	At3g56690		-	3,5
887	calmodulin-binding protein-related	At2g38800		2,6	3,8
888	calmodulin-domain protein kinase isoform 7	At5g12480	CPK7	-	4,3
889	calmodulin-related protein, putative	At5g42380		3,8	31,5
890	calmodulin-related protein, putative	At3g01830		-	22,3
891	touch-responsive protein	At2g41100	TCH3	-	4,1
892	calcineurin B-like protein 10 (CBL10)	At4g33000		-	0,1
893	calcium-binding EF hand family protein	At1g05150		-	0,3
894	calcium-binding EF hand family protein	At4g38810		-	0,2
895	calcium-binding RD20 protein (RD20)	At2g33380		-	0,1
896	calcium-dependent protein kinase, putative	At3g19100		-	0,3
897	calcium-transporting ATPase 4	At2g41560		-	0,2
898	calmodulin-binding family protein	At3g22190		-	0,3
899	calmodulin-binding family protein	At4g23060		-	0,1
900	calmodulin-binding family protein	At3g49260		-	0,2
901	calreticulin 2 (CRT2)	At1g09210		-	0,3
902	**HORMONES**				
903	**Auxin**				
904	auxin-responsive GH3 family protein	At5g13320		-	21,7
905	UDP-glucoronosyl/UDP-glucosyl transferase family protein	At1g05680		-	7,6
906	similar to auxin down-regulated protein ARG10	At3g22850		2,8	2,8
907	auxin efflux carrier family protein	At1g76520		-	0,3
908	auxin transport protein, putative	At1g70940	PIN3	-	0,2
909	auxin transport protein, putative	At2g01420	PIN4	-	0,1
910	auxin efflux carrier protein, putative	At1g23080	PIN7	-	0,1
911	auxin/aluminum-responsive protein, putative	At5g19140		-	0,3
912	auxin-responsive AUX/IAA family protein	At4g29080	PAP2	-	0,1
913	auxin-responsive factor	At2g33860	ETT	-	0,2
914	auxin-responsive family protein	At4g22620		-	0,2
915	auxin-responsive family protein	At4g34760		-	0,1
916	auxin-responsive family protein	At1g29430		-	0,1
917	auxin-responsive family protein	At2g46690		-	0,1
918	auxin-responsive family protein	At1g56150		-	0,3
919	auxin-responsive GH3 family protein	At4g03400	DFL2	-	0,1
920	auxin-responsive protein	At1g04250	AXR3	-	0,2
921	auxin-responsive protein	At4g12980		-	0,3
922	auxin-responsive protein	At4g14560	IAA1	-	0,1
923	auxin-responsive protein	At3g23030	IAA2	-	0,2
924	auxin-responsive protein	At3g23050	IAA7	-	0,2
925	auxin-responsive protein	At2g22670	IAA8	-	0,3
926	auxin-responsive protein	At1g04550	IAA12	-	0,3

Row	Description	Locus[2]	Protein	t/c ratio[3]	
	Functional categories[1]			IS12	S12
927	auxin-responsive protein	At3g04730	IAA16	-	0,2
928	auxin-responsive protein	At5g25890	IAA28	-	0,3
929	auxin-responsive protein	At1g04240	SHY2	-	0,1
930	auxin-responsive protein	At4g34750		-	0,2
931	auxin-responsive protein	At4g38860		-	0,04
932	auxin-responsive protein	At4g38840		-	0,1
933	auxin-responsive protein	At2g21210		-	0,1
934	auxin-responsive protein-related	At1g72430		-	0,2
935	axial regulator YABBY1	At2g45190	AFO	-	0,3
936	dormancy/auxin associated family protein	At2g33830		-	0,2
937	dormancy/auxin associated family protein	At1g56220		-	0,2
938	IAA-amino acid hydrolase 6, putative	At1g44350	ILL6	-	0,3
939	similarity to axi 1 protein	At3g30300		-	0,2
940	TCP family transcription factor, putative	At3g47620		-	0,2
941	TCP family transcription factor, putative	At5g08330		-	0,1
942	transcription factor MONOPTEROS (MP)	At1g19850	MP	-	0,3
943	UDP-glucoronosyl/UDP-glucosyl transferase family protein	At1g24100		-	0,2
944	expressed protein	At3g02250		-	0,3
945	**Brassinosteroid**				
946	brassinosteroid insensitive 1 [LRR24]	At4g39400	BRI1	-	0,3
947	cell elongation protein	At3g19820	DWF1	-	0,1
948	delta 7-sterol-C5-desaturase	At3g02580	STE1	-	0,3
949	steroid 22-alpha-hydroxylase	At3g50660	DWF4	-	0,3
950	**Abscisic acid**				
951	ABA-responsive protein-related	At5g13200		-	4
952	abscisic acid-responsive HVA22 family protein	At2g36020		-	11,6
953	molybdenum cofactor sulfurase	At1g16540		-	3
954	protein farnesyltransferase beta subunit	At5g40280	ERA1	-	5
955	phosphoinositide-specific phospholipase C	At5g58670	PLC1	-	0,3
956	3'(2'),5'-bisphosphate nucleotidase	At5g63980	SAL1/FRY1		0,3
957	ABA-responsive protein	At1g74520	HVA22A	-	0,3
958	ABA-responsive protein	At1g69700	HVA22C	-	0,2
959	**Ethylene**				
960	ethylene receptor, putative	At3g04580	EIN4	-	3,2
961	ethylene-responsive protein, putative	At1g09740		-	7
962	ethylene-responsive transcriptional coactivator, putative	At3g24500		3,3	11
963	member of the ERF subfamily B-2 of ERF	At2g47520		-	3,1
964	member of the ERF subfamily B-3 of ERF	At4g17490	ERF6	-	4,1
965	member of the ERF subfamily B-4 of ERF	At2g33710		-	13,9
966	member of the ERF subfamily B-5 of ERF	At1g22985		4,1	8,2
967	member of the ERF subfamily B-5 of ERF	At2g46310		-	12,1
968	oxidoreductase, 2OG-Fe(II) oxygenase family protein	At3g46480		-	4,5
969	universal stress protein (USP) family protein	At3g53990		-	3,3
970	2-oxoglutarate-dependent dioxygenase, putative	At2g25450		-	0,2
971	esterase, putative	At2g23610		-	0,2
972	member of the ERF subfamily B-3 of ERF	At5g47220		-	0,2
973	member of the ERF subfamily B-3 of ERF	At5g07580		-	0,1
974	member of the ERF subfamily B-3 of ERF	At5g61590		-	0,1
975	member of the ERF subfamily B-4 of ERF	At5g61890		-	0,2
976	member of the ERF subfamily B-6 of ERF	At5g25190		-	0,2
977	putative dioxygenase	At2g30830		-	0,1
978	universal stress protein (USP) family protein	At3g62550		-	0,1
979	universal stress protein (USP) family protein	At3g11930		-	0,1
980	**Jasmonate**				
981	lipoxygenase	At1g55020	LOX1	-	4,1
982	lipoxygenase, putative	At1g72520		-	3
983	allene oxide cyclase family protein	At1g13280	AOC4	-	0,1
984	allene oxide synthase	At5g42650	AOS	-	0,2
985	lipoxygenase	At3g45140	LOX2	-	0,2
986	lipoxygenase, putative	At1g17420	LOX3	-	0,1
987	12-oxophytodienoate reductase	At2g06050	OPR3	-	0,2
988	jacalin lectin family protein	At3g16470	JR1	-	0,04
989	jacalin lectin family protein	At3g16460		-	0,2
990	kelch repeat-containing protein	At1g54040	ESP	-	0,1
991	carboxyl methyltransferase family protein	At3g44860		-	0,2
992	**Cytokinin**				
993	two-component responsive regulator family protein	At2g01760		-	0,2
994	two-component responsive regulator	At2g40670	ARR16	-	0,1
995	histidine kinase	At5g35750	AHK2	-	0,3
996	**Gibberellin**				
997	similar to gibberellin 2-oxidase	At1g30040		-	28,5
998	gibberellin response modulator	At1g14920	GAI	-	0,2
999	gibberellin-responsive protein, putative	At1g74670		-	0,1
1000	gibberellin response modulator	At2g01570	RGA1	-	0,3
1001	ent-kaurenoic acid hydroxylase, putative	At2g32440	KAO2	-	0,3
1002	2-oxoglutarate-dependent dioxygenase, putative	At4g03060	AOP2	-	0,04
1003	gibberellin-regulated family protein	At5g14920		-	0,1
1004	**RESPONSE TO ABIOTIC AND BIOTIC STIMULI**				
1005	GCN5-related N-acetyltransferase (GNAT) family protein	At2g32030		4,2	28,1
1006	GCN5-related N-acetyltransferase (GNAT) family protein	At2g32020		7,5	9,3
1007	phosphoribosylanthranilate isomerase, putative	At1g29410	PAI3	2,3	-
1008	12-oxophytodienoate reductase, putative	At1g17990		-	0,3
1009	ACT domain containing protein	At1g69040	ACR4	-	0,2
1010	ATP-binding-cassette transporter	At4g04770	ABC1	-	0,3
1011	chloroplast signal recognition particle component	At2g47450	CAO	-	0,2

Row	Description	Locus[2]	Protein	t/c ratio[3]	
	Functional categories[1]			IS12	S12
1012	CP12 domain-containing protein	At3g62410	CP12-2	-	0,3
1013	cytochrome P450 79B2, putative	At4g39950	CYP79B2	-	0,1
1014	cytochrome P450 83B1	At4g31500	CYP83B1	-	0,2
1015	cytochrome P450 family protein	At4g13770	CYP83A1	-	0,1
1016	cytochrome P450, putative	At2g22330	CYP79B3	-	0,05
1017	dienelactone hydrolase family protein	At3g23570		-	0,3
1018	expressed protein	At5g55120		-	0,2
1019	expressed protein	At3g28840		-	0,2
1020	ferritin 1	At5g01600	FER1	-	0,1
1021	jacalin lectin family protein	At1g52040	MBP1	-	0,04
1022	pirin, putative	At3g59220	PRN	-	0,2
1023	ripening-responsive protein, putative	At5g65380		-	0,1
1024	RNA-dependent RNA polymerase	At3g49500	RDR6	-	0,3
1025	similar to homeobox protein knotted-1 like 4	At5g25220	KNAT3	-	0,3
1026	stress-responsive protein, putative	At1g29395	COR414-TM1	-	0,3
1027	subtilisin-like protease	At2g04160	AIR3	-	0,3
1028	Toll-Interleukin-Resistance	At1g72930	TIR	-	0,2
1029	transporter-related	At5g13750		-	0,2
1030	wound-responsive family protein	At1g19660		-	0,3
1031	**Heat**				
1032	23.6 kDa mitochondrial small heat shock protein M	At4g25200	HSP23.6	-	26,6
1033	23.5 kDa mitochondrial small heat shock protein (M)	At5g51440	HSP23.5	85,2	114,2
1034	17.7 kDa class II heat shock protein 17.6A C-II	At5g12030	HSP17.7	-	28
1035	17.6 kDa class I small heat shock protein C-I	At1g53540	HSP17.6C	-	4,2
1036	17.6 kDa class I small heat shock protein (CI)	At2g29500	HSP17.6BI	4,9	5,8
1037	17.6 kDa class I heat shock protein (CI)	At1g59860	HSP17.6A	36,8	111,2
1038	17.6 kDa class II heat shock protein C-II	At5g12020	HSP17.6	-	4,1
1039	17.4 kDa class I heat shock protein C-I	At3g46230	HSP17.4	-	44,4
1040	chaperonin	At3g23990	HSP60	-	3,1
1041	heat shock protein 70, putative / HSP70, putative	At3g12580		22,6	71,3
1042	heat shock protein 70, putative	At1g79920		-	4
1043	heat shock protein 70, mitochondrial, putative	At4g37910		-	3,9
1044	heat shock cognate 70 kDa protein 3	At3g09440	HSC70-3	-	3
1045	heat shock cognate 70 kDa protein 2	At5g02490	HSP70-2	2	13,3
1046	co-chaperone grpE protein, putative	At5g55200		6,1	9,5
1047	heat shock protein 81-2 (HSP81-2)	At5g56030	HSP81-2	-	3,1
1048	heat shock protein 81-1 (HSP81-1)	At5g52640	HSP81-1	9,5	52,1
1049	heat shock protein 101 (HSP101)	At1g74310	HSP101	4,6	15,1
1050	heat shock protein 100, putative / HSP100, putative	At2g25140		2,6	6,6
1051	DNAJ heat shock protein, putative	At5g22060	AtJ2	-	4,8
1052	DNAJ heat shock N-terminal domain-containing protein	At1g71000		-	132,1
1053	DNAJ heat shock N-terminal domain-containing protein	At2g35720		2,1	4,8
1054	DNAJ heat shock N-terminal domain-containing protein	At5g37440		-	3,9
1055	DNAJ heat shock N-terminal domain-containing protein	At1g74250		-	3
1056	DNAJ heat shock N-terminal domain-containing protein	At5g03030		2,5	2,9
1057	DNAJ heat shock family protein	At2g20560		-	10,5
1058	DNAJ heat shock family protein	At4g28480		2,2	5,7
1059	DNAJ heat shock N-terminal domain-containing protein	At5g18140		-	0,3
1060	DNAJ heat shock N-terminal domain-containing protein	At5g16650		-	0,3
1061	DNAJ heat shock N-terminal domain-containing protein	At4g09350		-	0,2
1062	DNAJ heat shock N-terminal domain-containing protein	At2g47440		-	0,1
1063	heat shock protein-related	At5g57710		-	0,3
1064	26.5 kDa class P-related heat shock protein P	At4g21870		-	0,1
1065	**Drought**				
1066	member of the DREB subfamily A-2	At2g38340		67	530,6
1067	member of the DREB subfamily A-2	At2g40350		5,6	22,3
1068	member of the DREB subfamily A-2	At5g05410	DREB2A	-	9,6
1069	member of the DREB subfamily A-2	At3g11020	DREB2B	-	3,1
1070	member of the DREB subfamily A-5	At3g50260		-	5,3
1071	drought-responsive family protein	At1g02750		-	3,9
1072	member of the DREB subfamily A-4	At4g16750		-	0,3
1073	member of the DREB subfamily A-4	At1g01250		-	0,1
1074	member of the DREB subfamily A-4	At4g32800		-	0,1
1075	member of the DREB subfamily A-4	At5g11590	TINY2	-	0,2
1076	member of the DREB subfamily A-5	At1g19210		-	0,3
1077	member of the DREB subfamily A-5	At1g74930		-	0,1
1078	member of the DREB subfamily A-6	At2g23340		-	0,1
1079	member of the DREB subfamily A-6	At1g64380		-	0,2
1080	member of the DREB subfamily A-6	At2g22200		-	0,3
1081	dehydration-responsive protein-related	At2g03480		-	0,2
1082	dehydration-responsive protein-related	At1g04430		-	0,2
1083	dehydration-responsive family protein	At4g00750		-	0,3
1084	dehydration-responsive family protein	At4g18030		-	0,2
1085	hydrophobic protein	At3g05890	RCI2B	-	0,2
1086	hydrophobic protein, putative	At4g30650		-	0,2
1087	hydrophobic protein, putative	At4g30660		-	0,2
1088	dehydration-responsive protein	At5g25610	RD22	-	0,3
1089	early-responsive to dehydration stress protein	At3g25760	ERD12	-	0,2
1090	dehydration-responsive protein-related	At1g78240		-	0,3
1091	**Stress**				
1092	adenine-DNA glycosylase-related	At4g12740		-	3,6
1093	chlorophyll A-B binding family protein	At3g22840	ELIP1	-	48,5
1094	DEAD/DEAH box helicase, putative	At3g53110	LOS4	-	3,1
1095	DNA repair protein RAD54, putative	At3g19210		-	4,1
1096	isochorismate synthase 1 (ICS1)	At1g74710	ICS1	-	23,6

Row	Description	Locus[2]	Protein	t/c ratio[3]	
	Functional categories[1]			IS12	S12
1097	pentatricopeptide (PPR) repeat-containing protein	At1g18900		-	3.2
1098	pentatricopeptide (PPR) repeat-containing protein	At1g74750		-	3.2
1099	recA family protein	At3g32920		-	3.2
1100	stress-inducible protein, putative	At1g62740		-	5.6
1101	stress-inducible protein, putative	At4g12400		-	43.2
1102	UMUC-like DNA repair family protein	At5g44740		-	3.5
1103	UMUC-like DNA repair family protein	At5g44750		2.2	3.7
1104	universal stress protein (USP) family protein	At3g03270		5.5	8.8
1105	DNA-damage-repair/toleration protein	At3g12610	DRT100	-	0.1
1106	methyladenine glycosylase family protein	At1g80850		-	0.2
1107	methyladenine glycosylase family protein	At5g44680		-	0.3
1108	pentatricopeptide (PPR) repeat-containing protein	At2g17033		-	0.3
1109	ribonuclease 1	At2g02990	RNS1	-	0.1
1110	**Pathogen**				
1111	avirulence-responsive protein	At1g33960	AIG1	-	10.2
1112	avirulence-responsive protein, putative	At1g33970		-	3.2
1113	chitinase, putative	At3g47540		3.5	16.5
1114	copine BONZAI1	At5g61900	BON1	-	5.4
1115	CPR5 protein, putative	At5g64930	CPR5	-	3.1
1116	cytochrome P450 71B15, putative (CYP71B15)	At3g26830	PAD3	-	15.2
1117	disease resistance family protein	At1g47890		-	5.3
1118	disease resistance family protein	At2g34930		2.9	-
1119	disease resistance family protein / LRR family protein	At3g05360		-	20.6
1120	disease resistance protein (NBS-LRR class), putative	At3g14470		-	3.9
1121	disease resistance protein (TIR class), putative	At2g32140		-	15.9
1122	disease resistance protein (TIR class), putative	At1g57630		2.2	26.3
1123	disease resistance protein (TIR-NBS class), putative	At1g66090		2.6	16.3
1124	disease resistance protein (TIR-NBS-LRR class), putative	At1g56540		-	4.1
1125	disease resistance protein (TIR-NBS-LRR class), putative	At5g51630		-	4.6
1126	disease resistance protein (TIR-NBS-LRR class), putative	At3g44400		-	5.1
1127	disease resistance protein (TIR-NBS-LRR class), putative	At4g11170		-	9.4
1128	disease resistance protein (TIR-NBS-LRR class), putative	At5g41740		-	11.9
1129	disease resistance protein (TIR-NBS-LRR class), putative,	At5g46470		-	3.2
1130	double-stranded RNA-binding domain-containing protein	At1g09700	HYL1	-	3.5
1131	enhanced disease susceptibility 5	At4g39030	EDS5	-	3.4
1132	expressed protein	At1g29690	CAD1	-	4
1133	expressed protein	At3g17800		-	5
1134	glutamate receptor family protein	At5g48400		-	4.3
1135	glycosyl hydrolase family 18 protein	At4g19810		-	8.8
1136	glycosyl hydrolase family 81 protein	At5g15870		2.2	17.6
1137	guanylate-binding family protein	At1g03830		-	10
1138	harpin-induced family protein	At2g35980	YLS9	-	71.1
1139	immediate-early fungal elicitor family protein	At3g02840		-	7.1
1140	legume lectin family protein	At3g16530		3.5	7.2
1141	macrophage migration inhibitory factor family protein	At3g51660		2	4.2
1142	phytoalexin-deficient 4 protein	At3g52430	PAD4	-	8.3
1143	pseudo-response regulator 9	At2g46790	APRR9	-	37.6
1144	putative DNA repair protein (XPB1) mRNA	At5g41370	XPB1	-	3.9
1145	RAR1 disease resistance protein	At5g51700	PBS2	-	3.4
1146	Toll-Interleukin-Resistance (TIR) domain-containing protein	At2g20145		-	3.7
1147	ankyrin repeat family protein	At4g14400	ACD6	-	0.2
1148	avirulence-responsive protein-related	At4g31310		-	0.2
1149	coronatine-induced protein 1 (CORI1)	At1g19670	CLH1	-	0.03
1150	Coronotine induced gene	At4g23600	CORI3	-	0.2
1151	disease resistance family protein	At2g15080		-	0.1
1152	disease resistance protein (CC-NBS-LRR class), putative	At1g53350		-	0.2
1153	disease resistance protein (CC-NBS-LRR class), putative	At5g63020		-	0.3
1154	disease resistance protein (TIR class), putative	At1g61100		-	0.2
1155	disease resistance protein (TIR-NBS class), putative	At1g72890		-	0.3
1156	disease resistance protein (TIR-NBS class), putative	At1g72920		-	0.1
1157	disease resistance protein (TIR-NBS class), putative	At1g72940		-	0.1
1158	disease resistance protein (TIR-NBS-LRR class), putative	At4g19530		-	0.1
1159	disease resistance protein (TIR-NBS-LRR class), putative	At5g46270		-	0.2
1160	disease resistance-responsive family protein	At1g65870		-	0.1
1161	disease resistance-responsive family protein	At4g23690		-	0.3
1162	pathogenesis-related protein, putative	At4g25780		-	0.1
1163	pathogenesis-related thaumatin family protein	At4g38670		-	0.3
1164	pathogenesis-related thaumatin family protein	At1g75800		-	0.2
1165	pathogen-responsive alpha-dioxygenase, putative	At1g73680		-	0.3
1166	pectate lyase, putative	At3g54920	PMR6	-	0.2
1167	plant defensin-fusion protein, putative	At2g02130		-	0.2
1168	plant defensin-fusion protein, putative	At2g02100		-	0.1
1169	seven transmembrane MLO family protein	At5g53760	MLO11	-	0.2
1170	thionin, putative	At1g66100		-	0.1
1171	transferase family protein, similar to hypersensitivity-related hsr201 protein	At3g48720		-	0.1
1172	trypsin inhibitor, putative	At2g43550		-	0.1
1173	trypsin inhibitor, putative	At2g43530		-	0.1
1174	trypsin inhibitor, putative	At2g43520	ATTI2	-	0.2
1175	trypsin inhibitor, putative	At2g43535		-	0.1
1176	vegetative storage protein 1	At5g24780	VSP1	-	0.1
1177	**Misc**				
1178	germin, putative	At1g18970	GLP4	3.1	4
1179	germin-like protein	At3g62020	GLP10	7.1	12
1180	germin-like protein, putative	At1g18980		26.6	36
1181	dehydrin	At1g76180	ERD14	2.1	2.8

Row	Description	Locus[2]	Protein	t/c ratio[3]	
	Functional categories[1]			IS12	S12
1182	Bet v I allergen family protein	At1g24020		-	0,02
1183	Bet v I allergen family protein	At1g70830		-	0,1
1184	dehydrin (ERD10),	At1g20450	LTI29	-	0,3
1185	germin-like protein, putative	At3g10080		-	0,1
1186	major latex protein-related	At1g70890		-	0,04
1187	major latex protein-related	At4g23670		-	0,1
1188	major latex protein-related	At3g26450		-	0,2
1189	ozone-responsive stress-related protein	At1g01170		-	0,3
1190	pollen Ole e 1 allergen and extensin family protein	At4g08685	SAH7	-	0,3
1191	**Cellular redox state**				
1192	glutaredoxin family protein	At1g03850		-	7.4
1193	glutaredoxin family protein	At3g28850		-	3,1
1194	glutathione peroxidase, putative	At4g31870	GPX7	-	3.2
1195	non-symbiotic hemoglobin 1	At2g16060	HB1	-	9
1196	NPK1-related protein kinase, putative	At1g09000	ANP1	-	5
1197	peroxidase, putative	At4g08770		-	16,5
1198	peroxiredoxin type 2, putative	At1g60740		7,4	92.4
1199	plastocyanin-like domain-containing protein	At5g20230		-	3,1
1200	catalase	At1g20620	CAT3	-	0,2
1201	cytochrome b5 domain-containing protein	At1g60660		-	0,3
1202	cytochrome b5, putative	At2g46650		-	0,04
1203	dehydroascorbate reductase, putative	At1g19570		-	0,1
1204	gamma-glutamyltranspeptidase family protein	At4g29210		-	0,3
1205	glutaredoxin family protein	At2g41330		-	0,3
1206	glutathione synthetase	At5g27380	GSH2	-	0,2
1207	heme oxygenase 2	At2g26550	HO2	-	0,2
1208	L-ascorbate oxidase, putative	At5g21105		-	0,3
1209	non-symbiotic hemoglobin 2	At3g10520	AHB2	-	0,3
1210	peroxidase 12 (PER12)	At1g71695		-	0,2
1211	peroxidase 21 (PER21)	At2g37130		-	0,1
1212	peroxidase 42 (PER42)	At4g21960	PRXR1	-	0,1
1213	peroxidase, putative	At5g40150		-	0,2
1214	rubredoxin family protein	At5g51010		-	0,3
1215	superoxide dismutase (Fe) / iron superoxide dismutase 3	At5g23310	FSD3	-	0,3
1216	thioredoxin family protein	At5g06690		-	0,2
1217	thioredoxin family protein	At5g61440		-	0,3
1218	thioredoxin, putative	At5g16400		-	0,3
1219	**Cell Cycle**				
1220	cell cycle control protein-related	At1g17130		-	3.2
1221	cell cycle control protein-related,	At3g43250		-	18.5
1222	cell division cycle protein 48	At3g09840	CDC48	2,2	4.4
1223	cell division cycle protein 48, putative	At3g53230		17.7	48.2
1224	cell division cycle protein 48, putative	At5g03340		2	7
1225	cell division cycle protein 48-related	At1g05910		-	3
1226	cyclin, putative	At1g77390		-	4.4
1227	cyclin-dependent kinase, putative	At5g10270		-	4.5
1228	meiotic recombination protein, putative	At3g22880	ATDMC1	-	4.2
1229	peptidyl-prolyl cis-trans isomerase	At3g25230	ROF1	2,2	5.7
1230	peptidyl-prolyl cis-trans isomerase	At2g21130		2.1	2.5
1231	peptidyl-prolyl cis-trans isomerase cyclophilin-type family protein	At1g01940		4,2	13
1232	peptidyl-prolyl cis-trans isomerase, putative	At2g38730		2.5	4.2
1233	peptidyl-prolyl cis-trans isomerase, putative	At5g48570		4,1	15
1234	ribosome recycling factor family protein	At3g01800		-	4,2
1235	cell division protein ftsH, putative	At3g02450		-	0,3
1236	chloroplast division protein, putative	At3g52750		-	0,3
1237	cyclin family protein	At3g21870		-	0,2
1238	cyclin, putative	At5g43080		-	0,3
1239	kip-related protein 2	At3g50630	ICK2	-	0,2
1240	peptidyl-prolyl cis-trans isomerase cyclophilin-type family protein	At1g74070		-	0,1
1241	UVB-resistance protein-related	At5g11580		-	0,3
1242	**TRANSCRIPTION**				
1243	AP2 domain-containing transcription factor, putative	At3g61630		2,6	24,5
1244	ARID/BRIGHT DNA-binding domain-containing protein	At1g76510		2,3	2.7
1245	ASF1-like anti-silencing protein, putative	At1g66740		-	3.5
1246	basic helix-loop-helix (bHLH) family protein	At2g42300		2.1	2.8
1247	bZIP family transcription factor	At3g51960		2,6	5.1
1248	bZIP transcription factor family protein	At3g54620		-	3.1
1249	bZIP transcription factor family protein	At3g10800		-	4,3
1250	bZIP transcription factor family protein	At1g42990		-	4.8
1251	C protein immunoglobulin-A-binding beta antigen-related	At1g05490		-	14,6
1252	CCR4-NOT transcription complex protein, putative	At1g27820		2.2	3.5
1253	CCR4-NOT transcription complex protein, putative	At1g06450		3.1	4.5
1254	CCR4-NOT transcription complex protein, putative	At1g15920		4.5	8
1255	DDT domain-containing protein	At5g08630		-	3,3
1256	DNA-binding protein RAV2 (RAV2)	At1g68840	RAV2	-	3.3
1257	DNA-binding protein-related	At2g38250		3	11.8
1258	DNA-directed RNA polymerase I(A) and III©	At2g29540	RPC14	2,3	3
1259	Dof-type zinc finger domain-containing protein	At1g21340		-	6,7
1260	expressed protein	At4g35940		-	3.1
1261	expressed protein	At1g61620		-	3,2
1262	expressed protein	At2g26780		3,8	6.8
1263	expressed protein	At4g14530		-	20.5
1264	expressed protein	At1g20220		-	3.3
1265	glycine-rich protein	At1g65440	GTB1	-	3.7
1266	heat shock factor protein 2	At3g02990	HSFA1E	-	5,7

Row	Description	Locus[2]	Protein	t/c ratio[3]	
	Functional categories[1]			IS12	S12
1267	heat shock transcription factor family protein	At2g26150	HSFA2	3.5	14.1
1268	heat shock transcription factor family protein	At5g03720	HSFA3	-	3.5
1269	heat shock transcription factor 21	At4g18880	HSFA4A	-	5.8
1270	heat shock factor protein, putative	At1g67970	HSFA8	-	6.2
1271	heat shock factor protein 7	At4g11660	HSFB2B	-	4.2
1272	heat shock transcription factor family protein	At1g77570		-	5.7
1273	high mobility group (HMG1/2) family protein	At4g11080		-	4.1
1274	histone H3, putative	At1g13370		-	7.6
1275	MADS-box protein (AGL18)	At3g57390	AGL18	2.1	2.9
1276	myb family transcription factor	At3g18100	MYB4R1	2,3	3,9
1277	myb family transcription factor	At3g10590		-	6.3
1278	myb family transcription factor	At2g13960		-	7
1279	myb family transcription factor	At1g17460	TRFL3	2.6	7.1
1280	myb family transcription factor (MYB50)	At1g57560		-	6.5
1281	NF-X1 type zinc finger family protein	At1g10170		3	10.9
1282	NIMIN1	At1g02450		-	3.3
1283	no apical meristem (NAM) family protein	At1g02220	ANAC003	-	5
1284	no apical meristem (NAM) family protein	At1g32870	ANAC013	3.1	5.5
1285	no apical meristem (NAM) family protein	At3g04060	ANAC046	-	6.1
1286	no apical meristem (NAM) family protein	At3g10490	ANAC051	2.7	11.6
1287	no apical meristem (NAM) family protein	At3g10500	ANAC053	-	5.5
1288	no apical meristem (NAM) family protein	At3g49530	ANAC062	-	3.1
1289	no apical meristem (NAM) family protein	At5g04410	ANAC078/NAC2	-	3.2
1290	no apical meristem (NAM) family protein	At5g09330	ANAC082	2.6	6.2
1291	no apical meristem (NAM) family protein	At5g18270	ANAC087	6.5	27.1
1292	no apical meristem (NAM) family protein	At5g22380	ANAC090	-	5.7
1293	no apical meristem (NAM) family protein	At5g39820	ANAC094	412.1	807.3
1294	no apical meristem (NAM) family protein	At5g61430	ANAC100	2.9	6.3
1295	no apical meristem (NAM) family protein	At5g64060	ANAC103	10.2	25.5
1296	PAZ domain-containing protein	At1g31290		7.3	13.3
1297	PAZ domain-containing protein	At1g31280	AGO2	2.8	14.6
1298	PHD finger family protein	At1g33420		-	6.5
1299	PHD finger family protein	At5g63900		-	6.8
1300	PHD finger family protein	At5g09790		-	6,7
1301	PHD finger protein-related	At1g26800		-	3.6
1302	PHD finger protein-related	At1g32800		-	4.7
1303	PHD finger transcription factor, putative	At5g58610		13	13
1304	proline-rich family protein	At5g14540		-	3.5
1305	rhomboid family protein	At3g17611		4.5	10.4
1306	RNA recognition motif (RRM)-containing protein	At4g32720		-	3.3
1307	scarecrow transcription factor family protein	At3g46600		2.1	3.7
1308	similar to myb family transcription factor	At5g27610		-	89.1
1309	similar to N2,N2-dimethylguanosine tRNA methyltransferase family protein	At3g02320		-	3.6
1310	SNF2 domain-containing protein	At2g18760		-	3,2
1311	SNF2 domain-containing protein	At5g66750	DDM1	-	3.3
1312	SNF2 domain-containing protein	At1g11100		-	5.2
1313	SNF2 domain-containing protein	At5g07810		-	5.3
1314	SNF2 domain-containing protein	At1g61140		-	4.5
1315	SNF2 domain-containing protein	At1g05480		-	60
1316	SNF7 family protein	At5g04850		-	3.9
1317	SNF7 family protein	At3g10640		2.1	6.8
1318	tesmin/TSO1-like CXC domain-containing protein	At2g20110		3	9.2
1319	transcription factor jumonji (jmi) family protein	At4g20400		4.9	6.9
1320	transcription factor jumonji (jmjC) domain-containing protein	At1g63490		-	3.4
1321	transcription initiation factor IIB-1	At2g41630	TFIIB	3	4.9
1322	transcriptional activator, putative	At3g07220		-	3.2
1323	U-box domain-containing protein	At5g37490		-	3.8
1324	WRKY family transcription factor	At1g62300	WRKY6	-	5.8
1325	WRKY family transcription factor	At2g23320	WRKY15	-	3
1326	WRKY family transcription factor	At2g30250	WRKY25	-	6.7
1327	WRKY family transcription factor	At5g24110	WRKY30	-	129.3
1328	WRKY family transcription factor	At2g38470	WRKY33	2.4	13.3
1329	WRKY family transcription factor	At2g46400	WRKY46	-	5.4
1330	WRKY family transcription factor	At2g40750	WRKY54	-	3.2
1331	WRKY family transcription factor	At2g40740	WRKY55	-	3.2
1332	WRKY family transcription factor	At2g21900	WRKY59	-	15.9
1333	WRKY family transcription factor	At5g13080	WRKY75	2.3	-
1334	zinc finger (AN1-like) family protein	At4g12040		-	3,1
1335	zinc finger (AN1-like) family protein	At3g28210	PMZ	23.4	82.9
1336	zinc finger (B-box type) family protein	At2g47890		2.6	4.1
1337	zinc finger (B-box type) family protein	At1g78600		-	6.2
1338	zinc finger (C2H2 type) family protein	At5g03740	HD2C	2.2	3.1
1339	zinc finger (C2H2 type) family protein	At4g25610		-	3.2
1340	zinc finger (C2H2 type) family protein	At2g24500	FZF	-	3.2
1341	zinc finger (C2H2 type) family protein	At2g01650	PUX2	-	3.2
1342	zinc finger (C2H2 type) family protein	At2g37430		-	15.1
1343	zinc finger (C3HC4-type RING finger) family protein	At1g18660		-	3
1344	zinc finger (C3HC4-type RING finger) family protein	At4g28370		-	3,4
1345	zinc finger (C3HC4-type RING finger) family protein	At2g30580		2.2	4.2
1346	zinc finger (C3HC4-type RING finger) family protein	At4g11370		2.2	4.2
1347	zinc finger (C3HC4-type RING finger) family protein	At3g05200	ATL6	-	4.4
1348	zinc finger (C3HC4-type RING finger) family protein	At3g19910		-	4.6
1349	zinc finger (C3HC4-type RING finger) family protein	At1g14200		-	4.8
1350	zinc finger (C3HC4-type RING finger) family protein	At5g27420		-	5
1351	zinc finger (C3HC4-type RING finger) family protein	At2g20030		-	8

Row	Description	Locus[2]	Protein	t/c ratio[3]	
	Functional categories[1]			IS12	S12
1352	zinc finger (C3HC4-type RING finger) family protein	At1g08050		-	9
1353	zinc finger (C3HC4-type RING finger) family protein	At1g03770		-	9.5
1354	zinc finger (C3HC4-type RING finger) family protein	At4g14365		-	11
1355	zinc finger (CCCH-type) family protein	At2g32930	ZFN2	-	3
1356	zinc finger (CCCH-type) family protein	At2g40140		-	5.6
1357	zinc finger (CCCH-type) family protein	At1g68200		-	6
1358	zinc finger (CCCH-type/C3HC4-type RING finger) family protein	At5g06420		2.1	4.4
1359	zinc finger (FYVE type) family protein	At3g43230		-	3.1
1360	zinc finger (HIT type) family protein	At4g28820		2.5	3.3
1361	zinc finger (MYND type) family protein	At2g17900	SDG37	-	3.7
1362	zinc finger protein-related	At1g05890		2.8	5
1363	29 kDa ribonucleoprotein, chloroplast, putative	At1g60000		-	0.1
1364	AP2 domain-containing transcription factor	At2g28550	TOE1	-	0.2
1365	AP2 domain-containing transcription factor, putative	At2g39250	SNZ	-	0.1
1366	AP2 domain-containing transcription factor, putative	At1g22190		-	0.2
1367	AP2 domain-containing transcription factor, putative	At3g54990	SMZ	-	0.2
1368	aspartyl protease family protein	At1g01300		-	0.1
1369	aspartyl protease family protein	At3g18490		-	0.2
1370	aspartyl protease family protein	At3g61820		-	0.1
1371	aspartyl protease family protein	At5g10760		-	0.2
1372	axial regulator	At4g00180	YAB3	-	0.2
1373	basic helix-loop-helix (bHLH) family protein	At2g18300		-	0.1
1374	basic helix-loop-helix (bHLH) family protein	At4g36540		-	0.1
1375	basic helix-loop-helix (bHLH) family protein	At1g68810		-	0.1
1376	basic helix-loop-helix (bHLH) family protein	At3g07340		-	0.2
1377	basic helix-loop-helix (bHLH) family protein	At4g17880		-	0.2
1378	basic helix-loop-helix (bHLH) family protein	At5g50915		-	0.2
1379	basic helix-loop-helix (bHLH) family protein	At2g46510		-	0.2
1380	basic helix-loop-helix (bHLH) family protein	At5g65640		-	0.2
1381	basic helix-loop-helix (bHLH) family protein	At5g46690		-	0.3
1382	basic helix-loop-helix (bHLH) family protein	At4g00050		-	0.3
1383	basic helix-loop-helix (bHLH) family protein	At3g57800		-	0.2
1384	basic helix-loop-helix (bHLH) protein	At1g32640	MYC2	-	0.1
1385	bZIP transcription factor family protein	At2g18160	GBF5	-	0.3
1386	CCAAT-binding transcription factor family protein	At2g34720		-	0.3
1387	CCAAT-box binding transcription factor subunit B	At5g47640		-	0.1
1388	CCAAT-box binding transcription factor subunit B	At4g14540		-	0.1
1389	chloroplast nucleoid DNA-binding protein-related	At1g09750		-	0.1
1390	CXC domain protein	At3g22780	TSO1	-	0.3
1391	DC1 domain-containing protein	At2g19650		-	0.1
1392	DC1 domain-containing protein	At2g21830		-	0.1
1393	DC1 domain-containing protein	At4g01350		-	0.2
1394	DNA-binding family protein	At1g63480		-	0.2
1395	DNA-binding protein RAV1	At1g13260	RAV1	-	0.2
1396	DNA-binding protein, putative	At1g01030		-	0.2
1397	Dof-type zinc finger domain-containing protein	At1g29160		-	0.05
1398	Dof-type zinc finger domain-containing protein	At5g60850	OBP4	-	0.1
1399	Dof-type zinc finger domain-containing protein	At5g60200		-	0.2
1400	eukaryotic rpb5 RNA polymerase subunit family protein	AT3G57080		-	0.3
1401	exocyst subunit EXO70 family protein	At5g59730		-	0.2
1402	expressed protein	At1g29950		-	0.3
1403	expressed protein	At4g00950		-	0.3
1404	expressed protein	At5g09460		-	0.3
1405	expressed protein	At2g42190		-	0.2
1406	expressed protein	At5g64340		-	0.3
1407	expressed protein	At3g13000		-	0.3
1408	expressed protein	At5g23920		-	0.2
1409	heat shock transcription factor family protein	At3g24520	HSFC1	-	0.3
1410	high mobility group (HMG1/2) family protein	At5g23420		-	0.1
1411	high mobility group (HMG1/2) family protein	At1g76110		-	0.04
1412	histone H1, putative	At1g06760		-	0.3
1413	histone H1.2	At2g30620		-	0.2
1414	histone H1/H5 family protein	At3g18035	HON4	-	0.3
1415	histone H2A, putative	At5g59870		-	0.1
1416	histone H2A, putative	At1g51060		-	0.2
1417	histone H2A, putative	At4g27230		-	0.3
1418	histone H2A, putative	At5g27670		-	0.3
1419	histone H2B	At3g45980		-	0.2
1420	histone H2B, putative	At2g28720		-	0.2
1421	histone H2B, putative	At5g22880		-	0.3
1422	histone H2B, putative	At3g46030		-	0.3
1423	histone H3	At5g65360		-	0.1
1424	histone H4	At2g28740	HIS4	-	0.2
1425	histone H4	At1g07820		-	0.3
1426	histone H4	At1g09200		-	0.1
1427	histone H5	At3g45930		-	0.1
1428	histone H5	At3g27360		-	0.3
1429	histone H6	At5g10390		-	0.1
1430	histone H6	At3g53730		-	0.2
1431	histone H7	At5g10400		-	0.1
1432	histone H7	At5g59690		-	0.1
1433	homeobox protein	At4g32980	ATH1	-	0.1
1434	homeobox protein knotted-1 like 4	At5g11060	KNAT4	-	0.2
1435	homeobox-leucine zipper family protein	At3g61150		-	0.3
1436	homeobox-leucine zipper protein 16	At4g40060	HB16	-	0.3

Row	Description	Locus[2]	Protein	t/c ratio[3]	
	Functional categories[1]			IS12	S12
1437	homeobox-leucine zipper protein 2	At5g47370	HAT2	-	0,2
1438	homeobox-leucine zipper protein 5	At5g65310	HB5	-	0,1
1439	homeobox-leucine zipper protein protodermal factor 2	At4g04890	PDF2	-	0,2
1440	homeobox-leucine zipper transcription factor	At2g34710	PHB	-	0,3
1441	homeobox-leucine zipper transcription factor	At4g32880	HB-8	-	0,1
1442	inositol-1(or 4)-monophosphatase, putative	At3g02870		-	0,2
1443	inositol-1(or 4)-monophosphatase, putative	At3g02830		-	0,1
1444	KH domain-containing protein	At5g06770		-	0,3
1445	LOB domain family protein	At3g11090		-	0,1
1446	LOB domain protein 37	At5g67420		-	0,3
1447	MADS-box family protein	At1g22590		-	0,2
1448	MADS-box protein (AGL3)	At2g03710		-	0,2
1449	methionine sulfoxide reductase domain-containing protein	At4g04830		-	0,03
1450	methionine sulfoxide reductase domain-containing protein	At4g04840		-	0,2
1451	methyl-CpG-binding domain-containing protein	At3g15790	MBD11	-	0,2
1452	mitochondrial transcription termination factor-related	At2g34620		-	0,1
1453	mitochondrial transcription termination factor-related	At2g36000		-	0,3
1454	mitochondrial transcription termination factor-related	At4g38160		-	0,2
1455	mutase family protein	At1g77060		-	0,3
1456	myb family transcription factor	At4g38620	MYB4	-	0,1
1457	myb family transcription factor	At4g09460	MYB6	-	0,2
1458	myb family transcription factor	At1g66230	MYB20	-	0,1
1459	myb family transcription factor	At5g61420	MYB28	-	0,1
1460	myb family transcription factor	At5g07690	MYB29	-	0,1
1461	myb family transcription factor	At3g28910	MYB30	-	0,2
1462	myb family transcription factor	At5g07700	MYB76	-	0,3
1463	myb family transcription factor	At1g74430	MYB95	-	0,2
1464	myb family transcription factor	At5g62470	MYB96	-	0,2
1465	myb family transcription factor	At3g46130	MYB111	-	0,04
1466	myb family transcription factor	At1g14350	MYB124	-	0,1
1467	myb family transcription factor	At1g56650	PAP1	-	0,1
1468	myb family transcription factor	At1g18710		-	0,02
1469	myb family transcription factor	At5g37260		-	0,1
1470	myb family transcription factor	At4g37260		-	0,1
1471	myb family transcription factor	At1g49010		-	0,1
1472	myb family transcription factor	At1g71030		-	0,2
1473	myb family transcription factor	At2g30420		-	0,2
1474	myb family transcription factor	At1g19000		-	0,3
1475	myb family transcription factor	At5g15310		-	0,3
1476	myb family transcription factor	At1g19510		-	0,3
1477	myb family transcription factor	At2g23290		-	0,3
1478	myb family transcription factor	At2g37630	AS1	-	0,1
1479	no apical meristem (NAM) family protein	At2g02450	ANAC034/035	-	0,2
1480	NPR1/NIM1-interacting protein 3	At1g09415		-	0,2
1481	ovule development protein, putative	At1g79700		-	0,2
1482	ovule development protein, putative	At1g16060		-	0,3
1483	PAC motif-containing protein	At2g02710		-	0,3
1484	PAZ domain-containing protein	At1g69440	AGO7	-	0,3
1485	PHD finger family protein	At3g14740		-	0,3
1486	plant-specific transcription factor YABBY family protein	At2g26580		-	0,2
1487	proliferating cell nuclear antigen 1	At1g07370	PCNA1	-	0,3
1488	pseudo-response regulator 3	At5g60100		-	0,3
1489	PUR alpha-1 protein	At2g32080		-	0,3
1490	remorin family protein	At3g57540		-	0,2
1491	RNA polymerase sigma subunit SigA	AT1G64860	SIGA	-	0,2
1492	RNA polymerase sigma subunit SigB	AT1G08540	SIGB	-	0,3
1493	RNA polymerase sigma subunit SigD	AT5G13730	SIGD	-	0,1
1494	RNA polymerase sigma subunit SigF	AT2G36990	SIGF	-	0,3
1495	scarecrow transcription factor family protein	At5g41920		-	0,2
1496	scarecrow transcription factor family protein	At5g66770		-	0,3
1497	SET domain-containing protein	At4g30860		-	0,3
1498	similar to aspartyl protease family protein	At5g07030		-	0,3
1499	similar to zinc finger (C2H2 type) family protein	At2g28200		-	0,2
1500	similar to zinc finger (C2H2 type) family protein	At4g17810		-	0,3
1501	speckle-type POZ protein-related	At3g48360		-	0,1
1502	squamosa promoter-binding protein-like 11	At1g27360		-	0,1
1503	squamosa promoter-binding protein-like 2	At5g43270	SPL2	-	0,3
1504	TAZ zinc finger family protein	At5g67480		-	0,2
1505	TCP family transcription factor 3	At1g53230	RAV1	-	0,2
1506	TCP family transcription factor, putative	At1g69690		-	0,2
1507	TCP family transcription factor, putative	At1g35560		-	0,3
1508	TCP family transcription factor, putative	At2g31070		-	0,3
1509	telomeric DNA-binding protein, putative	At3g12560	TRFL9	-	0,3
1510	transcription factor jumonji (jmjC) domain-containing protein	At3g20810		-	0,2
1511	transcription factor LIM, putative	At1g10200		-	0,2
1512	transcription factor-related	At2g27230		-	0,2
1513	transcriptional coactivator p15	At5g09240		-	0,3
1514	transcriptional factor B3 family protein	At3g06160		-	0,3
1515	trihelix DNA-binding protein	At5g28300		-	0,3
1516	trihelix DNA-binding protein	At1g76890	GT2	-	0,2
1517	trihelix DNA-binding protein, putative	At1g33240	GTL1	-	0,2
1518	WRKY family transcription factor	At4g24240	WRKY7	-	0,3
1519	WRKY family transcription factor	At4g01720	WRKY47	-	0,3
1520	WRKY family transcription factor	At2g25000	WRKY60	-	0,2
1521	zinc finger (B-box type) family protein	At1g68520		-	0,1

Row	Description	Locus[2]	Protein	t/c ratio[3]	
	Functional categories[1]			IS12	S12
1522	zinc finger (B-box type) family protein	At3g07650	COL9	-	0,2
1523	zinc finger (B-box type) family protein	At5g24930		-	0,3
1524	zinc finger (B-box type) family protein	At5g57660		-	0,3
1525	zinc finger (C2H2 type) family protein	At2g41940	ZFP8	-	0,1
1526	zinc finger (C2H2 type) family protein	At3g58070		-	0,1
1527	zinc finger (C2H2 type) family protein	At1g68130		-	0,2
1528	zinc finger (C2H2 type) family protein	At1g24625		-	0,2
1529	zinc finger (C3HC4-type RING finger) family protein	At1g04020		-	0,2
1530	zinc finger (C3HC4-type RING finger) family protein	At3g61460	BRH1	-	0,2
1531	zinc finger (C3HC4-type RING finger) family protein	At5g63780		-	0,1
1532	zinc finger (C3HC4-type RING finger) family protein	At1g49200		-	0,2
1533	zinc finger (C3HC4-type RING finger) family protein	At1g49230		-	0,04
1534	zinc finger (C3HC4-type RING finger) family protein	At1g76410		-	0,3
1535	zinc finger (C3HC4-type RING finger) family protein	At2g37580		-	0,2
1536	zinc finger (C3HC4-type RING finger) family protein	At2g01150	RHA2B	-	0,3
1537	zinc finger (C3HC4-type RING finger) family protein	At2g15580		-	0,2
1538	zinc finger (C3HC4-type RING finger) family protein	At4g13100		-	0,3
1539	zinc finger (C3HC4-type RING finger) family protein	At4g17245		-	0,2
1540	zinc finger (C3HC4-type RING finger) family protein	At4g28270		-	0,1
1541	zinc finger (C3HC4-type RING finger) family protein	At5g42200		-	0,3
1542	zinc finger (C3HC4-type RING finger) family protein	At5g47610		-	0,2
1543	zinc finger (C3HC4-type RING finger) family protein	At1g22500		-	0,04
1544	zinc finger (C3HC4-type RING finger) family protein	At5g22920		-	0,1
1545	zinc finger (C3HC4-type RING finger) family protein	At1g17970		-	0,2
1546	zinc finger (C3HC4-type RING finger) family protein	At5g41400		-	0,3
1547	zinc finger (C3HC4-type RING finger) family protein	At4g30400		-	0,2
1548	zinc finger (C3HC4-type RING finger) family protein	At3g61550		-	0,2
1549	zinc finger (C3HC4-type RING finger) family protein	At2g38970		-	0,3
1550	zinc finger (CCCH-type) family protein	At2g25900	CTH	-	0,2
1551	zinc finger (CCCH-type) family protein	At2g19810		-	0,3
1552	zinc finger (CCCH-type) family protein	At2g05160		-	0,04
1553	zinc finger (CCCH-type) family protein	At3g51950		-	0,2
1554	zinc finger (CCCH-type) family protein	At5g12440		-	0,2
1555	zinc finger (CCCH-type) family protein	At5g16540	ZFN3	-	0,2
1556	zinc finger (DHHC type) family protein	At1g69420		-	0,2
1557	zinc finger (GATA type) family protein	At3g60530		-	0,03
1558	zinc finger (GATA type) family protein	At3g06740		-	0,3
1559	zinc finger (MYND type) family protein	At5g50450		-	0,3
1560	zinc finger (Ran-binding) family protein	At3g15680		-	0,2
1561	zinc finger homeobox family protein	At4g24660		-	0,2
1562	zinc finger protein, putative	At1g32540	LOL1	-	0,3
1563	**TRANSPORT**				
1564	**ABC-Transporter**				
1565	ABC transporter family protein, AbcA	At3g47730	ATH1	2,6	5,1
1566	ABC transporter-related	At3g21080		2.6	6
1567	ABC transporter family protein	At5g60740	WBC29	5.9	8.2
1568	ABC transporter family protein	At5g02270	NAP9	2.8	11
1569	ABC transporter family protein	At3g13100	MRP7	3.6	35.7
1570	multidrug resistant (MDR) ABC transporter	At2g47000	PGP4	35.5	70.4
1571	multidrug resistant (MDR) ABC transporter, putative	At3g62150	MDR17	11.4	120.9
1572	ABC transporter family protein	At5g44110	NAP2/POP1	-	3.1
1573	ABC transporter family protein	At1g03905		-	3.7
1574	ABC transporter family protein	At1g71330	NAP5	-	4.3
1575	ABC transporter family protein	At3g47780	ATH6	-	8.4
1576	ABC transporter family protein	At1g15520	PDR12	-	23.1
1577	ABC transporter family protein	At3g55130	WBC19	-	0,1
1578	ABC transporter family protein	At2g39350	WBC1	-	0,1
1579	ABC transporter family protein	At2g07680	MRP11	-	0,1
1580	ABC transporter family protein	At1g17840	WBC11	-	0,2
1581	ABC transporter family protein	At1g51500	CER5	-	0,2
1582	ABC transporter family protein	At2g26910	PDR4	-	0,2
1583	ABC transporter family protein	At3g21250	MRP6	-	0,2
1584	glutathione-conjugate transporter, putative	At3g62700	MRP10	-	0,2
1585	similar to multidrug resistance P-glycoprotein, putative	At4g25960	MDR2	-	0,2
1586	ABC transporter family protein	At1g67940	NAP3	-	0,3
1587	ABC transporter family protein	At1g71960	WBC26	-	0,3
1588	ABC transporter family protein	At2g01320	WBC7	-	0,3
1589	**Amino acid transporter**				
1590	amino acid transporter family protein	At5g02180		2,6	3,3
1591	amino acid transporter family protein	At4g35180		-	5,6
1592	amino acid permease 6	At5g49630	AAP6	-	0,2
1593	amino acid permease, putative	At5g01240		-	0,2
1594	amino acid permease, putative	At2g38120	AUX1	-	0,3
1595	amino acid transporter family protein	At5g15240		-	0,3
1596	amino acid transporter family protein	At3g56200		-	0,1
1597	amino acid transporter family protein	At5g23810	AAP7	-	0,3
1598	amino acid transporter family protein	At1g47670		-	0,1
1599	amino acid transporter family protein	At5g65990		-	0,3
1600	proline transporter, putative	At2g36590	PROT3	-	0,1
1601	**Calcium**				
1602	calcium-transporting ATPase 4	At1g07670		-	3,1
1603	two-pore calcium channel	At4g03560	TPC1	-	0,3
1604	calcium exchanger	At2g38170		-	0,2
1605	**Cations**				
1606	cation/hydrogen exchanger, putative	At5g41610	CHX18	-	14,9

Row	Description	Locus[2]	Protein	t/c ratio[3]	
	Functional categories[1]			IS12	S12
1607	member of Zinc transporter (ZAT) family	At2g29410	MTPB1	4,9	11,1
1608	metal transporter, putative	At1g05300	ZIP5	-	0,2
1609	bile acid:sodium symporter family protein	At2g26900		-	0,3
1610	zinc transporter	At2g46800	ZAT	-	0,3
1611	magnesium/proton exchanger	At2g47600	MHX	-	0,3
1612	bile acid:sodium symporter family protein	At4g12030		-	0,2
1613	sodium proton exchanger	At5g27150	NHX1	-	0,3
1614	sodium:solute symporter family protein	At5g45380		-	0,3
1615	NRAMP metal ion transporter 4	At5g67330	NRAMP4	-	0,3
1616	**Ion channel**				
1617	cyclic nucleotide-binding transporter 1 / CNBT1	At3g17700	CNCG20	-	3,8
1618	cyclic nucleotide-binding transporter 2 / CNBT2	At3g17690	CNGC19	-	13,3
1619	cyclic nucleotide-regulated ion channel	At1g01340	CNGC10	-	10,1
1620	cyclic nucleotide-regulated ion channel, putative	At4g01010	CNGC13	-	3,2
1621	porin family protein	At1g50400		-	3
1622	chloride channel protein	At5g40890	CLC-A	-	0,2
1623	chloride channel-like (CLC) protein	At5g33280		-	0,3
1624	anion exchange family protein	At2g47160	BOR1	-	0,1
1625	voltage-gated chloride channel family protein	At4g35440	CLC-E	-	0,1
1626	cyclic nucleotide-regulated ion channel, putative	At2g46450	CNGC12	-	0,3
1627	cyclic nucleotide-regulated ion channel	At5g15410	DND1	-	0,1
1628	cyclic nucleotide-regulated ion channel	At5g54250	DND2	-	0,2
1629	**Lipid**				
1630	lipid transfer protein (LTP) family protein	At1g55260		-	0,1
1631	lipid transfer protein (LTP) family protein	At2g13820		-	0,2
1632	lipid transfer protein (LTP) family protein	At3g43720		-	0,2
1633	lipid transfer protein (LTP) family protein	At4g33550		-	0,3
1634	lipid transfer protein (LTP) family protein	At5g05960		-	0,2
1635	lipid transfer protein (LTP) family protein	At2g45180		-	0,3
1636	lipid transfer protein (LTP) family protein	At2g10940		-	0,2
1637	lipid transfer protein (LTP) family protein	At3g18280		-	0,2
1638	lipid transfer protein 6	At3g08770	LTP6	-	0,2
1639	lipid transfer protein, putative	At2g15050		-	0,1
1640	lipid transfer protein-related	At2g44300		-	0,3
1641	lipid transfer protein 3	At5g59320	LTP3	-	0,2
1642	nonspecific lipid transfer protein 5	At3g51600	LTP5	-	0,3
1643	lipid transfer protein-related	At1g27950		-	0,1
1644	nonspecific lipid transfer protein 2	At2g38530	LTP2	-	0,1
1645	**Mate efflux**				
1646	MATE efflux family protein	At2g04070		3,3	13,1
1647	MATE efflux family protein	At1g15180		8,8	4,2
1648	MATE efflux family protein	At2g04040		-	5,4
1649	MATE efflux family protein	At2g04050		-	14,4
1650	MATE efflux protein-related	At4g38380		-	5,1
1651	MATE efflux family protein	At4g22790		-	0,3
1652	MATE efflux family protein	At2g04080		-	0,3
1653	MATE efflux family protein	At1g61890		-	0,2
1654	MATE efflux family protein	At4g21910		-	0,1
1655	MATE efflux family protein	At5g17700		-	0,3
1656	MATE efflux family protein	At5g44050		-	0,3
1657	MATE efflux family protein	At3g26590		-	0,2
1658	**Mitochondrial transport**				3,8
1659	ADP, ATP carrier protein, mitochondrial, putative	At4g28390		-	3,8
1660	mitochondrial import inner membrane translocase subunit Tim17	At1g20350	TIM17-1	2,7	30,8
1661	mitochondrial import receptor subunit TOM20-4	At5g40930	TOM20-4	2,2	4
1662	mitochondrial substrate carrier family protein	At4g27940		2,2	4,7
1663	mitochondrial substrate carrier family protein	At4g26180		-	6,8
1664	mitochondrial substrate carrier family protein	At3g53940		-	4,1
1665	expressed protein, putative	At3g62650		-	0,3
1666	mitochondrial substrate carrier family protein	At5g01500		-	0,3
1667	**Misc**				
1668	ammonium transporter 2 (AMT2),	At2g38290	AMT2	-	4,5
1669	anion-transporting ATPase, putative	At1g01910		-	3,3
1670	ara4-interacting protein, putative	At4g11740	SAY1	3,1	5,4
1671	chloroplast protein import component-related	At4g03320		11,1	184,5
1672	chromosome-associated kinesin, putative	At5g60930		2,9	2,6
1673	coatomer protein epsilon subunit family protein	At2g34840		-	4,3
1674	cytokinesis-related Sec1 protein, putative	At4g12120	SEC1B	2,9	9,4
1675	dynamin-like protein 6	At1g10290	ADL6	-	3,7
1676	exocyst subunit EXO70 family protein	At3g09520		-	6,8
1677	exocyst subunit EXO70 family protein	At3g14090		-	3,2
1678	expressed protein	At1g76010		2,2	2,9
1679	haloacid dehalogenase-like hydrolase family protein	At3g25610		-	8,1
1680	heavy-metal-associated domain-containing protein	At5g52750		-	4
1681	heavy-metal-associated domain-containing protein	At5g52760		-	5
1682	heavy-metal-associated domain-containing protein	At1g55780		2,8	4,8
1683	importin alpha-1 subunit, putative	At3g06720	IMP	2	2,9
1684	importin alpha-2 subunit	At4g02150		2,2	4,7
1685	integral membrane transporter family protein	At5g54860		-	4,7
1686	kinesin motor protein-related	At1g09170		-	8,3
1687	kinesin motor protein-related	At3g10310		-	3,9
1688	kinesin motor protein-related	At5g27000	ATK4	-	3,3
1689	lipocalin, putative	At5g58070		3,4	4,1
1690	nuclear transport factor 2 (NTF2) family protein	At1g69250		-	4,1
1691	nucleoporin family protein	At1g59660		-	7,5

Row	Description	Locus[2]	Protein	t/c ratio[3]	
	Functional categories[1]			IS12	S12
1692	phagocytosis and cell motility protein ELMO1-related	At3g03610		3	5.2
1693	pre-mRNA splicing factor-related	At4g03430		2.5	7.6
1694	protease inhibitor/seed storage/lipid transfer protein (LTP) family protein	At1g62510		-	9.2
1695	protease inhibitor/seed storage/lipid transfer protein (LTP) family protein	At3g22600		-	4.7
1696	protease inhibitor/seed storage/lipid transfer protein family protein	At5g64080		3.5	9.6
1697	SEC14 cytosolic factor family protein	At1g22180		-	4
1698	SEC14 cytosolic factor family protein	At1g75170		-	4.1
1699	splicing factor, putative	At4g38780		3.9	3.6
1700	transducin family protein / WD-40 repeat family protein	At2g30050		-	3
1701	transport protein-related	At3g62770	ATAG18A	-	4.8
1702	VHS domain-containing protein	At5g16880		-	5.3
1703	xanthine/uracil permease family protein	At1g60030		3.7	5.5
1704	ATPase 2, plasma membrane-type, putative	At4g30190	AHA2	-	0.2
1705	ATPase, plasma membrane-type, putative	At5g62670		-	0.1
1706	heavy-metal-associated domain-containing protein	At2g36950		-	0.2
1707	SEC14 cytosolic factor family protein	At3g51670		-	0.3
1708	SEC14 cytosolic factor family protein	At1g72150		-	0.3
1709	triose phosphate/phosphate translocator, putative	At3g01550		-	0.3
1710	vacuolar ATP synthase subunit E, putative	At1g64200		-	0.3
1711	**Nitrate**				
1712	nitrate/chlorate transporter	At1g12110		-	0.04
1713	nitrate transporter	At2g26690		-	0.1
1714	**Nucleotides**				
1715	purine permease-related	At1g57990	PUP18	-	8.6
1716	permease	At5g03555		-	0.3
1717	purine permease family protein	At4g18210	PUP10	-	0.2
1718	**Oligopeptide transporter**				
1719	proton-dependent oligopeptide transport (POT) family protein	At5g01180		-	3.3
1720	oligopeptide transporter OPT family protein	At5g64410	OPT4	-	0.2
1721	proton-dependent oligopeptide transport (POT) family protein	At1g32450		-	0.1
1722	proton-dependent oligopeptide transport (POT) family protein	At1g52190		-	0.01
1723	proton-dependent oligopeptide transport (POT) family protein	At1g68570		-	0.1
1724	proton-dependent oligopeptide transport (POT) family protein	At1g69870		-	0.2
1725	proton-dependent oligopeptide transport (POT) family protein	At2g40460		-	0.2
1726	proton-dependent oligopeptide transport (POT) family protein	At3g01350		-	0.2
1727	proton-dependent oligopeptide transport (POT) family protein	At3g16180		-	0.2
1728	proton-dependent oligopeptide transport (POT) family protein	At3g47960		-	0.1
1729	proton-dependent oligopeptide transport (POT) family protein	At5g13400		-	0.1
1730	proton-dependent oligopeptide transport (POT) family protein	At5g14940		-	0.2
1731	**Phosphate**				
1732	mitochondrial phosphate transporter, putative	At3g48850		-	13.5
1733	phosphate translocator-related	At1g12500		-	0.2
1734	phosphate transporter family protein	At3g26570	PHT2;1	-	0.2
1735	phosphate transporter, putative	At3g23430	PHO1	-	0.3
1736	**Potassium**				
1737	potassium channel tetramerisation domain-containing protein	At5g55000	FIP2	-	3.5
1738	member of Stelar K+ outward rectifying channel (SKOR) family	At4g22200	AKT3	-	0.2
1739	outward rectifying potassium channel, putative	At4g01840	KCO5	-	0.3
1740	potassium transporter family protein	At1g60160		-	0.2
1741	potassium transporter, putative	At5g14880		-	0.3
1742	potassium transporter, putative	At2g40540	KT2	-	0.2
1743	**Sugar**				
1744	sugar transporter, putative	At2g48020		3.1	2.9
1745	glucose transporter (STP1)	At1g11260		-	0.3
1746	hexose transporter, putative	At5g61520		-	0.2
1747	integral membrane protein, putative	At1g19450		-	0.3
1748	sucrose transporter	At1g71880	SUC1	-	0.1
1749	sugar transporter family protein	At4g04750		-	0.1
1750	sugar transporter, putative	At1g77210		-	0.3
1751	sugar transporter, putative	At4g02050		-	0.2
1752	sugar transporter-related	At1g08900		-	0.1
1753	sugar-porter family protein 1	At5g27350	SFP1	-	0.1
1754	transporter-related	At1g79410		-	0.2
1755	transporter-related, low similarity to GDP-fucose transporter	At5g57100		-	0.3
1756	transporter-related, low similarity to hexose transporter	At4g35300		-	0.3
1757	**Sufate**				
1758	sulfate transporter (ST1)	At3g51895		-	0.3
1759	sulfate transporter	At1g78000	SULTR1;2	-	0.2
1760	sulfate transporter family protein	At3g12520	SULTR4;2	-	0.2
1761	sulfate transporter	At1g77990	AST56	-	0.2
1762	sulfate transporter	At5g10180	AST68	-	0.2
1763	**vesicle-trafficking**				
1764	expressed protein/v-SNARE	At4g14450	BET12	-	5.7
1765	Golgi SNARE protein membrin 12	At5g50440	MEMB12	2.3	2.6
1766	SNAP25 homologous protein SNAP33	At5g61210	SNAP33	-	3.4
1767	synaptobrevin-related family protein	At4g15780	VAMP724	-	3.5
1768	syntaxin 52	At1g79590	SYP52	-	5.1
1769	syntaxin 121	At3g11820	SYP121	-	4.3
1770	syntaxin, putative	At3g52400	SYP122	-	8.7
1771	**water channel**				
1772	aquaglyceroporin	At4g18910		-	0.3
1773	aquaporin, putative	At2g39010		-	0.2
1774	aquaporin, putative	At3g54820		-	0.1
1775	delta tonoplast integral protein	At3g16240	DELTA-TIP	-	0.1
1776	major intrinsic family protein	At4g23400		-	0.3

Row	Description	Locus[2]	Protein	t/c ratio[3]	
	Functional categories[1]			IS12	S12
1777	major intrinsic family protein	At4g17340	tonoplast	-	0,1
1778	plasma membrane intrinsic protein 1A	At3g61430	PIP1A	-	0,1
1779	plasma membrane intrinsic protein 1B	At2g45960	PIP1B	-	0,1
1780	plasma membrane intrinsic protein 1C	At1g01620	PIP1C	-	0,1
1781	plasma membrane intrinsic protein 2A	At3g53420	PIP2A	-	0,1
1782	plasma membrane intrinsic protein 2C	At2g37180	RD28	-	0,1
1783	plasma membrane intrinsic protein, putative	At4g00430	TMP-C	-	0,1
1784	plasma membrane intrinsic protein, putative	At2g16850		-	0,2
1785	small basic membrane integral family protein	At3g56950		-	0,3
1786	tonoplast intrinsic protein, putative	At3g26520	TIP2	-	0,2
1787	**DEVELOPMENT**				
1788	COP9 signalosome complex subunit 1	At3g61140	FUS6	-	4
1789	COP9 signalosome complex subunit 3	At5g14250	COP13	2.5	4.1
1790	COP9 signalosome complex subunit 4	At5g42970	COP8	2.2	4
1791	COP9 signalosome complex subunit 7	At1g02090	FUS5	-	5.6
1792	COP9 signalosome subunit 6	At5g56280	CSN6A	2.1	3.7
1793	COP9 signalosome subunit, putative	At4g14110	COP9	-	4.4
1794	embryo-abundant protein-related	At3g54150		2.7	20.5
1795	embryo-abundant protein-related	At2g41380		2.7	10.6
1796	embryo-abundant protein-related	At1g55450		-	3.7
1797	expressed protein	At3g04630	WDL1	3.5	-
1798	expressed protein	At1g68765	IDA	-	84.7
1799	haloacid dehalogenase-like hydrolase family protein	At5g44730		2.3	2.8
1800	late embryogenesis abundant 3 family protein	At1g02820		-	16.1
1801	late embryogenesis abundant 3 family protein	At4g02380	SAG21	-	6.8
1802	late embryogenesis abundant protein, putative	At2g46140		2.8	3.3
1803	leaf senescence protein-related	At5g51640	YLS7	-	3.1
1804	patatin, putative, similar to patatin-like latex allergen	At2g26560		2	9.3
1805	root hair defective 3 GTP-binding (RHD3) family protein	At5g45160		-	3.4
1806	senescence-associated protein-related	At1g19200		-	3.7
1807	senescence-associated protein-related SAG102	At4g17670	SAG102	-	3.3
1808	SWAP /surp domain-containing protein	At5g23080	TGH	-	4.4
1809	transducin family protein	At5g52250		-	7.5
1810	transducin family protein / WD-40 repeat family protein	At2g20330		-	3
1811	WD-40 repeat family protein /	At5g52820		-	3.6
1812	1-deoxy-D-xylulose 5-phosphate synthase, putative	At4g15560		-	0,3
1813	acid phosphatase class B family protein	At5g44020		-	0,1
1814	caleosin-related family protein	At1g70670		-	0,2
1815	CONSTANS-like protein-related	At1g07050		-	0,1
1816	family II extracellular lipase 3	At1g75900		-	0,1
1817	integral membrane family protein	At1g43650		-	0,2
1818	integral membrane family protein	At3g56620		-	0,3
1819	late embryogenesis abundant protein, putative	At3g50790		-	0,1
1820	male sterility MS5 family protein	At1g04770		-	0,1
1821	nodulin family protein	At4g34950		-	0,3
1822	nodulin family protein	At5g14120		-	0,1
1823	nodulin family protein	At2g16660		-	0,3
1824	nodulin MtN21 family protein	At3g28100		-	0,3
1825	nodulin MtN21 family protein	At2g40900		-	0,3
1826	nodulin MtN21 family protein	At3g28050		-	0,2
1827	nodulin MtN21 family protein	At1g75500		-	0,1
1828	nodulin MtN21 family protein	At2g37450		-	0,1
1829	nodulin MtN21 family protein	At2g37460		-	0,2
1830	nodulin MtN21 family protein	At4g08300		-	0,2
1831	nodulin MtN21 family protein	At3g28080		-	0,1
1832	nodulin MtN21 family protein	At3g28130		-	0,1
1833	nodulin MtN21 family protein	At4g01450		-	0,2
1834	nodulin MtN21 family protein	At4g08290		-	0,3
1835	nodulin MtN3 family protein	At3g48740		-	0,2
1836	nodulin MtN3 family protein	At4g15920		-	0,1
1837	nodulin MtN3 family protein	At5g23660	MTN3	-	0,1
1838	nodulin, putative	At1g76800		-	0,2
1839	nodulin-related	At4g19450		-	0,3
1840	patatin-related	At3g63200		-	0,03
1841	senescence-associated protein, putative	At5g46700		-	0,3
1842	senescence-associated protein-related	At1g78020		-	0,2
1843	senescence-associated protein-related	At1g22160		-	0,2
1844	senescence-associated protein-related	At3g22550		-	0,2
1845	senescence-associated protein-related	At1g53885		-	0,03
1846	senescence-associated protein-related	At2g44670		-	0,3
1847	**Large enzyme family**				
1848	**Oxidases**				
1849	amine oxidase family protein	At3g59050		-	0,3
1850	amine oxidase family protein	At4g29720		-	0,3
1851	copper amine oxidase family protein	At1g31680		-	0,02
1852	copper amine oxidase family protein	At4g12280		-	0,1
1853	copper amine oxidase, putative	At3g43670		-	0,1
1854	copper amine oxidase, putative	At1g31690		-	0,1
1855	flavin-containing monooxygenase family protein	At1g62540		-	0,1
1856	flavin-containing monooxygenase family protein	At1g62560		-	0,03
1857	**Glucosidases**				
1858	alpha-galactosidase, putative	At5g08370		-	0,1
1859	alpha-galactosidase, putative	At5g08380		-	0,2
1860	glycosyl hydrolase family 1 protein	At1g52400	BGL1	-	0,1
1861	glycosyl hydrolase family 1 protein	At3g62750		-	0,2

Row	Description	Locus[2]	Protein	t/c ratio[3]	
	Functional categories[1]			IS12	S12
1862	glycosyl hydrolase family 1 protein	At1g26560		-	0,1
1863	glycosyl hydrolase family 1 protein	At3g18080		-	0,1
1864	glycosyl hydrolase family 1 protein	At4g21760		-	0,3
1865	glycosyl hydrolase family 1 protein	At1g02850		-	0,2
1866	glycosyl hydrolase family 1 protein	At3g06510	SFR2	-	0,2
1867	**GDSL-lipases**				
1868	GDSL-motif lipase, putative	At1g28610		-	0,3
1869	GDSL-motif lipase, putative	At1g28570		-	0,1
1870	GDSL-motif lipase, putative	At1g28580		-	0,2
1871	GDSL-motif lipase, putative	At1g31550		-	0,1
1872	GDSL-motif lipase, putative	At1g54030		-	0,3
1873	GDSL-motif lipase/hydrolase family protein	At3g05180		-	0,1
1874	GDSL-motif lipase/hydrolase family protein	At4g26790		-	0,2
1875	GDSL-motif lipase/hydrolase family protein	At1g29660		-	0,1
1876	GDSL-motif lipase/hydrolase family protein	At1g29670		-	0,04
1877	GDSL-motif lipase/hydrolase family protein	At1g33811		-	0,3
1878	GDSL-motif lipase/hydrolase family protein	At1g67830		-	0,2
1879	GDSL-motif lipase/hydrolase family protein	At2g03980		-	0,1
1880	GDSL-motif lipase/hydrolase family protein	At2g04570		-	0,1
1881	GDSL-motif lipase/hydrolase family protein	At2g38180		-	0,3
1882	GDSL-motif lipase/hydrolase family protein	At3g14220		-	0,2
1883	GDSL-motif lipase/hydrolase family protein	At3g16370		-	0,1
1884	GDSL-motif lipase/hydrolase family protein	At4g28780		-	0,1
1885	GDSL-motif lipase/hydrolase family protein	At5g45950		-	0,03
1886	GDSL-motif lipase/hydrolase family protein	At5g55050		-	0,3
1887	GDSL-motif lipase/hydrolase family protein	At3g26430			0,3
1888	lipase, putative	At1g28600			0,3
1889	**Beta1,3 glucan hydrolases**				
1890	glycosyl hydrolase family 17 protein	At1g32860		-	5,6
1891	glycosyl hydrolase family 17 protein	At3g04010		-	7,1
1892	glycosyl hydrolase family 17 protein	At3g13560		-	0,3
1893	glycosyl hydrolase family 17 protein	At5g42720		-	0,3
1894	glycosyl hydrolase family 17 protein	At5g42100		-	0,2
1895	glycosyl hydrolase family protein 17	At5g35740		-	0,2
1896	beta-1,3-glucanase	At3g57240	BG3	-	0,3
1897	**Glutathione S-transferases,**				
1898	glutathione S-transferase, putative	At2g29490	GSTU1	17,8	13,9
1899	glutathione S-transferase, putative	At2g29480	GSTU2	-	5,3
1900	glutathione S-transferase, putative	At2g29460	GSTU4	2.1	10.7
1901	glutathione S-transferase, putative	At3g09270	GSTU8	2.5	4.7
1902	glutathione S-transferase, putative	At5g62480	GSTU9	8	168.7
1903	glutathione S-transferase, putative	At1g74590	GSTU10	2.5	38.4
1904	glutathione S-transferase, putative	At1g78340	GSTU22	4.6	8.1
1905	glutathione S-transferase, putative	At1g17170	GSTU24	9,1	21,7
1906	glutathione S-transferase, putative	At1g17180	GSTU25	124.7	236.7
1907	glutathione S-transferase	At5g41210	GSTT1	-	0,3
1908	glutathione S-transferase, putative	At2g30860	GSTF9	-	0,3
1909	glutathione S-transferase, putative	At3g03190	GSTF11	-	0,1
1910	glutathione S-transferase, putative	At5g17220	GSTF12	-	0,1
1911	glutathione S-transferase, putative	At2g29440	GSTU6	-	0,3
1912	glutathione S-transferase, putative	At1g59700	GSTU16	-	0,2
1913	glutathione S-transferase, putative	At1g10360	GSTU18	-	0,2
1914	glutathione S-transferase, putative	At1g78370	GSTU20	-	0,1
1915	glutathione S-transferase, putative	At1g17190	GSTU26	-	0,3
1916	glutathione S-transferase, putative	At3g43800	GSTU27	-	0,2
1917	**UDP-Glycosyltransferases**				
1918	alpha 1,4-glycosyltransferase family protein	At3g09020		3.3	11,9
1919	glycosyl transferase family 8 protein	At1g06780		2.3	2.8
1920	UDP-glucoronosyl/UDP-glucosyl transferase family protein	At2g15480		3.4	21,6
1921	UDP-glucoronosyl/UDP-glucosyl transferase family protein	At2g26480		2.1	4.7
1922	UDP-glucoronosyl/UDP-glucosyl transferase family protein	At2g15490		-	106
1923	coniferyl alcohol glucosyltransferase	At3g50740		-	0,1
1924	exostosin family protein	At4g13990		-	0,3
1925	exostosin family protein	At5g62220		-	0,2
1926	glycosyl transferase family 8 protein	At1g13250		-	0,2
1927	glycosyl transferase family 8 protein	At1g24170		-	0,1
1928	glycosyl transferase family 8 protein	At1g70090		-	0,2
1929	glycosyl transferase family 8 protein	At4g02130		-	0,2
1930	glycosyl transferase family 8 protein	At5g47780		-	0,3
1931	glycosyltransferase family 14 protein	At5g15050		-	0,3
1932	UDP-glucoronosyl/UDP-glucosyl transferase family protein	At1g06000		-	0,2
1933	UDP-glucoronosyl/UDP-glucosyl transferase family protein	At1g22370		-	0,3
1934	UDP-glucoronosyl/UDP-glucosyl transferase family protein	At2g30150		-	0,1
1935	UDP-glucoronosyl/UDP-glucosyl transferase family protein	At2g31750		-	0,2
1936	UDP-glucoronosyl/UDP-glucosyl transferase family protein	At2g31790		-	0,1
1937	UDP-glucoronosyl/UDP-glucosyl transferase family protein	At3g21750		-	0,1
1938	UDP-glucoronosyl/UDP-glucosyl transferase family protein	At3g21760		-	0,1
1939	UDP-glucoronosyl/UDP-glucosyl transferase family protein	At3g46670		-	0,2
1940	UDP-glucoronosyl/UDP-glucosyl transferase family protein	At4g14090		-	0,04

(1) Transcripts were grouped according to biological function GO (Gene Ontology) terms. Genes with unknown biological functions were excluded from table 8.3.

(2) The annotation of the genes derived from TAIR, the Arabidopsis Information Resource (http://arabidopsis.org).

(3) Data derived from three independent experiments. Differentially expressed genes were filtered by the Welch's t-test ($p \leq 0.05$) and MTC.
Grey filling designates t/c ratios ≥ 2 (IS12) and ≥ 3 (S12); no filling designates t/c ratios ≤ 0,5 (IS12) and ≤ 0,333 (S12).

(*) Abbreviations for the extracellular domains of receptor-like protein kinases (RLKs): CrRLK1, Catharanthus roseus RLK1; DUF26, domain of unknown function 26; K, kinase; LEC, legume lectin; LRR, leucine-rich repeat; SD, S-locus glycoprotein-like domain; TK, transmembrane/kinase; WAKL, wall-associated kinase like.

Table 8.4 Sporulation efficiency of powdery mildew on syl_404 upon syringolin treatment

M3 population	Experiment No.	Sporulation efficiency [%][1]		
		weak sporulation	intermediate sporulation	heavy sporulation
wild type	1	44	34	22
	2	88	10	2
syl_404	1	23	29	48
	2	32	27	41

(1) Sporulation efficiency was evaluated according to the scheme presented in table 4.13.

Table 8.5 Sporulation efficiency of powdery mildew on the wild type, syl_404 and backcross syl_404_bc1, syl_404_bc2 upon syringolin treatment

Plant material	Experiment No.	Sporulation efficiency [%][1]		
		weak sporulation	intermediate sporulation	heavy sporulation
wild type	1	52	31	17
	2	67	30	3
	3	88	12	0
	4	94	6	0
	5	67	30	3
	6	55	26	19
syl_404	1	5	32	63
	2	19	18	63
	3	42	28	30
	4	34	20	46
	5	62	33	5
	6	30	29	41
syl_404_bc1	1	4	17	79
	2	52	22	26
	3	36	25	39
	4	11	45	44
	5	69	14	17
	6	30	30	40
syl_404_bc2	1	15	55	30
	2	28	28	44
	3	39	35	26
	4	15	41	44
	5	68	29	3
	6	29	37	34

(1) Sporulation efficiency was evaluated according to the scheme presented in table 4.13.

Table 8.6 Functional groups of genes exhibiting m/wt ratios ≥ 3 and ≤ 0,333 in syl_404 upon control and/or syringolin treatment

Row	Description	Locus[2]	m/wt ratio		t/c ratio[5]	
	Functional categories[1]		Control[3]	SylA[4]	wt	syl_404
	RESPONSE TO ABIOTIC AND BIOTIC STIMULI					
	Jasmonic acid signalling					
1	12-oxophytodienoate reductase	At2g06050	**5,74**	**2,07**	**0,36**	**0,13**
2	allene oxide cyclase, putative	At3g25780	**14,74**	3,84	1,23	**0,32**
3	aminotransferase, putative	At2g24850	**37,71**	0,60	3,30	**0,05**
4	jacalin lectin family protein	At3g16470	**7,33**	0,14	**0,21**	**0,004**
5	jasmonic acid carboxyl methyltransferase	At1g19640	**7,06**	4,74	0,38	**0,25**
6	lipoxygenase, putative	At1g72520	**8,43**	1,22	**17,01**	**2,47**
7	lipoxygenase, putative	At1g17420	**7,90**	**10,62**	0,32	**0,44**
8	plant defensin-fusion protein, putative (PDF1.2b)	At2g26020	**7,34**	0,56	0,96	**0,07**
9	plant defensin-fusion protein, putative (PDF1.3)	At5g44420	**5,03**	0,53	0,82	**0,09**
10	plant defensin-fusion protein, putative (PDF2.2)	At2g02100	1,09	**0,08**	**0,17**	**0,01**
11	plant defensin-fusion protein, putative (PDF2.3)	At2g02130	**0,44**	**0,10**	**0,37**	**0,08**
12	steroid sulfotransferase, putative	At1g32640	**4,35**	**1,45**	**0,45**	**0,15**
13	vegetative storage protein 2	At5g24780	**32,76**	0,06	0,38	**0,001**
14	**Abscisic acid/ Dehydration stress**					
15	ABA-responsive protein (HVA22d)	At4g24960	**1,75**	**3,88**	0,83	**1,84**
16	ABA-responsive protein-related	At3g02480	**491,60**	**142,80**	6,67	1,94
17	calcium-binding RD20 protein	At2g33380	**9,65**	**30,09**	**0,11**	**0,33**
18	coronatine-responsive tyrosine aminotransferase	At4g23600	**8,97**	1,69	**0,13**	**0,02**
19	dehydration-responsive protein, putative	At1g31850	0,88	**0,22**	**0,59**	**0,15**
20	dehydrin	At5g66400	**4,23**	**5,12**	**1,31**	**1,59**
21	dehydrin	At1g20440	**4,70**	**7,49**	0,89	1,42
22	dehydrin	At1g20450	**7,18**	**18,56**	**0,24**	0,62
23	dehydrin xero2	At3g50970	**34,65**	**20,46**	**6,96**	**4,11**
24	dehydrin, putative	At4g38410	**24,07**	2,81	0,51	**0,06**
25	early-responsive to dehydration stress protein (ERD12)	At3g25760	**3,74**	**2,10**	**0,23**	**0,13**
26	GRAM domain-containing protein	At5g13200	**4,20**	**2,43**	**8,41**	**4,87**
27	late embryogenesis abundant protein, putative	At1g01470	**3,49**	**3,33**	1,35	1,29
28	lectin protein kinase, putative	At5g01540	**4,05**	1,03	**17,29**	**4,40**
29	lipid transfer protein 3	At5g59320	**7,05**	**3,41**	**0,32**	**0,16**
30	lipid transfer protein 4	At5g59310	**42,28**	10,67	0,61	**0,15**
31	pirin, putative	At3g59220	**6,47**	1,04	0,83	**0,13**
32	plasma membrane intrinsic protein 1A	At3g61430	**3,04**	0,85	**0,16**	**0,04**
33	protein phosphatase 2C, putative	At5g59220	**5,12**	**5,29**	1,23	1,27
34	protein phosphatase 2C, putative	At3g11410	**1,26**	**3,95**	**0,23**	0,72
35	protein phosphatase 2C, putative	At3g05640	**4,94**	**5,23**	0,25	**0,27**
36	**Pathogen**					
37	broad-spectrum mildew resistance RPW8 family protein	At3g50480	**4,50**	0,64	**4,57**	0,65
38	chitinase, putative	At2g43620	**14,27**	**2,84**	**2,73**	**0,54**
39	chitinase, putative	At2g43570	21,12	**3,75**	**29,15**	**5,18**
40	disease resistance family protein	At2g34930	**5,88**	**2,57**	**2,70**	1,18
41	disease resistance protein (TIR-NBS class), putative	At1g72940	0,96	**0,26**	**0,57**	**0,15**
42	disease resistance response protein-related	At3g13650	1,12	**3,72**	1,38	**4,59**
43	enhanced disease susceptibility 5	At4g39030	**4,31**	**1,42**	**8,88**	**2,92**
44	macrophage migration inhibitory factor family protein	At5g57170	**0,28**	**0,37**	**0,40**	0,53
45	macrophage migration inhibitory factor family protein	At3g51660	**3,30**	1,88	**12,85**	**7,34**
46	myrosinase-binding protein, putative	At1g52040	**4,17**	0,21	**0,05**	**0,003**
47	patatin-related	At3g54950	**3,59**	**1,79**	**3,53**	1,76
48	pathogenesis-related protein 5	At1g75040	**4,13**	0,92	1,66	**0,37**
49	pathogenesis-related thaumatin family protein	At4g36010	**18,46**	**2,42**	**19,23**	**2,52**
50	polygalacturonase inhibiting protein 1	At5g06860	**5,61**	1,38	0,43	**0,11**
51	polygalacturonase inhibiting protein 2	At5g06870	**6,70**	0,58	**0,08**	**0,01**
52	protein with putative ankyrin	At4g14400	**0,65**	**0,06**	**0,36**	**0,03**
53	thaumatin, putative	At4g38660	**0,19**	0,77	0,03	0,13
54	Toll-Interleukin-Resistance (TIR) domain-containing protein	At1g72930	0,73	**0,19**	0,45	**0,12**
55	trypsin inhibitor, putative	At2g43510	**18,01**	**3,80**	**2,36**	0,50
56	trypsin inhibitor, putative	At2g43550	1,48	**0,08**	**0,13**	**0,01**
57	**Cellular redox state**					
58	arginine decarboxylase 2 (SPE2)	At4g34710	**3,94**	**1,99**	**3,97**	**2,00**
59	catalase 3 (SEN2)	At1g20620	**1,23**	**0,08**	**0,29**	**0,02**
60	dehydroascorbate reductase, putative	At1g19570	**3,06**	**1,30**	**0,20**	**0,08**
61	FAD-binding domain-containing protein	At4g20830	**4,33**	**1,32**	**6,52**	**1,99**
62	late embryogenesis abundant 3 family protein	At4g02380	**5,49**	0,95	**60,73**	**10,52**
63	myb family transcription factor (MYB75)	At1g56650	**5,24**	1,24	0,29	0,07
64	peroxidase 21 (PER21) (P21) (PRXR5)	At2g37130	**14,02**	0,44	0,11	**0,003**
65	peroxidase 33 (PER33) (P33) (PRXCA)	At3g49120	**5,34**	**1,77**	**4,89**	**1,62**
66	peroxidase 42	At4g21960	**0,66**	**0,09**	**0,22**	**0,03**
67	peroxidase, putative	At5g64120	**9,01**	**1,69**	1,46	**0,27**
68	peroxidase, putative	At5g05340	**17,71**	0,76	0,80	0,03
69	plastocyanin-like domain-containing protein	At5g20230	**11,46**	1,10	**17,31**	**1,67**
70	**Drug stress response**					
71	glutathione S-transferase, putative	At3g09270	9,52	**3,02**	23,05	**7,31**
72	glutathione S-transferase, putative	At1g02930	**7,22**	0,99	**21,58**	**2,97**
73	glutathione S-transferase, putative	At3g43800	**0,50**	**0,32**	**0,17**	**0,11**

Row	Description	Locus[2]	m/wt ratio		t/c ratio[5]	
	Functional categories[1]		Control[3]	SylA[4]	wt	syl_404
74	glutathione S-transferase, putative (ERD9)	At1g10370	**11,94**	**1,60**	**7,20**	0,97
75	MATE efflux protein-related	At5g52050	**6,23**	2,30	0,40	**0,15**
76	**Ethylene/ Senescence**					
77	ERF domain protein 9 (ERF9)	At5g44210	**4,30**	0,30	0,88	0,06
78	ethylene-responsive element-binding factor 2 (ERF2)	At5g47220	**4,32**	1,48	0,55	**0,19**
79	ethylene-responsive protein, putative	At1g05710	**3,39**	1,02	1,53	0,46
80	hevein-like protein (HEL)	At3g04720	**4,71**	**0,29**	0,64	**0,04**
81	senescence-associated protein	At4g35770	**19,47**	2,08	1,12	**0,12**
82	**Heat**					
83	17.4 kDa class I heat shock protein	At3g46230	0,96	**5,90**	15,20	**93,62**
84	17.4 kDa class III heat shock protein	At1g54050	1,47	**8,39**	0,20	1,12
85	17.6 kDa class II heat shock protein	At5g12020	4,04	**11,84**	3,71	**10,86**
86	17.6 kDa class I small heat shock protein	At1g53540	5,22	**24,22**	7,23	33,53
87	17.6 kDa class I small heat shock protein	At2g29500	0,88	**5,82**	3,41	**22,48**
88	17.7 kDa class II heat shock protein	At5g12030	5,99	**24,92**	16	**66,51**
89	heat shock protein 70, putative / HSP70, putative	At3g12580	**3,73**	**1,39**	**151,80**	**56,51**
90	heat shock protein 70, putative / HSP70, putative	At1g16030	1,08	**3,37**	1,55	**4,84**
91	heat shock protein-related	At2g03020	**1,57**	**5,83**	0,99	**3,69**
92	**Auxin**					
93	amino acid permease, putative (AUX1)	At2g38120	**0,26**	0,25	**0,12**	0,12
94	auxin-responsive family protein	At4g22620	**4,88**	1,22	0,98	0,24
95	auxin-responsive family protein	At4g34760	**0,30**	0,51	**0,07**	0,11
96	auxin-responsive family protein	At1g56150	**3,42**	0,25	0,56	**0,04**
97	auxin-responsive GH3 family protein	At4g27260	**4,62**	5,19	0,13	0,15
98	auxin-responsive GH3 protein, putative (DFL-1)	At5g54510	**5,86**	**2,11**	**3,62**	1,30
99	auxin-responsive protein, putative	At1g29510	**0,24**	0,28	**0,08**	0,09
100	auxin-responsive protein, putative	At1g75580	**3,82**	1,37	0,12	0,04
101	auxin-responsive protein, putative	At2g21210	**0,40**	**0,11**	**0,09**	**0,02**
102	auxin-responsive protein, putative	At4g38860	**0,30**	0,09	**0,03**	**0,01**
103	IAA-amino acid hydrolase 6, putative	At1g44350	**5,82**	**3,34**	0,31	**0,18**
104	**others**					
105	2-oxoacid-dependent oxidase, putative	At3g49620	**315,70**	0,75	64,05	**0,15**
106	beta-amylase (CT-BMY)	At4g17090	0,75	**0,33**	**0,22**	**0,09**
107	cell elongation protein	At3g19820	**0,55**	**0,17**	**0,30**	**0,09**
108	cold-responsive protein	At2g42540	**4,54**	**3,59**	**2,57**	**2,03**
109	CP12 domain-containing protein	At3g62410	**0,61**	**0,28**	**0,39**	**0,18**
110	gibberellin-regulated family protein	At5g14920	**0,60**	**0,03**	**0,22**	**0,01**
111	gibberellin-regulated protein 4	At5g15230	**0,36**	**0,18**	**0,35**	**0,17**
112	gigantea protein (GI)	At1g22770	**4,19**	**1,24**	**4,70**	**1,39**
113	glycosyl hydrolase family 17 protein	At3g57260	**9,15**	**2,12**	**0,65**	**0,15**
114	hydrophobic protein, putative	At4g30660	1	**0,32**	**0,32**	**0,10**
115	low-temperature-responsive protein 78	At5g52310	**4,95**	**8,41**	1,01	**1,72**
116	mannitol dehydrogenase, putative	At4g37990	**61,14**	**85,32**	2,26	3,15
117	MERI-5 protein	At4g30270	**13,56**	**1,45**	**5,05**	0,54
118	metallothionein-like protein 1C	At1g07610	**3,19**	**5,39**	1,11	1,88
119	nitrate reductase 1	At1g77760	**4,68**	1,34	1,24	**0,36**
120	non-symbiotic hemoglobin 2	At3g10520	**0,50**	**0,18**	**0,35**	**0,13**
121	patatin, putative	At2g26560	**6,03**	**0,64**	**47,22**	**5,00**
122	prolifera protein	At4g02060	**0,25**	1,40	0,16	0,92
123	pseudo-response regulator 7 (APRR7)	At5g02810	**3,18**	**1,70**	**4**	**2,14**
124	pseudo-response regulator 9	At2g46790	1,81	**4,49**	6,19	**15,32**
125	RuBisCO subunit binding-protein alpha subunit, chloroplast	At2g28000	**0,33**	**0,38**	1,18	1,35
126	RuBisCO subunit binding-protein beta subunit, chloroplast	At1g55490	**0,30**	**0,36**	0,53	**0,64**
127	serine carboxypeptidase S10 family protein	At4g30610	**0,24**	0,85	**0,09**	0,33
128	steroid sulfotransferase, putative	At2g03760	**4,50**	**0,68**	**19,92**	**3,00**
129	sucrose synthase / sucrose-UDP glucosyltransferase (SUS1)	At5g20830	**3,38**	**2,71**	**4,37**	**3,50**
130	Toll-Interleukin-Resistance (TIR) domain-containing protein	At2g20145	**3,20**	0,96	**5,00**	**1,50**
131	tubulin beta-8 chain (TUB8) (TUBB8)	At5g23860	**0,32**	**1,54**	0,53	**2,57**
132	xyloglucan:xyloglucosyl transferase	At2g06850	**0,69**	**0,26**	**0,25**	**0,09**
133	xyloglucan:xyloglucosyl transferase	At5g57560	**4,55**	**1,68**	**12,25**	**4,52**
134	**General stress response**					
135	coronatine-responsive protein	At1g19670	**5,89**	0,69	**0,07**	**0,01**
136	expressed protein	At5g50200	**3,38**	**1,68**	**5,54**	**2,76**
137	methyladenine glycosylase family protein	At1g80850	**0,26**	0,26	**0,16**	0,16
138	protease inhibitor, putative	At2g38870	**5,57**	**1,92**	**3,51**	1,21
139	stress-responsive protein, putative	At2g23680	**3,42**	0,72	**3,58**	0,75
140	universal stress protein (USP) family protein	At3g11930	1,12	**0,26**	**0,24**	**0,05**
141	universal stress protein (USP) family protein	At3g62550	1,06	**0,19**	**0,16**	**0,03**
142	**ELECTRON PATHWAYS**					
143	alcohol dehydrogenase	At1g77120	2,66	**14,87**	0,38	**2,15**
144	chlorophyll A-B binding protein (LHCB2:4)	At3g27690	**3,38**	**2,76**	**0,51**	**0,42**
145	cytochrome b5, putative	At2g46650	**3,78**	0,47	**0,11**	**0,01**
146	cytochrome P450 71A13, putative	At2g30770	**20,32**	1,58	**21,62**	**1,68**
147	cytochrome P450 71B23, putative (CYP71B23)	At3g26210	**3,91**	**0,56**	**3,91**	**0,56**
148	cytochrome P450 71B26, putative	At3g26290	**5,71**	0,97	1,15	**0,20**
149	cytochrome P450 81D1	At5g36220	**6,95**	1,60	1,24	**0,29**
150	cytochrome P450 family protein	At3g48520	**29,54**	1,77	0,61	**0,04**
151	cytochrome P450 family protein	At1g16410	**3,98**	0,31	0,13	**0,01**

Row	Description	Locus[2]	m/wt ratio		t/c ratio[5]	
	Functional categories[1]		Control[3]	SylA[4]	wt	syl_404
152	cytochrome P450, putative	At4g37370	**3,36**	**1,21**	**47,64**	**17,19**
153	cytochrome P450, putative	At2g45570	2,37	**15,87**	1,36	**9,14**
154	cytochrome P450, putative	At3g03470	**3,50**	**1,51**	**4,30**	**1,85**
155	dihydrolipoamide dehydrogenase 1	At3g16950	**0,55**	**0,14**	0,78	**0,19**
156	FAD-binding domain-containing protein	At1g30700	29,55	**3,04**	**205,30**	**21,13**
157	FAD-binding domain-containing protein	At4g20860	**6,49**	1,47	**17,81**	4,04
158	FAD-binding domain-containing protein	At5g44400	**0,21**	0,24	**0,24**	0,27
159	FAD-binding domain-containing protein	At2g34810	**7,07**	2,10	**0,28**	**0,08**
160	ferredoxin family protein	At4g14890	0,58	**0,20**	**0,16**	**0,05**
161	ferredoxin-related	At3g16250	**0,45**	**0,29**	**0,23**	**0,15**
162	flavin-containing monooxygenase family protein	At1g62570	**2,18**	**8,54**	**0,34**	1,32
163	flavin-containing monooxygenase family protein	At1g12200	0,64	**0,29**	1,33	0,59
164	fructose-bisphosphate aldolase, putative	At4g26530	**0,43**	**0,28**	**0,45**	**0,29**
165	GDSL-motif lipase/hydrolase family protein	At1g53990	2,45	**3,02**	15,17	18,70
166	GDSL-motif lipase/hydrolase family protein	At3g48460	**5,04**	**4,02**	0,91	**0,72**
167	glucose-6-phosphate 1-dehydrogenase / G6PD (ACG12)	At5g40760	**3,04**	1,55	2,81	1,43
168	glutamate decarboxylase, putative	At2g02010	**90,79**	1,34	**1817**	**26,84**
169	glutaredoxin family protein	At1g64500	**0,18**	1,03	1,48	**8,27**
170	glutaredoxin family protein	At1g28480	**7,96**	**1,68**	**8,59**	**1,82**
171	glycosyl transferase family 20 protein	At1g60140	**3,64**	**1,62**	0,62	**0,28**
172	glycosyl transferase family 20 protein	At4g17770	**0,53**	**0,21**	**0,27**	**0,10**
173	oxygen evolving enhancer 3 (PsbQ) family protein	At3g01440	**0,42**	**0,20**	**0,14**	**0,07**
174	pfkB-type carbohydrate kinase family protein	At2g31390	**1,83**	**3,06**	**2,79**	**4,67**
175	pfkB-type carbohydrate kinase family protein	At1g69200	**0,33**	0,55	1,02	1,72
176	plastocyanin-like domain-containing protein	At4g12880	**0,35**	**0,33**	**0,23**	**0,22**
177	pyridine nucleotide-disulphide oxidoreductase family protein	At1g07180	**5,13**	**1,68**	**13,81**	**4,52**
178	pyruvate kinase, putative	At5g52920	**0,50**	**0,33**	0,91	0,60
179	pyruvate kinase, putative	At3g22960	**0,60**	**0,25**	**0,89**	0,38
180	thioredoxin H-type 5	At1g45145	**7,14**	**2,54**	**6,66**	**2,37**
181	trehalose-6-phosphate phosphatase, putative	At4g22590	2,57	**3,06**	1,80	2,15
182	**SIGNALTRANSDUCTION**					
183	aspartate/glutamate/uridylate kinase family protein	At3g18680	**0,33**	**0,18**	**0,38**	**0,20**
184	CBL-interacting protein kinase 11	At2g30360	**7,66**	**2,68**	**2,89**	1,01
185	DNA-damage-repair/toleration protein, putative	At3g12610	**0,22**	**0,22**	**0,12**	**0,13**
186	gibberellin-responsive protein, putative	At1g74670	**0,14**	**0,21**	**0,09**	**0,14**
187	leucine-rich repeat family protein	At1g68780	**0,27**	0,42	0,24	0,37
188	leucine-rich repeat family protein	At3g20820	**0,53**	**0,33**	**0,14**	**0,09**
189	leucine-rich repeat family protein / protein kinase family protein	At5g25930	**3,17**	1,04	**19,78**	**6,45**
190	leucine-rich repeat family protein / protein kinase family protein	At2g37050	**0,55**	**0,30**	**0,49**	**0,27**
191	leucine-rich repeat transmembrane protein kinase, putative	At4g39270	**3,26**	1,26	**7,52**	**2,90**
192	leucine-rich repeat transmembrane protein kinase, putative	At1g09970	**4,30**	0,86	**2,84**	**0,57**
193	leucine-rich repeat transmembrane protein kinase, putative	At1g68400	**0,25**	1,11	0,11	0,49
194	leucine-rich repeat transmembrane protein kinase, putative	At1g35710	**1,56**	**0,33**	1,13	**0,24**
195	leucine-rich repeat transmembrane protein kinase, putative	At3g56370	**0,21**	0,41	**0,12**	0,23
196	leucine-rich repeat transmembrane protein kinase, putative	At1g48480	**0,33**	0,47	**0,16**	**0,22**
197	leucine-rich repeat transmembrane protein kinase, putative	At5g51560	**0,30**	0,33	**0,14**	0,15
198	leucine-rich repeat transmembrane protein kinase, putative	At3g28040	**0,54**	**0,15**	**0,13**	**0,04**
199	PRLI-interacting factor L, putative	At1g80480	**0,33**	**0,34**	0,95	0,97
200	protein kinase family protein	At2g18890	**0,33**	0,59	0,21	0,37
201	protein kinase family protein	At5g01020	**0,53**	**0,28**	**0,49**	**0,26**
202	protein kinase family protein	At3g20860	**3,22**	**1,96**	1,95	1,18
203	protein kinase-related	At1g33940	**0,31**	1,13	**0,50**	**1,86**
204	Ras-related GTP-binding protein, putative	At5g60860	**2,35**	**3,37**	**0,71**	1,02
205	receptor-like protein kinase 5 (RLK5)	At4g23140	**3,91**	0,36	1,62	0,15
206	serine/threonine protein kinase (PK19)	At3g08720	**3,76**	**1,37**	**6,53**	**2,37**
207	wall-associated kinase 1 (WAK1)	At1g21250	2,30	**0,25**	0,85	**0,09**
208	WD-40 repeat family protein	At5g53500	**0,33**	0,50	**0,28**	0,42
209	**TRANSCRIPTION**					
210	antitermination NusB domain-containing protein	At4g26370	**0,47**	**0,27**	**0,45**	**0,25**
211	AP2 domain-containing transcription factor, putative	At2g20880	**37,10**	4,45	1,72	**0,21**
212	basic helix-loop-helix (bHLH) family protein	At5g46690	**0,30**	0,42	**0,20**	0,28
213	bZIP transcription factor family protein	At3g58120	**0,15**	0,74	**0,05**	0,25
214	expressed protein	At4g12750	1,36	**0,27**	1,85	0,37
215	member of the DREB subfamily A-5 of ERF	At3g50260	**6,33**	1,14	**12,87**	**2,32**
216	member of the DREB subfamily A-5 of ERF	At1g74930	**0,33**	**2,70**	**0,12**	0,96
217	member of the DREB subfamily A-5 of ERF	At1g21910	**3,43**	1,80	1,32	0,69
218	member of the DREB subfamily A-6 of ERF	At4g28140	**31,66**	**12,64**	2,43	0,97
219	member of the DREB subfamily A-6 of ERF	At1g64380	**6,75**	1,44	0,30	**0,06**
220	member of the ERF subfamily B-3 of ERF	At5g61590	0,83	**0,28**	**0,12**	**0,04**
221	member of the ERF subfamily B-4 of ERF	At5g13330	**14,97**	3,17	1,68	**0,36**
222	member of the ERF subfamily B-4 of ERF	At5g61890	**12,37**	0,69	0,47	**0,03**
223	member of the ERF subfamily B-4 of ERF	At1g43160	**856,70**	7,85	1,59	**0,01**
224	member of the ERF subfamily B-6	At3g25890	0,78	**0,22**	**0,60**	**0,17**
225	mitochondrial transcription termination factor-related	At4g38160	**0,46**	**0,15**	**0,26**	**0,08**
226	myb family transcription factor	At4g05100	**32,56**	**181,60**	0,17	0,96
227	myb family transcription factor	At4g21440	**9,68**	10,91	0,43	**0,49**
228	myb family transcription factor	At5g67300	**4,95**	**2,47**	**0,64**	**0,32**
229	myb family transcription factor (MYB96)	At5g62470	**3,36**	1,14	**0,34**	**0,12**

Row	Description	Locus[2]	m/wt ratio		t/c ratio[5]	
	Functional categories[1]		Control[3]	SylA[4]	wt	syl_404
230	myb-related transcription factor	At2g46830	9,97	**7,09**	8,97	**6,38**
231	no apical meristem (NAM) family protein	At1g01010	**5,12**	1,06	**4,59**	0,95
232	no apical meristem (NAM) family protein	At4g27410	**5,76**	**5,52**	0,64	0,62
233	no apical meristem (NAM) family protein	At1g52890	**26,20**	14,09	0,49	**0,27**
234	ovule development protein, putative	At2g41710	0,94	**0,28**	**2,29**	0,68
235	scarecrow-like transcription factor 13 (SCL13)	At4g17230	**3,35**	**1,35**	**4,25**	**1,71**
236	speckle-type POZ protein-related	At3g48360	**0,54**	**0,17**	**0,10**	**0,03**
237	TAZ zinc finger family protein	At4g37610	**0,33**	1,26	**0,33**	1,28
238	TAZ zinc finger family protein	At5g67480	**4,05**	**0,80**	**0,32**	**0,06**
239	transcription factor jumonji (jmjC) domain-containing protein	At3g20810	**0,47**	**0,08**	**0,33**	**0,06**
240	transcription regulatory protein SNF5, putative (BSH)	At3g17590	**0,73**	**0,24**	**1,52**	0,51
241	WRKY family transcription factor	At5g49520	**21,61**	**4,50**	4,63	0,97
242	WRKY family transcription factor	At5g46350	**4,99**	**2,13**	2,20	0,94
243	WRKY family transcription factor	At5g07100	**7,09**	1,33	4,02	0,75
244	WRKY family transcription factor	At4g31800	**11,39**	**2,03**	**4,17**	0,74
245	WRKY family transcription factor	At4g23810	**2,48**	**0,16**	**5,81**	**0,38**
246	WRKY family transcription factor	At4g18170	**11,07**	6,88	0,60	**0,37**
247	WRKY family transcription factor	At5g22570	**4,57**	0,36	1,76	**0,14**
248	WRKY family transcription factor	At2g30250	**3,91**	1,18	**11,51**	**3,47**
249	zinc finger (B-box type) family protein	At5g57660	**4,30**	**3,89**	**0,28**	**0,25**
250	zinc finger (B-box type) family protein	At1g68520	**0,76**	**0,20**	**0,12**	**0,03**
251	zinc finger homeobox family protein	At5g65410	**0,28**	0,57	0,48	0,97
252	**PROTEIN METABOLISM**					
253	33 kDa secretory protein-related	At5g48540	**3,56**	**0,69**	**8,07**	1,57
254	33 kDa secretory protein-related	At1g04520	**0,25**	0,51	0,26	0,53
255	50S ribosomal protein L18 family	At3g20230	**0,52**	**0,29**	**0,31**	**0,17**
256	60S ribosomal protein L12 (RPL12C)	At5g60670	0,50	**0,32**	1,04	0,66
257	armadillo/beta-catenin repeat family protein	At1g60190	**2,66**	**9,21**	0,73	**2,53**
258	aspartyl protease family protein	At3g18490	0,77	**0,31**	**0,25**	**0,10**
259	aspartyl protease family protein	At5g10760	**3,36**	0,18	0,35	**0,02**
260	band 7 family protein	At3g01290	**3,22**	0,83	**15,82**	**4,10**
261	chaperonin, putative	At3g13470	**0,33**	**0,57**	**2,54**	**4,44**
262	chloroplast nucleoid DNA-binding protein-related	At1g09750	**0,29**	**0,34**	**0,10**	**0,12**
263	cysteine proteinase, putative	At2g27420	**0,24**	1,20	0,16	0,81
264	cysteine proteinase, putative	At4g11310	**8,79**	0,77	0,45	**0,04**
265	DNAJ heat shock N-terminal domain-containing protein	At5g03030	**4,05**	**1,81**	**4,24**	1,90
266	elongation factor 1B alpha-subunit 1 (eEF1Balpha1)	At5g12110	**0,27**	0,40	**1,67**	2,42
267	expressed protein	At3g27210	**3,32**	2,11	0,78	0,50
268	expressed protein	At1g60010	0,89	**0,30**	**0,28**	**0,09**
269	FtsH protease, putative	At1g79560	**0,30**	**0,28**	0,69	0,63
270	galactosyltransferase family protein	At1g27120	**0,18**	1,01	**0,31**	1,71
271	histone H2A, putative	At5g59870	**0,33**	1,06	**0,20**	**0,64**
272	histone H2A.F/Z	At3g54560	**0,28**	**3,16**	**0,55**	**6,16**
273	histone H2B, putative	At5g22880	**0,33**	0,52	0,35	0,55
274	histone H3	At5g10400	**0,32**	1,03	**0,16**	0,52
275	IAA-amino acid hydrolase 3 / IAA-Ala hydrolase 3 (IAR3)	At1g51780	**9,21**	**1,87**	**2,07**	**0,42**
276	lectin protein kinase family protein	At5g60300	**4,44**	1,00	0,86	**0,19**
277	leucine-rich repeat family protein	At1g49750	0,77	**0,22**	**0,32**	**0,09**
278	microtubule associated protein family protein	At5g55230	0,63	**0,20**	**0,22**	**0,07**
279	nucleosome assembly protein (NAP) family protein	At1g74560	0,80	**0,31**	1,62	**0,63**
280	palmitoyl protein thioesterase family protein	At5g47330	**9,44**	2,17	**0,14**	**0,03**
281	palmitoyl protein thioesterase family protein	At4g17470	**13,29**	2,16	0,19	**0,03**
282	peptidyl-prolyl cis-trans isomerase, putative	At5g58710	0,71	**0,32**	1,25	0,56
283	protein kinase family protein	At3g18750	**0,20**	1,18	0,75	**4,40**
284	protein kinase family protein	At4g11890	**5,23**	1,06	**11,15**	2,26
285	protein kinase family protein	At1g33260	**6,51**	0,67	0,88	**0,09**
286	protein kinase family protein	At1g21590	0,76	**0,21**	**0,27**	**0,08**
287	protein kinase family protein	At4g23210	**8,73**	1,38	**4,08**	0,65
288	ribosomal protein L7Ae/L30e/S12e/Gadd45 family protein	At4g12600	**0,76**	**0,32**	**2,70**	1,12
289	serine carboxypeptidase S10 family protein	At3g02110	**0,31**	0,49	**0,22**	0,35
290	serine carboxypeptidase S10 family protein	At5g08260	0,68	**0,22**	0,51	**0,16**
291	serine carboxypeptidase S10 family protein	At2g35780	0,75	**0,31**	**0,21**	**0,09**
292	subtilase family protein	At1g32940	**4,43**	**1,46**	**93,12**	**30,67**
293	subtilase family protein	At5g51750	**0,30**	0,44	**0,21**	0,30
294	subtilase family protein	At1g20160	**3,50**	0,44	0,20	**0,03**
295	U-box domain-containing protein	At1g66160	**3,58**	**2,03**	**3,94**	2,23
296	zinc finger (C3HC4-type RING finger) family protein	At1g08050	**3,18**	**2,09**	**10,81**	**7,12**
297	zinc finger (CCCH-type) family protein	At2g28450	1,07	**0,29**	**3,65**	0,99
298	**TRANSPORT**					
299	2-isopropylmalate synthase 1 (IMS1)	At1g74040	0,54	**0,32**	1,06	0,63
300	4-alpha-glucanotransferase, putative	At5g64860	0,54	**0,06**	**0,27**	**0,03**
301	ABC transporter family protein	At2g26910	**0,13**	**0,14**	**0,24**	0,25
302	ABC transporter family protein	At2g39350	**20,76**	3,60	0,36	**0,06**
303	acetyl-CoA C-acyltransferase 1	At5g48880	**3,12**	**1,69**	**0,34**	**0,18**
304	ADP, ATP carrier protein 2, mitochondrial	At5g13490	**4,64**	**2,42**	**5,81**	**3,03**
305	AICARFT/IMPCHase bienzyme family protein	At2g35040	**0,54**	**0,29**	0,91	0,49
306	amino acid permease family protein	At4g21120	**10,42**	2,13	3,53	0,72

Row	Description	Locus[2]	m/wt ratio		t/c ratio[5]	
	Functional categories[1]		Control[3]	SylA[4]	wt	syl_404
307	amino acid permease I (AAP1)	At1g58360	**1,69**	**3,06**	**0,36**	**0,65**
308	amino acid transporter family protein	At2g41190	**2,40**	**5,07**	0,67	1,41
309	amino acid transporter family protein	At1g47670	**0,31**	0,08	**0,14**	0,04
310	aquaporin, putative	At3g54820	**6,83**	1,19	0,59	**0,10**
311	auxin efflux carrier family protein	At2g17500	**3,27**	**4,62**	0,97	1,37
312	auxin transport protein, putative	At2g01420	**0,63**	**0,31**	**0,12**	**0,06**
313	beta-ketoacyl-CoA synthase family protein	At5g04530	**0,20**	0,33	**0,19**	0,31
314	beta-ketoacyl-CoA synthase, putative	At1g04220	**4,18**	0,68	0,26	**0,04**
315	bifunctional aspartate kinase	At4g19710	**0,51**	**0,28**	0,76	**0,43**
316	bifunctional aspartate kinase	At1g31230	0,95	**0,32**	**0,39**	**0,13**
317	bile acid:sodium symporter family protein	At4g12030	**3,31**	1,00	**0,43**	**0,13**
318	bile acid:sodium symporter family protein	At2g26900	**0,63**	**0,29**	**0,27**	**0,13**
319	branched-chain amino acid aminotransferase, putative	At3g19710	**5,21**	0,31	**0,09**	**0,01**
320	C4-dicarboxylate transporter/malic acid transport family protein	At5g24030	**3,20**	2,34	0,48	**0,35**
321	calcium-transporting ATPase 4	At2g41560	**0,77**	**0,20**	**0,32**	**0,08**
322	carboxyl methyltransferase family protein	At3g44860	**36,63**	2,24	1,55	**0,09**
323	cation exchanger, putative (CAX7)	At5g17860	**10,46**	**1,93**	3,69	0,68
324	copper chaperone (CCH)-related	At5g50740	**0,18**	0,62	0,12	0,43
325	cyclin family protein	At1g47210	**0,26**	1,34	**0,43**	2,25
326	cyclin family protein	At3g21870	**0,30**	0,63	**0,22**	0,46
327	dihydrolipoamide S-acetyltransferase (LTA2)	At3g25860	**0,55**	**0,33**	**0,51**	**0,30**
328	dihydrolipoamide S-acetyltransferase, putative	At1g34430	**0,58**	**0,30**	0,65	**0,33**
329	DNA (cytosine-5-)-methyltransferase (ATHIM)	At5g49160	**0,23**	**0,54**	**0,58**	1,34
330	embryo-abundant protein-related	At4g22530	**3,64**	0,78	3,01	**0,64**
331	ferritin 1	At5g01600	**4,48**	**3,62**	**0,31**	**0,25**
332	GCN5-related N-acetyltransferase (GNAT) family protein	At2g39030	**113,50**	1,31	1,57	**0,02**
333	glucosyltransferase-related	At4g16590	**12,63**	0,40	1,18	0,04
334	glutamate-1-semialdehyde 2,1-aminomutase 2 (GSA 2)	At3g48730	**0,45**	**0,33**	**0,45**	**0,33**
335	glycoside hydrolase family 77 protein	At2g40840	0,76	**0,32**	**0,19**	**0,08**
336	glycoside hydrolase starch-binding domain-containing protein	At5g26570	**0,57**	**0,28**	**0,37**	**0,18**
337	glycosyl transferase family 2 protein	At4g13410	**7,00**	9,12	0,05	0,06
338	glycosyl transferase family 2 protein	At1g24070	**5,10**	0,25	0,51	**0,02**
339	glycosyl transferase family 48 protein	At5g13000	0,55	**0,31**	0,48	**0,27**
340	glycosyltransferase family protein	At4g27570	**4,32**	2,14	1,10	0,54
341	heavy-metal-associated domain-containing protein	At1g51090	**3,19**	**2,54**	1,55	1,24
342	hexose transporter, putative	At5g26340	**9,27**	0,73	**6,35**	0,50
343	high-affinity nitrate transporter, putative	At3g45060	**10,13**	1,19	0,39	**0,05**
344	homocysteine S-methyltransferase 3 (HMT-3)	At3g22740	**4,09**	1,41	0,15	0,05
345	imidazole glycerol phosphate synthase hisHF, chloroplast	At4g26900	0,63	**0,30**	0,79	**0,37**
346	kinesin motor family protein	At4g24170	14,52	**5,16**	49,44	17,57
347	kinesin motor protein-related	At1g09170	0,46	**4,62**	3,44	34,96
348	kinesin motor protein-related	At3g50240	**0,22**	0,22	**0,16**	0,16
349	lipid transfer protein, putative	At2g15050	**0,77**	**0,21**	**0,11**	**0,03**
350	lysine and histidine specific transporter, putative	At5g40780	**4,19**	**0,68**	**3,54**	**0,57**
351	mannitol transporter, putative	At4g36670	**7,81**	0,76	0,78	**0,08**
352	MATE efflux family protein	At3g23550	**10,37**	**0,22**	**12,40**	**0,26**
353	MATE efflux family protein	At1g61890	**13**	**3,58**	0,43	**0,12**
354	mitochondrial import inner membrane translocase subunit	At4g26670	**0,63**	**0,23**	**0,49**	**0,18**
355	mitochondrial substrate carrier family protein	At5g27520	**5,16**	**2,45**	3,09	1,47
356	multidrug resistance P-glycoprotein, putative	At1g28010	**8,34**	0,49	0,82	**0,05**
357	nitrate/chlorate transporter (NRT1.1) (CHL1)	At1g12110	**1,50**	**0,32**	**0,12**	**0,03**
358	nonspecific lipid transfer protein 5	At3g51600	1,09	**0,14**	**0,47**	**0,06**
359	oligopeptide transporter OPT family protein	At5g55930	**6,99**	0,97	0,91	**0,13**
360	oligopeptide transporter OPT family protein	At4g16370	**0,55**	**0,22**	**0,23**	**0,09**
361	oligopeptide transporter OPT family protein	At4g27730	**4,39**	0,47	0,19	0,02
362	O-methyltransferase family 2 protein	At1g76790	**11,15**	0,86	0,80	**0,06**
363	O-methyltransferase N-terminus domain-containing protein	At5g42760	**0,23**	1,11	0,84	**4,04**
364	O-methyltransferase, putative	At1g21100	2,56	**0,17**	**9,47**	0,64
365	phosphatidate cytidylyltransferase family protein	At3g45040	**3,61**	**1,60**	**4,44**	1,97
366	proline transporter, putative	At2g36590	**12,94**	2,09	0,14	**0,02**
367	protease inhibitor/seed storage/lipid transfer protein	At1g62510	**4,50**	**2,69**	**8,31**	**4,97**
368	protease inhibitor/seed storage/lipid transfer protein	At3g22600	**37,53**	**2,18**	**45,56**	**2,64**
369	protease inhibitor/seed storage/lipid transfer protein	At5g48490	**0,21**	**1,68**	**0,13**	1,05
370	protease inhibitor/seed storage/lipid transfer protein	At4g12470	**9,41**	0,86	4,19	**0,38**
371	protease inhibitor/seed storage/lipid transfer protein	At2g10940	**0,28**	**0,35**	**0,21**	**0,26**
372	protease inhibitor/seed storage/lipid transfer protein	At4g22470	**20,92**	2,18	1,54	0,16
373	protease inhibitor/seed storage/lipid transfer protein	At3g22620	**24,51**	8,31	0,45	0,15
374	protease inhibitor/seed storage/lipid transfer protein	At5g55450	1,05	**0,07**	1,00	0,07
375	protease inhibitor/seed storage/lipid transfer protein	At3g22120	0,83	**0,07**	**0,24**	**0,02**
376	proton-dependent oligopeptide transport (POT) family protein	At5g46050	**17,78**	0,50	2,12	**0,06**
377	proton-dependent oligopeptide transport (POT) family protein	At3g47960	**3,69**	**0,48**	**0,20**	**0,03**
378	proton-dependent oligopeptide transport (POT) family protein	At1g52190	**0,36**	**0,05**	**0,17**	**0,02**
379	SEC14 cytosolic factor family protein n	At1g72160	1,15	**0,32**	**0,30**	**0,08**
380	Skb1 methyltransferase family protein	At4g31120	1,00	**0,30**	**2,23**	0,66
381	sodium/dicarboxylate cotransporter, putative	At5g47560	**0,62**	**3,33**	**0,21**	1,10
382	spermidine synthase, putative	At5g53120	**5,03**	**3,87**	**3,54**	**2,72**
383	sterol 24-C-methyltransferase, putative	At5g13710	0,78	**0,28**	**0,32**	**0,12**

Row	Description	Locus[2]	m/wt ratio		t/c ratio[5]	
	Functional categories[1]		Control[3]	SylA[4]	wt	syl_404
384	sucrose transporter / sucrose-proton symporter (SUC1)	At1g71880	**1,97**	**0,25**	**0,23**	**0,03**
385	sucrose-phosphate synthase, putative	At4g10120	**0,30**	0,58	**0,16**	**0,30**
386	sulfotransferase family protein	At5g07010	**94,33**	3,60	0,55	**0,02**
387	transferase family protein	At5g61160	13,72	**0,28**	**60,84**	1,26
388	transferase family protein	At2g40230	**6,50**	0,91	1,16	**0,16**
389	transferase family protein	At2g39980	**3,21**	0,83	0,32	**0,08**
390	transferase family protein	At5g01210	**3,04**	0,43	**0,53**	**0,07**
391	transferase family protein	At5g39050	**5,05**	0,97	**9,92**	**1,91**
392	transporter-related	At4g17550	1,48	**3,28**	1,97	**4,37**
393	UDP-glucoronosyl/UDP-glucosyl transferase family protein	At4g15490	**3,11**	**2,30**	**1,54**	1,14
394	UDP-glucoronosyl/UDP-glucosyl transferase family protein	At2g43820	**4,16**	**3,47**	1,34	1,11
395	UDP-glucoronosyl/UDP-glucosyl transferase family protein	At2g30140	**3,19**	0,95	**2,40**	0,72
396	vacuolar sorting receptor, putative	At4g20110	**3,90**	1,32	**5,71**	1,93
397	xyloglucan:xyloglucosyl transferase, putative	At3g44990	**0,19**	1,08	**0,05**	**0,27**
398	xyloglucan:xyloglucosyl transferase, putative	At4g03210	**0,20**	0,76	0,04	0,16
399	xyloglucan:xyloglucosyl transferase, putative	At4g30290	**9,15**	2,53	0,23	**0,06**

(1) Transcripts were grouped according to biological function GO (Gene Ontology) terms. Genes with unknown biological functions were excluded from table 8.6.

(2) The annotation of the genes derived from TAIR, the Arabidopsis Information Resource (http://arabidopsis.org).

(3) Data derived from two independent experiments: m/wt ratios were calculated from the data derived from control-treated syl_404 and wild-type plants. Genes that passed statistical filtering based on Student's t-test ($p \leq 0.05$) are highlighted in bold.

(4) Data derived from two independent experiments: m/wt ratios were calculated from the data derived from syringolin-treated syl_404 and wild-type plants. Genes that passed statistical filtering based on Student's t-test ($p \leq 0.05$) are highlighted in bold.

(5) Data derived from two independent experiments. t/c ratios were calculated from data derived from wildtype (wt) and syl_404 plants. Genes that passed statistical filtering based on Student's t-test ($p \leq 0.05$) and MTC are highlighted in bold.

Table 8.7 Microarray experiments in databases compared to syringolin experiments

Experiment name	Replicates	References	Database	Statistical Test	MTC
Anoxia	2	Loreti et al., 2005	NCBI[1]	Student' s t-test	No
Drought	2	Kudla/Ulm, Germany	NASC[2]	Student' s t-test	No
Pseudomonas syringae	3	Nürnberger/Halle, Germany	NASC	Welch' s t-test	Yes
Flagellin	2	Zipfel et al., 2004	NCBI	Student' s t-test	No
Ozone	3	A. Shirras/Lancaster, UK	NASC	Student' s t-test	No
Cycloheximide	2	Y. Shimada/Saitama, Japan	NASC	Student' s t-test	No
Heat	2	C. Leaver/Oxford, UK	NASC	Student' s t-test	No
Senescence	2	C. Leaver/Oxford, UK	NASC	Student' s t-test	No
Fumonisin	4	P. McCabe/Dublin, IR	NASC	Welch' s t-test	Yes

(1) National Centre for Biotechnology Information.

(2) Nottingham Arabidopsis Stock Centre.

9 Acknowledgements

In the first place, I would like to thank Prof. Dr. Robert Dudler for giving me the opportunity to work in his group. I am very grateful for his support and endless encouragements during difficult periods of work. He greatly assisted me with scientific writing.

I also wish to thank Prof. Dr. Beat Keller for taking charge of the co-referate.

I am much obliged to Andrea Patrignani and Uli Wagner for their help and excellent supervision during long lasting sessions of gene chip hybridisation and data analysis.

I thank Prof. Dr. Felix Keller for his generous help with the HPLC and Prof. Dr. Rosmarie Honegger for specifying the powdery mildew isolate.

The encouragement and support of Beatrice Scherrer have been invaluable to me. Your friendship, simply put, has greatly improved several difficult periods of work and has contributed to feel home in Switzerland.

I am grateful for the assistance, generosity, and advice I received from Barbara Schellenberg. I especially thank you for critically reading the manuscript.

I wish to thank Olaf Abderhalden and Rémy Bruggmann for the warm reception in the group, for their technical support, and for facilitating my first steps in Switzerland.

I would like to thank all the other members of the group, especially Roshani Shakya, Simone Rau and Zsuzsa Hasenkamp.

I extend many thanks to Theres Imhof-Klimm for her generous help, to Nabila Yahiaoui, Susanne Brunner, Silvia Travella, Urs Ochsner and all the other members of the Beat Keller group. In particular, I thank Dani Stutz for solving all my computer problems.

I am especially grateful to my partner Daniel Maring for his love and patience during intensive periods of work. I thank you not only for enduring every emotion and the countless hours of detachment but for believing in me all these years.

Last but far from least, I would like to thank my parents who made my education possible, for their support, and enthusiasm. I wish to thank my sister for listen to all my complaints and for her immense encouragements. They all have made this work possible.

10 Curriculum vitae

Name	Kathrin Michel
Date of birth	May 22, 1976
Place of origin	Mainz, Deutschland
1982-1986	Primary school in Mainz
1986-1995	Secondary school in Mainz
1995-2001	Undergraduate studies at the University of Giessen
March 1999	Practical training at Roche Diagnostics, Mannheim
October 2001	Diploma in biology, University of Giessen
2002-2006	Ph.D. thesis at the Institute of Plant Biology at the University of Zürich